JUL 8 1935

DO NOT TAKE FROM LIBRARY

THE PHYSICAL REVIEW

VOLUME 48 *Second Series* NUMBER 1

JULY 1, 1935

Published for the

AMERICAN PHYSICAL SOCIETY

by the

AMERICAN INSTITUTE OF PHYSICS
Incorporated

LANCASTER, PA., AND NEW YORK, N. Y.

THE AMERICAN PHYSICAL SOCIETY

OFFICERS OF THE SOCIETY

R. W. WOOD, *President*
The Johns Hopkins University
Baltimore, Maryland

F. K. RICHTMYER, *Vice President*
Cornell University
Ithaca, New York

W. L. SEVERINGHAUS, *Secretary*
Columbia University
New York, New York

G. B. PEGRAM, *Treasurer*
Columbia University
New York, New York

JOHN T. TATE, *Editor*
University of Minnesota
Minneapolis, Minnesota

L. B. LOEB, *Local Secretary for the Pacific Coast*
University of California
Berkeley, California

THE PHYSICAL REVIEW

BOARD OF EDITORS

JOHN T. TATE, *Editor*

J. W. BUCHTA, *Assistant Editor*

Associate Editors

K. K. DARROW
J. C. HUBBARD
A. E. RUARK
A. ELLETT
L. A. TURNER
G. E. UHLENBECK
W. V. HOUSTON
R. S. MULLIKEN
I. I. RABI

THE PHYSICAL REVIEW, which was established in 1893, is a journal of experimental and theoretical physics. It is published for the American Physical Society by the American Institute of Physics Incorporated. There are two volumes annually with twelve issues in each volume.

Manuscripts for publication should be submitted to John T. Tate, University of Minnesota, Minneapolis, Minnesota.

Proof and all correspondence concerning papers in the process of publication, should be addressed to the Editorial Secretary, American Institute of Physics, 11 East 38th Street, New York, New York.

Subscription price: United States and Possessions and Canada, $15.00; Foreign, $16.50. Subscriptions and orders for back numbers should be addressed to Prince and Lemon Streets, Lancaster, Pennsylvania, or to the American Institute of Physics, 11 East 38th Street, New York, New York.

Advertising is not accepted for the *Physical Review* but attention is called to the *Review of Scientific Instruments with Physics News and Views*, a companion publication of the Institute, and a medium through which the field of physics can be reached most effectively. Rates and other information will be furnished on request to the Editorial Secretary.

Changes of address and complaints of failure to receive the *Physical Review*, in the case of members of the American Physical Society, should be addressed to the Treasurer; in the case of other subscribers, to the Editorial Secretary. New copies can be sent free in response to complaints of non-delivery only if notice of non-delivery is received within three months of date of issue.

The Physical Review is published semi-monthly at Prince and Lemon Streets, Lancaster, Pennsylvania.

Entered at the Post Office at Lancaster, Pennsylvania, as second class matter.

Acceptance for mailing at special rate of postage provided for in section 1103, Act of October 3, 1917, authorised September 6, 1926.

THE
PHYSICAL REVIEW
A Journal of Experimental and Theoretical Physics
VOL. 48, NO. 1 JULY 1, 1935 SECOND SERIES

Schematic Representation of the Anomalous Scattering by Suitable Nuclear Fields

LEE H. HORSLEY, *Department of Physics, University of Kansas*
(Received May 3, 1935)

An attempt to represent Pose's data on the collision of α-particles and protons by a schematic nuclear model has led to results which are consistent with other information concerning the position of nuclear energy levels. The picture obtained seems also to apply to the results of Wenzel concerning the scattering of α-particles by other light elements.

§1. INTRODUCTION

THE theory of scattering of particles provides a relation between the scattering of the particles and the positions of the virtual nuclear energy levels.[1]

The purpose of this paper is to give an analysis of the virtual nuclear energy levels responsible for the anomalous scattering observed by several authors and to connect the position of these virtual levels with that of the stable nuclear quantum states. We shall see that this description of the scattering data makes it possible to account for all main features given by the experiments (position and height of maxima and minima), and that it is only a question of more detailed calculations to give still more accurate representations. It is doubtful, however, whether the present data are sufficiently reliable to base more detailed calculations on them and to get more complete information on an "intranuclear field" than is furnished by the relative position of the nuclear levels.

We should like to emphasize, therefore, that the following considerations are exclusively based on qualitative arguments for which the present experiments are certainly reliable (in regard to approximate heights and position of maxima, etc.), although they could evidently be adapted to fit more detailed experimental data by slightly modifying the proposed schematic nuclear model.

We shall find that the investigation of the nuclear scattering provides us with a helpful means for examining the structure of light nuclei and to attribute a definite arrangement to the interfering nuclear levels. For this purpose the approximate analysis of the data at present available may be regarded as sufficiently accurate.

We notice that a maximum scattering occurs in the neighborhood of a virtual energy level, if the latter belongs to an energy value, E, which is small compared to U, Fig. 1. This can easily be shown by a consideration of the scattering in the case of the potential hole shown. For example, for an s scattering the cross section is given by the expression

$$Q_0 = |C_0|^2 \lambda^2/\pi,$$

where

[1] *Viz.*, e.g., *Handbuch der Radiologie*, 2nd ed., Vol. 6/1, Leipzig, 1933, p. 343.

$$|C_0|^2=\frac{(\sin k_2R\cos k_1R-(k_2/k_1)\sin k_1R\cos k_2R)^2}{1+(k_2^2/k_1^2-1)\cos^2 k_2R} \tag{1}$$

$$k_1=(2\pi/h)[2m(+E)]^{\frac{1}{2}} \quad \text{and} \quad k_2=(2\pi/h)[2m(E+U)]^{\frac{1}{2}}.$$

Further, the condition that a stable eigenvalue exists for $E<0$ is

$$\tan k_2R=-k_2/\kappa=[(U+E)/-E]^{\frac{1}{2}}, \tag{2}$$

where $\kappa=(2\pi/h)[2m(-E)]^{\frac{1}{2}}$.

Now if $-E$ is very small compared to U (which means that the virtual level is very near the point $E=0$, Fig. 1), then $\tan k_2R=\infty$ and k_2R may have the values $\pi/2, 3\pi/2, \cdots (n+1)\pi/2$. For very small incident energies $k_1\to 0$, and the above expression (1) reduces to its maximum value $|C_0|^2=\cos^2 k_1R\to 1$. That is, for the case in which E is small compared to U the scattering coefficient and the scattering have maximum values. In the same way it can be shown that the p, d, etc., scatterings have maximum values in a virtual energy level in the neighborhood of $E=0$.

§2. The Energy Levels in a Rectangular Potential Hole

According to what we have said above, the systematic behavior of the anomalous scattering will thus depend on the level scheme of the scattering nuclei.

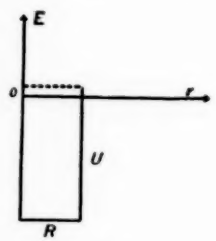

Fig. 1.

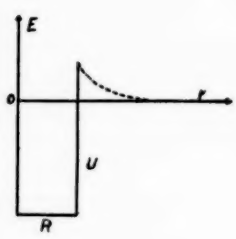

Fig. 2.

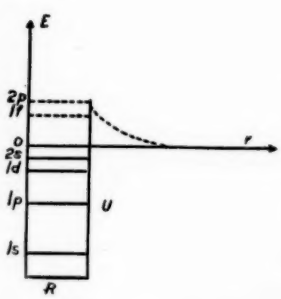

Fig. 3.

The exact shape of the "intranuclear field" is not known, but we can roughly represent a nucleus by the schematic model shown in Fig. 2, which previously has been successfully applied to nuclear problems by Condon and Gurney[2] and Gamow.[3]

It is easily seen that the relative position of the stable and virtual energy levels in Fig. 2 will depend only slightly upon a change of the shape of the potential hole. We can therefore restrict ourselves to the consideration of the level system in a simple rectangular potential hole. We find that the consecutive levels have to be described as

$$1s,\ 1p,\ 1d,\ 2s,\ 1f,\ 2p,\ \cdots,$$

where the first number (principal quantum number) determines in the usual way the number of nodes of the radial eigenfunctions, and the symbols s, p, d, f, etc. refer, respectively, to the orbital momenta

$$(h/2\pi)^2 l(l+1), \qquad l=0, 1, 2, 3, \cdots.$$

The lowest of these levels will be stable, the higher ones virtual energy levels (indicated by dotted lines, Fig. 3). By varying the depth of U in Fig. 3 we can evidently obtain any number of stable levels.

It will now be our task to determine the level picture (Fig. 3) for the nuclei investigated by analyzing the results of the anomalous scattering experiments. This will provide us with information which, to a high degree, is independent of detailed assumptions as to the nuclear radius R. A change of R within reasonable limits would only lead to a somewhat different value of the depth U to assume for each nucleus.

[2] Condon and Gurney, Nature **122**, 439 (1928).
[3] Gamow, Zeits. f. Physik **51**, 209 (1928).

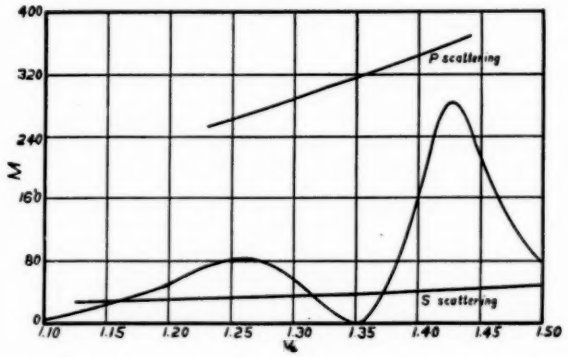

FIG. 4. S and P scattering according to Wenzel. Σ is the ratio of experimental scattering to Rutherford scattering.

§3. SCATTERING OF PROTONS BY α-PARTICLES

The procedure outlined above may be illustrated in greater detail by its application to Pose's[4] data on the collision of α-particles and protons at large angles ($\theta=180°$). The curves s and p (Fig. 4) are Wenzel's[5] maxima curves which indicate the values of the ratio

$$\Sigma=\frac{\text{experimental scattering}}{\text{Rutherford scattering}},$$

which cannot be exceeded if only s, respectively p, scattering occurs.

We conclude at once from Fig. 4 that the actually observed α-proton scattering is mainly due to a p resonance which will be found slightly modified by the influence of the s scattering.

§4. THE REPRESENTATION OF POSE'S CURVE

A preliminary calculation, using simply a rectangular potential hole (as in Fig. 1) showed that it is easy to account roughly for the shape of Pose's experimental curve (Fig. 4) if we choose the characteristics of the potential hole in order to place the p level very near to $E=+0$. (E.g., $R=4\times10^{-13}$ cm, $U=2.2\times10^{-5}$ erg.) This alone furnishes a maximum of Σ of the correct height, but does not account for the comparative sharpness of the maximum in Fig. 4.

[4] Pose and Diebner, Zeits. f. Physik **90**, 773 (1934).

[5] Wenzel, Zeits. f. Physik **90**, 754 (1934). A slight error in Wenzel's calculations (Wenzel uses the expression $D_l=-\cos(\gamma_l-G_l)e^{i(\gamma_l+G_l)}$ instead of the correct value $D_l=-\cos(\gamma_l-G_l)e^{i\gamma_l}$) does not affect the curves shown appreciably.

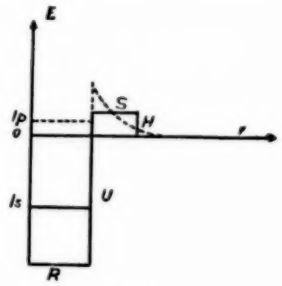

FIG. 5.

However, since the energy of the colliding particles in Rose's experiments (considered for the system with the center of gravity at rest) is of the order

$$E=\tfrac{1}{2}\left[\frac{M_\alpha}{1+M_\alpha/M_p}\right]V_\alpha{}^2=800{,}000\text{ ev},$$

we must take into account the coulomb repulsion outside the nuclear dimensions for the more exact treatment. The coulomb repulsion obviously adds a low potential barrier to Fig. 1 and reduces the width of the virtual p level in proportion just in the sense required by the experimental data.

The schematic model finally adopted in our calculations is shown in Fig. 5.

The differential scattering cross section included in the solid angle $d\Omega$ and depending upon an s and a p term is

$$dQ_{0,\,1}=(\lambda^2/4\pi^2)\,|\,C_0+3C_1P_1\,(\cos\theta)\,|^2d\Omega$$

and in our case, since $\theta=180°$, becomes

$$dQ_{0,\,1}=(\lambda^2/4\pi^2)\,|\,C_0-3C_1\,|^2d\Omega, \qquad (3)$$

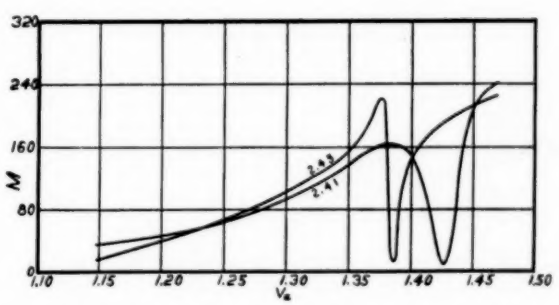

FIG. 6. S and P scattering according to the present theory.

where

$$2C_0+1=-\frac{A_0e^{\kappa S}(k_1R-i\kappa R)+B_0e^{-\kappa S}(k_1R+i\kappa R)}{A_0e^{\kappa S}(k_1R+i\kappa R)+B_0e^{-\kappa S}(k_1R-i\kappa R)}e^{-2ik_1(R+S)},$$

$$2C_1+1=-\frac{A_1e^{\kappa S}P\ +B_1e^{-\kappa S}Q}{A_1e^{\kappa S}P^*+B_1e^{-\kappa S}Q^*}e^{-2ik_1(R+S)},$$

and

$$A_0=\sin k_2R+\frac{k_2R}{\kappa R}\cos k_2R;\quad B_0=\sin k_2R-\frac{k_2R}{\kappa R}\cos k_2R,$$

$$A_1=(1/k_2R+k_2R/\kappa R+k_2R/\kappa^2R^2)\sin k_2R-\cos k_2R,$$

$$B_1=(-1/k_2R+k_2R/\kappa R-k_2R/\kappa^2R^2)\sin k_2R+\cos k_2R,$$

$$P=-ik_1(R+S)+ik_1/\kappa+i\kappa/k_1-\kappa(R+S),$$

$$Q=-ik_1(R+S)-ik_1/\kappa-i\kappa/k_1+\kappa(R+S),$$

$$k_1=(2\pi/h)(2\mu E)^{\frac{1}{2}};\quad k_2=(2\pi/h)(2\mu(E+U)^{\frac{1}{2}},$$

$$\kappa=(2\pi/h)(2\mu(H-E)^{\frac{1}{2}};\quad \mu=M\alpha/(1+M_\alpha/M_p).$$

By dividing (3) by the Rutherford scattering, namely

$$dQ=(4e^4/4\mu^2v_\alpha{}^4\sin^4\theta/2)d\Omega$$

we obtain finally, in the two cases which have been calculated, the curves shown in Fig. 6. It is seen that the resonance becomes much narrower and it would be merely a matter of further calculations to find a more suitable scattering field and obtain a closer representation of the curve in Fig. 4.

§5. The Structure of Light Nuclei

We have thus found that the collision of α-particles and protons is represented by the interaction energy indicated in Fig. 5, and is characterized by the stable $1s$ level, the $1p$ level being already metastable. We can interpret Fig. 5 as the level picture of the proton in the nuclear field of the α-particle.

This representation fits nicely into the picture we have to assume for the α-particle. The $1s_p$ level* is occupied by two protons and two neutrons, and therefore gives a completed shell in agreement with the very high packing energy of the α-particle. No other stable level exists in this case, which would lead to a stable Li_5 nucleus.

If we add simultaneously a proton and a neutron to the α-particle, the interaction of these causes an increase of the depth U in Fig. 5, the $1p_p$ level becomes stable, and accounts for the small packing energy of the Li_6 nucleus. We

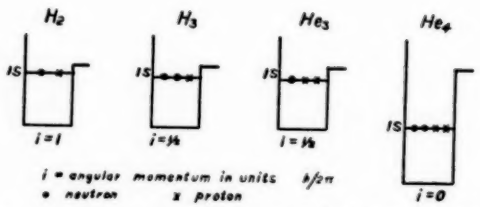

FIG. 7. Protons and neutron levels in light nuclei.

can also place an additional neutron in the $1p_p$ level, corresponding to Li_7.

By taking into account the degeneracy of the different levels it is easy to build up in this way a scheme of all light elements up to A_{36}, the $1p$ and $1d$ levels being successively occupied by protons and neutrons. This scheme was proposed first by Bartlett.[6]

It can easily be shown, however, that this scheme applies only to nuclei up to Li_7 and that a different picture must be devised for heavier nuclei. For, by adding an additional proton to Li_7 we would obtain a highly unstable aggregate which, according to Cockcroft and Walton,[7] disintegrates to give two α-particles.

It will be an important task to make an attempt to account for the nuclear spins based on the nuclear model outlined here. The nuclear spins, however, depend on the relative strength of the different types of coupling between the elementary particles. This is not known and no predictions can be made at present in this respect except for the four lightest nuclei (Fig. 7).[8]

§6. α-Particle Levels in Light Nuclei

We have seen that the scheme to build up light nuclei from protons and neutrons fails to hold for nuclei heavier than Li_7 because of the intranuclear formation of α-particles. We can follow this process somewhat more closely by considering the anomalous scattering of α-particles. For the interaction of an α-particle with a light nucleus Fig. 3 again holds qualitatively, provided we understand the occurring levels to be α levels in this case.

* The subscripts p, n and α attached to the level symbols s, p, d, etc. in what follows refer to the proton, neutron and α-particle, respectively. For our purposes, however, it will be sufficient to assume the proton and neutron levels as identical.

[6] Bartlett, Phys. Rev. **41**, 370 (1932); **42**, 145 (1932).

[7] Cockcroft and Walton, Proc. Roy. Soc. **A137**, 229 (1932).

[8] A more detailed investigation of these questions will be given in a paper by P. M. Strickler in which the lowest nuclear energy states are discussed from the point of view of the systematics of isotopes.

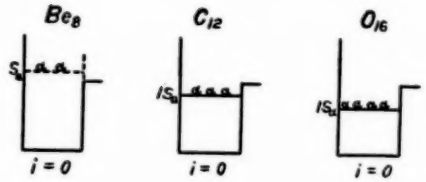

FIG. 8.

The collision of α-particles with helium nuclei has been measured by Rutherford and Chadwick[9] and a simple application of Wenzel's method (taking care, however, in regard to the symmetry of the eigenfunctions for identical particles) shows the scattering to be an s_α scattering.

Taylor[10] tried to account for this scattering by considering a virtual $2s_\alpha$ level but shows that this assumption leads to untenable results regarding the mass defect of a Be_8 nucleus. We shall therefore regard the $\alpha-$He scattering as a $1s_\alpha$ scattering. This means that no stable Be_8 nucleus can exist, its lowest level ($1s_\alpha$) occurring several million electron volts above $E=0$.

$\alpha\rightarrow Li_{6,7}$

No experiments are known in this case. Since the $1s_\alpha$ level is already stable ($B_{10,11}$ exist) we would have to expect a $1p_\alpha$ scattering at fairly high energies.

$\alpha\rightarrow Be_9$

Only little evidence is known for this interaction. Rietzler's[11] data on Be_9 show that the scattering has to be at least a p_α scattering and therefore we identify it with a $1p_\alpha$-resonance, probably at fairly high energies.

$\alpha\rightarrow B_{10,11}$

In this case Wenzel's analysis of Rietzler's measurements gives a distinct p_α resonance at about 5.0×10^6 electron volts. We can identify this level with the $1p_\alpha$ level of Fig. 3.

$\alpha\rightarrow C_{12}$

Rietzler's experiments also give a distinct p_α resonance in this case at about 4×10^6 electron volts, which again indicates a $1p_\alpha$ level of slightly decreased energy compared with boron. This fits nicely into our picture.

$\alpha\rightarrow F_{19}$

No scattering experiments are known but Pose[12] has found a resonance disintegration for this element which might correspond to a virtual $1d_\alpha$ level.

$\alpha\rightarrow Al_{27}$

Rietzler's measurements indicate the occurrence of a $2s_\alpha$ resonance at high energies. At lower energies Pose[13] finds a resonance level which should be identified with the $1d_\alpha$ level. It has been pointed out earlier that Pose's resonance level cannot be regarded as an s_α level. Recent experiments by Duncanson and Miller[14] show that this level has a high multiplicity which could be attributed to a d_α level.

Similar experiments for magnesium show less resonance levels in the energy range covered. We could also expect that the resonance level of magnesium is shifted to higher energy values compared with aluminum.

The α level scheme for the lighter nuclei is given in Fig. 8.

§7. THE STRUCTURE OF HEAVIER NUCLEI

Regarding nuclei of the type Be_9, B_{10}, B_{11}, etc., evidently a mixed description, using proton and neutron levels as well as α-levels will have to be applied.

The α-particles will all have to be assumed in the lowest level, $1s_\alpha$. A difficulty arises, however, in regard to the additional neutron-proton levels.

Let us consider for example the Be_9 nucleus. By building this nucleus up from two ap-

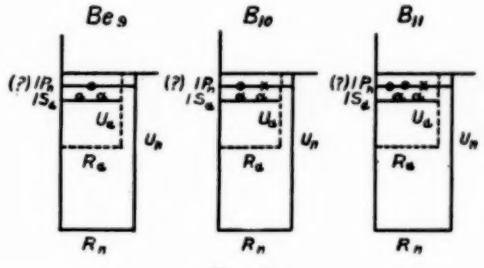

FIG. 9.

[9] Rutherford and Chadwick, Phil. Mag. **4**, 605 (1927).
[10] Taylor, Proc. Roy. Soc. **A134**, 103 (1931).
[11] Rietzler, Proc. Roy. Soc. **A134**, 528 (1931).
[12] Pose, Zeits. f. Physik **72**, 528 (1931).
[13] Pose, Zeits. f. Physik **64**, 1 (1930).
[14] Duncanson and Miller, Proc. Roy. Soc. **A146**, 396 (1934).

proaching α-particles and a neutron we see that the neutron plays a similar role as the binding electron in the case of a positive hydrogen molecule ion (H_2^+). Making use of the results of the theory of the two-center problem and remembering that the lowest neutron level in the field of a single α-particle is $1p_n$ (*viz.*, §4, Fig. 5) we realize that the neutron level after the two α-particles have been brought together could hardly be an s_n level, but could become a p_n, d_n, or f_n level. The lowest level is thus probably a p_n level. This leads to the representation shown in Fig. 9. In a similar way nuclei consisting of more than two α-particles could be represented. We notice here however that our picture furnishes several different possibilities for the nuclear spins.

If we proceed to still heavier nuclei our picture leads to the possibility that the relative position of the lowest proton—neutron and α levels may become shifted so that more than three of the lighter particles may remain separated without a tendency to unite in the formation of an α-particle.

No definite conclusions, however, can be obtained in this respect. We should like only to lay emphasis on the fact that the shift of the levels in question can experimentally be followed by a systematical investigation of anomalous scattering processes with protons and neutrons.

No experimental data are known for the anomalous scattering of protons by heavier nuclei. From our picture we could predict that for Li_6 and Li_7 at fairly high energies a $1d_p$ resonance would occur, etc.

No predictions can at present be made for still heavier elements, as we have seen that then our picture becomes incorrect. It would be, however, of great importance to know something in this case concerning the position and classification of proton levels from experiments. From the experimental point of view it might be more convenient to obtain the necessary information from the scattering of neutrons. Since the light nuclei seem to be fairly symmetrically built of protons and neutrons, a similar picture as for protons is to be expected to hold for neutrons interacting with light nuclei.

We thus shall expect a $1s_n$ scattering for collisions of neutrons with protons, α $1p_n$ scattering for neutrons and helium nuclei, etc. No sufficiently accurate experiments are available at present for the scattering of neutrons by light nuclei, but we can see that such experiments could furnish an important support for the views expressed here.

§8. Conclusions

We should like to conclude from this investigation that the wave-mechanical treatment of nuclear processes is not restricted to phenomena in which a particle moving outside the nucleus is affected as it was assumed in the early treatments of nuclear collisions. It seems to us that for light nuclei, at least, a fairly consistent picture can be obtained also in the case in which a heavy particle is bound inside a nucleus and that its energy levels can be designated in the well-known manner.

No conclusions, however, can be obtained in this way on the question of whether a treatment of this kind can be complete. A further investigation will have to show whether the picture obtained here will provide us with a sufficient basis to consider the question of nuclear spins. In addition to this it must be regarded as highly questionable whether the phenomena of β-emission will not force us to assume a more adequate general scheme.

The author wishes to express his thanks to Professor F. E. Kester for the opportunity to work in his department and especially to Dr. G. Beck for valuable assistance and many helpful suggestions in the development of this paper.

On the Fermi Theory of β-Radioactivity

E. J. KONOPINSKI AND G. E. UHLENBECK, *Department of Physics, University of Michigan*

(Received May 3, 1935)

A comparison of Fermi's formula for the distribution in energy of the electrons and positrons emitted by radioactive bodies with the observed spectra seems to show that a basic factor in it, the statistical factor, is not asymmetric enough. Since about the same degree of asymmetry is common to the spectra of light and heavy nuclei and of positron and electron emitters, it cannot be ascribed to another factor in the Fermi formula, depending on the nuclear field. A weight factor is introduced to provide the required asymmetry by changing the form of the Fermi interaction energy. It is shown that two almost equivalent points of view can be employed in attacking this problem and that a certain uniqueness in the form of the interaction law can be obtained within the requirements laid down by Fermi. The modified distribution formula, which holds strictly only for light nuclei, is then shown to give a much more satisfactory agreement with the data than the original formula.

§1. INTRODUCTION

FOLLOWING a suggestion by Pauli that the continuous character of the β-disintegration spectra may be due to the emission of a second, unobserved particle together with each electron, Fermi[1] has developed a theory of β-decay, which is in general agreement with the experimental facts. This second particle, the neutrino, makes possible the fulfillment of the conservation laws, and owes its ability to escape detection to its zero charge, and to the smallness of its mass and its magnetic moment.[2]

The mathematical formulation of the Fermi theory is quite analogous to the quantum theory of radiation. Corresponding to the transition of an atom from an excited state to the normal state with emission of a light quantum, there is the transition of a heavy particle in the nucleus from a "neutron state" to a "proton state" with emission of an electron and a neutrino. This can be represented by the reaction:

$$N \rightarrow P + e^- + n. \tag{1}$$

In the case of positron emitters, on the other hand, one has:

$$P \rightarrow N + e^+ + n' \tag{2}$$

representing the transition from the proton state of the heavy particle to the neutron state. Here the second particle should properly be called, according to Fermi's formulation of the theory, an "antineutrino."[3]

One can write the result Fermi obtains for the probability of emission of an electron or positron with an energy (including the rest energy) between W and $W+dW$ and a maximum energy W_0:[4]

$$P(W)dW = G^2 |M|^2 F(Z, W)(W_0 - W)^2 \times (W^2-1)^{1/2} W dW. \tag{3}$$

From this follows the lifetime τ according to:

$$1/\tau = \int_1^{W_0} P(W)dW. \tag{4}$$

In (3), G is a dimensionless constant which measures the strength of the coupling between the heavy particle and the "electron-neutrino field." To explain the slowness of β-decay, Fermi has to assume this constant to be very small, of the order of magnitude 10^{-13}.[5] M is a matrix element (containing the wave functions of the heavy particle), which enters into the theory in the same way that the matrix element of the dipole moment enters radiation theory. Fermi connects the two curves of Sargent's[6] well-known graph relating the lifetime and the maximum energy with "allowed" and "forbidden" transitions, corresponding to different values of $|M|^2$ and in analogy to the dipole and quadripole transitions of radiation theory. $F(Z, W)$ is given by:

$$F(Z, W) = \{4/[\Gamma(3+2\gamma)]^2\}(2p\rho)^{2\gamma} \times e^{\pi\alpha ZW/p} |\Gamma(1+\gamma+i\alpha ZW/p)|^2, \tag{5}$$

[1] E. Fermi, Zeits. f. Physik **88**, 161 (1934).

[2] For attempts to observe the neutrino through its magnetic moment, compare J. Chadwick and D. E. Lea, Proc. Camb. Phil. Soc. **30**, 59 (1934); M. E. Nahmias, Proc. Camb. Phil. Soc. **31**, 99 (1935).

[3] G. C. Wick, Atti Lincei **19**, 319 (1934). See also §3.

[4] Here and in the following are used the rational relativistic units. The unit of energy is mc^2; of time, $mc^3/\hbar$; of length, the Compton wavelength, $\hbar/mc$. Ordinary formulae are put into these units by setting m, $\hbar$ and c equal to unity and e^2 to the fine-structure constant $\alpha = e^2/\hbar c$.

[5] This G is related to the g of Fermi by: $G = gm^2c/(2\pi^2)^{\frac{1}{2}}\hbar^3$.

[6] B. W. Sargent, Proc. Roy. Soc. **A139**, 659 (1933).

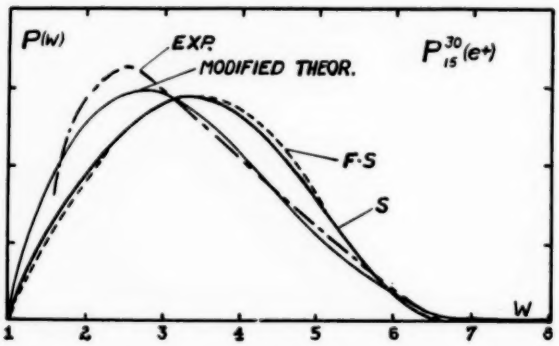

FIG. 1.

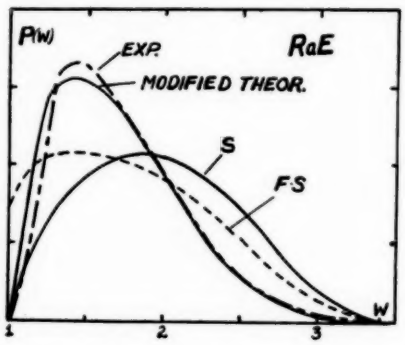

FIG. 2.

FIG. 1. Comparison of the positron distributions given by the statistical factor S, the Fermi formula FS and the modified Fermi formula (see § 4) with the experimental curve of Ellis and Henderson.[19] For S, FS and the experimental curve, $W_0=6.54$. For the modified distribution, $W_0=8$. The areas under the curves are made equal to each other.

FIG. 2. Comparison of the electron distributions given by the statistical factor S, the Fermi formula FS and the modified Fermi formula (see § 4) with the experimental curve for Ra E given in the article of Sargent.[12] For all curves, $W_0=3.4$. The areas under each are made equal.

where ρ is the radius of the nucleus, $p=(W^2-1)^{\frac{1}{2}}$ and $\gamma=(1-\alpha^2Z^2)^{\frac{1}{2}}-1$. This represents the influence of the Coulomb field of the nucleus on the energy distribution; for $Z=0$ it reduces to unity.[7] The remainder of (3) will be referred to as the "statistical factor" and will be symbolized by S.

Such a statistical factor will always occur in the expression for the energy distribution between two particles.[8] It is proportional to the volume in phase space or the number of states into which each particle can go, thus: $S\sim p_e^2p_n^2dp_edp_n$. This is put in terms of energies for the purpose of comparison with observed spectra and is made independent of quantities connected with the unobserved neutrino by taking into account energy conservation.

§2. Comparison with Experiment

Whatever success the Fermi theory may have in explaining the form of the electron and positron spectra is mainly due to the statistical factor. S plotted against W gives a distribution curve having the general shape of the observed distributions (see Figs. 1 and 2). The asymmetry of the curve comes from the difference in the masses of the two emitted particles.[9] The factor $F(Z, W)$ has little effect on the form of the distribution curves for light nuclei (compare S and SF in Fig. 1).[10] For the heavy nuclei, $F(Z, W)$ has quite an appreciable effect (see Fig. 2). Although it shifts the maximum toward lower electron energies as the experimental data require, it brings in the serious difficulty that it predicts too many slow electrons.[11] Because fast electrons are less influenced by the nuclear attraction, these effects of F will be less marked for spectra with higher maximum energy.

The comparison in Figs. 1 and 2 of the theoretical and experimental distributions for typical, noncomplex positron and electron spectra[12] seems to indicate that the basic

[7] Z must be taken positive for electron emitters and negative for positron emitters. Following Fermi we have taken the mass of the neutrino zero. For a finite mass μ, $F(Z, W, \mu)$ is a more complicated function, which for $Z=0$ reduces to $1+\mu/W(W_0-W+\mu)$.

[8] Compare G. E. Uhlenbeck and S. Goudsmit, Physica, in press.

[9] For a neutrino mass equal to the electron mass the corresponding statistical factor would give a perfectly symmetrical curve. The maximum is shifted toward lower electron energies for smaller neutrino masses. The data, as we shall see, require a strongly asymmetric curve, so that in the present form of the theory, we certainly must take the neutrino mass zero, which Fermi had already done on other grounds.

[10] The theory proposed by Beck and Sitte (Zeits. f. Physik **86**, 105 (1933)) takes as the second particle a positron, which is then again captured by the nucleus. Because now the masses of the two particles between which the energy is divided are *equal*, one must depend entirely on the nuclear field to provide the asymmetry in the distribution. It seems then difficult to account for the similarity of the experimental distributions for heavy and light nuclei and for positron and electron emitters.

[11] G. Beck and K. Sitte, Zeits. f. Physik **89**, 259 (1934); R. L. Dolecek, Phys. Rev. this issue, p. 13. We want to thank Dr. Dolecek for allowing us to see his paper before its publication.

[12] The data for P used here are taken from C. D. Ellis and W. J. Henderson, Proc. Roy. Soc. **A146**, 206 (1934):

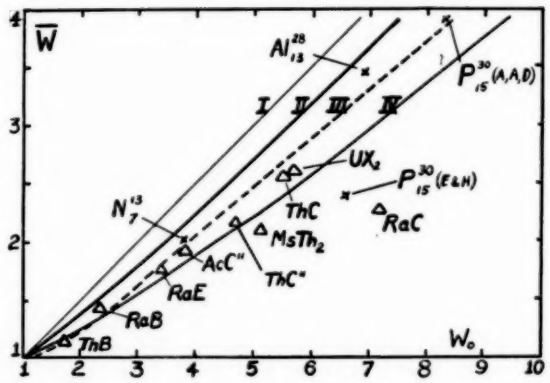

FIG. 3. Comparison of the experimental average energies with theory: I, perfectly symmetrical distribution; II, distribution given by S ($\mu=0$, $Z=0$); III, distribution given by FS with $\mu=0$, $Z=82.2$ (applicable only to the experimental points given by the triangles); IV, distributions given by the modified Fermi theory (see §4) with $\mu=0$, $Z=0$. ${}_{15}P^{30}$ (E & H) is the value taken from Ellis and Henderson's[19] results, and ${}_{15}P^{30}$ (A, A & D) from Alichanian, Alichanow and Dzelepow's data. The experimental values for W_0 are used; if the theoretical end points (see Figs. 5, 6 and 7) were used for ${}_{13}Al^{28}$, ${}_{7}N^{13}$ and ${}_{15}P^{30}$ (A, A & D), these points would lie almost on curve IV

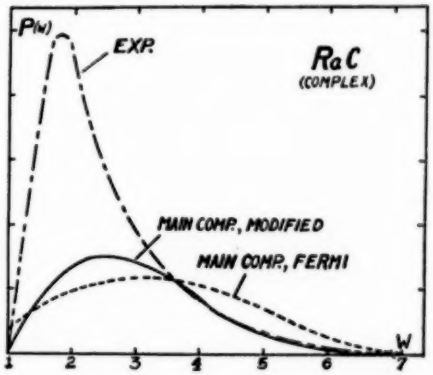

FIG. 4. The main component (weight 0.5) of the complex Ra C spectrum as given by the Fermi and the modified (see §4) theories compared with the observed Ra C spectrum. $W_0=7.16$ for all curves. The area of each component is made equal to one-half the area under the experimental curve.

statistical factor does not give a sufficiently asymmetrical distribution. This is further confirmed when one considers the average energies defined by:

$$\bar{W}=\tau\int_1^{W_0} WP(W)dW$$

as a function of W_0 (see Fig. 3). The experimental average energies deviate systematically from the theoretical values computed from the purely statistical distributions in a direction corresponding to greater asymmetry (the straight line represents the average energies of perfectly symmetrical distributions). Taking $F(Z, W)$ into account helps the agreement with the average energies of the β-ray spectra of the heavy elements, although the actual form as we have seen is not represented very well. For the positron emitters the slight (in their case) influence of Z tends to make the distributions more symmetric instead of less as required. It is true that perhaps many of the experimental points are not directly comparable with the theory because of the complex nature of the corresponding spectra. The spectrum of Ra C, for instance, is quite surely the result of a superposition of several spectra having various upper limits. An attempt was made, following Ellis and Mott,[13] to construct the Ra C curve out of properly weighed components computed from the theory. The result depends very much on what one takes for the populations, which are quite uncertain. One is only sure that the component with the greatest upper limit has at least a population 0.5. We have therefore drawn in Fig. 4 only this main component of the theoretical curve, giving it one-half the area of the experimental curve. Because of the lack of asymmetry of the theoretical curve it is clear that no agreement can be obtained.

compare with this Fig. 5, §4. The Ra E curve was obtained from B. W. Sargent, Proc. Camb. Phil. Soc. **24**, 538 (1932).

§3. THE FERMI INTERACTION "ANSATZ"

To see how the Fermi theory can be modified so as to agree better with experiment it is necessary to examine more closely the fundamental "Ansatz" made for the interaction of the heavy particle with the electron-neutrino field. In analogy to radiation theory the interaction term of the total Hamiltonian is made up of the scalar product of two polar four-vectors, and is written:

[13] C. D. Ellis and N. F. Mott, Proc. Roy. Soc. **A141**, 502 (1933), composed the Ra C spectrum of curves made geometrically similar to the Ra E distribution curve. The upper limit and the weight of each component were calculated from the known energy levels of the product nucleus (Ra C') and their populations as obtained from γ-ray data. These populations must be revised according to the later experimental results of Rutherford, Lewis and Bowden, Proc. Roy. Soc. **A142**, 347 (1933).

$$H=Q[A_0+(\vec{\alpha}_{\text{heavy}}\cdot\vec{A})]+Q^*[A_0^* +(\vec{\alpha}_{\text{heavy}}\cdot\vec{A})^*]. \quad (6)$$

Here Q and Q^* are the Heisenberg matrices:

$$Q=\begin{pmatrix}0 & 1\\ 0 & 0\end{pmatrix}, \quad Q^*=\begin{pmatrix}0 & 0\\ 1 & 0\end{pmatrix},$$

which operate on the inner coordinate ρ of the heavy particle, which in turn determines whether the particle is a neutron ($\rho=+1$) or a proton ($\rho=-1$). Q corresponds to the proton to neutron transition and Q^* to the reverse. The components of $\vec{\alpha}_{\text{heavy}}$ are the Dirac matrices which operate on the spin coordinate of the heavy particle.[14] The four vector A is built up out of the quantized wave functions ψ and φ of the electron and neutrino according to:

$$A_0=\psi\delta\varphi, \quad \vec{A}=\psi\delta\vec{\alpha}\varphi, \quad (7)$$

where $$\delta=\begin{pmatrix}0 & -1 & 0 & 0\\ 1 & 0 & 0 & 0\\ 0 & 0 & 0 & 1\\ 0 & 0 & -1 & 0\end{pmatrix}.$$

The above choice of A is made to insure that a neutron to proton transition is accompanied by the creation of an electron and a neutrino. This becomes clear when ψ and φ are developed as follows:

$$\psi=\sum_s a_s\psi_s, \qquad \varphi=\sum_\sigma b_\sigma\varphi_\sigma,$$
$$\psi_s^*=\sum_s a_s^*\psi_s^*, \quad \varphi^*=\sum_\sigma b_\sigma^*\varphi_\sigma^*. \quad (8)$$

According to the method of second quantization,[15] a_s^* and b_σ^* are operators indicating the creation of an electron in state s and a neutrino in state σ; a_s and b_σ are correspondingly the destruction operators. Introducing (8) into (7), one sees that H will now contain the combinations $Q^*a_s^*b_\sigma^*$ and Qa_sb_σ. The first combination is responsible for the electron emission and the second for the positron emission. To see this one must remember that in order to obtain a definite upper limit of the spectrum, Fermi must assume that the negative energy states of *both* the electron and the neutrino are filled in the Dirac fashion. In the electron emission term, $Q^*a_s^*b_\sigma^*$, s and σ refer to the positive states of the light particles. In the positron emission term, the s and σ must be negative states because the destruction of an electron and a neutrino in negative states is equivalent to the creation of a positron and an antineutrino.

Of course it is arbitrary to connect the neutrino with the emission of an electron and the antineutrino with the positron emission. Physically one could just as well interchange the roles of the neutrino and antineutrino. Formally this can be done by constructing a four vector A' in which the wave function of one particle is coupled with the complex conjugate of the other wave function; this will produce in the Hamiltonian combinations $Q^*a_s^*b_\sigma$ and $Qa_sb_\sigma^*$. The only possibility for such a four vector is:

$$A_0'=\psi\varphi^*, \quad \vec{A}'=\psi\vec{\alpha}^*\varphi^*, \quad (9)$$

which is analogous to the familiar current four vector. The choices (7) and (9) are the only two possible polar four-vectors involving products of wave functions only. This can perhaps most easily be seen with the spinor notation.[16] The ψ becomes then the pair of spinors $\psi_{\dot{m}}$, χ_l and φ correspondingly $\Psi_{\dot{m}}$, X_l. Combining these into four vectors one finds immediately that there are essentially only four possible, of which two are polar and two axial. The two polar ones are:

$$a_{\dot{m}l}=\psi_{\dot{m}}\mathrm{X}_l-\Psi_{\dot{m}}\chi_l, \quad a_{\dot{m}l}'=\psi_{\dot{m}}\Psi_l+\mathrm{X}_{\dot{m}}\chi_l$$

which correspond to A and A', respectively.

One can easily verify that the use of (9) instead of (7) in the Fermi theory gives *exactly* the same results if the neutrino mass μ is zero, as should also be expected from the physical standpoint. If μ is not zero the statistical factor in the distribution formula is the same whether A or A' is used. In the factor $F(Z, W, \mu)$ there are some sign changes so that for $Z=0$ the factor referred to in footnote 7 becomes $1-\mu/W(W_0-W+\mu)$. The influence of this factor is very

[14] Fermi neglects the terms involving $\vec{\alpha}_{\text{heavy}}$ because they are roughly of the order v/c times the magnitude of the first term. Here v is the velocity of the *heavy* particle in the nucleus, so that v/c is about 0·1. One uses here the Dirac equation for the heavy particle only formally to show the analogy with radiation theory. See also Dolecek, reference 11.

[15] See Pauli, *Handbuch der Physik*, Vol. 24, No. 1, p. 199. In Fermi's paper the formulae defining a_s and a_s^* have to be interchanged.

[16] See, e.g., Laporte and Uhlenbeck, Phys. Rev. **37**, 1380 (1931).

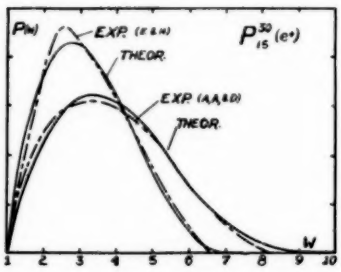

FIG. 5.

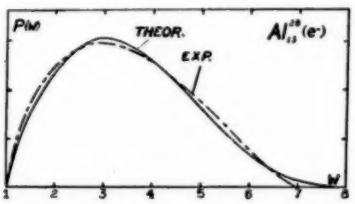

Fig. 6.

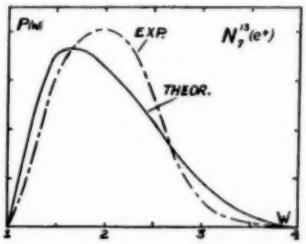

FIG. 7.

FIG. 5. The experimental distributions for the positrons from $_{15}P^{30}$ as given by Ellis and Henderson[19] with $W_0=6.54$ and by Alichanian, Alichanow and Dzelepow[19] with $W_0=8.34$. According to the modified Fermi theory, $W_0=8$ and 10.6.

FIG. 6. Comparison of the distributions of the electrons from radio-aluminum as given by the experiments of Alichanian, Alichanow and Dzelepow[19] and by the modified theory. Experimental $W_0=6.97$. Theoretical $W_0=8.8$.

FIG. 7. Distributions of positrons from radio-nitrogen as given by the experiments of Alichanian, Alichanow and Dzelepow[19] and by the modified theory. Experimental $W_0=3.84$, theoretical $W_0=4.4$.

small and does *not* improve the agreement with experiment. Hereafter we will always take $\mu=0$.

§4. A Modification of the Interaction Ansatz

As we saw in §2, the experimental data both for light and heavy nuclei, whether they are electron or positron emitters, seem to give the impression that the basic distribution is more asymmetrical than the one provided by the statistical factor S. If we may believe this, one must require even for $Z=0$ in addition to the always present statistical factor a weight factor which gives preference to low electron energies or high neutrino energies. This requirement could be fulfilled in a simple, empirical way by multiplying (3) by a power of the neutrino energy W_0-W. In terms of the formalism of the Fermi theory, this is accomplished by introducing derivatives of the neutrino wave functions into the Ansatz for the interaction energy.

We will show that one can construct essentially only one polar four vector involving the wave functions of the electron and the derivatives of the neutrino wave functions. To do this, we shall employ the second point of view, mentioned in §3 in which the emission of an antineutrino is connected with the electron emission. Using the γ_i matrices and the notation of Pauli,[17] we can form only the following three polar four vectors:

$$B_i=\psi\dagger\partial\varphi/\partial x_i,$$
$$C_i=\psi\dagger M_{ia}\partial\varphi/\partial x_a, \quad M_{ij}=\gamma_i\gamma_j\delta_{ij}, \qquad (10)$$
$$D_i=\psi\dagger\gamma_i(\gamma_a\partial\varphi/\partial x_a).$$

Remembering that the wave equation of the neutrino, with $\mu=0$, is: $\gamma_a\partial\varphi/\partial x_a=0$, one sees that D_i is identically zero. Furthermore, the first component of C_i, for example, is:

$$\psi\dagger\gamma_1\left(\gamma_2\frac{\partial\varphi}{\partial x_2}+\gamma_3\frac{\partial\varphi}{\partial x_3}+\gamma_4\frac{\partial\varphi}{\partial x_4}\right)$$
$$=\psi\dagger\gamma_1\left(-\gamma_1\frac{\partial\varphi}{\partial x_1}\right)=-\psi\dagger\frac{\partial\varphi}{\partial x_1},$$

so that $C_i=-B_i$. The only vector which remains, B_i, can be written with the Dirac matrices, leaving off a factor i:

$$B_0=\psi^*\beta\partial\varphi/\partial t, \quad \vec{B}=\psi^*\beta\,\text{grad}\,\varphi. \qquad (11)$$

Besides the vectors (10), there are, of course, possible three more if we adopt the original viewpoint of Fermi, connecting the electron with the neutrino emission, which again reduce to one when the neutrino wave equation is applied. Since, for $\mu=0$, the two points of view always give the same result there remains really only the vector B_i.[18]

Substituting the vector B_i for A_i in the derivation of the Eq. (3) for the distribution, following Fermi's calculations closely and making

[17] Pauli, *Handbuch der Physik*, Volume 24, No. 1, p. 220.

[18] With the spinor notation both sets of vectors are obtained at the same time just as a^*_{nl} and $a^*_{nl'}$ in §3. One can then make the analogous reduction to one vector and in this way the proof of the uniqueness of B_i is perhaps made more convincing.

the same approximations, one obtains with $Z=0$:

$$P(W)dW = G^2|M|^2(W_0-W)^4(W^2-1)^{\frac{1}{2}}WdW. \quad (12)$$

If Z were not put equal to zero one has again to multiply (12) with the factor $F(Z, W)$ given by (5).

In Figs. 1, 5, 6 and 7 the distribution given by (12) is compared with the experimental data[19] for $_{15}P^{30}$, $_{7}N^{13}$ (positron emitters) and $_{13}Al^{28}$ (electron emitter). In these cases the factor F is negligible, and it seems that (12) gives the required asymmetry. Because it appears that the experimental values for the upper limits are not very certain, and because the curve (12) tails off very slowly to zero near W_0, so that the end would be hardly observable, we have adjusted the upper limits somewhat.[20] In Fig. 3 this would shift the points for P and Al to the right and bring them nearly on the theoretical curve IV. For Ra E (12) also represents the observed distribution rather well as is seen in Fig. 2. However, in this case F is *not* negligible and should be included. As in the Fermi theory the theoretical distribution will then *not* go to zero for $W=1$, so that the change in the interaction energy does *not* remove this difficulty.

§5. Concluding Remarks

1. The choice of B in the interaction energy fulfills just as A all the *a priori* requirements which Fermi set down at the beginning of his paper. Besides the fact that B seems to give better agreement with the data, it may have significance that in B enter the energy and impulse operators of the neutrino. The neutrino has been introduced to fulfill the conservation laws, so that we may perhaps say that the energy and the impulse of the neutrino are its only observable properties.

2. We have also considered other forms of the interaction energy involving derivatives both of the electron and the neutrino wave functions, with the hope of diminishing the influence of $F(Z, W)$ for the heavy elements near $W=1$. By using the neutrino wave equation the number of independent polar four vectors containing the derivatives of both wave functions narrows down to two:

$$K_i=\frac{\partial\psi\dagger}{\partial x_\alpha}\gamma_i\frac{\partial\varphi}{\partial x_\alpha}, \quad L_i=\frac{\partial\psi\dagger}{\partial x_\alpha}\gamma_\alpha\frac{\partial\varphi}{\partial x_i}.$$

For $Z=0$ L_i reduces to B_i. We did not succeed however, either with these vectors or with a linear combination of them, in bringing down the distribution curve near $W=1$ and keeping the required asymmetry at the same time.

3. Our modification of the form of the interaction energy does not of course affect Fermi's explanation of Sargent's law, nor does it change the order of magnitude of G. The essential difficulty of the Fermi theory as pointed out by Nordsieck and Tamm[21] therefore remains. Because of the smallness of G the interaction between the neutron and the proton through the electron-neutrino field is much too weak to account for the experimental results on neutron-proton scattering. Nordsieck computes the cross section for inelastic scattering (the colliding neutron is transformed into a proton, emitting an electron and a neutrino) and finds a convergent result of the order G^2d^2 where $d=e^2/mc^2$. The elastic collision cross section comes out even smaller ($\sim G^4d^2(M/m)^2\alpha^{-2}$) if the integral occurring in it, which diverges as $\int^\infty dp/p$, may be cut off at $p\sim 1/\alpha$ and considered of the order of magnitude unity. With the modified interaction these calculations are changed essentially only in the fact that the integral in the elastic cross section diverges as $\int^\infty pdp$. If we may again take the upper limit as $1/\alpha$ this would make the elastic cross section at least $(137)^4$ times as large as Nordsieck's value. This is, however, by far not enough to remove the discrepancy.

[19] Ellis and Henderson, Proc. Roy. Soc. **A146**, 206 (1934); Alichanow, Alichanian and Dzelepow, Zeits. f. Physik **93**, 350 (1935). The experimental curves for P disagree with each other. We have shown them both in Figs. 1 and 5. The fact that each can be fitted by a theoretical curve indicates that they have the same kind of asymmetry.

[20] Increasing the upper limits will also tend to remove the discrepancy between Chadwick's value for the mass of the neutron and the value given by Curie and Joliot (Nature **133**, 721 (1934)). Raising the upper limit and the kinetic energy of the neutron together by about 1.5 MEV would bring down the Curie-Joliot mass to the Chadwick value. If (12) really represents the form of the β-ray spectrum, an error of this order of magnitude can easily be understood, especially for the spectra with high upper limits.

[21] A. Nordsieck, Phys. Rev. **46**, 234 (1934); Ig. Tamm, Nature **133**, 981 (1934).

Discussion of the β-Decay Theory

R. L. DOLECEK, *Department of Physics, University of Kansas*

(Received May 3, 1935)

A method is developed which allows one to calculate, according to the Fermi treatment, the energy distribution of the β-electrons for any assumptions on the angular momentum balance. The evaluation of the distribution functions show disagreement with the experimental data for heavy radioactive nuclei. The distribution curves support the criticism of the Fermi treatment given by Beck and Sitte.

§1. INTRODUCTION

EARLY investigations of the radioactive β-decay phenomena lead to difficulties in the theoretical treatment of the β-emission. These difficulties are principally based on the fact that if we confine our attention to the observable radiations emitted from radioactive sources, there is no conservation of mechanical integrals of motion.[1]

It has been common in all attempts made until now, to account for the experimental evidence by treating the β-decay, at least formally, as a double process in which beside the emitted β-electron a second particle occurs in the equations. Beck and Sitte[2] have tried to connect the β-emission with the well-established phenomenon of the electron pair production according to the Dirac theory of the electron. Following this hypothesis they have been led to assume that one of the two particles is subsequently to be treated as captured by the nucleus without conservation of mechanical integrals. Their analysis of the empirical data leads to the important result that another assumption, in addition to the introduction of the second particle is required. The purpose of this assumption is to exclude the emission of slow electrons as particles of lowest angular momentum.

A somewhat similar formalism has been proposed by Fermi.[3] Fermi assumes the second particle to be a neutrino which has the spin momentum $h/4\pi$, zero charge and Fermi statistics. An additional assumption required by the Fermi theory is that the mass of the neutrino be zero. Beck and Sitte[4] immediately criticized Fermi's treatment because of the lack of an assumption similar to that they had found indispensable for accounting for the experimental data. Fermi stated[5] however, that while experimental results might be questionable for low emission energies, the neutrino hypothesis would fit the experimental curves upon the inclusion of higher values of angular momentum transfer.

It is the purpose of this paper to present a convenient way of calculating Fermi's integrals. This treatment yields the immediate calculation of the emission curves for any assumption on the angular momentum balance. The results confirm the cited criticism[4] of Fermi's paper, and lead to even a more distinct disagreement with experimental evidence than was previously estimated.

§2. THE PRINCIPAL ASSUMPTIONS OF THE FERMI THEORY

In the following treatment of Fermi's theory we will make these assumptions:—

(1) The laws of conservation of mechanical quantities hold.
(2) The emission probability of electrons and neutrinos is proportional to the respective density functions.
(3) Processes involved in the β-decay take place entirely within nuclear dimensions.

Assumptions 1 and 2 are also characteristic, at least formally, of the treatment by Beck and Sitte. Assumption 3, however, is not included in their treatment. Assumption 1, which implies at least the formal use of the conservation laws, can hardly be dispensed with. The abandonment of

[1] N. Bohr, J. Chem. Soc., Faraday Lectures, 349 (1932).
[2] Beck and Sitte, Zeits. f. Physik **86**, 105 (1933).
[3] Fermi, Zeits. f. Physik **88**, 161 (1934).
[4] G. Beck and K. Sitte, Zeits. f. Physik **89**, 259 (1934); K. Sitte, Report of the International Conference on Physics, London, 1934.
[5] Fermi, Zeits. f. Physik **89**, 522 (1934).

assumption 3 would lead immediately to the production of a pair of differently charged particles in order to account for a differential conservation of charge. It is seen therefore that the abandonment of assumption 3 leads to the theory of Beck and Sitte.

Thus the only possible generalization in agreement with the Fermi-Heisenberg point of view would concern assumption 2. We shall see in the following discussion that the consequences of these three assumptions are not in agreement with experimental evidence. Therefore, from the point of view of Fermi and Heisenberg, assumption 2 will have to be abandoned. It would be well to recall here that this assumption is valid for all wave emission processes known to date.[6]

Denying assumption 2, which denial certainly should be considered allowable,[7] leads us to say that the β-decay is a process different from all known wave emissions and therefore must be described by some unknown type of interaction function. Such a function, however, would have to be founded on definite physical arguments which can hardly be formulated at the present.

In order to examine the Fermi theory we will consider the consequences of assumptions 1 to 3. We have, then, for the probability of β-emission an absolute square of an invariant expression which can be written,

$$\text{Const.}\,|\int\{UA^0V^*+\Sigma U\alpha_iA^iV^*\}d\tau|^2, \quad (1)$$

where U is the eigenfunction of the neutron in the initial nucleus, V the eigenfunction of the proton in the final nucleus and α_i Dirac matrices. In Eq. (1) the Dirac theory is assumed for both particles which certainly is incompatible with the experimental evidence of Stern and Rabi. It will be shown however, (§3) that the discussion is valid for any relativistic expression of a type (1). A^0, A^1, A^2, A^3 are the components of a four vector which depends upon the eigenfunctions of the emitted electrons (ψ) and the eigenfunctions of the emitted neutrino (ψ'). Two assumptions for a four vector are possible

$$A^0=\psi^*\psi', \quad A^i=\psi^*\alpha_i\psi', \quad i=1,2,3, \quad (2)$$

corresponding to the emission of an electron and an anti-neutrino and therefore similar to the treatment by Beck and Sitte, or

$$A^0=\psi\delta\psi', \quad A^i=\psi\delta\alpha_i\psi', \quad \delta=\begin{pmatrix}0 & -1 & 0 & 0\\ 1 & 0 & 0 & 0\\ 0 & 0 & 0 & 1\\ 0 & 0 & -1 & 0\end{pmatrix} \quad (3)$$

corresponding to the emission of an electron and a neutrino in the positive part of its energy spectrum. In the event $m'=0$ (neutrino of zero mass) both cases are mathematically equivalent.[8]

ψ here is understood to refer to an electron emitted with the energy W (including the rest energy). ψ' represents a neutrino of energy W' where evidently

$$W+W'=\Delta E \quad (4)$$

if ΔE is the energy liberated by the transformed nucleus.

Regarding the nucleus as a spherical system, all of the involved eigenfunctions may be expressed in terms of radial functions and spherical harmonics familiar from the Dirac theory of the electron. U and V are assumed to be given. U refers, in particular, to a special angular momentum of the initial nuclear state (neutron) and V to the angular momentum of the final state (proton). Thus the angular dependence of U and V have to be regarded as given spherical harmonics. Their radial dependence is not known in detail but we may represent them by Bessel functions extended over a region of nuclear dimensions R.

In the same way ψ and ψ' (in polar coordinates) will refer to well-defined angular momenta of the emitted electron and neutrino. As we are only interested in the total number of emitted particles, without regard to their angular momenta, (1) has to be worked out for every possible pair of solutions ψ and ψ'. The sum over all of these possible transitions is then to be taken.[9]

---

[6] *Viz.*, e.g., G. Beck, Reports of the International Conference of Physics, London 1934.

[7] E. J. Konopinski and G. E. Uhlenbeck, Phys. Rev., this issue, p. 7. I wish to thank Professor Uhlenbeck and Mr. Konopinski for allowing me to see their paper before its publication.

[8] See reference 7. This point has been clarified in discussions with Professor Uhlenbeck. I wish to express my thanks to Professor Uhlenbeck for these discussions.

[9] This implies that emission possibilities in which different angular momenta are involved may be regarded as independent processes.

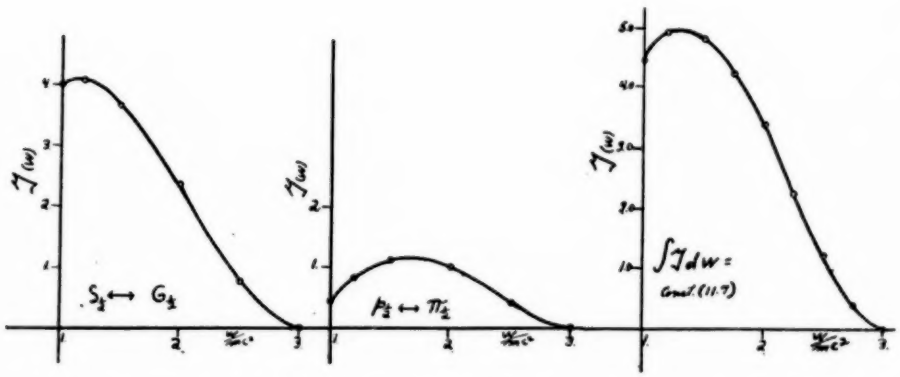

FIG. 1. Shape of the probability curve for zero transfer of angular momentum by the nucleus.

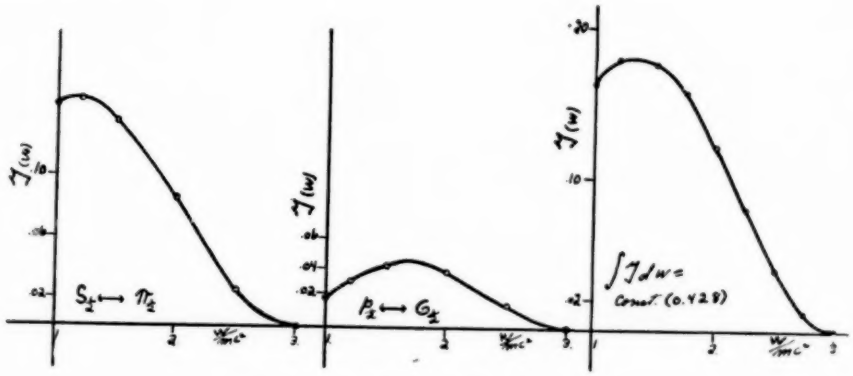

FIG. 2. Transfer of $h/2\pi$ by the nucleus.

Eq. (1) thus becomes an infinite series which, however, can be simplified. First we note that the integration of the angular functions immediately eliminates all terms in which the sum of the angular momenta of the produced pair of particles does not equal the angular momentum transferred by the nucleus; (conservation of angular momentum). Furthermore only those transitions which belong to small values of angular momentum for the particles need be taken into account. This is due to the fact that the probabilities for the emission of particles which have angular momenta differing by one unit are in the proportion $(R/\lambda)^2$; where R again is the nuclear radius, λ the wavelength of the emitted particle.

It will be shown in (§3) that only the following transitions need be taken into consideration:

(1) No angular momentum transferred from the nucleus,

$$S_{1/2}\longleftrightarrow\sigma_{1/2}, \quad P_{1/2}\longleftrightarrow\pi_{1/2}. \tag{5a}$$

(2) Transfer of angular momentum $h/2\pi$ by the nucleus,

$$S_{1/2}\longleftrightarrow\pi_{1/2}, \quad P_{1/2}\longleftrightarrow\sigma_{1/2} \tag{5b}$$

(3) Transfer of angular momentum $2h/2\pi$ by the nucleus,

$$\begin{aligned} &S_{1/2}\longleftrightarrow\delta_{3/2}, \quad P_{3/2}\longleftrightarrow\pi_{1/2}, \\ &P_{1/2}\longleftrightarrow\pi_{3/2}, \quad D_{3/2}\longleftrightarrow\sigma_{1/2}, \end{aligned} \tag{5c}$$

where I have used the well known notations $S_{\frac{1}{2}}$, $P_{\frac{1}{2}}$, $P_{\frac{3}{2}}\cdots$ for the electronic states and similarly $\sigma_{\frac{1}{2}}$, $\pi_{\frac{1}{2}}$, $\pi_{\frac{3}{2}}$ for the corresponding states of the neutrino.

§3. Influence of the Relativistic Terms

We shall now investigate the dependence of (1) on the relativistic interaction terms A^1, A^2, A^3. Taking (1) for any single transition we can first integrate over the angular variables and—neglecting higher powers of (R/λ)—we obtain

expressions of the following type:

$$J(W)=\text{Const.}\,|\int\Xi(r)\{a\cdot\chi(r)+b\cdot\varphi(r)\}r^2dr|^2 \quad (6)$$

for transitions involving $\sigma_{\frac{1}{2}}$, $\pi_{\frac{1}{2}}$, $\cdots$ states, or

$$J(W)=\text{Const.}\,|\int\Phi(r)\{a'\varphi(r)+b'\chi(r)\}r^2dr|^2 \quad (7)$$

for transitions involving $\pi_{\frac{1}{2}}$, $\delta_{\frac{1}{2}}$, $\cdots$ states.

$\Xi(r)$ and $\Phi(r)$ are Bessel functions referring to the neutrino. $\chi(r)$ and $\varphi(r)$ are the radial eigenfunctions for the electron. The ratio of b/a and b'/a' is of the order v/c or v'/c; v' and v being the velocities of the neutron and the proton in the nucleus. These ratios are about 1/10.

We note that in our approximation $\varphi(r)$ and $\chi(r)$ have the form,

$$\varphi\sim(\gamma+\kappa)\cdot(W-1)^{\frac{1}{2}}-i\cdot\alpha\cdot(W+1)^{\frac{1}{2}},$$
$$\chi\sim(\gamma-\kappa)\cdot(W+1)^{\frac{1}{2}}-i\cdot\alpha\cdot(W-1)^{\frac{1}{2}},$$

where W is measured in units mc^2, $\gamma=\{\kappa^2-\alpha^2\}^{\frac{1}{2}}$. κ represents the angular momentum quantum number which takes the values ±1, ±2, ±3, $\cdots$ and α the fine structure constant times the atomic number Z.

By using these expressions it can be shown that

$$\chi=\{i\alpha/(\kappa-\gamma)\}\varphi. \quad (8)$$

(8) permits one to reduce (6) and (7) to the first-nonrelativistic-terms only. The relativistic terms, however, though they do not change the shape of $J(W)$ may affect this quantity by a constant factor of the order one for heavy elements ($\alpha\sim1$).

§4. The Decay Formulae

The decay formulae (6) and (7) thus become reduced to the form:

$$J(W)=\text{Const}\cdot D\cdot(W')^{2\mu}\cdot(W^2-1)^{(\gamma-\frac{1}{2})}\,|\,(\gamma-\kappa)\cdot(W+1)^{\frac{1}{2}}-i\alpha(W-1)^{\frac{1}{2}}\,|^2, \quad (6')$$

$$J(W)=\text{Const}\cdot D\cdot(W')^{2\mu}\cdot(W^2-1)^{(\gamma-\frac{1}{2})}\,|\,(\gamma+\kappa)\cdot(W-1)^{\frac{1}{2}}-i\alpha(W+1)^{\frac{1}{2}}\,|^2 \quad (7')$$

with the abbreviations

$$D=B^2\frac{2^{2\gamma}R^2(R/\Lambda)^{2(\gamma+\mu)}\,|\,\Gamma(\gamma+i\alpha W)/(W^2-1)^{\frac{1}{2}}\,|^2}{|\,\Gamma(2\gamma+1)\,|^2\{1\cdot3\cdot5\cdots(2\mu-1)\}^2(\gamma+\mu+1)^2},$$

$$B=\int f(\theta,\varphi)(w^\alpha w'^\beta-w^\beta w'^\alpha)\sin\theta d\theta d\varphi,$$

$f(\theta,\varphi)$ determines the angular momentum transfer of the nucleus, it is a constant for the transfer zero and a spherical harmonic for higher transitions. w and w' are the spherical harmonics familiar from Dirac's theory of the electron. $\mu=|\kappa'|$ represents the angular momentum quantum number of the neutrino. $\Lambda=h/2\pi mc$.

The evaluation of (6′) and (7′) yield the following curves which are to be compared with experimental curves and data.

§5. Discussion of the Theoretical Curves

In comparing the emission curves with experimental data the discrepancy at low emission energies is evident. Experimentally few emitted particles are detectable at low emission energies;[10] one recognizes in the curves the plausibility of the additional assumption stated by Beck and Sitte. It is also to be noticed that the higher order transitions do not improve the agreement with experimental curves by having their maxima shifted to higher emission energies.[11]

The calculations for transfer of $(h/2\pi)$ yield a total probability which is of the order 1/30 of that for the case of zero transfer. It does not depend on the ratio of $(R/\lambda)^2$ as Fermi thought. Remembering that $1/\tau=\int J(W)dw$ we cannot of course reconcile this with the Sargent curves in which the factor is about 1/1000 for $\Delta E=3\,mc^2$. The corrections could hardly account for the discrepancy by saying that the first Sargent curve represents the sum of these two which we have not been able, experimentally, to differentiate between. Let us consider this possibility, however, and determine whether the transfer of

[10] Especially in experiments concerning the case of Ra *E*.

[11] The same difficulty is discussed in the treatment of Konopinski and Uhlenbeck. See this issue, p. 7.

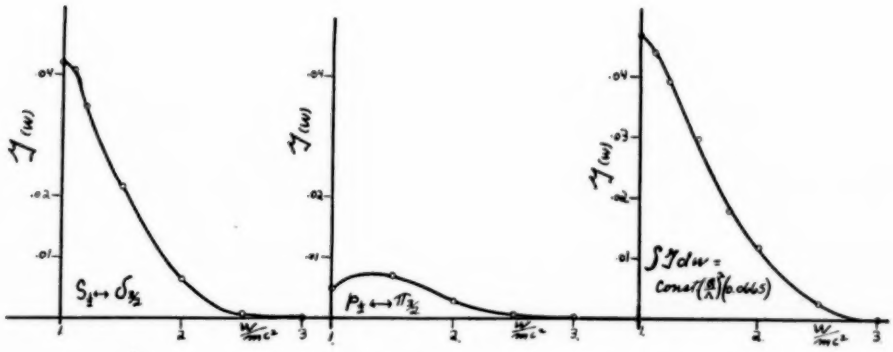

FIG. 3. Transfer of $2h/2\pi$ by the nucleus.

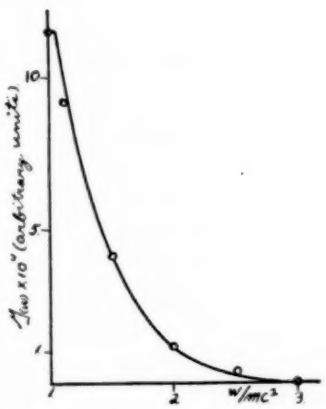

FIG. 4. Transfer of $4h/2\pi$ by the nucleus.

angular momentum $2h/2\pi$ would fit the second curve. We observe that the transitions $P_{\frac{1}{2}} \longleftrightarrow \pi_{\frac{1}{2}}$ and $D_{\frac{1}{2}} \longleftrightarrow \sigma_{\frac{1}{2}}$ give no appreciable contribution and have therefore been omitted from Fig. 3.

The ratio of the total probability for transfer of $2h/2\pi$ to that for zero transfer is less than 1/300,000. The emission characteristics as calculated are hardly reconcilable with experimental data therefore and they do not become better reconciled with the inclusion of higher ordered transitions as it was thought the case might be.

The large ratio in the total emission probability of the transfer $2h/2\pi$ to zero transfer suggests the possibility of explaining the weak radioactivity of potassium and rubidium as being due to a transition of large angular momentum transfer. Calculation of transfer of angular momentum $4h/2\pi$ gives the curve in Fig. 4 for the total probability.

Experimentally, in the case of potassium and rubidium, two well-defined groups are found in the continuous β-spectrum. The theoretical emission curve as calculated does not indicate the presence of the two groups of this type.

The foregoing discussion of the Fermi theory based upon the simplified method developed for the evaluation of the probability integrals has shown disagreement with experimental evidence. The calculations have given curves similar to those obtained by Fermi. These curves, however, do not become better upon the inclusion of higher ordered transitions nor do they agree with experimental evidence when applied to the radioactivity of potassium and rubidium. The discussion supports the criticism by Beck and Sitte which cites the indispensability of an additional assumption necessary to prevent the emission of slow electrons.

The author wishes to express his indebtedness to Dr. Beck under whose direction this work was done.

Shapes and Wavelengths of *K* Series Lines of Elements Ti 22 to Ge 32

J. A. BEARDEN AND C. H. SHAW,* *Rowland Physical Laboratory, Johns Hopkins University*

(Received March 13, 1935)

A double crystal spectrometer was used to measure the widths at half-maximum and the indices of asymmetry of the principle *K* series lines of the elements Ti 22 to Ge 32. When sufficient intensity was available, measurements were made in three orders of diffraction, namely, in the (1−2), (1+1) and (1+2) positions. Curves of width *vs.* atomic number and degree of asymmetry *vs.* atomic number are different in the various orders. These differences are discussed. Measurements were also made of the widths of certain satellites and of their intensities and displacements relative to an adjacent line. The diffraction angles of the peaks of the lines were determined with precision in two orders and wavelengths calculated. Comparisons are made with single crystal photographic spectrometer work and the higher degree of accuracy obtained in the present work is pointed out.

INTRODUCTION

MEASUREMENTS of the shapes and wavelengths of certain x-ray lines have been made by previous investigators with both single[1] and double[2] crystal spectrometers. In studies on line shapes with either type of instrument the effect of the crystal diffraction patterns must be considered. However, the limitations imposed on the slit system to utilize fully the resolving power of the crystals are more easily realized with the double crystal than with the single crystal instrument. In addition, it has been shown that the double crystal spectrometer is capable of measuring x-ray wavelengths with a precision equal to or greater than that attained with the single crystal system.

The purpose of the present work was first, to determine accurately the shape and thus the asymmetry of the lines of the *K* series of the elements from Ti 22 to Ge 32, and to study the correlation between the asymmetry of the lines and atomic number; secondly, to measure with high precision the diffraction angles from a calcite crystal in the first and second orders. The wavelengths of these lines have been calculated using the usual assumed grating constant of calcite ($d_\infty = 3.02945$A) in order that the results could be directly compared with previous measurements by other methods.

APPARATUS

The double crystal spectrometer was made by the Societé Genevoise. The first crystal was mounted on a slide midway between the target and the second crystal and perpendicular to a line joining them,[3] providing a rapid and simple means of changing the wavelength setting. The second crystal table was mounted on the precision circle spindle in such a way that it could be rotated relative to the circle in order that any given angle could be measured on different parts of the divided circle. Four carefully calibrated microscopes read the precision circle. Since two lines ten minutes apart were read in each microscope, eight angular readings were obtained for each individual setting of the circle. This arrangement considerably reduced the error due to random variations in the rulings. The circle was calibrated every five degrees to 0.2 second of arc by the four-microscope method. The appropriate correction as obtained from the calibration curve was applied to the measured angle. The accuracy of the divided circle can be judged from the fact that the largest correction applied to any measured angle was only 0.3 second.

Each crystal holder was constructed so that the crystal was supported at three points on its reflecting surface and held in place by pins and springs on the other side of the crystal and directly opposite the supporting points. This type

* National Research Fellow, Cornell University.

[1] *Shapes:* N. Seljakow, A. Krasnikow and T. Stellezky, Zeits. f. Physik **45**, 548 (1927); A. Larsson, Phil. Mag. **3**, 1136 (1927); J. H. van der Tuuk, Zeits. f. Physik **41**, 326 (1927), (*L* series). *Wavelengths:* Siegbahn, *Spectroscopie der Rontgenstrahlen*, 2nd ed.

[2] *Shapes:* Reference 1, S. K. Allison, Phys. Rev. **44**, 63 (1933); L. G. Parratt, Phys. Rev. **44**, 695 (1933); **45**, 364 (1934); **46**, 749 (1934); F. K. Richtmyer and S. W. Barnes, Rev. Sci. Inst. **5**, 351 (1934); L. G. Parratt, Rev. Sci. Inst. **5**, 395 (1934); J. H. Williams, Phys. Rev. **45**, 71 (1934); Phys. Rev. **37**, 1431 (1931); L. P. Smith, Phys. Rev. **46**, 343 (1934); F. K. Richtmyer and S. W. Barnes, Phys. Rev. **46**, 352 (1934); F. K. Richtmyer, S. W. Barnes and E. Ramberg, Phys. Rev. **46**, 843 (1934). *Wavelengths:* A. H. Compton, Rev. Sci. Inst. **2**, 365 (1931); J. H. Williams, Phys. Rev. **40**, 636 (1932); **40**, 791 (1932); J. A. Bearden, Phys. Rev. **43**, 92 (1933).

[3] P. A. Ross, Phys. Rev. **39**, 550 (1932).

of mounting eliminates the possibility of warping the crystal. That no warp was present was verified by the observation that the (1 − 1) width was independent of the width of the x-ray beam.

The cone bearing on the spindle of the spectrometer which supported the second crystal was adjusted in the following manner. One of the mirrors of a Michelson interferometer was placed in the second crystal holder parallel to, and on, the axis of rotation.[4] If the spindle were loose, the fringes would not return to their original position when the table was pushed backward or forward and released.

Before the Michelson mirror was removed, a telescope with a Gauss eyepiece was placed perpendicular to the spectrometer axis with the aid of the mirror. The calcite crystal was substituted for the interferometer mirror and adjusted parallel to the axis of rotation by means of the telescope. Thus the reflecting surface of the crystal was on the axis of rotation within 0.01 mm and parallel to it within 15 seconds.

The next adjustment was that of setting the first crystal parallel to the second. This was accomplished by placing the crystals in the (1 − 1) position and adjusting until a strong x-ray line was reflected onto a fluorescent screen. If the crystals were not parallel, the line came in from the top or bottom and disappeared at the bottom or top as the second crystal was rotated. The first crystal was tilted until the line came in uniformly from the side. A final adjustment was then made by obtaining the minimum width of the (1 − 1) rocking curve.

Sixty cycle a.c. was supplied by a generator driven by a d.c. motor operated from the campus supply. The speed control described in another paper[5] was used to maintain the primary voltage constant to 0.1 percent. Four oil-immersed kenotrons rectified the high voltage and a 0.5 mfd condenser was used to reduce the voltage ripple. The high voltage was measured by a microammeter in series with a 50 meghom Taylor resistance. The filament of the broad-focus cathode was operated from a transformer.

It is well known that second to variations of supply voltage, the small changes of gas pressure in an x-ray tube are the chief cause of variations of the intensity of the x-rays. Such bursts of gas cause a variation in the flow of thermionic current in the tube. Two methods have been tried in an effort to overcome this difficulty. In the first method the potential drop through a resistance connected in series with the x-ray tube was partially balanced by a battery and the residual voltage applied to the grid of a thyratron tube which paralleled the resistance in the primary of the filament transformer. The intensity could be controlled to one percent when the filament transformer was supplied by 500-cycle current and the 0.5 mfd condenser was employed in the high voltage circuit. The arrangement was not satisfactory when 60-cycle current was used and the condenser was disconnected.

A more convenient and equally effective method is the balanced x-ray filament high voltage circuit. Although this circuit has previously been given in the literature,[6] it has not been widely used and the principle of operation has not been described so far as the authors are aware. Fig. 1 gives the diagram of the circuit.

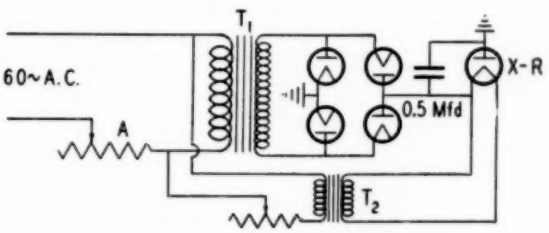

FIG. 1. Balanced x-ray filament-high voltage circuit.

This arrangement is designed to correct for changes of space charge, charges on the walls of the tube and minute changes of gas pressure. If for any of these reasons the current through the x-ray tube increases, the reaction through the high voltage transformer T_1 is such as to increase the current through the primary circuit, thus decreasing the voltage across the filament transformer. The cooling of the filament which results reestablishes the normal current through the x-ray tube. In like manner a decrease of current through the tube produces the reverse reaction. The optimum value of the resistance A depends, of course, upon the reactance of the transformer

[4] J. A. Bearden, Phys. Rev. **37**, 1210 (1931).
[5] J. A. Bearden and C. H. Shaw, Rev. Sci. Inst. **5**, 292 (1934).
[6] J. A. Bearden, Phys. Rev. **29**, 20 (1927).

T_1 and the impedance of the x-ray tube. For most x-ray circuits a resistance of not less than 4 ohms has been found satisfactory.

The copper target of the x-ray tube was mounted rigidly and permanently in a vertical position. The target was cut at an angle of 12 degrees with the horizontal and the focal spot thus acted as the first height limiting slit for the spectrometer. The glass body of the tube could be lowered over the target and the ground joint between tube and target made tight with picein wax. This arrangement made possible the change of targets without disturbing its alignment with the crystals of the spectrometer. Those metals which could be electroplated, namely Cr, Mn, Fe, Co, Ni and Zn were plated onto the target from solutions of chemically pure salts. The Ti, Va and Ge metals were finely divided either by crushing or filing and a small quantity pounded into the copper face of the target. Thermal contact between the powdered metal and the water-cooled copper was sufficient to prevent melting except in a few small regions. About 70 percent of the target was covered by the metal. Two samples each of Ti and Va were used: One Va sample was a 92 percent commercial alloy containing 2 percent Mo, 2 percent Fe and small amounts of other metals, and the other sample of Va was 99.7 percent pure with traces of Fe and Si (0.1 percent each). The first sample of Ti was of unknown purity and the second was exceptionally pure—spectroscopically free of Fe. Since Ga has a melting point of 30°C and a boiling point of 2000°C, it can be used in an x-ray tube even though it is in the liquid state. A small quantity of Ga metal was rubbed onto the copper target, to which it adhered, although there was no evidence of amalgamation.

For all the work with the first crystal in the first order, the first slit (projection of the focal spot) was 1 mm high, the second was 8 mm and they were separated by 53 cm. For the curves taken in the (2+2) order the second slit was reduced to 3 mm. No slits were used to limit the horizontal divergence of the incident beam.

The ionization chamber was constructed of iron,[7] carefully sandpapered inside and filled with argon. Alpha-particles were recorded about five minutes apart on the average. The ionization current was measured by an FP54 pliotron arranged in the circuit described by DuBridge and Brown.[8] A leakage resistance of 10^{11} ohms was used. In measuring the weakest lines (ionization current of 10^{-14} amp.) a voltage sensitivity of 200,000 mm/volt was employed. Such readings were accurate to two percent.

The ionization current circuit was constructed so that either an electrometer or the vacuum tube could be used to measure the ionization current. For the measurement of strong lines the vacuum tube has two main advantages over the electrometer. First, the direct deflection method is more convenient and permits of greater speed in the making of observations, which greatly reduces the errors due to slow shifts in the apparatus. Second, since the sensitivity may be varied easily, a change from the measurement of a weak line to the measurement of a strong line can be accomplished without altering the operating conditions of the x-ray tube.

For weak lines there is still some question as to which method is more precise. In either the electrometer or the vacuum tube method there are two principle limitations on the accuracy of measurement of an ionization current. The first of these is the statistical variation in the number of ionizing particles produced in the chamber by the entering radiation. For ionization currents of 10^{-14} ampere and for a time of observation of one minute the average deviation from the mean is about 0.5 percent. The second limitation is the random emission of alpha-particles from radioactive contamination on the walls of the chamber. If an electrometer is being used to measure the ionization current, the longer range alpha-particles may be detected; however, the average range particles cannot be detected and will therefore contribute an appreciable error to any given reading. Because of its high sensitivity, the vacuum tube possesses the advantage that even short range alpha-particles may be detected and their effect eliminated from the reading. In the case of the vacuum tube, the period of the galvanometer and the electrical time constant of the grid circuit are usually about fifteen seconds. This would increase the average deviation of readings except for the

[7] J. A. Bearden, Rev. Sci. Inst. **4**, 271 (1933).

[8] L. DuBridge and H. Brown, Rev. Sci. Inst. **4**, 532 (1933).

fact that a greater effective time of observation may be obtained by observing the fluctuations of the galvanometer and estimating the average position. This method was found to be satisfactory for times of observation up to two minutes.

In the present experiments it was found that ionization currents of 10^{-14} ampere could be measured about equally well with either the electrometer or the vacuum tube. The convenience of operation of the vacuum tube system, however, made its use preferable for the measurement of both strong and weak lines.

Study of Crystals

Several pairs of calcite crystals were tested before a pair giving the (1−1) width predicted by theory[9] was found. The effect of etching with HCl was also tried and was found to decrease the (1−1) width within about 5 percent of the theoretical value at 1.54A. Table I gives the

Table I. *Effect of treatment on (1−1) width at 1.54A for several different pairs of calcite crystals.*

Origin of crystals	Treatment	Width (1−1) (seconds)
Montana I	ground and polished	38
	Wash HCl	11.1
	Repeat	11.1
Montana II	cleaved	11.5
	Wash HCl	10.4
Spain I	cleaved	10.2
Spain II	cleaved	11.0
Iceland	cleaved	10.4
Argentina	cleaved	9.8

treatment and (1−1) width in seconds for Cu $K\alpha$ radiation (1.54A) for the several pairs of crystals tested.

The Argentina pair of crystals was used in all the subsequent work in the present paper. No change of (1−1) width could be found over a period of a year. A further test of the Argentina crystals was made by observing the (1−1) width as a function of wavelength from 1.1A to 2.5A. Fig. 2 shows the results. The open circles represent the theoretical width of perfect calcite crystals as calculated by Allison and Parratt.[9] It

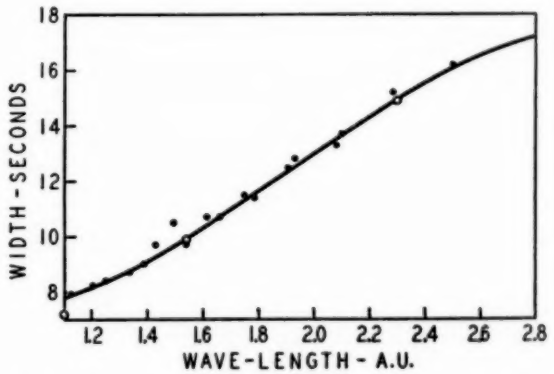

Fig. 2. Rocking curve widths at half-maximum as a function of wavelength for crystals employed in the present work. The open circles are theoretical values.

is apparent that these crystals are as "perfect" as any previously used.

In order to utilize the full resolving power of the crystals, the slits limiting the vertical divergence should be of such heights that the geometrical resolving power is not less than the resolving power of the crystals themselves. The geometrical resolving power for the double crystal spectrometer is given by[10]

$$\lambda/d\lambda = 4/\varphi_m^2, \qquad (1)$$

where φ_m is the maximum vertical divergence in radians from the central ray. In the present apparatus for the $(1\pm n)$ order the geometrical resolving power was 50,000, and was increased to 250,000 in the (2+2) order by narrowing the second vertical slit to 3 mm.

In the $(n+n)$ positions the physical resolving power of the crystals is expressed by[11]

$$\lambda/d\lambda = \lambda D/w, \qquad (2)$$

where D = dispersion and w = full width in radians at half maximum of the rocking curve in the $(n-n)$ position. The full width of the (2−2) curve was measured for Cu $K\alpha$ (1.54A) and Ge $K\alpha$ (1.25A) and found to be 2.4″ and 1.7″, respectively. The physical resolving power in the (1+1) position is 11,000 for Cu $K\alpha$ and 10,000 for Ge $K\alpha$, while in the (2+2) order it is 100,000 in both cases. Thus it is seen that the resolving power in all cases is limited by the diffraction patterns of the crystals.

[9] S. K. Allison, Phys. Rev. **41**, 1 (1932); L. G. Parratt, Phys. Rev. **41**, 561 (1932).

[10] L. G. Parratt, Phys. Rev. **46**, 749 (1934).

[11] S. K. Allison, Phys. Rev. **38**, 203 (1931).

TABLE II. *Widths at half-maximum of K series lines in seconds.*

LINE	ORDER	Ge	Ga	Zn	Cu	Ni	Co	Fe	Mn	Cr	Va	Ti
	1−2	18.3	19.9	22.4	25.3	28.1	37.2	48.7	59.0	61.4	76.0	
	1+1	31.8	33.0	36.9	39.9	43.8	55.5	68.4	76.5	75.5	75.6	80.9
	(1+1)[12]					50.5		73.5	80	80	86	94.5
$K\alpha_1$	(1+1)[13]	30		36	41	45	58	72				
	1+2	43.6	47.0	51.0	56.5	61.5	81.1	104.2	122.8			
	1−3			49.4								
	1+3			79.2								
	2−1				25.7							
	2+1				56.7							
	2+2	55.5			72.5							
	1−2	18.7	19.9	25.3	32.8	36.8	45.3	56.8	65.9	79.0	104.3	
	1+1	33.9	34.6	43.1	51.5	59.0	69.6	80.1	89.8	90.4	99.5	109.7
	(1+1)[12]					64		85	95	103	114	121
$K\alpha_2$	(1+1)[13]	32		41	54	58	67	76				
	1+2	45.4	49.0	60.9	77.9	87.4	105.6	123.9	144.4			
	1−3			58.5								
	1+3			95.5								
	1−2	32.0	34.0	38.0	42.5	46.3	50.0	48.2	53.6	58.0	71.5	
$K\beta_{1,3}$	1+1	57.2	59.3	63.5	72.5	75.7	77.8	73.2	76.5	77.4	87.4	110.2
	1+2	83.6	88.5	94.5	109.6	112.5	113.8	110.3	115.9	119.6		
$K\beta_{2,5}$	1+1	37.0	64.3	91.0	——	99.2	115	119	139.3	135.0	141	

RESULTS

Widths of lines

The widths of the $K\alpha_1(K-L_{III})$, $K\alpha_2(K-L_{II})$ and $K\beta_{1,3}(K-M_{II,III})$ lines were measured in the (1−2), (1+1) and (1+2) positions and in general were found to be slightly different in the various orders. The low intensities of the $K\beta_2(K-N_{II,III})$ and $K\beta_5(K-M_{IV,V})$ lines allowed them to be measured in the (1+1) order only. Four determinations were made of each line width and in general the maximum variation was not greater than one percent. No attempt was made to resolve the $K\alpha$ lines into components because not enough information on their shapes is available to perform the resolution in an analytical manner.

The widths of the K series lines obtained in the present work are shown in Table II together with measurements made by previous investigators.[12, 13] The only previous results for which accuracy was claimed are those by Allison and Parratt. In both cases the α_1 and α_2 lines only were studied in the (1+1) order. Parratt's results are in every case wider than the present measurements. For Ti $K\alpha_1$ his value is about 14 seconds wider than the present width. This point has been rechecked with the two different samples of Ti mentioned before and has also been measured on our apparatus with Parratt's target and in each case the width was 81.0±0.4 seconds. Some of Allison's values are lower than those obtained in the present work, but the differences lie within the estimated experimental errors.

Fig. 3 shows the variations of the line widths in volts with atomic number. It is apparent that in this atomic number region such curves are not simple functions. The various maxima and minima observed seem without doubt to be real.

On referring to Fig. 4 it will be seen why the curves in Fig. 3 for the $\beta_{1,3}$ line rise for higher atomic numbers. The β_1 and β_3 lines are just beginning to show a separation at Ni 28, and at Ge 32 the dual characteristic is quite apparent. For lower atomic numbers the α lines are somewhat wider than the component lines because here the resolution is not complete.

A correction was made for the effect of the $K\beta_{1,3}$ doublet on the shape of the $K\beta_2$ and $K\beta_5$ lines. The intensity curve was carried to several minutes of arc on either side of the weaker line and the base line drawn in. Subtraction of this base line from the observed curve gave the shape of the line. Because this base line cannot be determined very accurately, the estimated error in the width of $K\beta_{2,5}$ is 5 percent. Since the $K\beta_{2,5}$ line for Cu 29 is an unresolved doublet the width is abnormally large, being 125 seconds. So far as these experiments show, the line $K\beta_2$ is entirely absent from Ti 22 to Ni 28, leaving $K\beta_5$ as the strong line in this region. At Cu 29 the doublet structure indicates the appearance of $K\beta_2$, which is as yet relatively weak. At Zn 30 the intensity of the $K\beta_5$ line has decreased markedly and the intensity of the $K\beta_2$ line in-

[12] L. G. Parratt, Phys. Rev. **44**, 695 (1933).
[13] S. K. Allison, Phys. Rev. **44**, 63 (1933).

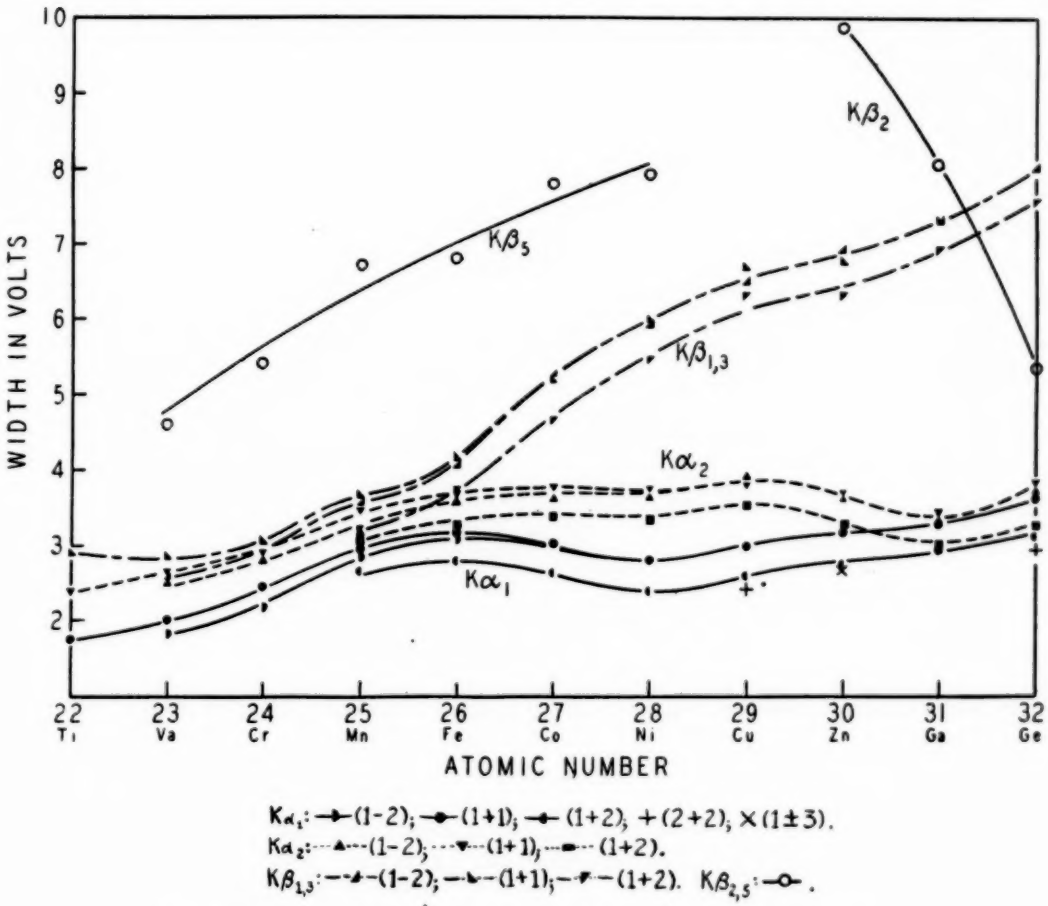

FIG. 3. Widths at half-maximum of lines as a function of atomic number.

creased so that the relative intensities are reversed. Fig. 5 shows these lines for several elements.

It will be observed that for lower atomic numbers the width curve for the $(1-2)$ order lies below that for the $(1+1)$ order, while at higher atomic numbers they coincide. This indicates that the resolving power for lower atomic numbers in the $(1-2)$ order must be greater than that in the $(1+1)$ in spite of the decreased dispersion. The resolving power in the $(1+1)$ and $(1-2)$ for the Cu $K\alpha$ and Ti $K\alpha$ wavelengths may be calculated as follows. Eq. (2) requires the width of the rocking curve in the parallel position. For the calculation of the resolving power in the $(1+1)$ position we use the width in the $(1-1)$ order. In the (1 ± 2) positions, however, the value to use is not obvious, but it lies somewhere between the $(1-1)$ and $(2-2)$ widths. To obtain the width of the single crystal diffraction pattern from the width of the $(n-n)$ curve, it has been assumed that the former is of the Gaussian error shape.[11] On this assumption the width of the single crystal diffraction pattern in the nth order is given by

$$w_a = w_{(n-n)}/\sqrt{2}$$

and the w value (Eq. (2)) in the (1 ± 2) order should be the square root of the sum of the squares of the first and second order single crystal diffraction patterns. For Cu $K\alpha$ radiation this becomes

$$w = [w^2_{(1-1)}/2 + w^2_{(2-2)}/2]^{\frac{1}{2}}$$
$$= [(9.8)^2/2 + (2.4)^2/2]^{\frac{1}{2}} = 7.1 \text{ sec.}$$

The $(1-1)$ width for Ti $K\alpha$ is about 17.4″ (Fig. 2). If we arbitrarily choose 5″ for the $(2-2)$ width, the value of w is about 12.5″. Using these values the resolving powers as calculated are shown in Table III.

Thus the resolving power in the $(1-2)$ and

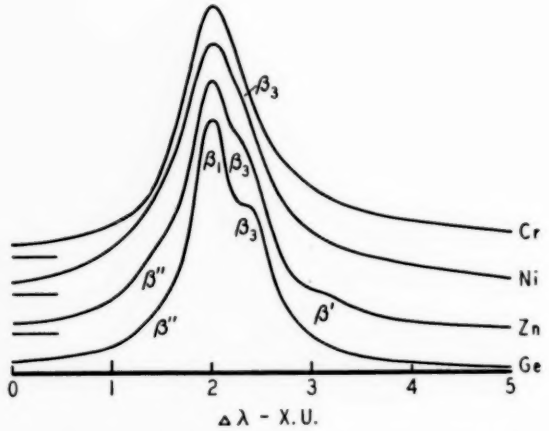

FIG. 4. $K\beta_{1,3}$ doublet. No separation can be seen for atomic numbers less than Ni 28.

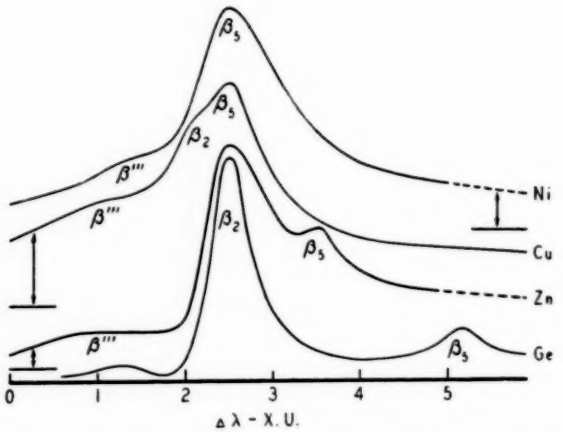

FIG. 5. $K\beta_2$ and $K\beta_5$. $K\beta_2$ was not observed for atomic numbers less than Cu 29.

TABLE III. *Resolving power of crystals employed.*

ORDER \ λ	1.54A	2.74A
1+1	11,000	12,000
1−2	9,200	26,000
1+2	24,000	42,000

(1+1) are the same for the higher atomic numbers and the curves should be of the same width, while at the lower atomic numbers the resolving power of the (1−2) is considerably greater than that of the (1+1) and the width is correspondingly less. Whether one assumes a Gaussian, classical[14] or other reasonable shape for the single crystal diffraction pattern, probably leaves these general conclusions unaltered.

[14] A. Hoyt, Phys. Rev. **40**, 477 (1932).

Asymmetries of lines

The index of asymmetry of an x-ray line has been defined[13] as the ratio of the part of the full width at half-maximum lying to the long wavelength side of the maximum ordinate to that on the short wavelength side. Four independent determinations of each index were made and the average deviation from the values listed in Table IV was usually not greater than 2 percent. Especial care was taken in the measurement of the asymmetry of Fe $K\alpha_1$ in the three orders and the error is thought to be not greater than one percent.

Fig. 6 shows a graph of the variation of the index of asymmetry with atomic number. Here again the curve for the β-line rises sharply for

TABLE IV. *Indices of asymmetry of K series lines.*

LINE	ORDER	Ge	Ga	Zn	Cu	Ni	Co	Fe	Mn	Cr	Va	Ti
	1−2	1.03	1.08	1.08	1.11	1.12	1.28	1.54	1.41	1.32	1.18	
	1+1	1.04	1.05	1.12	1.13	1.22	1.39	1.61	1.52	1.37	1.27	1.24
	(1+1)[12]					1.35		1.65	1.60	1.30		
	(1+1)[13]				1.4	1.1	1.5	1.8				
$K\alpha_1$	1+2	1.06	1.08	1.06	1.15	1.22	1.40	1.66	1.52	1.48		
	1−3			1.04								
	1+3			1.08								
	2−1				1.12							
	2+1				1.12							
	2+2	1.04			1.10							
	1−2	1.08	1.10	1.19	1.20	1.18	1.25	1.22	1.13	1.00	0.87	
	1+1	1.10	1.20	1.33	1.31	1.19	1.30	1.26	1.20	1.03	0.94	0.84
	(1+1)[12]					1.35		1.40	1.35			
$K\alpha_2$	1+2	1.11	1.14	1.34	1.29	1.21	1.30	1.30	1.24			
	1−3			1.30								
	1+3			1.32								
	1−2	2.00	1.79	1.43	1.17	1.23	1.67	1.64	1.36	1.45	1.46	
$K\beta_{1,3}$	1+1	1.96	1.83	1.48	1.09	1.30	1.68	1.75	1.40	1.53	1.54	1.73
	1+2	2.09	1.78	1.67	1.19	1.32	1.78	1.81	1.42	1.57		
$K\beta_{2,5}$	1+1	1.21	2.93	3.02	——	1.75	2.06	2.44	2.34	2.54	2.90	

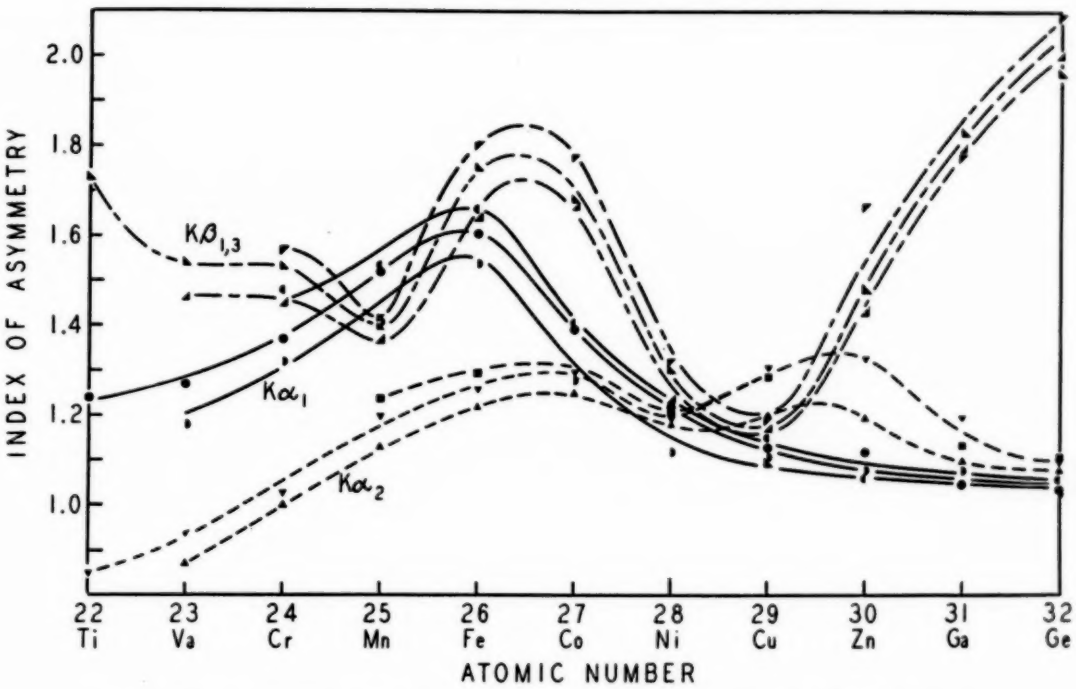

FIG. 6. Indices of asymmetry of lines as a function of atomic number. See Fig. 3 for legend.

high atomic numbers because β_1 and β_3 are not of the same intensity (Fig. 4). The indices for low atomic number are somewhat too high for the α_1-lines and too low for the α_2-lines because the lines are not completely resolved. The variation of asymmetry with order of diffraction increases in the order (1−2), (1+1), (1+2). This is contrary to what one would at first expect since the single crystal diffraction pattern in the second order is certainly much narrower than that in the first order. A possible explanation may be the following: As the crystal is rotated to obtain the intensity curve in any given order the two single crystal patterns slip over one another and give a contribution at any particular point equal to the integral of the product of the two curves. The theoretical single crystal diffraction patterns are not symmetrical[9] and the asymmetry is in the direction to augment the true line asymmetry. In the (1−1) position the theoretical patterns are equal and oppositely superimposed, so that all asymmetry disappears. In the (1+1) order the patterns are superimposed in the same direction and the asymmetry is correspondingly greater. Assuming that the first and second order single crystal diffraction patterns have different degrees of asymmetry we find the situation is somewhat altered in the (1±2) orders. In the (1−2) order the two patterns are superimposed oppositely so that the asymmetry of the one partially nullifies that of the other, and the curve is more nearly symmetrical than that in the (1+1). Bearing in mind the manner in which these curves combine, let us examine the conditions in the (1+2). Although the second order single crystal pattern is narrower than that of the first, a greater degree of asymmetry of the second order pattern may possibly be the determining factor in fixing the crystal contribution to the asymmetry of the measured line. On this interpretation, then, the present data indicate that the second order single crystal diffraction pattern is more asymmetrical than the first. It will be noticed from Table IV that for both Cu 29 and Ge 32 the (2+2) asymmetry is less than the (1+2) value. In this case, apparently, the single crystal patterns are so narrow that the degree of asymmetry no longer plays an important part in determining the line shape. It is interesting to note that the ratio of (1+1) width to (1−1) is 4, while that of the (2+2) to the (2−2) is about 30.

Attention is called to the fact that Ga 31 was

used in the liquid state, while the other elements were in the solid state. The curves show no marked irregularity for either width or asymmetry for Ga, indicating that the state has little influence on the widths of the K series lines in this particular region of atomic number. This is probably not true for the lower atomic number elements because the electrons involved in the K transitions are not so well shielded from external influence. It seems reasonable that the same factors would be involved in any observed change of width with state as are involved in the alloy effect.[15] Since no change with state was observed for Ga one would expect that the alloy effect would likewise be negligible. The Ge 32 metal used was of unknown purity, but for these reasons it is thought that the widths and asymmetries are within experimental error of those for pure Ge.

No difference greater than the experimental error was detected for the widths and asymmetries of the $K\alpha$ and $K\beta$ lines of the pure and impure samples of Ti 22 and Va 23.[16] It is possible that the particular kind of impurity present affected the widths of the lines very little, or that the effect produced by one impurity was cancelled by that of another.

The question of the origin of the asymmetry of the lines was raised by Seljakow, Krasnikow and Stellezky.[1] They suggested that there might be some connection with the fact that the M shells are being filled in the region from Sc 21 to Cu 29, where their experiments indicated that the asymmetry disappears. Inspection of Fig. 6 shows that the asymmetry is greater than unity for elements whose M shells are filled, namely, Cu, Zn, Ga and Ge. If the crystals were contributing greatly to the asymmetry in this region one would hardly expect the asymmetry to be changing with wavelength or atomic number to any appreciable extent. Thus it appears that there is little or no connection between the degree to which the inner shells are filled and the asymmetries of the lines. In all probability the answer will be found in asymmetries of the energy levels.

A test of the dependence of the width and asymmetry on the exciting voltage was also made for the Fe $K\alpha_1$ line using the filtered supply. No change greater than the experimental error of one percent was found from 10 kv to 35 kv or greater than the error of 5 percent at 8 kv, which is only 15 percent above the excitation potential.

Satellites

Accompanying the β_1 and β_5-lines were certain satellites, some of whose characteristics could be measured roughly. Table V gives the widths of the satellites at half maximum and the ratios of the areas of the adjacent line to that of the satellite. The strongest and most easily measured of these lines was the β' line on the long wavelength side of $\beta_{1,3}$. In general it was possible to measure this line in two or three orders. No β' satellite was detected in any order for Ti, Va, Cr, Ni or Ge. The next most prominent of the satellites measured, β'', was observed for the elements of higher atomic number only and to the short

TABLE V. *Satellite widths at half-maximum and intensities relative to an adjacent diagram line.*

Element	Order	Width (X.U.)	Ratio areas $\beta_{1,3}/\beta'$
		β' Line	
Mn	1−2	1.5	32
	1+1	1.5	30
	1+2	1.2	73
Fe	1−2	1.5	55
	1+1	1.4	73
Co	1−2	0.83	82
	1+1	.77	98
	1+2	.75	89
Ni	None		
Cu	1−2	.38	100
	1+1	.55	73
	1+2	.52	75
Zn	1+1	.32	220
	1+2	.25	200
Ga	1+1	.25	400
	1+2	.25	400
Ge	None		
		β'' Line	
			$\beta_{1,3}/\beta''$
Cu	1+2	.36	120
Zn	1+1	.29	120
	1+2	.33	60
Ga	1+1	.36	81
	1+2	.29	60
Ge	1−2	.29	100
	1+1	.33	87
	1+2	.30	95
		β''' Line	
			β_5/β'''
Mn		.47	280
Fe		.88	65
Co		.58	100
Ni		.62	70
Cu		1.1	—
			β_2/β'''
Zn		1.1	15
Ga		None	
Ge		.58	17

[15] L. G. Parratt, Phys. Rev. **45**, 364 (1934).

[16] However, a sample of MnO_2 gave the $K\alpha_1$ width 15 percent higher than that from pure Mn.

wavelength side of the $\beta_{1,3}$ doublet. No trace of this satellite was found from Ti 22 to Ni 28. The intensity relative to the $\beta_{1,3}$ doublet is substantially constant in this range. The satellites, β''', accompanying the $\beta_{2,5}$ lines were very difficult to measure. The maximum ionization current due to the satellite was not much greater than 10^{-15} ampere so it was necessary to measure the region of the satellite several times. The satellites as well as the $\beta_{2,5}$ lines themselves could be measured in the (1+1) order only. The intensity for the Ga $K\beta_2$ line was so weak that it was impossible to detect the satellite. However, in the case of Cr 24 the satellite should have shown up if it existed. No indication of its presence was found.

Wavelengths

Glancing angles corresponding to the peaks of the lines were measured in both first and second orders from the second crystal. For those lines showing structure the position of maximum intensity was measured. At the present time line shapes are not known with sufficient accuracy to allow components to be drawn. It is very probable that the components are not symmetrical in any case and in order to locate the peaks of the components one must know something about the degree of asymmetry and either their widths or separation.

In determining a glancing angle the position of the peak was taken alternately in the $(1\pm n)$ order until three independent determinations of the angle had been made. The temperature of the crystals was read to 0.1°C at every determination and usually did not change during a complete observation by more than 0.3°C. The angle between the $(1+n)$ and $(1-n)$ positions with 180° subtracted represented twice the diffraction angle. Three corrections must be applied to the measured angle in order to obtain the Bragg angle θ: (1) The temperature correction for crystal expansion; (2) the correction due to slit height; and, (3) the calibration correction of the divided circle.

The linear coefficient of expansion, 1.02×10^{-5} per °C, computed by C. D. Cooksey and D. Cooksey[17] was used to reduce the measured angle to the angle corresponding to 18°C, as follows,

$$d\theta'' = 2.10\ (t-18)\tan\theta.$$

The slit correction was made from the expression[18]

$$d\theta'' = 2\times10^{5}[(a^2+b^2)/24L^2]\tan\theta,$$

where a and b are the heights of the two slits and L is their distance apart.[19] The circle correction was made from the calibration curve as described above.

The crystals used were taken from the same sample of Argentina calcite that Bearden used to determine the grating space of calcite.[20] The density was found to be within experimental error of the average $\rho=2.71030$ g/cc at 20°C of several crystals from widely different localities. At 18°C this increases to $\rho=2.71046$ g/cc according to the linear expansion coefficient found by Cooksey.[17] The grating space as computed by Bearden[20] is $d_{\infty}=3.02810$A at 18°C on the assumption of Millikan's value for $e=4.768\times10^{-10}$ e.s.u.

The determination of the true value of the grating constant of any crystal depends essentially on the value assigned to the electronic charge, which is not accurately known. Since diffraction angles can be measured to 0.001 percent most writers have used for calcite the arbitrarily assumed grating constant $d_{\infty}=3.02945$A. The ruled grating wavelength measurements of Bearden[4] differ from those obtained with calcite crystals by about 0.22 percent.[21] These values

[17] C. D. Cooksey and D. Cooksey, Phys. Rev. **36**, 85 (1930).

[18] J. H. Williams, Phys. Rev. **40**, 636 (1932).

[19] See, however, Compton and Allison, *X-Rays in Theory and Experiment*, p. 737, where it is concluded that any correction for slit height is meaningless. Parratt has recently shown (Phys. Rev.) that Williams' correction should be

$$d\theta'' = 2\times10^{5}[(a+b)^2/24L^2]\tan\theta.$$

If this correction formula is used instead of the one above the Ge $K\alpha_1$ result in the first order is lowered by one part in 400,000, while the Ti $K\alpha_1$ value in the second order is lowered by one part in 200,000. Compton and Allison point out that a correction should be made for the effect of the asymmetry of the single crystal diffraction pattern on the position of the peak of the measured line. The correction is in such a direction as to *increase* the measured wavelength and is uncertain because these asymmetries are not accurately known.

[20] J. A. Bearden, Phys. Rev. **38**, 2089 (1931).

[21] E. Bäcklin, Nature **135**, 32 (1935). With improved experimental technique he now finds for the Al $K\alpha$ line

$$\frac{\lambda\ \text{grating}-\lambda\ \text{crystal}}{\lambda\ \text{crystal}} = 0.218\ \text{percent}$$

instead of the 0.14 percent as previously found. The new value agrees very satisfactorily with the value obtained by Bearden.[4]

have also been confirmed by refraction measurements on quartz[22] and on diamond.[23] The value of the calcite grating constant calculated from the ruled grating measurements is $d_{\infty}=3.03560$A. This is probably a much more precise value of the grating constant than can be obtained from the usual crystal constants. Since ruled grating experiments are in progress from which a more accurate value of d_{∞} may be obtained, it was thought best to retain the Siegbahn arbitrary value for the present computations. Thus all wavelengths in the present paper have been calculated with the following values of the grating constant

$$d_1=3.02904\text{A}, \qquad d_2=3.02934, \qquad d_3=3.02940.$$

Beyond 2.3A the correction for anomalous dispersion becomes appreciable and was made according to Siegbahn.[24] For shorter wavelengths the corrective term for refractive index was taken as $\delta/\lambda^2=3.69\times10^{-6}$.

Tables VI and VII give the wavelengths of the K series lines of the various elements together with previous results from single crystal photographic spectrometer work. Very little seems to have been done on second order measurements and consequently not many comparisons can be made. In the present work the agreement between the results obtained in the first and second orders indicate the high accuracy that has been attained by this method. It will be seen that the single crystal measurements of previous investigators are generally in satisfactory agreement with the new values except for Ti and Va. The previous measurements on Ti and Va for which the highest accuracy was claimed are those of v. Friesen.[25] For the Ti $K\alpha_1$, $K\alpha_2$, $K\beta$ lines his values are, respectively, about 10″, 5″ and 6″ higher than the results in the present experiments. The angular separation of the Ti $K\alpha_1$ and $K\alpha_2$ was carefully measured and found to be 279.0″ in the (1+1) position, whereas v. Friesen obtained a value corresponding to 270″. These disagreements were so great that the measurements were repeated quite carefully. The diffraction angle obtained by v. Friesen for Va $K\beta_5$ is 37″ greater than that from the present work. In view of the repeated measurements and also the fact that our Va $K\beta_5$ value is within experimental error of the $(\nu/R)^{\frac{1}{2}}$ curves, it appears that v. Friesen's measurements are in error.

Attention should also be called to the determinations for Ge 32 and Ga 31. The accuracy for Ge has been considerably increased, as judged by the agreement between first and second orders. The last measurement on the K series of Ga was made in 1917 by Uhler and Cooksey[26] with an estimated accuracy of a few seconds of arc.

The arrangement of apparatus was such that the ionization chamber could not be carried to a large enough angle to observe the (1+2) order of Ti 22 and Va 23, although the (1−2) order could be measured. To measure the second order diffraction angle in these cases the following procedure was used. The angle between the (1−1) and (1−2) positions was measured. The first-order diffraction angle was added to this measured angle, after making the necessary allowance for slit and temperature correction, thus giving the second-order diffraction angle. The appropriate slit and temperature corrections were then applied to this resultant angle.

The $(\nu/R)^{\frac{1}{2}}$ values for the $K\alpha_1$ lines in the present work vary from a smooth curve by an average deviation of 0.001 percent, while the deviation in previous work is about 0.003 percent. This indicates that greater accuracy has been achieved by the double crystal spectrometer than with the photographic spectrometers.

No attempt has been made to correct the diffraction angles for the overlapping of the α_1 and α_2 lines. In the case of the β_1 line the diffraction angles for the elements Ni 28 to Ge 32 are too large, because of the doublet characteristic of the line. The intensity of the $K\beta_5$ line was so low for Ga 31 that it could not be measured. As previously mentioned, the Cu 29 $K\beta_{2,5}$ is a doublet and here the longer wavelength component has been assumed to be the β_5 line. In the region from Va 23 to Ni 28 the present values of the wavelengths of $K\beta_5$ are lower than previous measurements have indicated. This may be due to the

[22] J. A. Bearden and C. H. Shaw, Phys. Rev. **46**, 759 (1934).
[23] J. A. Bearden, Phys. Rev. **47**, 811 (1935).
[24] M. Siegbahn, *Spectroscopie der Röntgenstrahlen*, 2nd ed., p. 45.
[25] S. v. Friesen, Zeits. f. Physik **58**, 781 (1929).
[26] H. S. Uhler and C. D. Cooksey, Phys. Rev. **10**, 645 (1917).

TABLE VI.

El.	Obs.	$K\alpha_1$ line—KL_{III} First order $\theta_{18°C}$	λ	Second order $\theta_{18°C}$	λ	$K\alpha_2$ line—KL_{II} First order $\theta_{18°C}$	λ	Second order $\theta_{18°C}$	λ
Ti	I	26°55′15.0″	2.742866A	64°52′54.5″	2.742872A	26°57′34.5″	2.746518A	65° 2′36.8″	2.746491A
	II	26 55 25.0	2.74311			26 57 39.5	2.74665		
Va	I	24 21 23.1	2.498428	55 33 43.4	2.498417	24 23 45.7	2.502243	55 41 23.1	2.502229
	II	24 21 23.1	2.49842			24 23 44.5	2.50221		
Cr	I	22 9 33.3	2.285000	48 57 45.3	2.284974	22 11 56.3	2.288889		
	III	22 9 34.5	2.285033			22 11 57.0	2.288907		
Mn	I	20 15 25.5	2.097507	43 49 12.3	2.097504	20 17 48.3	2.101442	43 55 24.7	2.101446
	III	20 15 25.4	2.097506			20 17 49.8	2.101489		
Fe	I	18 35 52.4	1.932070	39 37 35.0	1.932049	18 38 13.6	1.936000	39 43 22.7	1.935979
	III	18 35 52.6	1.932075			18 38 14.1	1.936013		
	IV	18 35 52.3	1.932067	39 37 34.8	1.932046	18 38 13.2	1.935989		
	V	18 35 52.7	1.932078						
Co	I	17 8 22.3	1.785314	36 6 35.3	1.785295	17 10 39.8	1.789173	36 12 1.1	1.789158
	III	17 8 21.4	1.785287	36 6 33.2	1.785273	17 10 40.3	1.789187	36 12 1.7	1.789169
Ni	I	15 50 57.3	1.654505	33 6 14.9	1.654512	15 53 12.9	1.658336	33 11 25.9	1.658336
	III	15 50 57.2	1.654503	33 6 9.7	1.654450	15 53 13.5	1.658353	33 11 24.0	1.658315
Cu	I	14 42 4.0	1.537400	30 29 51.6	1.537400	14 44 18.5	1.541220	30 34 53.4	1.541218
		(2±1) order		(2±2) order				(2±2) order	
	I	14 42 4.4		30 29 52.1				30 34 52.8	
	VI	14 42 3.9	1.537397	30 29 51.2	1.537397	14 44 19.3	1.541243		
	V	14 42 4.1	1.537402						
	V	14 42 3.9	1.537397						
Zn	I	13 40 30.1	1.432219	28 12 54.2	1.432218	13 42 44.1	1.436042	28 17 50.8	1.436055
				(1±3) order				(1±3) order	
	I			45 9 59.4	1.432217			45 19 14.7	1.436045
	VII, VIII	13 40 28.4	1.432170			13 42 43.7	1.436032		
Ga	I	12 45 11.4	1.337329	26 11 49.8	1.337337	12 47 27.7	1.341233	26 16 45.9	1.341238
	IX	12 45 5	1.337152			12 47 15	1.340869		
Ge	I	11 55 19.2	1.251478	24 24 3.7	1.251483	11 57 36.7	1.255429	24 28 58.6	1.255426
	VIII, X	11 55 13.0	1.25130			11 57 29.1	1.25521		

TABLE VII.

El.	Obs.	$K\beta_{1,3}$ line—KM_{III} First order $\theta_{18°C}$	λ	Second order $\theta_{18°C}$	λ	$K\beta_2$ line—$KM_{IV,V}$ First order $\theta_{18°C}$	λ	$K\beta_2$ line—$KN_{II,III}$ First order $\theta_{18°C}$	λ
Ti	I	24°27′48.8″	2.508744A						
	II	24 27 54.9	2.50890						
Va	I	22 6 19.6	2.279730	48°48′40.0″	2.279708A	21 57′12.9″	2.26485A		
	II	22 6 22.0	2.27979			21 57 50.0	2.26586		
Cr	I	20 5 12.1	2.080597	43 22 41.8	2.080587	19 56 42.4	2.06653		
	III	20 5 11.7	2.080586			19 56 49.0	2.06671		
Mn	I	18 20 27.4	1.906301	38 59 46.7	1.906274	18 12 36.3	1.89316		
	III	18 20 23.6	1.906195			18 12 40.0	1.89327		
Fe	I	16 49 11.6	1.752991	35 21 25.3	1.752987	16 41 48.7	1.74054		
	III	16 49 12.5	1.753013			16 41 58.0	1.74080		
Co	I	15 29 8.1	1.617483	32 16 18.8	1.617479	15 22 7.6	1.60558		
	III	15 29 6.5	1.617436			15 22 9.0	1.60562		
Ni	I	14 18 26.0	1.497080	29 36 57.2	1.497048	14 11 40.3	1.48553		
	III	14 18 24.8	1.497045			14 11 43.0	1.48561		
Cu	I	13 15 29.7	1.389364	27 17 57.9	1.389378	13 9 2	1.37828		
	VI	13 15 29.2	1.389349			13 9 0.6	1.378236		
Zn	I	12 19 11.6	1.292610	25 15 29.2	1.292609	12 13 8	1.28220	12°12′29.4″	1.281067A
	VII	12 19 9.3	1.292546			12 12 58	1.2819	12 12 29.4	1.281068
Ga	I	11 28 37.4	1.205409	23 26 52.6	1.205422			11 21 45.2	1.19354
	IX	11 28 30	1.20520					11 21 54.0	1.1938
	VIII	11 28 38.0	1.20543						
Ge	I	10 43 3.6	1.126618	21 49 59.4	1.126627	10 37 36	1.1172	10 36 6.0	1.11457
	VIII, X	10 43 6.8	1.12671			10 37 44	1.1174	10 36 8.2	1.11463

Tables VI, VII. I—Present results; II—Sten v. Friesen, Zeits. f. Physik **58**, 781 (1929); III—S. Eriksson, Zeits. f. Physik **48**, 360 (1928); IV—A. Larsson, Zeits. f. Physik **41**, 507 (1927); V—M. Siegbahn, Ark. Mat., Astr. o. Fysik (A) **21**, Nr. 21 (1929); VI—Ina Wennerlöf, Ark. Mat., Astr. o. Fysik (A) **22**, Nr. 8 (1930); VII—B. Edlén, Zeits f. Physik **52**, 364 (1928); VIII—H. Beuthe, Zeits. f. Physik **60**, 603 (1930); IX—H. S. Uhler and C. D. Cooksey, Phys. Rev. **10**, 645 (1917); X—A. Leide, Comptes rendus **180**, 1203 (1925).

TABLE VIII. *Wavelengths of satellites.*

Element	Order		λ
		β' Line $\lambda\beta' - \lambda\beta_{1,3}$	
Mn	1−2	4.0 X.U.	
	1+1	4.2	1.9101A
	1+2	3.2	
Fe	1−2	3.0	
	1+1	3.1	1.7560
Co	1−2	2.2	
	1+1	2.2	1.6197
	1+2	2.2	
Ni	None		
Cu	1−2	1.4	1.3907
	1+1	1.3	
	1+2	1.3	
Zn	1+1	1.2	1.2938
	1+2	1.2	
Ga	1+1	1.0	1.2064
	1+2	1.0	

Element	Order		λ
		β'' Line $\lambda\beta_{1,3} - \lambda\beta''$	
Cu	1+2	1.0 X.U.	1.3884A
Zn	1+1	.62	1.2920
	1+2	.59	
Ga	1+1	.59	1.2048
	1+2	.63	
Ge	1−2	.62	1.1260
	1+1	.61	
	1+2	.59	
		β''' Line $\lambda\beta_5 - \lambda\beta'''$	
Mn	1+1	2.0 X.U.	1.8912A
Fe		1.9	1.7386
Co		1.8	1.6038
Ni		1.2	1.4843
Cu		1.5	1.3768
		$\lambda\beta_2 - \lambda\beta'''$	
Zn		1.6	1.2795
Ga		None	
Ge		1.4	1.1133

fact that these lines are very asymmetrical and hence on a photographic plate the center of gravity may not coincide with the position of maximum intensity. The $K\beta_2$ line disappears abruptly at Cu 29, at least so far as these experiments show. In any event, it would be so close to $K\beta_5$ for atomic numbers less than that of Cu that the two could not be resolved.

Because of the large width and the fact that they are usually superimposed on the side of a stronger line the positions of the various satellites were not determined very accurately. Some check is possible where the satellites were observed in more than one order. Table VIII gives the wavelength data for these satellites in decreasing order of wavelength.

We are indebted to Drs. L. G. Parratt and L. P. Smith for helpful discussions and to Dr. Lewis V. Judson of the Bureau of Standards for valuable aid in the calibration of the divided circle. The Geneva Society spectrometer was a generous donation by Dr. A. L. Loomis of Tuxedo Park. The samples of pure Va and Ti metals were kindly supplied by the Vanadium Corporation of America and the Titanium Alloy Manufacturing Company.

JULY 1, 1935 PHYSICAL REVIEW VOLUME 48

A Measurement of the Absolute Probability of *K*-Electron Ionization of Silver by Cathode Rays

J. C. CLARK, *Stanford University*

(Received April 23, 1935)

The method of Ross's balanced foils was used to separate the $K\alpha$ quanta from the thin silver foil target radiation. The x-ray energy was absorbed in CH_3Br and SO_2 in a standard ionization chamber and the ionization currents measured by means of a Compton electrometer and calibrated ionization system. Stockmeyer's value for the energy per ion pair for these gases was used to compute the number of quanta absorbed in the chamber. The number of Ag *K* ionizations per bombarding electron was then calculated, after the necessary target and absorption corrections. Measurements were made on 10 thin targets of average thickness 0.17 micron, and the *K*-electron ionization cross section for silver for 70.0 kv electrons was determined to be $\Phi(U) = (4.80 \pm 0.43) \times 10^{-23}$ cm². The measurements of relative probabilities of *K* electron ionization for silver by Webster, Hansen and Duveneck are normalized at 70.0 kv, ($U = 2.75$) by the above value of $\Phi(U)$, and these experimental data compared with classical quantum theory and the wave mechanics theories of Massey, Mohr and Burhop, Soden and Wetzel. The theories of Soden and Wetzel compare more favorably with the experimental data than those of Massey, Mohr and Burhop, or indeed with the classical theory.

I. INTRODUCTION

THE problem of determining the probability of *K*-electron ionization by electron impact has been studied both theoretically and experimentally by numerous authors. Theoretical solutions have been given for hydrogen,[1] helium,[1, 2] silver[3, 4] and mercury,[3] and the experimental determinations cover hydrogen,[5] helium[6] and silver.[7] The experimental work on silver by

[1] H. S. W. Massey and C. B. O. Mohr, Proc. Roy. Soc. **A140**, 613 (1933).
[2] W. W. Wetzel, Phys. Rev. **44**, 25 (1933).
[3] D. Graf Soden, Ann. d. Physik **19**, 409 (1934).
[4] E. H. S. Burhop and W. W. Wetzel have given solutions as yet unpublished, but discussed in the theoretical section of this paper.
[5] J. T. Tate and P. T. Smith, Phys. Rev. **39**, 270 (1932).
[6] P. T. Smith, Phys. Rev. **36**, 1293 (1930).
[7] D. L. Webster, W. W. Hansen and F. B. Duveneck, Phys. Rev. **43**, 851 (1933).

Webster, Hansen and Duveneck covers measurements of the relative probabilities of K-electron ionization by cathode rays as a function of their kinetic energy. The experiments herewith reported have been performed to determine the absolute probability of K-electron ionization of silver by 70.0 kv cathode rays.

For the case where the probability determination is made by measuring the absolute intensity of characteristic x-rays emitted by a target of solid material, the absolute probability is defined[7] most conveniently as (the probability of ionization) ÷ (the number of atoms per unit area of the target). This identifies it as the cross-section area of each atom effective for ionization, denoted as $\Phi(U)$. Thus

$$\Phi(U)=(N_{KI}/N_E)/nX_0, \qquad (1)$$

where N_{KI} is the number of K-electron ionizations produced by N_E electrons striking a target of thickness X_0, the target containing n atoms per cubic centimeter. The number of K ionizations is determined in this experiment in terms of the ionization current produced by absorbing a known fraction of the x-ray quanta in a standard ionization chamber, and the already measured[8] value of the energy required to produce a pair of ions in the absorbing gas used in the ionization chamber.

II. The Balanced Foil Method

When 70.0 kv electrons interact with silver atoms to produce x-rays, both characteristic and continuous x-rays are produced. For effectively separating the $K\alpha$ line energy from the series of higher terms, as well as from the continuous spectrum energy, the method suggested by Ross,[9] using balanced thin metallic foils, was used. This method utilizes thin foils of nearly adjacent elements in the periodic table, whose thicknesses are adjusted so that the absorption curves of each foil exactly coincide except in the region between their K absorption limits. The wide apertures allowable by the balanced foil method, makes possible the measurement of the small number of quanta obtained from the thin film targets which would otherwise be impossible by the usual methods of analysis. Since a large part of the energy of the K series is associated with the $K\alpha$ lines, a region of the spectrum including only these lines is measured and proper corrections are made to include all of the K series energy in the computation of $\Phi(u)$. The balanced foils most suitable for determining the $K\alpha$ line energy are rhodium (45), and masurium (43). However, masurium is not available, so it is necessary to use molybdenum (42). The K limit of Mo is 58 X.U. above, while the Rh K limit is 27 X.U. below that of the wavelength of the silver $K\alpha$ lines. This gives a band of continuous energy 85 X.U. in extent which is measured with the $K\alpha$ line energy. The correction for this continuous energy is treated separately, below.

III. Apparatus

The general assembly of apparatus is shown diagrammatically in Fig. 1. The x-ray tube with removable anode and cathode is entirely enclosed in a lead house, and the x-rays to be measured allowed to escape only through an opening controlled by an electromagnetic shutter. This shutter is actuated by a selector switch and standard clock circuit which permits duplication of exposure-time intervals estimated to be accurate to ±0.05 second. After passing through two thin aluminum windows in the tube, one being 0.040 mm thick on the side of the target to shield electrostatically the thin silver foil, and the other being the tube window 0.075 mm thick, the x-rays pass through air until they encounter the balanced foils. These foils are mounted on a holder which allows either the Mo or the Rh foil to be placed in the x-ray path. The beam is next limited by a circular aperture in a thick lead plate, this opening defining the solid angle of x-ray energy entering the standard ionization chamber from the target. In the chamber the quanta are partially absorbed by either methyl bromide (used during measurements for seven of the ten silver targets), or sulphur dioxide, (used for the remaining three targets), and their intensity measured in terms of the ionization produced. The ionization current is measured by means of a Compton electrometer.

The second ionization chamber shown in Fig. 1 is used with the calcite crystal to determine the

[8] W. Stockmeyer, Ann. d. Physik **404**, 71 (1932).
[9] P. A. Ross, Phys. Rev. **28**, 425 (1926).

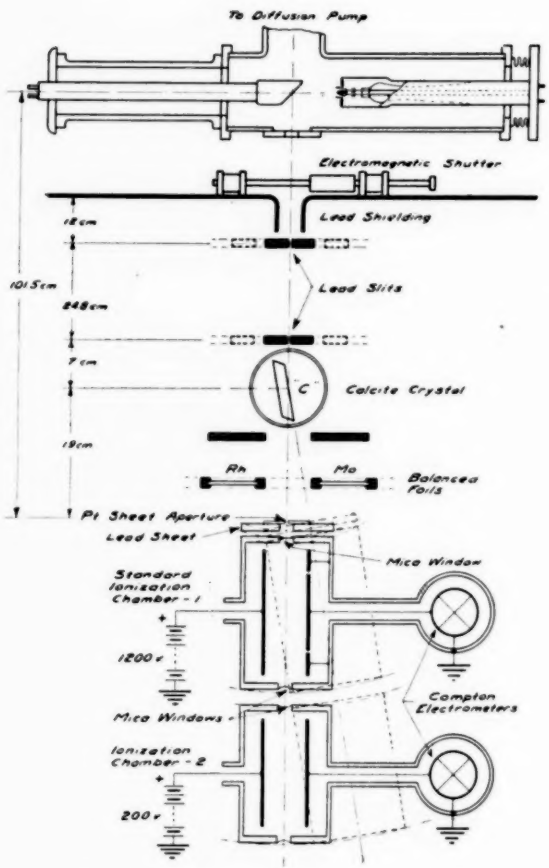

FIG. 1. General assembly of apparatus.

absorption coefficient of the gas in the standard chamber as a function of wavelength. Both chambers are therefore mounted on a movable carrier which rotates about the axis of the crystal "*C*." The crystal is placed in the path only when spectrometer measurements are being made. When the crystal is removed, the standard chamber axis is properly aligned with the x-ray tube window and target.

The high voltage power source used during these experiments[9] utilizes a 500-cycle current, the output voltage of the transformer being rectified and filtered so that the ripple voltage is only 4 volts at 10 milliamperes. The high voltage was measured by means of an electrostatic voltmeter[10] which had just recently been calibrated[11] by means of standard cells and resistors checked by the U. S. Bureau of Standards. During all exposures of x-rays into the standard ionization chamber, as well as for the various correction determinations, the x-ray tube voltage and current were maintained very constant by means of manually operated controls in the high voltage source circuit.

The x-ray tube cathode heater circuit, consisting of the electrical wiring, batteries, meters and various controls, is entirely electrostatically shielded.[11] This shielding prevents the possibility of corona currents being included with the x-ray tube current. This precaution is absolutely necessary for this experiment because the corona currents may be many times greater than the feeble tube currents generally employed, namely, 25–60 microamperes. The microammeter used to measure these currents was calibrated in its operating position during each run by means of a standard potentiometer circuit and a standardized 10,000-ohm resistor.

The x-ray tube is shown diagrammatically in Fig. 2a. It will be noticed that the principal section of the tube is made of brass, kept at cathode potential. This central brass tube is insulated from the anode and grounded diffusion pump by means of standard sections of Pyrex glass flanged pipes, two inches in internal diameter. The cathode holder is adjustable from the exterior by means of flexible metal bellows. Pinhole pictures were taken to make sure that the focal spot was in the middle of the target, and that it was sufficiently broad to allow maximum tube currents to be used. Ionization chamber measurements were frequently made to make sure that no x-rays were produced from field currents within the tube. Similar measurements were made to determine the magnitude of the extraneous radiation emitted from places on the target assembly other than the focal spot. These latter measurements were made with normal tube currents flowing, but without the thin silver film mounted on the holder.

The target of the x-ray tube is shown diagrammatically in Fig. 2b. The silver foils used for the target were commercial thin silver leaf, very much like gold leaf, and of average thickness 0.17 micron. These films were strong enough to support their own weight when placed across the end of the aluminum supporting tube, thus elim-

[10] H. Clark, Rev. Sci. Inst. **1**, 615 (1930).
[11] P. Kirkpatrick and P. A. Ross, Phys. Rev. **45**, 456 (1934).

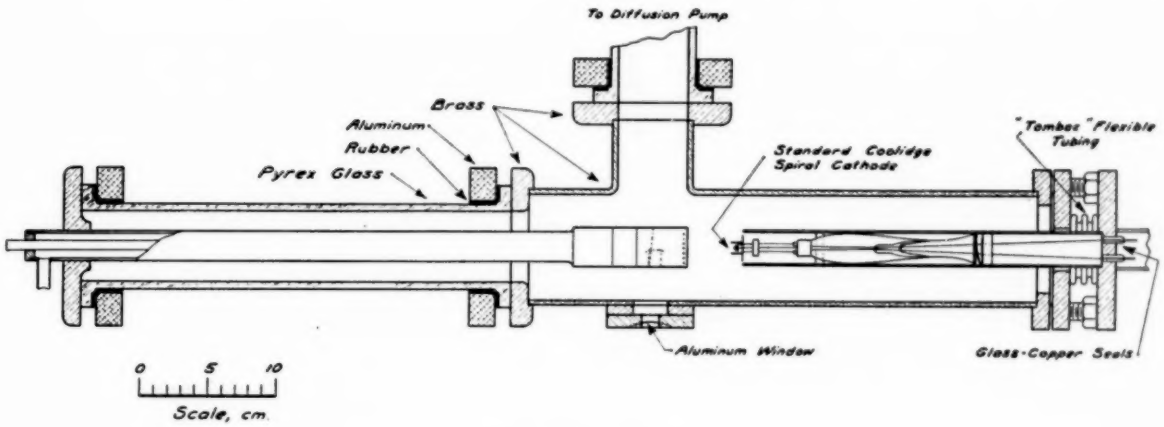

FIG. 2a. X-ray tube.

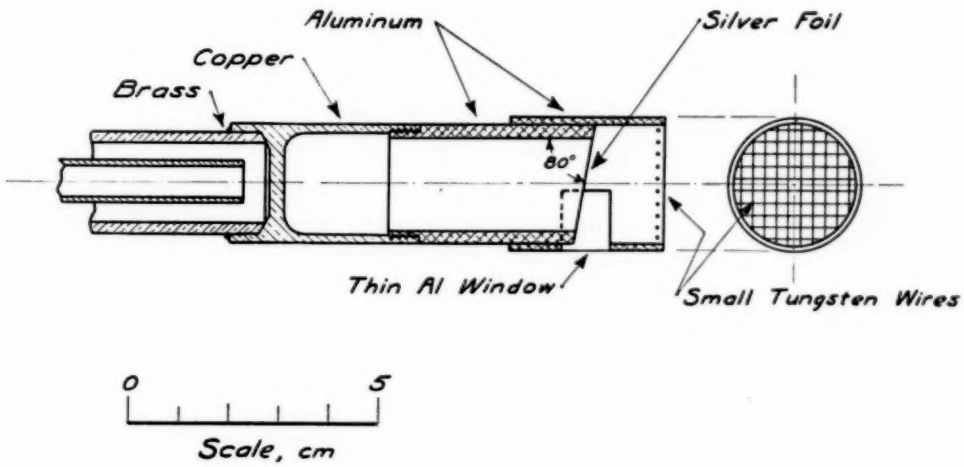

FIG. 2b. Detail of target.

inating the necessity of a backing target. The thin wall aluminum cylinder used to support the film is threaded to a copper rod, which furnishes the back end of the target and which is soldered to a brass supporting tube extending to the anode end of the x-ray tube. The aluminum supporting tube is made long enough so those electrons which pass straight through the film will not experience collisions with any material which is in the optical path of the measuring apparatus. The front end of the aluminum tube is ground off to make an angle very nearly equal to 80 degrees with its longitudinal axis, thus placing the silver foil at the same angle with respect to the direction of the incident electrons from the cathode.

The ionization chamber is shown diagrammatically in Fig. 3. The main cylinder and end plates are made of brass, and the seals are designed so that the gas pressure within the chamber may be greater or less than atmospheric. The standard collector plate, guard plates and potential plate are made of 1/16-inch sheet aluminum. The collector plate is supported between the guard plates by the terminal used for making connection to the electrometer circuit. The terminal is held rigidly in place by an amber bushing, which also insulates it electrically from the grounded chamber walls. The guard electrodes are connected to the grounded chamber, and are mounted in the same plane as the collector electrode. The potential electrode is bent so the electric field between the plates is very nearly uniform, thus causing all of the ions which are produced by the x-rays in the column of gas defined by the collector plate

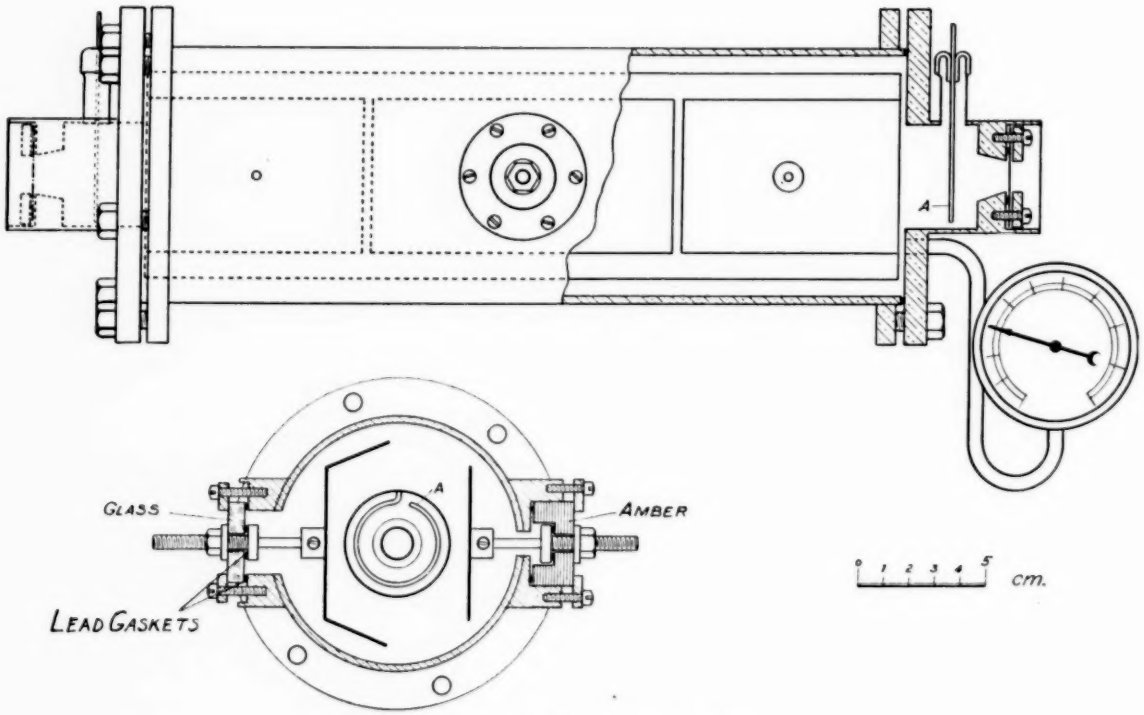

FIG. 3. Standard ionization chamber.

to be carried to electrodes. The nature of the electric field in the region of the collector plate, at right angles to, and along the chamber axis was determined by mapping the equipotential lines. Mapping the field was accomplished by means of a dimensional model of the chamber placed in a tray of water, connecting the proper elements to a 1000-cycle oscillator, and probing the field produced with a telephone head set. The potential and collector plates are placed far enough apart so that photoelectrons produced along the path of the x-rays lose all of their energy to the gas before reaching the plates.

The windows of the ionization chamber are thin sheet aluminum 0.078 mm thick. The ring electrodes, marked *A* in Fig. 3, at each end of the chamber were maintained at a potential of 200 volts above that of the chamber to collect photoelectrons produced by x-rays passing through the windows. These electrodes were not necessary for this experiment since relatively high pressures were used for both gases. Fuse wire gaskets were used throughout in the assembly of this apparatus.

The ionization system consists of the ionization chamber, an electrically shielded connection between the collector electrode and the electrometer, and the Compton electrometer. The electrometer sensitivity was approximately 4000 mm/volt. The electrical capacity of the ionization system was determined in terms of two standardized cylindrical condensers, using the method described by R. Rinkel.[12] The capacities of the cylindrical condensers, which were exactly similar except for their length, were calculated, and a correction due to the distortion of the electric field at ends of the condensers was determined by a series of measurements as outlined in the above method. The capacity of the ionization system as a function of the electrometer deflection was then determined in terms of the corrected capacities of the standard condensers. A Leeds and Northrup type K potentiometer and a U. S. Bureau of Standards certified standard cell was used during all ionization system calibrations.

[12] R. Rinkel, Physik. Zeits. **33**, 544 (1932).

IV. Corrections

Target corrections

The electrons, upon entering the target, experience many minor deflections from their straight paths, thus increasing their path length through the film target. Some of these electrons may bend[13] more than 90° and thus be rediffused through the target film, while others may go straight through the film and pass along the hollow supporting tube to the copper base. A part of those striking the copper base may also experience rediffusion and find their way back through the silver foil target. These three diffusion effects will increase the number of K ionizations per electron striking the target. Another effect is that due to electron retardation while passing through the target, which reduces the energy of the electron and thus reduce the number of K ionizations. There is also the effect of fluorescence within the target. That is, continuous spectrum x-rays of wavelength shorter than those of the K series may be absorbed on their way out of the target by atoms which emit K series quanta, thus increasing the number of K ionizations per electron. Of the above effects the corrections for the rediffusion of the electrons from the copper end of the target, the electron retardation, and the fluorescence effect, have been calculated by the methods used by Webster, Hansen and Duveneck[7] and found to be negligible. The corrections for the remaining two effects are now discussed following the procedure applied by the above authors.

Diffusion within the target. If the observed intensity of the K quanta is i and the intensity corrected for diffusion is i_d, then the diffusion correction k_d is $i_d \div i$. This is shown to be[7] given by $k_d = 1/(1+\lambda_0/2)$. In this expression λ_0 is the value of λ at $x = X_0$ where X_0 is the thickness of the silver foil target, and λ is the most probable angle of deflection of an electron deflected by multiple scattering when passing through a substance. As given by Bothe,[14]

$$\lambda = \frac{8.0}{V}\,\frac{V+511}{V+1022}\,Z\left(\frac{\rho x}{A}\right)^{\frac{1}{2}},$$

where λ is expressed in radians if the electron is at a distance x microns from the forward side of the target, Z, A and ρ are the atomic number, atomic weight in grams, and density in grams per cubic centimeter, respectively, and V is the accelerating potential of the electron, in kilovolts. In this experiment 70.0 kv electrons were used with silver foil targets of mean thickness 0.17 micron, making $\lambda = 0.373$ and $k_d = 0.935$. From the assumptions used in Bothe's formula together with those involved in deducing the expression for k_d, the probable error in k_d is estimated to be ± 1.0 percent.

Rediffusion within the target. Bothe[14] gives for the ratio of electrons which rediffuse from a target of thickness x to the number incident,

$$p_x = p(1-e^{-2\alpha x})/(1-p^2e^{-2\alpha x}),$$

where α is Lenard's "practical absorption coefficient" for the incident electrons, and p is the ratio of electrons which rediffuse from a massive target to the number incident. Schonland[15] gives $p = 0.39$ for Ag and shows it is independent of V. The absorption coefficient α for silver and 70.0 kv electrons is about[16] 4.2×10^3 cm^{-1}. Accordingly, for 0.18 micron Ag foils $p_x = 0.05$, and for $x = 0.09$ micron, $p_x = 0.03$. Thus three percent of the electrons entering the target penetrate to a depth equal to one-half the target thickness and then return to the entering surface. If the rediffused electrons pass straight into the target, reversed their direction and returned in straight paths out, the fact that approximately half of the rediffused electrons penetrate to only one-half the total target thickness eliminates any rediffusion correction for this case. However, the electrons experience multiple collisions within the target and have very crooked paths, which means that those electrons which do penetrate half-way through the target before being reversed undoubtedly travel considerably farther than one target thickness while they are in the target. In any event, the rediffusion correction is small and because there is not enough known about the paths of the electrons while in the target, an evaluation of this correction cannot be made.

Auger effect correction. The ratio of the number

[13] Bothe[14] gives const. $\times \theta e^{-\text{const.}\times\theta^2} d\theta$ for the angular distribution of diffused electrons.

[14] W. Bothe, *Handbuch der Physik*, 1927, Vol. 24, Chap. I, Sec. 9.

[15] B. F. J. Schonland, Proc. Roy. Soc. **A108**, 187 (1925).

[16] Andrade, *The Structure of the Atom*, C. Bell and Sons, London, 3rd ed., p. 15.

of K quanta produced (N_{KQ}) to the number of K ionizations (N_{KI}), defined as the fluorescence efficiency, w_K, has been measured by several observers[17] for various elements. From these data the value $0.72=w_K$ for silver will be here used. The number of K quanta may be calculated in terms of the measured number of $K\alpha$ quanta from the relation

$$N_{KQ}=N_{K\alpha}\frac{(I\lambda)_{K\alpha}+(I\lambda)_{K\beta}+(I\lambda)_{K\gamma}}{(I\lambda)_{K\alpha}}. \quad (2)$$

In this equation $N_{K\alpha}$ denotes the number of $K\alpha_1$ and $K\alpha_2$ quanta measured, and $(I\lambda)_{K\alpha}$, etc., are quantities proportional to the number of $K\alpha$ quanta, and I and λ denote the intensity and wavelength, respectively, of the lines. Using the relative intensities of the Ag K series lines as given by Siegbahn,[18] we obtain N_{KI}

$$N_{KI}=(1.16/w_K)N_{K\alpha}. \quad (3)$$

Ratio of line to continuous energies

In this experiment N_{KI} is determined in terms of $N_{K\alpha}$ as shown above. However, since the method of balanced thin foils does not completely separate the $K\alpha$ line energy from the band of continuous energy, it is necessary to obtain a measure of the ratio of the $K\alpha$ line energy to the energy of the continuous spectrum between the K limits of the foils for the thin silver target radiation. In this case, the area is taken to mean $\int_{\nu_2}^{\nu_1} i(\nu)d\nu$, where $i(\nu)d\nu$ denotes the intensity of the radiation for a frequency range $d\nu$ at the frequency ν. Numerical values of this quantity were obtained from planimeter measurements on spectral curves obtained by means of a Bragg spectrometer. The continuous radiation from a thin silver target is very weak, but spectral curves have been obtained throughout the spectral region necessary for this ratio determination. These curves were run at the voltage for which the ionization cross section was determined, namely 70.0 kv, and a correction for the second order continuous spectrum was necessary. Kirkpatrick[19] has outlined a method for obtaining the second order correction. The procedure involves determining the intensity of x-rays of wavelength λ and $\lambda/2$ reflected from the crystal with and without a film of material of known thickness and absorption coefficients for the two wavelengths, intercepting the x-ray beam. As previously stated the directly reflected beam of continuous energy is very weak (an electrometer deflection of approximately 2 mm is obtained during a 60-sec. exposure with the tube current and voltage 50 microamperes and 70.0 kv, and the silver foil target 0.17 micron thick), and it becomes impossible to accurately measure this radiation when an absorbing film is placed in the path. The intensity of the radiation of wavelength $\lambda/2$ can, however, be determined by multiplying the intensity of the thin target continuous energy for the first-order crystal reflection by the ratio of the "second-order crystal reflection" to the "first-order crystal reflection." In this case, "first-order crystal reflection" denotes the energy of wavelength λ reflected from the crystal in unit time when the crystal is adjusted to reflect the wavelength λ. Likewise "second-order crystal reflection" denotes one-half of the energy of wavelength $\lambda/2$ reflected per unit time when the crystal is set to reflect the wavelength $\lambda/2$, one-half the energy being taken in order to correct for the crystal dispersion. Measurements of the ratio of crystal reflections were made using radiation from a thick silver target, and the above mentioned method given by Kirkpatrick. A molybdenum foil 0.04 mm thick was used for the absorbing film, and Richtmyer's[20] values for μ/ρ at λ_M and $\lambda_M/2$ were used, λ_M being the wavelength midway between the Rh and Mo K limits.

The results of five determinations of the ratio of line to continuous areas for 70.0 kv x-rays from two thin silver targets of average thickness 0.17 micron, corrections being made for the second order continuous energy gives.

$$k=A^L/A^C=3.41\pm0.13.$$

[17] P. Auger, Comptes rendus **182**, 1215 (1926); G. Locher, Phys. Rev. **40**, 484 (1932); D. K. Berkey, Phys. Rev. **45**, 437 (1934); A. H. Compton, Phil. Mag. **8**, 961 (1929); L. H. Martin, Proc. Roy. Soc. **A115**, 420 (1927); D. K. Berkey, Phys. Rev. **46**, 74 (1934); F. Harms, Ann. d. Physik **82**, 87 (1926); W. S. Stockmeyer, Ann. d. Physik **105**, 71 (1932); R. J. Stephenson, Phys. Rev. **46**, 73 (1934); M. Haas, Ann. d. Physik **16**, 473 (1932).

[18] M. Siegbahn, *Spektroskopie der Röntgenstrahlen*, 2nd ed., Julius Springer, Berlin, 1931, p. 355.

[19] P. Kirkpatrick, Phys. Rev. **22**, 37 (1923).

[20] F. K. Richtmyer, Phys. Rev. **30**, 759 (1927).

Correction for absorption in balanced foils

From the definition of the preceding paragraph we may write

$$A=A^L+A^C \quad \text{and} \quad A^L=Ak/(k+1).$$

However, it is not the energy proportional to A which is measured in the standard ionization chamber, but only that received by the chamber after the balanced foil absorption, which shall here be denoted by A_F. That is

$$A_F=\int_{\nu_1}^{\nu_2} i(\nu)\{e^{-[\mu_2(\nu)x_2]}-e^{-[\mu_1(\nu)x_1]}\}d\nu,$$

where ν_1 and ν_2 are the frequencies of the K limits, $\mu_1(\nu)$ and $\mu_2(\nu)$ the absorption coefficients, and x_1 and x_2 the thicknesses, of the Rh and Mo foils, respectively. By setting $R=A_F/A$, we have

$$A^L=(A_F/R)k/(k+1). \tag{4}$$

In this equation the value of k is already available and R may be obtained from

$$R=\frac{A^L[e^{-\mu_2(\nu)x_2}-e^{-\mu_1(\nu)x_1}]_{\nu=K\alpha}+A^C[e^{-\mu_2(\nu)x_2}-e^{-\mu_1(\nu)x_1}]_{\nu=\lambda_M}}{A^L+A^C},$$

where $\nu=K\alpha$ denotes the frequency of the Ag $K\alpha$ lines, and $\nu=\lambda_M$ is the frequency midway between the Rh and Mo K limits. For the balanced Mo and Rh foils used in this experiment Eq. (4) becomes

$$A^L=1.51A_F. \tag{5}$$

If we now denote the number of $K\alpha$ quanta which get through the foils during the exposure time interval by $N_{K\alpha}'$, and likewise let N_C' be the number of continuous quanta in the frequency range between the foil K limits which get through the foils in the same time interval, and further set $N_F=N_C'+N_{K\alpha}'$, then since the spectral areas previously defined are proportional to energy, we have

$$A^L/A_F=N_{K\alpha}\nu_{K\alpha}/N_F\nu_n=1.51, \quad \text{from (5)}.$$

In this equation ν_n is defined by

$$A_F\nu_n=A_L\nu_{K\alpha}[e^{-\mu_2(\nu)x_2}-e^{-\mu_1(\nu)x_1}]_{\nu=K\alpha}+A_C\nu_M[e^{-\mu_2(\nu)x_2}-e^{\mu_1(\nu)x_1}]_{\nu=M}. \tag{6}$$

Thus, from Eqs. (5) and (3) we have

$$N_{KI}=(1.75/w_K)(\nu_n/\nu_K)N_F. \tag{7}$$

General absorption corrections

It is seen from Fig. 1 that after leaving the target the x-rays travel through two thin aluminum films in the x-ray tube, one 0.040 mm thick and the other 0.075 mm thick. The rays next pass through 97.0 cm air, the balanced films and the front window of the ionization chamber which is 0.075 mm aluminum. Inside the chamber the rays first pass through the column of absorbing gas in the region of the front guard electrode before entering the region defined by the collector electrode. It is only those quanta absorbed in the collector electrode region which are measured. To obtain the fraction absorbed in this region, we define the following terms: let i_0 denote the intensity of the $K\alpha$ rays leaving the target i_1 and i_2 the intensity of the $K\alpha$ rays at the front and back e.m.f. of the collector electrode region, respectively, μ_1 the absorption coefficient for aluminum at $\lambda=$ Ag $K\alpha$, and y_1 the thickness of all the aluminum in the x-ray path, μ_2 and y_2 the absorption coefficient and thickness of the air from tube to chamber, μ_3 and y_3 the absorption coefficient and length of the absorbing gas in the chamber, from the front window to the front end of the collector plate, and y_4 the length of the standard collector plate. Then, neglecting the absorption due to the Mo and Rh foils (treated separately above) and calling the target intensity i_0' until this connection is added, we have

$$\begin{aligned} i_2&=i_0'\{e^{-[\mu_1 y_1+\mu_2 y_2+\mu_3(y_3+y_4)]}\} \\ i_1&=i_0'\{e^{-[\mu_1 y_1+\mu_2 y_2+\mu_3 y_3]}\}. \end{aligned} \tag{8}$$

Denoting the powers of the exponential terms involved in i_2 and i_1 by m_2 and m_1, respectively, and also denoting N_F' the number of quanta which get through the foils and are absorbed by the gas in the collector electrode region, we have

$$\frac{N_F}{N_F'}=\frac{i_0}{i_1-i_2}=\frac{1}{e^{-m_1}-e^{-m_2}}. \tag{9}$$

This last equation is correct only if all of the energy extracted from the x-ray beam in the standard collector electrode region is used to produce ions. Actually, this is not true when CH_3Br is the absorbing gas, since in this case fluorescent bromine rays are produced and some of these escape from the collector electrode region unabsorbed. This correction is discussed in the following paragraph.

Correction for unabsorbed fluorescent rays produced in the ionization chamber

When a beam of Ag $K\alpha$ rays pass through the column of gas a fraction of the incident energy is extracted according to the usual law of mass absorption. Part of the absorbed quanta are scattered by the absorbing gas atoms and the remainder interact with the gas atoms to produce photoelectrons and fluorescent x-rays of energy smaller than the incident quanta. The fluorescent rays are partially absorbed by the surrounding gas, producing photoelectrons. If the gas is maintained at sufficient pressure, and the ionization chamber electrodes are far enough apart, all of the energy of the photoelectrons, except those produced within a millimeter or two from the electrodes, will be absorbed by the gas to produce ions. In this experiment for the cases when CH_3Br is used as the absorbing gas, the relatively short fluorescent bromine K rays produced along the axis of the standard ionization chamber are not totally absorbed before they reach the collecting electrodes. A correction is therefore made to account for the energy contained in the unabsorbed Br K quanta. Practically all of the fluorescent bromine L and M quanta produced will be absorbed. A similar correction for the unabsorbed scattered Ag K quanta is negligibly small.

From the geometry of the ionization chamber it is seen that the correction for the unabsorbed fluorescent Br K quanta may be considered in the five following parts: I, the Br K quanta which pass through the boundary of an imaginary cylinder of mean radius "a" and length l, equal to 1/2 the distance between the chamber electrodes and the length of the collector electrode, respectively; II and III, the Br K quanta which leave the collector electrode region through the front and back ends of the above-mentioned imaginary cylinder; IV and V the Br K quanta which enter the collector electrode region through the front and back ends of the cylinder, originating from the front and back guard plate regions. If μ'_{Br} denotes the total absorption coefficient Br $K\alpha$ rays in CH_3Br, w the fluorescence efficiency of bromine, τ the photoelectric absorption coefficient for Ag K rays in CH_3Br, i_1 the intensity of the Ag $K\alpha$ rays at the front end of the collector electrode region, i_x the intensity of the Ag $K\alpha$ rays along the axis of the collector electrode region, i_f the intensity of the unabsorbed Br K rays escaping from the absorption region, then $di_x = -\mu_{Br} i e^{-\mu'_{Br} x} dx$, and the intensity of the Br K rays on a ring dz wide along the cylinder and at a distance r from their source along the axis of the cylinder, will be

$$di_f = di_x \left(\frac{\nu_{Br}}{\nu_{Ag}}\right) w \frac{\tau}{\mu_{Br}} e^{-\mu'_{Br} r} \frac{2\pi r \sin\theta}{4\pi r^2} dz \sin\theta,$$

where $r = [(z-x)^2 + a^2]^{\frac{1}{2}}$ and $\sin\theta = a/r$. For each of the five mentioned cases the above expression leads to an integral for i_f which must be calculated by graphical integration, as indeed was found by Stockmeyer[8] for similar calculations in his measurements on the energy per ion pair of various substances. Evaluation of the integrals for the above-mentioned five parts of the correction, leads to a final value of

$$(1+k_f) = 1.119 \pm 0.006, \qquad (10)$$

where $k_f = i_f/i_1$. Thus for the ionization measurements on Targets 1–8, during which CH_3Br was used in the ionization chamber, approximately 18 percent of the absorbed Ag $K\alpha$ energy escaped from the collector electrode region as fluorescent Br K quanta without producing ions in the chamber.

Saturation current correction in the ionization chamber

Webster and Yeatman[21] and Stockmeyer[8] have measured the electric field strength required to remove nearly all of the ions produced in the absorbing gases used here before recombination occurs. Their saturation curves show that a field strength of approximately 250 volts/cm is necessary to be sure that all but one percent of the ions formed will be collected before recom-

[21] D. L. Webster and R. M. Yeatman, J. Opt. Soc. Am. **17**, 254 (1928).

bination takes place. The electrodes of the ionization chamber used in this experiment were 5.0 cm apart, and a source of 1300 volts of Burgess radio "B" batteries were used. Saturation curves were made with x-ray intensities sufficient to produce ion currents twice as great as any measured during the actual tests to make sure that no more than one percent of the ions formed failed to reach the collecting plates. A one-percent correction is added to the ionization currents to correct for this lack of complete saturation.

Ionization cross section in terms of measured quantities

The method of balanced foils as used in this experiment requires two measurements of charge produced in the ionization chamber, the first being the charge accumulated on the collector plate of the ionization chamber during the exposure time interval and with the Rh foil in the x-ray path, denoted by Q_{Rh}, and second the similar charge (Q_{Mo}) collected when the Mo foil is in the path. The difference between these two charges is proportional to the number of quanta N_F'. Actually N_F' consists of $K\alpha$ quanta as well as the continuous quanta contained between the balanced foil K-limits. If all of these quanta are considered to be of one frequency only, namely, ν_n, as defined by Eq. (6), then the difference between the two charge measurements is

$$Q_{\mathrm{Rh}}-Q_{\mathrm{Mo}}=N_F'h\nu_n e/\epsilon, \qquad (11)$$

where h is Planck's constant, e the electronic charge and ϵ the energy required to produce a pair of ions in the absorbing gas. Combining Eqs. (3), (5), (9), (10), (11) we obtain for the total number of K ionizations produced by N_{CR} cathode rays in the time interval t,

$$N_{KI}=\frac{1.75}{W_K}\frac{4\pi}{\Delta\Omega}\frac{k_d(k_f+1)\epsilon}{eh\nu_K}\frac{Q_{\mathrm{Rh}}-Q_{\mathrm{Mo}}}{e^{-m_1}-e^{-m_2}}(1.01). \qquad (12)$$

In this equation the factor $\Delta\Omega$ is the solid angle subtended by the lead aperture directly in front of the ionization chamber with the focal spot on the target as the center, and 1.01 is the saturation current correction.

The number of electrons which strike the target during the exposure time interval t is $N_E=it/e$, where i is the tube current and e the electronic charge.

The number of atoms per unit cross section of the target is given by $nX_0=(L\rho/A)X_0$, where L represents Avogadro's number, ρ the density of the target material, A its atomic weight and X_0 the thickness of the target. In this case the thin silver foil is inclined at an angle of 80° with respect to the direction of the incident electrons, so the thickness becomes X_0 sec. 80°.

The expression for the ionization cross section (Eq. (1)) may now be written in the final form involving the quantities determined by the measurements. Thus

$$\Phi(U)=\frac{\frac{1.75}{it}\frac{4\pi}{\Delta\Omega}\frac{k_d(k_f+1)}{h\nu_{K\alpha}}\frac{Q_{\mathrm{Rh}}-Q_{\mathrm{Mo}}}{e^{-m_1}-e^{-m_2}}(1.01)}{(L\rho/A)X_0 \text{ sec. } 80^\circ}. \qquad (13)$$

In the above expression $\Phi(U)$ has the units of cm² if it is measured in ampere-seconds, $Q_{\mathrm{Rh}}-Q_{\mathrm{Mo}}$ in coulombs, ϵ and $h\nu_{K\alpha}$ in electron volts, ρ in g/cm³ and X_0 in cm. The *International Critical Tables* (1926) values for the atomic weight and density of silver were used and the I.C.T. values of Ag $K\alpha_1K\alpha_2$ were corrected according to Bearden's[22] results, making $h\nu_{K\alpha}=22{,}068$ electron volts. The value of the linear absorption coefficient for aluminum for $\lambda=559.4$ X.U. was computed from Jönsson's[23] empirical formula to be $\mu_{\mathrm{Al}}=7.81$ cm^{-1}. The linear absorption for air was taken from a curve of data represented by Siegbahn.* For air at 760 mm and 20°C at $\lambda=559.4$ X.U., $\mu_{\mathrm{air}}=0.00082$ cm^{-1}. The lead aperture used to define the x-ray beam was 4.69 ± 0.02 mm in diameter. This measurement was very kindly furnished by Mr. M. S. Hugo of the U. S. Government Gauge Laboratory at Stanford University. The distance from the focal spot to the lead aperture varied for various target measurements. For targets 1–4 this distance was 101.5 ± 0.3 cm for Targets 4–10 the x-ray tube was moved a small amount and this distance was 107.6 ± 0.3 cm. The error introduced in $4\pi/\Delta\Omega$ by the uncertainties in aperture diameter and focal spot to aperture distance is negligible. The values of the energy per ion pair for CH_3Br and

[22] J. A. Bearden, Phys. Rev. **43**, 92 (1933).

[23] E. Jönsson, Inaugural Dissertation, Upsala University, Sweden, 1928.

* M. Siegbahn, *Spektroskopie der Röntgenstrahlen*, 2nd ed., Table 227.

TABLE I. *Thickness of silver foils for targets.*

Method	Number of foils tested	Thickness per foil X_0
X-ray abs.	8	0.171 micron
" "	7	0.180
" "	6	0.153
Weight	1	0.171
		0.169±0.004 micron

SO_2 are those given by Stockmeyer[8, 24] as $\epsilon_{CH_3Br}=25.4$ electron volts, and $\epsilon_{SO_2}=29.7$ electron volts. These values are based on Eisel's[25] determination of ϵ for air to be 32.2 electron volts. Eisel gives his probable error to be ±1.5 percent, and allowing for an error in the relative measurements of Stockmeyer, the above values for ϵ are here taken to be correct to within ±2.5 percent.

V. TARGET THICKNESS

The thin silver foils used for targets were taken from the same lot as those used by Wesbter, Hansen and Duveneck.[7] These foils were obtained commercially under the name of pure silver leaf, and look and behave very much the same as gold leaf. They are prepared by a "beating" process and their thickness is not uniform.

[24] This work was completed in January, 1935, and since that time Gaertner, Ann. d. Physik **21**, 564 (1934), reports experiments on the determination of the energy per ion pair for air and gives the value $\mu_{air}=35.2$ electron volts. Also E. Arends, Ann. d. Physik **22**, 281 (1935), reports the fluorescence efficiency for silver $w_K=0.795$. These results would increase the value of $\Phi(U)$ reported here by one percent.

[25] A. Eisel, Ann. d. Physik **395**, 277 (1929).

Measurement of thickness by x-ray absorption

The absorption of x-rays of wavelength where the mass absorption coefficient of silver is accurately known is too small to measure for a single foil of such a small thickness (mean thickness 0.17 micron). In order therefore to use absorption methods several foils are placed in the x-ray path. Foils of this thickness are difficult to handle, and it is best not to remove them from the tissue paper booklet in which they are transported. In this experiment the absorption measurements were made at the Ag K limit, in which case the effect of the paper is eliminated from the thickness determinations. That is, if μ_a and μ_b denote the minimum and maximum absorption coefficient of silver at the K limit, respectively, I_a and I_b the corresponding intensities of the transmitted x-ray beam, and μ_p the absorption coefficient of the paper at this wavelength, then

$$I_a=I_0e^{-\mu_aNX_0-\mu_px}; \quad I_b=I_0e^{-\mu_bNX_0-\mu_px}$$

and

$$X_0=\frac{1}{N}\frac{\log(I_a/I_b)}{\mu_b-\mu_a},$$

where NX_0 represents the thickness of N silver foils. Measurements of x-ray intensities were made over a wavelength region of 100 X.U. above and below the K limit with the foils in the path. A spectral curve was plotted, and because of the width of the discontinuity the upper and lower portions of the curve were extended to the middle point of the discontinuity, in order to obtain the magnitude of the discontinuity accurately. This extrapolation was done by the λ^3 law, and Richtmyer's[20] values for μ/ρ at the K limit were used. The results of the thickness

TABLE II. *Film 1, test 1.* Tube voltage 70.0 kv, exposure time t 18.0 sec., tube current i 30.15 microamperes.

Balanced film	Electrometer deflection, mean of 5 expos.	Vltg. on ioniz. system to cause deflection	Capac. of ionizat'n syst. at this deflect'n	Charge collected
Rh	249.0 mm	0.0702 volt	118.5$\mu\mu$f	8.32×10^{-12} coul.
Mo	134.6	0.0398	114.5	4.56×10^{-12}
			uncorrected $Q_{Rh}-Q_{Mo}$	$=3.76\times10^{-12}$
	Extraneous radiation from places on target other than focal spot			
Rh	7.85 mm	0.0020 volt	110.6$\mu\mu$f	0.221×10^{-12}
Mo	6.00	0.0015	110.6	0.166×10^{-12}
			extraneous rdn. correction $Q_{Rh}-Q_{Mo}$	$=0.055\times10^{-12}$
			Resultant charge collected $Q_{Rh}-Q_{Mo}$	$=3.70\times10^{-12}$ coul.

TABLE III. *Values of $\Phi(U)$ for all silver films.*

Target	No. of tests	Mean $\Phi(U)$ ($\times 10^{23}$ cm^2)	Target	No. of tests	Mean $\Phi(U)$ ($\times 10^{23}$ cm^2)
1	2	4.58	6	6	4.28
2	2	5.04	7	3	4.40
3	1	5.13	8	3	6.37
4	9	3.68	9	3	4.52
5	5	5.51	10	3	4.46
				Average	4.80±0.16

measurements, together with a thickness determination by "*weighing*" are shown in Table I.

Measurement of thickness by weight measurements

The area and weight of one of the foils 89.094 cm^2 and 16.005 g was determined by a series of measurements with a Starrett steel scale and microscope and an F. Sartorious beam balance. The weights used were the laboratory standards of this department.

VI. RESULTS

A set of sample data are presented in Table II. From formula (13) the value of the ionization cross section for this test is therefore $\Phi(U) = 4.57\times10^{-20}$ cm^2. In the following Table III is shown the results of tests made on 10 thin silver foil targets. The ionization currents for Films 1–7 were produced by absorbing the x-rays in CH_3Br at approximately 680 mm Hg, while SO_2 at about 20 lbs./in.^{2} was used for Films 7–10. Only one test was obtained on Film 3 before it was punctured, either by melting or a sudden release of gas in the x-ray tube. Tube currents varying between 30 and 60 microamperes were used throughout the measurements, although it was found that these silver foils would not last more than an hour or so with currents over 50 microamperes. The probable error of ±0.16 is due to variations in the measurements of $(Q_{Rh}-Q_{Mo})$ and the variations in film thickness X_0.

Accuracy of results: It is seen from the report of this work that the measurements involved in the determination of $\Phi(U)$ are not direct, but that the final value is obtained from a number of very different physical measurements. Some of the measurements are those made by the author, while those involved in the determinations of certain constants and coefficients such as w_K, μ_{Al}, μ_{air}, ϵ, $I_{K\alpha}:I_{K\beta}$, etc., are the results of work by others. The errors in the measurements by the author are well known, and in the cases where the errors of other workers are not stated, a fair estimate is here assumed for the purpose of calculating the error of this work.

In the factor $1.75/w_K$, w_K was obtained from a graph drawn from the data of several observers,[16, 24] and estimated to be 0.72±3.0 percent while the term 1.75 is the result of two numerical values obtained from formula (2) and (4). In (2) the errors of each of $(I\lambda)$ are estimated to be correct to one percent and in (4) the factors k and R are computed to be correct to ±3.8 and ±4.96 percent, respectively. This makes the probable error in the fraction $1.75/w_K$ equal to ±7.6 percent. The probable errors in the factors $4\pi/\Delta\Omega$, $h\nu_{K\alpha}$ and $(L\rho/A)$ sec. 80° are considered negligibly small. In the factor $e^{-m_1}-e^{-m_2}$ the terms m_1 and m_2 consists of terms of the form (μx), each of which are estimated to be in error by 1.0 percent, making the probable error of the total factor $e^{-m_1}-e^{-m_2}$ equal to ±3.0 percent. As previously discussed the probable error in ϵ is estimated to be ±2.5 percent. The factors remaining are $(Q_{Rh}-Q_{Mo})$ and X_0. A measure of the error in these terms is available in the data given in Table II. Here the variation in $\Phi(U)$ is due to the variation in both $(Q_{Rh}-Q_{Mo})$ and X_0 and the probable error is ±3.3 percent. The probable error in the variations of the Q's can be calculated from data available, but not represented in this report, and is ±0.3 percent.

The most probable value of the resultant error in $\Phi(U)$, obtained by combining the above outlined errors is found to be ±9.0 percent, making the most probable value of $\Phi(U)$ obtained from these measurements equal to[24]

$$\Phi(U) = (4.80\pm0.43)\times10^{-25}\ \text{cm}^2.$$

VII. THEORETICAL

There have been several theoretical attempts given to the problem of the determination of the probability of inelastic scattering of electrons by atoms. The earlier predictions are based on the classical quantum theory, while the more recent theories involve the wave mechanics. The classical quantum theories of Davis,[26] Rosse-

[26] B. Davis, Phys. Rev. **11**, 433 (1918).

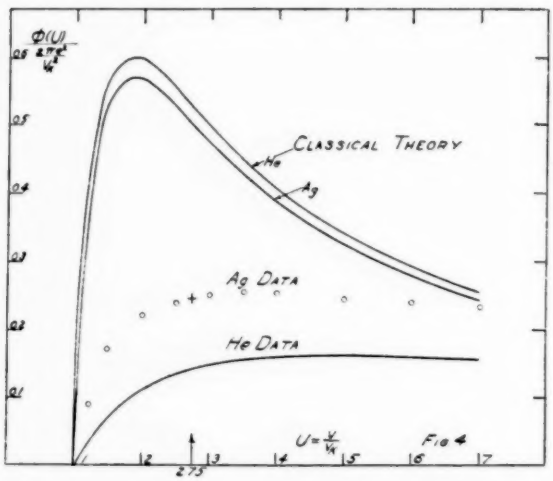

FIG. 4. Ionization cross sections *vs.* energy. Classical theory and an experiment compared for silver and helium.

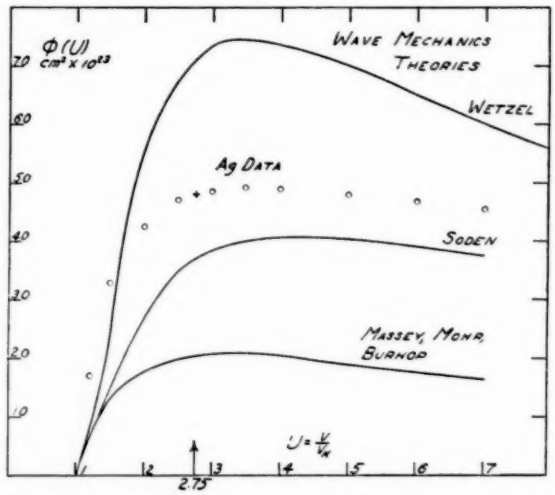

FIG. 5. Ionization cross section *vs.* energy. Wave-mechanical theories compared with data on silver.

land,[27] and Thomas[28] are fully discussed in the paper by Webster, Hansen and Duveneck.[7] Modifications of the nonrelativistic classical quantum theories to account for the deflection of the impinging electron before the ionizing impact are applied by the latter authors and the results, labeled "Classical theory," are shown in Fig. 4. In this figure P. T. Smith's[6] data on the absolute value of the ionization cross section for helium are shown together with data of Webster, Hansen and Duveneck on the relative probabilities of K electron ionization for silver. These relative measurements are normalized at $U=2.75$ by the absolute value of the ionization cross section for silver determined by the author. The curves show the classical theory represents a very rough approximation to the facts at high values of U, but that it is practically useless for $U<5$.

The wave mechanics theories appear to be leading to results which compare more favorably with the experimental data. However, all of the wave mechanics theories so far reported treat the interaction of the impinging electron with the K electron as a small perturbation in the same way as it is done in Born's theory of collisions. The approximation is valid only for electrons with kinetic energy large compared to the ionizing energy. It therefore seems quite certain that any theory based on Born's approximation cannot be expected to be accurate for a value of U as small as that used in this experiment, namely, $U=2.75$. Besides this most serious source of error, in all but Soden's paper, the orbits of the atomic electrons are treated as hydrogenic orbits; an assumption which is wrong and can only roughly be corrected by screening constants. It is probably due to the latter reason that the results of Burhop and Wetzel deviate more from the experimental values than those of Soden.

In Fig. 5 are shown Webster, Hansen, Duveneck and the present author's experimental data of the ionization cross section of silver as a function of U, compared with the wave mechanics theories. Three curves of Massey, Mohr and Burhop and Wetzel are taken from such curves contained in personal correspondence on this subject between these authors and Professor D. L. Webster during the interval between September, 1933 and May, 1934. It is evident from this correspondence that these curves represent only a first attempt at a solution of this problem for the case of silver.

[27] G. Rosseland, Phil. Mag. **45**, 65 (1923).
[28] L. H. Thomas, Proc. Camb. Phil. Soc. **23**, 829 (1927).

ACKNOWLEDGMENTS

The author wishes to express his appreciation for the many valuable suggestions and comments of Professors P. A. Ross, P. Kirkpatrick and F. Bloch, and in particular to thank Professor D. L. Webster, under whose guidance this work was done. He wishes also to acknowledge gratefully the financial support given by the Research Committee of Stanford University.

Direct and Fluorescence Excitation of the K Level in Thick Targets of Gold

K. B. STODDARD, *Stanford University*

(Received May 7, 1935)

The ratio P of the number of $K\alpha$ line quanta produced by direct cathode electron impact to the number of quanta produced by fluorescence as observed in the radiation from a thick gold target, is measured with normally emergent x-rays over a range of voltages extending from 1.3 to 2.2 times the K excitation voltage. P is found to vary from 0.195 at $U=1.3$ to 0.27 at $U=2.2$, where U is the ratio of tube voltage to K excitation voltage. The ratio Q of the probability of a cathode electron ionizing the K shell directly to the probability of a cathode electron exciting a continuous quantum of frequency greater than the K limit frequency is found to vary from 0.07 at $U=1.3$ to 0.11 at $U=2.2$. A discussion of the variation of P with atomic number found experimentally and that to be expected theoretically is given, still indicating a lack of agreement between theory and experiment.

INTRODUCTION

IT has been shown by recent papers[1–3] that the number of $K\alpha$ line quanta produced by direct cathode-electron impacts bears very nearly a constant ratio to the number of $K\alpha$ line quanta produced by fluorescence. This ratio, usually called the direct to indirect ratio P, shows a slight increase with voltage tending to become more nearly constant at the higher voltages. A definite idea of the change in P with voltage can be given from the recent work on copper.[3] P increases from 6.63 at twice the K excitation voltage for copper to 7.2 at 17.4 times this excitation voltage. In this case the increase of P with voltage was very nearly constant over the entire voltage range. Data on palladium[2] and silver[1] tend toward a constant P as the voltage increases.

In the work on copper[3] a comparison of the variation of P with atomic number, for a constant value of U determined from various experimental data for silver, palladium and copper was made with the theoretical variation of P with Z obtained from an elementary theoretical discussion. The result of the comparison showed a lack of satisfactory agreement between experiment and theory. Theory predicted that P should vary with $Z^{-4.8}$ with constant U, and the empirical data available indicated a variation with $Z^{-2.6}$. This deviation was considered to be outside the experimental limits of error. Any attempt to improve the theory resulted in a slightly wider deviation. The data, however, did not cover a sufficient number of different elements to make the experimental variation conclusive. It was to clarify this point that the present experiment was started, and in order to obtain as wide a spread of atomic numbers as possible, gold was chosen for the target material.

THEORY OF EXPERIMENT

The same experimental method of measurement of P used for copper[3] was used in this investigation. This method makes use of the ratio of the Au $K\alpha$ line intensity from a gold target to the Au $K\alpha$ line intensity from the same target covered with a palladium foil sufficiently thick to stop all the cathode electrons. In the latter case all the K excitation in the Au target is by fluorescence. The ratio P is obtained from the ratio of the two intensities stated above, together with certain calculations to be outlined below. Palladium was chosen for the foil material because the mean depth of production of the continuous rays had been measured previously for the voltage range here considered.[2]

In the following expressions all intensities are to be defined as energy per unit solid angle, per cathode electron.

The following symbols are defined as follows:

I = intensity of Au $K\alpha$ lines (unresolved) from the bare gold target;
d = part of I produced directly;
i = part of I produced by fluorescence;
i_+ = part of i that is produced at depths greater than $\bar{x}$, the mean depth of production of the continuous rays;
i_- = part of i produced at depths less than $\bar{x}$;
i_0 = intensity of Au $K\alpha$ lines from gold target covered with palladium foil.

The intensity from the bare gold target will be

[1] D. L. Webster, Proc. Nat. Acad. Sci. **14**, 339 (1928).
[2] W. W. Hansen and K. B. Stoddard, Phys. Rev. **43**, 701 (1933).
[3] K. B. Stoddard, Phys. Rev. **46**, 837 (1934).

composed of both direct and fluorescence rays. $I=d+i$ and as $P=d/i$ by definition, $P+1=I/i$. The expressions for i_+, i_-, and i_b are given immediately below.[3]

$$i_+=R[\exp(-\mu_{\alpha 2}\bar{x}_2)]F(V,0);\quad i_-=R\Phi(V,\bar{x}_2);$$

$$i_b=R[\exp(-\mu_{\alpha 1}x_1)]f(V,x_1-\bar{x}_1),$$

where

$$F(V,0)=\int_{\nu_k}^{\nu_0}(I(V,\nu)/\nu)(\mu_2/\mu_{\alpha 2})\log(1+\mu_{\alpha 2}/\mu_2)d\nu,$$

$$\Phi(V,x)=\int_{\nu_k}^{\nu_0}(I(V,\nu)/\nu)(\mu_2/\mu_{\alpha 2})\{[\exp(-\mu_{\alpha 2}x)][Ei\{(\mu_{\alpha 2}-\mu_2)x\}-\log|(1-\mu_{\alpha 2}/\mu_2)|]-Ei(-\mu_2 x)\}d\nu,$$

$$f(V,x)=\int_{\nu_k}^{\nu_0}(I(V,\nu)/\nu)(\mu_2/\mu_{\alpha 2})[\{\exp(a\mu_{\alpha 2}x)\}Ei\{-(a\mu_{\alpha 2}+\mu_1)x\}-Ei(-\mu_1 x)]d\nu,$$

$$R=\tfrac{1}{2}u_\alpha\nu_\alpha(\mu_k/\mu_2),$$

where $\mu_1=6.13\times10^{27}\,c^3\nu^{-3}+12)$ cm^{-1} absorption coefficient for Pd;[4]

$\mu_2=4.31\times10^{28}\,c^3\nu^{-3}+16.4)$ cm^{-1} absorption coefficient[4] for Au;

$\mu_{\alpha 1}=49.5$ cm^{-1} absorption coefficient of Pd for Au $K\alpha$ rays;[4]

$\mu_{\alpha 2}=73.2$ cm^{-1} absorption coefficient of Au for Au $K\alpha$ rays;[4]

$a=\mu_1/\mu_2$;

$\mu_K/\mu_2=0.82$ ratio of K absorption to total absorption in Au;

u_α = number of K electrons ejected that reappear as $K\alpha$ quanta;

ν_K = frequency of K discontinuity;

ν_0 = high frequency limit;

ν_α = Au α line frequency;

$\bar{x}_1$ and $\bar{x}_2$ are the mean depths of production of the continuous rays in Pd and Au, respectively;

x_1 thickness of Pd foil;

$I_1(V,\nu)=\delta k[(\nu_0-\nu)-bZ_{\mathrm{Pd}}\nu_0]$;

$I_2(V,\nu)=k[(\nu_0-\nu)-bZ_{\mathrm{Au}}\nu_0]$;

$b=1.2\times10^{-3}$ sec^{-1}.[5]

The above expressions for i_+, i_- and i_b are evaluated by numerical integration. The constant δ in $I_1(V,\nu)$ is evaluated for each voltage from the criterion that $I_1(V,\nu_\alpha)=I_2(V,\nu_\alpha)$; that is, the continuous spectrum intensities are matched at ν_α.

The expression for $P+1$ is

$$P+1=I/i=(I/i_b)[i_b/(i_++i_-)],$$

where I/i_b is the ratio of the intensity of the Au α lines without the foil to the intensity with the Pd foil, measured in the same units. The α line intensity produced directly is a fraction $P/P+1$ of the total.

The ratio Q of the probability of a cathode electron ejecting a K electron directly to the probability of a cathode electron exciting a continuous quantum of frequency greater than the K limit frequency as determined from a thick target, may be immediately evaluated from P with a small calculation.[6]

$$Q=iP\exp(\mu_{\alpha 2}\bar{x}_2)/[\mu_a\nu_a\int_{\nu_k}^{\nu_0}(I_2(V,\nu)/\nu)d\nu].$$

The results of the calculations obtained by numerical integration, together with the measurements and values for P and Q are given in Table I.

TABLE I. *Calculations and measurements leading to the values for P and Q.*

$U=V/V_K$	1.3	1.6	1.9	2.2
Calculated quantities				
i_+/D*	0.0545	0.168	0.319	0.49
i_-/D	0.0098	0.038	0.089	0.167
i/D	0.0643	0.206	0.408	0.657
i_b/D	0.0351	0.113	0.225	0.365
Measured quantities				
$\bar{x}_1\cdot10^4$ in cm	3.5	5.3	7.4	10.5
$\bar{x}_2\cdot10^4$ in cm	2.8	4.3	6.0	8.5
I/i_b	2.19	2.23	2.27	2.28
Results				
P	0.195	0.225	0.255	0.27
$P/P+1$	0.163	0.184	0.203	0.212
Q	0.07	0.088	0.103	0.11

*$D=Rk\nu_K$.

Experimental Discussion

In this experiment as in previous ones[1–3] the x-rays leave the target perpendicularly. The angle between the incident cathode electrons and the observed emergent x-rays is 60 degrees.

[4] F. K. Richtmyer, Phys. Rev. **27**, 1 (1926).

[5] Int. Crit. Tab. **6**, 46 (1929).

[6] The expression for Q given in reference 3 is incorrect. The numerical values for Q, however, are correct.

Dispersion of the x-ray beam was obtained by a Bragg spectrometer.

The mean depth of production $\bar{x}_2$ of the continuous rays in gold was measured by the method used by Webster and Hennings.[7] The mean depth $\bar{x}_1$ in palladium was obtained from a previous paper.[2] It is assumed in this work as before that the continuous rays of frequency greater than the K excitation frequency are all produced at the same average depth $\bar{x}$. The justification for this assumption has been discussed before.[3]

In obtaining the ratio I/i_b the first step was to measure the ratio of the line ordinate to the continuous ordinate $I_\alpha/I_{c\alpha}$ for the bare gold target. By keeping the spectrometer set-up unchanged, the corresponding ratio $i_\alpha/i_{c\alpha}$ was then obtained for the gold target covered with the palladium foil. Since the ratio I/i_b is really obtained by matching the continuous spectrum intensities in the two cases, it is essential that this be done for the continuous intensities correcting for target absorption.

Therefore

$$I/i_b=[(I_\alpha/I_{c\alpha})\exp(\mu_{\alpha 1}\bar{x}_1-\mu_{\alpha 2}\bar{x}_2)]/(i_\alpha/i_{c\alpha}).$$

When the slits on the spectrometer were set for a reasonable exposure time for the thin foil measurements, the resolution was such that it was impossible to obtain continuous spectrum points between the $K\alpha$ and $K\beta$ lines. Analytical interpolation was therefore resorted to, to obtain $I_{c\alpha}$ and $i_{c\alpha}$. The continuous spectrum was assumed to approximate a fourth power parabola. This form was chosen after examining the continuous spectrum curves used in measuring $\bar{x}_2$.

Discussion of Results

Before discussing the results certain errors involved in the measurement of P should be specifically pointed out. The error in the determination of I/i_b is approximately four percent. The major uncertainty here is due to the method of interpolation. Expansion in a Taylor's series about λ_α to obtain the continuous intensity at λ_α was used. Because of the symmetry of the continuous spectrum the cubic term was neglected and fifth and higher power terms discarded. It is unfortunate that a continuous point could not be obtained between the $K\alpha$ and $K\beta$ lines. This would have increased the accuracy of $I_{c\alpha}$ materially. Various other methods of interpolation such as approximate graphical ones, assuming the form of the continuous spectrum to approximate a cubic, etc., gave values for $I_{c\alpha}$ that differed from the average by as much as two percent. It is observed that the same uncertainty occurs in $i_{c\alpha}$ hence the influence on I_α/i_α is less. The intensity for the measured continuous points was determined with an accuracy of better than one percent by repeated measurements on each point.

Little accuracy can be claimed for the $\bar{x}$ measurements in Au. The sharp decline of the continuous spectrum intensity due to excessive transmission of the ionization chamber near the Au K limit made the extrapolation necessary in the determination of $\bar{x}$ very uncertain. This uncertainty led to a special investigation of the variation of $P+1$ with change in $\bar{x}_2$. It was found that an error of 15 percent (the probable error in the determination of the mean depth) in $\bar{x}_2$, caused an error of 2.3 percent in $P+1$. As long as $P\gg 1$, the influence on P of such an error in $\bar{x}_2$ is not important with reference to other errors in the experiment, but when $P<1$, as in the present case, it becomes relatively more important. For example although $P+1$ changes by 2.3 percent for a 15 percent change in $\bar{x}_2$, P changes by very nearly 12 percent. It should be pointed out that this line of argument also applies to the error in $P+1$ due to probable error in I/i_b. For an error of four percent in I/i_b the error in P is approximately 18 percent. These two sources of error and the way in which their effect is amplified indicates that the results for gold are relatively less accurate than the P and Q determinations for the other elements.[1-3]

Numerous assumptions are made in the development and evaluation of the expressions for i_+, and i_- and i_b. It is practically impossible to estimate the influence of errors introduced by these assumptions. It is thought, however, that a probable overall error of 30 percent in the determination of P will include all these uncertainties. A similar overall error is to be understood for the values for Q.

[7] D. L. Webster and A. E. Hennings, Phys. Rev. **21**, 301 (1923).

The results tabulated in Table I are in accord with other determinations[1-3] of P and Q. It is seen that the gradual increase of P and Q with U and the tendency toward a constant value for the higher voltages is also observed for gold.

In gold it is approximately four times as probable for the K shell to be ionized by fluorescence as for it to be ionized by cathode electron impact, while the probability of a cathode electron producing a K quantum is only about 1/10 of the probability of its producing a continuous quantum of frequency greater than the K limit frequency.

Variation of P and Q and Z

In a previous paper[3] the writer gave a simple theoretical argument indicating that P should vary as $Z^{-4.8}$ for a constant value of U. The empirical data then available indicated that P varied as $Z^{-2.6}$. The collected data for Ag, Pd, Cu and Au for several values of U are given in Table II. In Fig. 1 $\log P$ is plotted against $\log Z$ for $U=2$. It is seen that no constant power of Z will fit the data.

Table II. *P tabulated for various elements, for several values of U.*

U	1.5	2.0	2.5
P_{Cu}	6.60*	6.63	6.65
P_{Pd}	1.93*	1.97	1.99
P_{Ag}	1.85	1.89	1.92
P_{Au}	0.22	0.26	0.28*

* Extrapolated values.

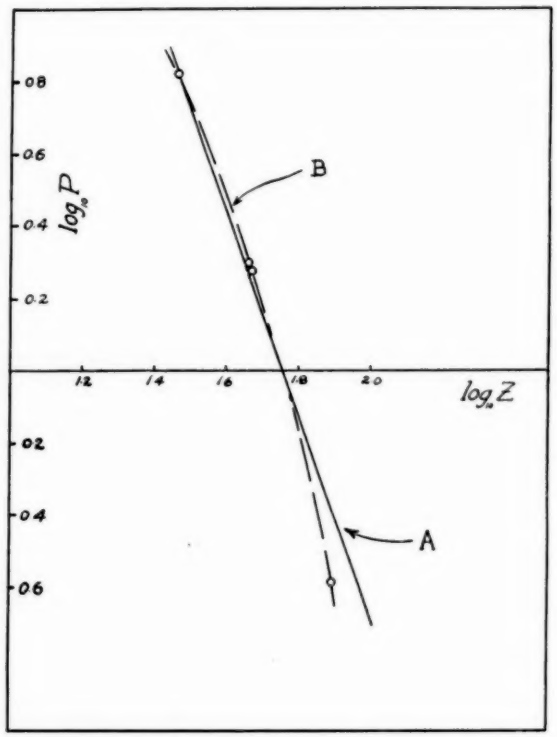

Fig. 1. $\log_{10} P$ plotted as a function of $\log_{10} Z$ for $U=2$.

If it is assumed that P should vary with Z to a constant power then the straight line A in Fig. 1 having an average slope of -2.78 for the three values of U given in Table II is the best fit. This assumes that the data for P are all of the same accuracy. Actually the data on Au are not as accurate as the other data and hence should be weighted less. This would decrease the absolute value of the slope slightly.

On the other hand the only reason for expecting P to vary with a constant power of Z is obtained from the theory given in the paper on copper.[3] This theory is incomplete. There are a number of factors which vary in a minor fashion with Z such as the rediffusion of cathode electrons, cathode electron retardation, μ_k/μ_2, etc. These were assumed to be independent of Z. If these assumptions are not made, it is evident that P will not vary with a constant power of Z. It so happens that the influence of these factors is very small in comparison with the factor $Z^{-4.8}$, and unless there is some factor omitted in the theoretical discussion or some assumption involved in the calculation of P that is not justified, the agreement between theory and experiment must be considered unsatisfactory. Discarding the notion that P should vary with a constant power of Z, one is no longer restricted to a straight line for the $\log P$ *vs.* $\log Z$ curve. The points in Fig. 1 are distributed in such a fashion that they do not indicate a unique curve. A parabola passed through the points of Fig. 1 shown by curve B will serve for the empirical variation of P with Z for interpolation purposes until more data are obtained. Curve B corresponds to the formula

$$\log_{10} P = -2.71 + \log_{10} Z(6.76 - 2.97 \log_{10} Z).$$

Interpolation according to this formula will be well within the experimental error.

The foregoing discussion applies equally well to Q as the variation with Z should be approximately the same as that for P.

Remarks on the Systematics of Isotopes

GUIDO BECK, *Department of Physics, University of Kansas*
(Received May 3, 1935)

A comparison between the older views on the structure of nuclei and recent ideas is given and possibilities are discussed which might guide to a decision between the two views.

§1

THE problem of the systematics of isotopes has been treated a number of years ago by several authors and it has been shown that there exist distinct regularities in the occurrence of stable isotopes which have to be regarded as an expression of the unknown laws governing the structure of atomic nuclei. These regularities being independent of the special assumptions on the nature of the elementary nuclear particles have since been proved to be fruitful especially in the important discovery of the heavy hydrogen.

In addition to this, these investigations have supported the view that the nuclear structure has to be described in terms of a peculiar interaction of heavy nuclear particles and electronic charges and that in particular the alpha-particle plays an important role as an intermediary subnuclear unit in the nuclear structure.

The discovery of the neutron since has led several authors to the conclusion that a consistent picture of the nuclear structure might be obtained by building up nuclear aggregates from protons and neutrons only. This assumption, indeed, would allow us to treat the problem according to the well-established laws of wave mechanics without taking into account the behavior of nuclear charges explicitly. As far as the systematics of isotopes is concerned even the opinion has been expressed that the older views definitely have to be abandoned and that the nuclear structure should be described only in terms of neutron and proton levels in the nucleus.

A careful and detailed investigation is required to decide to what extent each of these different views might be justified and this investigation will have to take into account all evidence furnished by experiments. The following remarks may be regarded as a preliminary introduction to the discussion of this problem which will be carried on in a series of detailed investigations on the various aspects of the nuclear phenomena.

§2

The peculiar situation we are faced with in nuclear physics requires two, at present independent, lines of attack. The first is concerned with the behavior of heavy particles interacting with nuclei and can at first be based on the nonrelativistic wave-mechanical treatment of these particles. The second attempt has to deal with the behavior of electronic charges in nuclear phenomena, starting from the highly developed theory of the electron. No reason exists at present to believe that more than these two problems have to be solved in order to obtain a complete understanding of the nuclear phenomena and there exists scarcely any disagreement of opinion that both of these problems in principle will have to be treated. But it seems to be a general opinion that the two problems in question can be separated to a large extent and that the second problem only will have to be solved *after* a general understanding of the nuclear structure has been obtained from the treatment of the heavy particles. The behavior of the electronic charges should then only account for the interaction of a proton and a neutron and for the structure of these two particles.

There exist, however, some doubts whether this separation of the two main problems can lead to fruitful results. The author would like to lay emphasis on the fact that the complete treatment of nuclear phenomena certainly requires the introduction of one entirely new point of view in order to account for the existing asymmetry of the phenomena with respect to the sign of the electric charge. This asymmetry has become especially obvious in the failure to detect a negative proton which—for symmetry reasons—should occur in disintegration processes with a probability similar to that of the occurrence of

positive protons. Though the assumption that only positive protons and neutrons exist in the nuclei accounts for the mentioned asymmetry, the necessity of introducing a new fundamental element into the theory excludes at once any safe conclusion that these new features will not show up also in other nuclear phenomena. We shall see later that the complex character of the radioactive beta-decay suggests that new elements will have to be introduced into the theory which are likely to be related to the asymmetry.

§3

As far as the problem of the heavy particles is concerned no definite results have been obtained to date as to whether we are allowed to speak about single particles inside the nucleus. Recently, P. Wenzel has been able to show that it is possible to ascribe to the virtual energy levels of light nuclei well-defined angular momentum quantum numbers and that these quantum numbers can be determined from observations of the anomalous scattering at large angles.[1] Wenzel's method has been applied by L. H. Horsley and his results show that there exists a marked and very simple regularity in the designation of the virtual levels of the various light elements.[2] Certainly Horsley's results have thus far to be regarded as an empirical regularity, but they show that the concept of a phenomenologically introduced intranuclear field can be applied with advantage *qualitatively*. We have, however, no evidence so far, to what extent *quantitative* conclusions can be based on Horsley's model.

In addition to that, Horsley's results suggest that the lightest nuclei of weight $4n$ have to be described in terms of alpha-particle aggregates. This view is also strongly supported by the known packing energies. These arguments, however, do not exclude the possibility that heavier nuclei might contain a number of protons and neutrons not bound in alpha-particles, but they exclude any scheme which deals with quantum levels of protons and neutrons only.

§4

The most detailed information on the behavior of nuclear charges is furnished by the radioactive beta-decay. The first attempt to proceed to a theory of this phenomenon has been made by Beck and Sitte. The formalism of this theory, which is based on Dirac's theory of the electron, seems sufficient to account for all observed facts, but additional evidence is required in order to test the various assumptions of the theory. The objections raised against the quoted treatment do not concern the connection of the theory with the experimental evidence but criticise the abandonment of the conservation laws. Fermi has given a modification of the theory of Beck and Sitte the purpose of which is to connect the beta-decay exclusively with the characteristics of the heavy nuclear particles. If such an attempt could be proved to be successful it certainly would lend considerable support to the view that the separate treatment of the two main nuclear problems is justified. It has been pointed out by Beck and Sitte that this might not be the case. R. L. Dolecek has undertaken to present Fermi's theory in a form in which the objections against Fermi's treatment become obvious and has shown that it leads to disagreement with the present experimental evidence.[3] Dolecek's results thus may be taken as an illustration for the views expressed in §2.

[1] P. Wenzel, Zeits. f. Physik **90**, 754 (1934).
[2] L. H. Horsley, Phys. Rev. **47**, 1 (1935).
[3] R. L. Dolecek, Phys. Rev. **47**, 13 (1935).

Linear Modifications in the Maxwell Field Equations

ROBERT SERBER,* *University of California, Berkeley*

(Received April 24, 1935)

Expressions, accurate to the first order in e^2, are obtained for the charge and current densities which, according to positron theory, are induced in vacuum by an electromagnetic field. Because the corresponding correction terms in the Maxwell field equations involve integral operators, it does not seem possible to treat the modified field equations by Hamiltonian methods.

THE theory of the positron introduces certain modifications in the classical electromagnetic field equations of Maxwell, which result in the equations of the field being no longer equivalent to a system of linear second order differential equations. These modifications arise from the interaction of the electromagnetic field with the continuous distribution of electrons in negative energy states envisaged by the theory. The interaction is treated by expanding the interaction terms in the Hamiltonian function in powers of the electronic charge; in the following we shall consider only effects in e^2. In this order the linearity of the equations is still preserved and the effect of the interaction can conveniently be expressed as the induction of a charge and current density in vacuum by the electromagnetic field.

STATIC FIELDS

We shall first investigate, using the methods recently formulated by Dirac[1] and Heisenberg,[2] the charge and current densities induced by a static field. The equations take their simplest form when written in terms of the Fourier amplitudes of the quantities involved; the Fourier amplitude of a function $f(\mathbf{r})$ corresponding to a propagation vector $\mathbf{k}$ will be written simply f.

The Fourier amplitude of the charge induced by an electrostatic field which is everywhere small compared to the critical field $F_c=m^2c^3/eh$ can be written[3]

$$\delta j_0=-(\alpha/4\pi^3)\chi(k)A_0=-(\alpha/\pi^2k^2)\chi(k)j_0, \quad (1)$$

where $j_0(\mathbf{r})$ is the charge density, $A_0(\mathbf{r})$ is the scalar potential, k is the magnitude of the propagation vector $\mathbf{k}$, and

$$\chi(k)=\int \frac{\epsilon\epsilon'-(q^2+1-\frac{1}{4}k^2)}{\epsilon\epsilon'(\epsilon+\epsilon')}e^{i(q\cdot R)}d\mathbf{q}, \quad (2)$$

$$\epsilon=[1+(\mathbf{q}+\tfrac{1}{2}\mathbf{k})^2]^{\frac{1}{2}}, \quad \epsilon'=[1+(\mathbf{q}-\tfrac{1}{2}\mathbf{k})^2]^{\frac{1}{2}}.$$

The second form of (1) is obtained from the first by means of the equation $\Delta A_0(\mathbf{r})=-4\pi j_0(\mathbf{r})$. From the integral (2) certain singular terms and normalization terms are still to be subtracted, after which the "off diagonal distance," $\boldsymbol{R}$, is to be put equal to zero. Explicit expressions for these subtractitive terms are given in Heisenberg's paper. Introducing the abbreviations $a^2=1+\frac{1}{4}k^2$, $v=\mathbf{q}\cdot\mathbf{k}/(q^2+a^2)$, we can write

$$\chi(k)=\tfrac{1}{2}\int (q^2+a^2)^{-\frac{1}{2}}v^{-1}\{(1+v)^{\frac{1}{2}}-(1-v)^{\frac{1}{2}}+(1+v)^{-\frac{1}{2}}-(1-v)^{-\frac{1}{2}}\}e^{i(q\cdot R)}d\mathbf{q}$$

$$+\tfrac{1}{4}k^2\int (q^2+a^2)^{-\frac{1}{2}}v^{-1}\{(1-v)^{-\frac{1}{2}}-(1+v)^{-\frac{1}{2}}\}e^{i(q\cdot R)}d\mathbf{q}. \quad (3)$$

On expanding the integrand of the first integral in (3) in powers of v we obtain, for this integral, the expression[4]

* National Research Fellow.

[1] P. A. M. Dirac, Proc. Camb. Phil. Soc. **30**, 150 (1934).

[2] W. Heisenberg, Zeits. f. Physik **90**, 209 (1934).

[3] See reference 2. It should be noted that we employ rational units, measuring length in terms of the Compton wavelength $\hbar/mc$, time in terms of $\hbar/mc^2$, and mass in terms of the electronic mass m.

[4] The Bessel function $K_n(z)$ which appears in (4) is that defined by Whittaker and Watson, *Modern Analysis*, §17.71. The integration formula used in obtaining (4) is given by Watson, *Theory of Bessel Functions*, §13.6. Watson's definition of $K_n(z)$ differs from that of *Modern Analysis* by a factor $(-1)^n$.

$$-\sum_{n=1}^{\infty}\frac{(-1)^n(4n)!}{2^{4n}[(2n)!]^2}\frac{2n}{2n+1}(\mathbf{k}\cdot\mathrm{grad}_R)^{2n}\int\frac{e^{i(q\cdot R)}}{(q^2+a^2)^{2n+\frac{1}{2}}}d\mathbf{q}$$

$$=\pi\sum_{n=1}^{\infty}\frac{(-1)^n 2n}{2^{2n-2}(2n+1)!}(\mathbf{k}\cdot\mathrm{grad}_R)^{2n}\frac{R^{2n-1}}{a^{2n-1}}K_{2n-1}(aR). \quad (4)$$

If one now examines the ascending series for $R^{2n-1}K_{2n-1}(aR)$ one sees that there are terms of two types: (a) an infinite series, whose leading term is of the form $R^{4n-2}(\log\frac{1}{2}aR+\text{const.})$; (b) a polynomial in R of degree $4(n-1)$. Hence, when the operator $(\mathbf{k}\cdot\mathrm{grad}_R)^{2n}$ is applied to terms of type (a), and $\mathbf{R}$ is permitted to approach zero, one obtains the result zero when $n>1$. From the terms of type (b) one obtains a contribution only from the term of degree $2n$. This contribution is

$$\frac{(-1)^{n-1}}{4}\frac{(n-2)!}{n!}a[(\mathbf{k}\cdot\mathrm{grad}_R)^{2n}R^{2n}]_{R=0}$$

$$=\frac{(-1)^{n-1}}{4}\frac{(n-2)!(2n)!}{n!}ak^{2n}.$$

The terms after the first in (3) thus give

$$\frac{\pi k^2}{2}\sum_{n=0}^{\infty}\frac{1}{(n+1)(2n+5)}\left(\frac{k}{2a}\right)^{2n+2}. \quad (5)$$

The second integral in (3) can be handled in the same way; the terms after the first are found to be

$$\frac{\pi k^2}{2}\sum_{n=0}^{\infty}\frac{1}{(n+1)(2n+3)}\left(\frac{k}{2a}\right)^{2n+2}. \quad (6)$$

Adding (5) and (6) and performing the summation, one obtains the result

$$\tfrac{2}{3}\pi k^2\log a$$

$$-\tfrac{1}{2}\pi k^2\int_0^1(1-x^2)\log[1+\tfrac{1}{4}k^2(1-x^2)]dx. \quad (7)$$

The first term in (4) and in the analogous series for the second integral in (3) are readily shown to give just the singular and normalization terms which, according to the theory, must be deleted, and in addition a term, $-\frac{2}{3}\pi k^2\log a$, which cancels the first term in (7). Hence

$$\chi(k)=$$

$$-\tfrac{1}{2}\pi k^2\int_0^{\pi/2}\cos^3\psi\log[1+\tfrac{1}{4}k^2\cos^2\psi]d\psi. \quad (8)$$

The calculation of the current density induced by a magnetostatic field is very similar. This current is given by

$$\delta\mathbf{j}=(\alpha/\pi^2k^2)\int\{[\epsilon\epsilon'+(q^2+1-\tfrac{1}{4}k^2)]\mathbf{j}-2\mathbf{q}(\mathbf{q}\cdot\mathbf{j})+\tfrac{1}{2}\mathbf{k}(\mathbf{k}\cdot\mathbf{j})\}[\epsilon\epsilon'(\epsilon+\epsilon')]^{-1}e^{i(q\cdot R)}d\mathbf{q} \quad (9)$$

The third term in the bracket vanishes in virtue of the condition $\mathrm{div}\mathbf{j}(\mathbf{r})=0$, i.e., $\mathbf{k}\cdot\mathbf{j}=0$. The remaining terms can be handled by the method used to evaluate (2). The only new point of interest arises in connection with the second term in the bracket, which apparently gives a dependence of the ith component of the induced current on the jth component of the inducing current. From this term, in the series analogous to (4) one obtains terms of the form

$$[\mathrm{grad}_R(\mathbf{j}\cdot\mathrm{grad}_R)(\mathbf{k}\cdot\mathrm{grad}_R)^{2n}R^{2n+2}]_{R=0}$$

$$=(2n+2)(2n)![k^{2n}\mathbf{j}+2n\mathbf{k}(\mathbf{k}\cdot\mathbf{j})k^{2n-2}].$$

Again using $\mathbf{k}\cdot\mathbf{j}=0$, we see that the contribution of j_i to δj_i in fact vanishes. One readily finds

$$\delta\mathbf{j}=-(\alpha/\pi^2k^2)\chi(k)\mathbf{j}, \quad (10)$$

with $\chi(k)$ as given by (8). The equality of the quite different looking integrals which appear in (1) and (9) might have been easily foretold by considerations, similar to those given in the following section, of the transformation properties of charge and current under a Lorentz transformation. The origin of the different representation of the function $\chi(k)$ in the two cases is to be found in the different meanings attached to canonical momentum in the presence and absence of a vector potential.

On recombining the Fourier components, we find for the charge and current densities induced by a static field[5]

$$\delta j_\lambda(\mathbf{r}')=\int U(r)\Delta \mathbf{j}_\lambda(\mathbf{r}'')d\mathbf{r}'',\ (\lambda=0,\ 1,\ 2,\ 3), \quad (11)$$

where $\mathbf{r}=\mathbf{r}'-\mathbf{r}''$,

$$U(r)=-(\alpha/16\pi^4)\int_0^{\pi/2}\cos^3\psi d\psi\int e^{i(k\cdot r)}\log(1+\tfrac{1}{4}k^2\cos^2\psi)k^{-2}d\mathbf{k}$$

$$=-(\alpha/4\pi^3 r)\int_0^{\pi/2}\cos^3\psi d\psi\int_0^{\infty}\sin kr\log(1+\tfrac{1}{4}k^2\cos^2\psi)k^{-1}dk$$

$$=(\alpha/4\pi^2 r)\int_0^{\pi/2}\cos^3\psi Ei(-2r\sec\psi)d\psi.$$

The exponential-integral function is obtained by deforming the path of the k integration to the imaginary axis, $\int_0^\infty=\frac{1}{2}[\int_0^{i\infty+0}+\int_0^{-i\infty+0}]$.

Varying Fields

The expressions (1) and (10) for the charge and current densities induced by a static field can readily be generalized to the case of an arbitrarily varying field. Let us consider a single Fourier component of the charge and current, $j_\lambda e^{i[(k\cdot r)-k_0 t]}$, $\lambda=0,\ 1,\ 2,\ 3$. If $k^2>k_0^2$ we can make a Lorentz transformation to a system moving with velocity $\mathbf{v}=k_0\mathbf{k}/k^2$; in this system the Fourier component becomes $j_\lambda' e^{i(K\cdot r')}$, where the length of the vector $\mathbf{K}$ is $K=|k^2-k_0^2|^{\frac{1}{2}}$. This however can be regarded as a Fourier component of a static field, which induces a charge and current given by (1) and (10). Upon transforming back to the original coordinate system we thus have

$$\delta j_\lambda=-(\alpha/\pi^2K^2)\chi(K)j_\lambda. \quad (12)$$

This equation has been established only when $k^2>k_0^2$, i.e., only for spacelike $\mathbf{K}$. In order to establish this result also for timelike $\mathbf{K}$, we have only to note that, for time varying potentials, the modification in the expression for the induced charge and current consists in replacing the factor $1/(\epsilon+\epsilon')$ in (2) by $(\epsilon+\epsilon')/[(\epsilon+\epsilon')^2-k_0^2]$. Since this is true irrespective of whether $\mathbf{K}$ is spacelike or timelike, it can immediately be concluded that (12) holds in either case. It should be noted however, that in consequence of our definition of K as $K=|k^2-k_0^2|^{\frac{1}{2}}$, K^2 must be replaced by $-K^2$ throughout (12) if $\mathbf{K}$ is timelike. The only difficulty which can arise comes from the possible vanishing of the denominator $(\epsilon+\epsilon')^2-k_0^2$. Since the minimum value of $(\epsilon+\epsilon')^2$ is $4+k^2$, this cannot occur if $\mathbf{K}$ is spacelike, or if $\mathbf{K}$ is timelike and $K<2$. That is to say, only the Fourier components of the field for which $\mathbf{K}$ is timelike and $K>2$ are capable of producing pairs, since only under these conditions can both energy and momentum be conserved. In performing integrations over such components the pair-production singularity must be avoided by deforming the path of the K integration into the complex plane.

Heisenberg's results (40) and (44) may readily be obtained from (12) by writing $j_0=j_0(\mathbf{k})\delta(k_0-k_0')$, and retaining only the first term in the expansion of $\chi(K)$ in powers of K^2.

We can now write the induced charge and current as an integral over four-space,

$$\delta j_\lambda(\mathbf{s}')=(\alpha/32\pi^5)\int_0^{\pi/2}\cos^3\psi d\psi\int\Lambda(s,\psi)\Box\Box j_\lambda(\mathbf{s}'')d\mathbf{s}'', \quad (13)$$

where the four-vector $\mathbf{s}=\mathbf{s}'-\mathbf{s}''$, $s=|r^2-t^2|^{\frac{1}{2}}$, and

$$\Lambda(s,\psi)=\int e^{i(K\cdot s)}\log(1\pm a^2K^2)K^{-4}d\mathbf{K}. \quad (14)$$

Here $a=\frac{1}{2}\cos\psi$ and the plus or minus sign is to be taken in (14) according as $\mathbf{K}$ is spacelike or timelike.

We now introduce hyperbolic coordinates:

[5] A discussion of this formula and some of its applications is given in the following paper by E. A. Uehling. The expression for the induced charge was originally obtained by Dr. Uehling by a somewhat different method of calculation.

The three space components of $\mathbf{K}$ are expressed in terms of the usual polar coordinates k, θ, Φ; while

$$k_0 = \pm K \cosh \varphi, \quad k = K \sinh \varphi,$$
$$d\mathbf{K} = K^3 \sinh^2 \varphi \sin \theta dK d\varphi d\theta d\Phi,$$

$0 < \varphi < \infty$, when $\mathbf{K}$ is timelike; and

$$k_0 = K \sinh \varphi, \quad k = K \cosh \varphi,$$
$$d\mathbf{K} = K^3 \cosh^2 \varphi \sin \theta dK d\varphi d\theta d\Phi,$$

$-\infty < \varphi < \infty$, when $\mathbf{K}$ is spacelike. We then have,[6] for timelike $\mathbf{s}$,

$$\Lambda(s, \psi) = 4\pi \int_0^\infty \log (1+a^2K^2) K^{-1} dK \int_{-\infty}^{\infty} e^{isK \sinh \varphi} \cosh^2 \varphi d\varphi$$
$$+ 8\pi \int_0^\infty \log (1-a^2K^2) K^{-1} dK \int_0^\infty \cos (sK \cosh \varphi) \sinh^2 \varphi d\varphi$$
$$= 8\pi \left[s^{-1} \int_0^\infty K_1(sK) \log (1+a^2K^2) K^{-2} dK + \tfrac{1}{2}\pi s^{-1} \int_0^\infty Y_1(sK) \log (1-a^2K^2) K^{-2} dK \right], \quad (15)$$

and for spacelike $\mathbf{s}$,

$$\Lambda(s, \psi) = 2\pi \int_0^\infty \log (1+a^2K^2) K^{-1} dK \int_{-\infty}^{\infty} \cosh^2 \varphi d\varphi \int_0^\pi e^{isK \cosh \varphi \cos \theta} \sin \theta d\theta$$
$$+ 4\pi \int_0^\infty \log (1-a^2K^2) K^{-1} dK \int_0^\infty \sinh^2 \varphi d\varphi \int_0^\pi \cos (sK \sinh \varphi \cos \theta) \sin \theta d\theta$$
$$= -8\pi \left[\tfrac{1}{2}\pi s^{-1} \int_0^\infty Y_1(sK) \log (1+a^2K^2) K^{-2} dK + s^{-1} \int_0^\infty K_1(sK) \log (1-a^2K^2) K^{-2} dK \right]. \quad (16)$$

The singularities which arise from the possibility of pair production make their appearance in the second integrals in (15) and in (16), which represent the contribution of timelike $\mathbf{K}$, when $K = 1/a$. In these integrals one is to suppose a cut made in the K plane from $1/a$ to infinity, and the symbol $\int_0^\infty$ is to be understood as meaning $\frac{1}{2}[\int_0^{\infty+i0} + \int_0^{\infty-i0}]$. The term in $1/sK$ in the ascending series for $K_1(sK)$ and for $Y_1(sK)$ does not converge at the lower limit of integration; however this singularity is only apparent, disappearing if the lower limit in both the K_1 and Y_1 integrals is put equal to ϵ, and ϵ is allowed to approach zero. The integrals are also singular when $s = 0$; this singularity we must investigate in detail.

When $s \neq 0$, the contour of the second integral in (16) may be deformed to the imaginary axis,

$$\int_0^\infty \equiv \tfrac{1}{2}\left[\int_0^{\infty+i0} + \int_0^{\infty-i0}\right] = \tfrac{1}{2}\left[\int_0^{i\infty} + \int_0^{-i\infty}\right];$$

we then obtain just the negative of the first integral in (16). Hence $\Lambda(s, \psi)$ vanishes, as it obviously must, when $\mathbf{s}$ is outside the light cone; no effects are propagated with a velocity greater than that of light.

The first integral in (15) can be treated in a similar manner provided $s \neq 0$; making the deformation

$$\int_0^\infty = \tfrac{1}{2}\left[\int_0^{i\infty+0} + \int_0^{-i\infty+0}\right]$$

we obtain the negative of the second integral in (15), and in addition another term,

$$(\pi^2/2s) \int_{1/a}^\infty J_1(sK) K^{-2} dK,$$

which results from the difference in the values

[6] The integral representations of the Bessel functions which are used in the derivation of (15) and (16), and, later, in the Appendix, can be obtained, by use of the recurrence formulae, from the representation of $Y_0(x)$ given in *Modern Analysis*, Chap. XVII, Example 26, and from the representations of $K_0(x)$ given in Example 40.

of $\log(1-a^2K^2)$ on the two sides of the cut.

We can thus write

$$\Lambda(s,\psi)=f(r,\psi)\delta(t+r)+\begin{cases}0, & \mathbf{s}\text{ spacelike.}\\ 4\pi^3 as^{-1}\int_1^\infty J_1(sK/a)K^{-2}dK, & \mathbf{s}\text{ timelike.}\end{cases}\tag{17}$$

The coefficient of the delta function can be most readily evaluated by noting that the integral over time of the second term in (17) vanishes. This integral is[7]

$$8\pi^3 a\int_1^\infty K^{-2}dK\int_0^\infty J_1(sK/a)(s^2+r^2)^{-\frac{1}{2}}ds$$
$$=8\pi^3 a\int_1^\infty I_1(rK/2a)K_1(rK/2a)K^{-2}dK=0,$$

since $K_1(z)\equiv 0$. Hence $f(r,\psi)=\int_{-\infty}^{\infty}\Lambda(s,\psi)dt$.

The evaluation of this integral, using the expressions (15) and (16) for $\Lambda(s,\psi)$, is given in the Appendix; we find

$$f(r,\psi)=8\pi^2 r^{-1}\int_0^\infty \sin Kr\log(1+a^2K^2)K^{-3}dK$$
$$=-8\pi^3 a^2 r^{-1}\int_1^\infty e^{-Kr/a}K^{-3}dK,\tag{18}$$

the second expression being obtained from the first by deforming the path of integration to the imaginary axis.

Eq. (13) can now be written

$$\delta j_\lambda(\mathbf{s}')=\int\Lambda_1(r)\{\Box\Box j_\lambda(\mathbf{s}'')\}d\mathbf{r}''+\int\Lambda_2(s)\Box\Box j_\lambda(\mathbf{s}'')d\mathbf{s}'',\tag{19}$$

where $\{\Box\Box j_\lambda(\mathbf{s}'')\}$ is the retarded value of $\Box\Box j_\lambda(\mathbf{s}'')$,

$$\Lambda_1(r)=-\frac{\alpha}{16\pi^2 r}\int_0^{\pi/2}\cos^5\psi d\psi\int_1^\infty e^{-2Kr\sec\psi}K^{-3}dK,$$

$$\Lambda_2(s)=\frac{\alpha}{8\pi^2 s}\int_0^{\pi/2}\cos^4\psi d\psi\int_1^\infty J_1(2Ks\sec\psi)K^{-2}dK.$$

The second integral in (19) is to be extended only over the interior of the light cone, and only over past values of the time. Our formalism of course, has made no distinction between past and future; this distinction first arises when we introduce boundary conditions to validate our neglect of surface integrals. A similar choice is involved in the first integral of (19), namely, in the use of the retarded, rather than the advanced value of $\Box\Box j_\lambda(\mathbf{s}'')$.

The second term in (19) represents an effect which is propagated with a velocity less than that of light. This can be pictured as due to the propagation of the electromagnetic pulse from an element of charge and current at $(\mathbf{r}'', t'')$ to within a few Compton wavelengths of $\mathbf{r}'$, and here the production (real or virtual) of a pair; one particle of this pair then reaches the point $\mathbf{r}'$, at a later time of course than the electromagnetic pulse.

It has already been shown that when $j_\lambda(\mathbf{s}'')$ is independent of time the second term in (19) vanishes. On transferring, by partial integration, one Laplacian from $j_\lambda(\mathbf{s}'')$ to $\Lambda_1(r)$, one again obtains the formula (11). Another interesting case is that of a charge and current $j_\lambda(\mathbf{s}'')=j_\lambda e^{i[(\mathbf{k}\cdot\mathbf{r})-k_0 t]}$. If $\mathbf{K}$ is spacelike one can transform to a Lorentz frame in which $k_0'=0$; in this frame the entire contribution is again from the first term in (19). However if $\mathbf{K}$ is timelike one finds that in the Lorentz frame in which $\mathbf{k}'=0$ the entire contribution comes from the second term in (19). In either case, of course, one obtains just (12).

The linear corrections introduced by positron theory in the equations of the electromagnetic field can be represented by replacing the field equation $\operatorname{div}\mathbf{E}(\mathbf{s}')=4\pi j_0(\mathbf{s}')$ by

$$\operatorname{div}\mathbf{E}(\mathbf{s}')-\int\Lambda(s)\Box\Box\operatorname{div}\mathbf{E}(\mathbf{s}'')d\mathbf{s}''=4\pi j_0(\mathbf{s}'),\tag{20}$$

where $\Lambda(s)=(\alpha/32\pi^5)\int_0^{\pi/2}\Lambda(s,\psi)\cos^3\psi d\psi$, and by a similar modification in the field equations involving $\mathbf{j}$. If $\mathbf{E}(\mathbf{s}')$ is expanded in powers of e^2, the first correction term is equivalent to (19), while the higher terms represent the effect of the charge induced by the induced charge, and so forth. These latter effects, of course, first appear when the interaction of the electron distribution with itself is taken into account. To the order in

[7] Watson, *Theory of Bessel Functions*, §13.6.

which we have been working, the correction terms vanish in the absence of a charge or current. This, however, will no longer be true in the next approximation, wherein the terms of order e^4, cubic in the fields and their derivatives, are taken into account. In consequence of the occurrence of integral operators in (20), it does not appear to be possible to treat the modified field equations by Hamiltonian methods. The situation here is analogous to that encountered in classical electrodynamics, where, when one attempts to eliminate the electromagnetic field from the equations of motion for the charge, one is also led to integral operators.

I have discussed this subject many times with Professor J. R. Oppenheimer and I wish to thank him for his generous advice. I am indebted also to Dr. E. A. Uehling for his kindness in placing at my disposal his earlier calculation of the induced charge.

Appendix

Evaluation of the integral $f(r,\psi)=\int_{-\infty}^{\infty}\Lambda(s,\psi)dt$.

The time integral of the first terms in (15) and (16) is

$$16\pi\int_0^{\infty}\frac{dK}{K^2}\log(1+a^2K^2)\times\left[\int_0^{\infty}\frac{K_1(sK)}{(s^2+r^2)^{\frac{1}{2}}}ds-\frac{\pi}{2}\int_0^{r}\frac{Y_1(sK)}{(r^2-s^2)^{\frac{1}{2}}}ds\right].$$

The expression in brackets can be written

$$[\,]=\int_0^{\infty}K_1(Kr\sinh\theta)d\theta-\tfrac{1}{2}\pi\int_0^{\pi/2}Y_1(Kr\sin\theta)d\theta,$$

or, introducing integral representations of the Bessel functions,[6]

$$\begin{aligned}[\,]&=-\int_0^{\infty}\cosh t\,dt\Big[\int_0^{\infty}e^{-Kr\cosh t\sinh\theta}d\theta\\&\quad-\tfrac{1}{2}\int_0^{\pi}\sin(Kr\cosh t\sin\theta)d\theta\Big]\\&=\tfrac{1}{2}\pi\int_0^{\infty}Y_0(Kr\cosh t)\cosh t\,dt\\&=-\tfrac{1}{4}\int_{-\infty}^{\infty}\int_{-\infty}^{\infty}\cos(Kr\cosh t\cosh s)\cosh t\,dt\,ds.\end{aligned}$$

If we now set $t=u+v$, $s=u-v$, and use the addition formulae for the circular and hyberbolic functions, we find that the variables separate, and we are finally left with only integrals of the form

$$\int_{-\infty}^{\infty}\cos(Kry^2)dy\quad\text{and}\quad\int_{-\infty}^{\infty}\sin(Kry^2)dy.$$

One easily obtains the result

$$[\,]=\tfrac{1}{2}\pi\sin Kr/Kr$$

and hence (18).

It remains to show that the second terms in (15) and (16) contribute nothing. The time integral of these terms is

$$16\pi\int_0^{\infty}\frac{dK}{K^2}\log(1-a^2K^2)\times\left[\frac{\pi}{2}\int_0^{\infty}\frac{Y_1(Krs)}{(1+s^2)^{\frac{1}{2}}}ds-\int_0^{1}\frac{K_1(Krs)}{(1-s^2)^{\frac{1}{2}}}ds\right].\tag{21}$$

Again making use of an integral representation of Y_1, we write

$$\frac{\pi}{2}\int_0^{\infty}\frac{Y_1(Krs)}{(1+s^2)^{\frac{1}{2}}}ds=-\int_0^{\infty}\cosh t\,dt\int_0^{\infty}\frac{\sin(Krs\cosh t)}{(1+s^2)^{\frac{1}{2}}}ds.\tag{22}$$

If the sine is now expressed in terms of exponentials, and the paths of the resulting integrals over s are deformed to the imaginary axis, we find that (22) is equal to

$$-\int_0^{1}\frac{ds}{(1-s^2)^{\frac{1}{2}}}\int_0^{\infty}e^{-Krs\cosh t}\cosh t\,dt=\int_0^{1}\frac{K_1(Krs)}{(1-s^2)^{\frac{1}{2}}}ds;$$

this just cancels the second term in (21).

Polarization Effects in the Positron Theory

E. A. UEHLING,* *University of California*

(Received April 24, 1935)

Some of the consequences of the positron theory for the special case of impressed electrostatic fields are investigated. By imposing a restriction only on the maximum value of the field intensity, which must always be assumed much smaller than a certain critical value, but with no restrictions on the variation of this intensity, a formula for the charge induced by a charge distribution is obtained. The existence of an induced charge corresponds to a polarization of the vacuum, and as a consequence, to deviations from Coulomb's law for the mutual potential energy of point charges. Consequences of these deviations which are investigated are the departures from the Coulombian scattering law for heavy particles and the displacement in the energy levels for atomic electrons moving in the field of the nucleus.

INTRODUCTION

ACCORDING to Dirac's theory of the positron an electromagnetic field will, in general, induce a charge and current distribution due to the creation and annihilation of electron-positron pairs. The induced fields produced by the electron-positron distribution may be regarded phenomenologically as corresponding to supplementary terms in Maxwell equations. Since one must demand the validity of these equations in sufficiently weak and slowly varying fields, i.e., the vanishing of the susceptibility of vacuum, these terms must depend upon higher powers of the field intensities and their derivatives. Both linear and nonlinear terms will be present. The latter correspond to a failure in the superposition principle for electromagnetic waves, and correspond, therefore, to the scattering of light by light, and of light by an electrostatic field, i.e., to the interaction in general of electromagnetic fields. The linear terms, on the other hand, correspond to a nonvanishing susceptibility of the vacuum. These terms are of importance whenever the fields vary appreciably in a distance of the order of $\hbar/mc$, under which circumstances an appreciable polarization of the electron-positron distribution can exist. It is this effect which we wish to investigate. In order to do so our considerations will be confined to the simplest possible circumstances, namely, those attendant upon an impressed rapidly varying external electrostatic field.[1]

Since the critical field strength of the theory is $F_c=m^2c^3/e\hbar$, our considerations will be valid only insofar as $|\mathcal{E}|$ may be supposed $\ll F_c$. The critical length of the theory is $\lambda_0=\hbar/mc$; no restrictions on the variations of the field in distances of this order will be imposed. In the impact of two point charges (protons for example) rapidly varying fields occur, and one may expect therefore, as has been pointed out by Furry and Oppenheimer,[2] deviations from the Coulomb law of force between them. Similar deviations will occur, also, for atomic electrons moving in the field of a nucleus, and these deviations will give rise to displacements in the position of the atomic energy levels.

The non-Maxwellian terms given by the theory of the positron do not in any way account for the stability of the elementary electrical particle. On the contrary, these terms correspond to an increase in its electromagnetic proper energy. The supplementary terms given by the positron theory are not, therefore, completely correct. However, terms of the same general character are capable of giving a stable electron, and it is of interest to determine in how far such terms lead to experimentally detectable results.

The formulism of the theory developed by Heisenberg will be used in our treatment of the problem.[3] For the case of electrostatic fields, these methods are fully equivalent to those of Furry and Oppenheimer,[2] since apart from the ambiguities introduced by gauge and Lorentz transformations, the infinite constant polarization of vacuum which appeared in their work can be simply ignored, and the finite deviations can be given an unambiguous meaning. It is more convenient, however, to work with expressions which are unconditionally convergent. Heisenberg, following a suggestion of Dirac,[4] was able to obtain

* National Research Fellow.

[1] The generalization of these results to rapidly varying electromagnetic fields is to be found in a paper of Serber appearing in this issue.

[2] Furry and Oppenheimer, Phys. Rev. **45**, 245 (1934).

[3] Heisenberg, Zeits. f. Physik **90**, 209 (1934).

[4] Dirac, Proc. Camb. Phil. Soc. **30**, 150 (1934).

such convergent expressions for the expectation values of physical quantities in the theory of the positron. This convergence is achieved by consideration of the density matrix in nondiagonal form, and subtraction from it of all singular contributions to the expectation values of electromagnetic and dynamical quantities. We shall not be concerned here with the arguments according to which the density matrix is defined, nor with the question of the uniqueness of the result. The definition is, of course, consistent with the vanishing of the susceptibility of vacuum in weak and slowly varying fields.

I. The Induced Charge Density

A general formula for the induced charge, arising from the existence of static external charges, and valid in those regions of space in which the external field intensity is small compared with the critical field, will be obtained. One considers the field to be adiabatically increased from zero to some constant value corresponding to the presence of the existing external charges, and determines the modified wave functions for the electrons by a first-order perturbation method. In accordance with the method of Dirac and Heisenberg a density matrix R_S is then defined such that $R_S=R-\frac{1}{2}R_F$, where R is the density matrix corresponding to the Dirac hole theory and R_F the density matrix for the distribution in which every energy level is occupied. All of these matrices are defined in nondiagonal form in the coordinates, the time, and the spin variables, and the result for the matrix R_S has been obtained by Heisenberg.[5] The first term of this expression is identified immediately with the highest singularity on the light cone. Heisenberg then finds the remaining singularities by developing the integrand in powers of $g(\mathbf{g}=\mathbf{p}'-\mathbf{p}''$ where $\mathbf{p}'$ and $\mathbf{p}''$ are the momenta corresponding to the electron and positron) valid for slowly varying fields. The result of the integration then shows that the remaining singularities correspond to the terms in the lowest power of g, and these terms are in consequence to be subtracted from the matrix R_S to form the matrix r which is to be identified with the physically significant portion of the density matrix representing only the deviations from that distribution in which all negative energy states are occupied and all positive states unoccupied. In the process of this identification, according to which just those terms corresponding to the lowest power g are taken to represent the remaining singularities, and arbitrary constant appearing in the formulation of these singular terms is fixed so that the induced charge over all space vanishes and the polarization in slowly varying fields is zero.

We now use Heisenberg's result to form the matrix r valid for rapidly varying fields. Subtracting the terms corresponding to the singularities and defining $(x_\rho=x_\rho'-x_\rho'',\ x_i'=x^{i'},\ x_0'=-x^{0'}=ct',x_\rho'+x_\rho''=2\mathfrak{y}_\rho,\mathbf{p}'=\mathbf{k}+\mathbf{g}/2,\mathbf{p}''=\mathbf{k}-\mathbf{g}/2)$ one obtains the result

$$(x'k'|r|x''k'')=-\frac{1}{256\lambda_0^2\pi^6\hbar}\int d\mathbf{r}'\int d\mathbf{g}\int d\mathbf{K}\frac{e}{c}A^0(\mathbf{r}')\{\exp i(\mathbf{r}'\cdot\mathbf{g}-\mathfrak{y}\cdot\mathbf{g}-\mathbf{K}\cdot\mathbf{x})\}$$
$$\times\{(\mathbf{K}\cdot\mathbf{g})^{-1}[(1+K^2+\tfrac{1}{2}\mathbf{K}\cdot\mathbf{g})(1+K^2+\tfrac{1}{4}g^2+\mathbf{K}\cdot\mathbf{g})^{-1/2}-(1+K^2-\tfrac{1}{2}\mathbf{K}\cdot\mathbf{g})(1+K^2+\tfrac{1}{4}g^2-\mathbf{K}\cdot\mathbf{g})^{-1/2}]$$
$$-\tfrac{1}{4}g^2(1+K^2)^{-3/2}+\tfrac{1}{4}(\mathbf{K}\cdot\mathbf{g})^2(1+K^2)^{-5/2}\}+\text{conj.},\qquad(1)$$

where $\lambda_0=\hbar/mc$, k' and k'' are the spin variables, all lengths are expressed in units of λ_0, and all momenta in units of mc. Since all infinities are now removed, one can go to the diagonal of the matrix r before performing the integrations. Integrating over the azimuthal angle of K, going to the diagonal $(x_\rho=0,\ k''=k')$, adding the conjugate, and simplifying, one obtains

$$(\mathfrak{y}k'|r|\mathfrak{y}k')=-\frac{1}{32\pi^5\lambda_0^2\hbar}\int d\mathbf{r}'\int\frac{d\mathbf{g}}{g}\int KdK\frac{e}{c}A^0(\mathbf{r}')\{\exp i\mathbf{g}\cdot(\mathbf{r}'-\mathfrak{y})\}$$
$$\times\int_{-1}^{1}\frac{du}{u}\{(1+K^2+\tfrac{1}{2}Kgu)(1+K^2+\tfrac{1}{4}g^2+Kgu)^{-1/2}-\tfrac{1}{8}Kgu(g^2(1+K^2)^{-3/2}-K^2g^2u^2(1+K^2)^{-5/2})\},\quad(2)$$

[5] Heisenberg, reference 3, Eq. (33).

where $u=\cos\vartheta$ is a new integration variable (ϑ is the polar angle between the vectors $\mathbf{K}$ and $\mathbf{g}$). When the integral over K is performed it is found that the subtractive terms are just sufficient to remove the divergences of the principal term. The result of this integration gives

$$(\mathfrak{y}k'|r|\mathfrak{y}k')=\frac{1}{256\pi^5\lambda_0\hbar}\int d\mathbf{r}'\int g^2 d\mathbf{g}\frac{e}{c}A^0(\mathbf{r}')\{\exp i\mathbf{g}\cdot(\mathbf{r}'-\mathfrak{y})\}\int_{-1}^{1}(1-u^2)\log\{(1+\tfrac{1}{4}g^2)^{1/2}+\tfrac{1}{2}gu\}du. \quad (3)$$

By introducing now the potential in terms of a continuous charge distribution

$$A^0(\mathbf{r}')=-A_0(\mathbf{r}')=\lambda_0{}^2\int\frac{\rho(\mathbf{r}'')d\mathbf{r}''}{|\mathbf{r}'-\mathbf{r}''|},\quad\int A_0(\mathbf{r}')\{\exp i\mathbf{r}'\cdot\mathbf{g}\}d\mathbf{r}'=\frac{4\pi\lambda_0{}^2}{g^2}\int\rho(\mathbf{r}')\{\exp i\mathbf{r}'\cdot\mathbf{g}\}d\mathbf{r}',$$

where $\rho(\mathbf{r}')$ is the charge density per unit volume measured in ordinary units, introducing the Laplacian, and summing over the spin variables k'

$$(\mathfrak{y}|r|\mathfrak{y})=\frac{\alpha}{16\pi^4 e}\int\frac{d\mathbf{g}}{g^2}\int\rho(\mathbf{r}')d\mathbf{r}'\Delta\{\exp i\mathbf{g}\cdot(\mathbf{r}'-\mathfrak{y})\}\int_0^1(1-u^2)\log\{1+\tfrac{1}{4}g^2(1-u^2)\}du, \quad (4)$$

where $\alpha=e^2/\hbar c$. The Laplacian considered as an operator on $\{\exp i\mathbf{g}\cdot\mathbf{r}'\}$ may be introduced as an operator on $\rho(\mathbf{r}')$ by partial integration. Integrating over the angle variables of g, one then obtains

$$(\mathfrak{y}|r|\mathfrak{y})=-\frac{\alpha}{4\pi^3 e}\int\Delta\rho(\mathbf{r}')d\mathbf{r}'\int_0^\infty\frac{db}{b}\frac{\sin\{2b|\mathbf{r}'-\mathfrak{y}|(1-u^2)^{-1/2}\}}{|\mathbf{r}'-\mathfrak{y}|}\int_0^1(1-u^2)\log(1+b^2)du. \quad (5)$$

Integrating now over b, and expressing all lengths again in ordinary units, one obtains an expression for the matter density given by

$$(\mathfrak{y}|r|\mathfrak{y})=(\alpha/4\pi^2 e)\int U(|\mathbf{r}'-\mathfrak{y}|)\Delta\rho(\mathbf{r}')d\mathbf{r}', \quad (6)$$

where

$$U(R)=\frac{1}{R}\int_0^1(1-u^2)li\{\exp-(2R/\lambda_0)(1-u^2)^{-1/2}\}du,$$
$$li(e^{-y})=\int_0^{e^{-y}}\frac{dt}{\log t}=\int_\infty^1 e^{-yz}\frac{dz}{z}=\mathcal{E}_i(y). \quad (7)$$

The induced charge is then

$$\delta\rho(\mathfrak{y})=(\alpha/4\pi^2)\int U(|\mathbf{r}'-\mathfrak{y}|)\Delta\rho(\mathbf{r}')d\mathbf{r}'. \quad (8)$$

The function $U(R)$ has an essential singularity at $R=0$, and falls rapidly to zero for values of R different from zero. Its behavior for small values of the argument can be found from the development of the logarithmic function

$$li(e^{-y})=\gamma+\log y+\sum_{n=1}^{\infty}\frac{(-1)^n y^n}{n(n!)}. \quad (8a)$$

Thus for small values of R

$$U(R)\sim(2/3R)[\gamma+\log R/\lambda_0+(5/6)+0(R)], \quad (9)$$

where $\gamma=0.5772$ is Euler's constant. One can show also that for large values of R

$$U(R)\sim-\frac{\pi^{1/2}}{4}\frac{\lambda_0{}^{3/2}}{R^{5/2}}e^{-2R/\lambda_0}[1+0(R^{-1})]. \quad (10)$$

The contribution to the induced charge exists therefore in those regions of space where the Laplacian of the inducing charge has a finite value and in a narrow fringe of space of the order of the Compton wavelength bordering on those regions. Since $U(R)$ is negative for all values of R, the sign of the induced charge is the same as that of the inducing charge in those regions of space where the Laplacian of the latter is negative. One may now obtain an approximate expression for the induced charge by developing

$\Delta\rho(\mathbf{r}')$ about the point $\mathbf{r}'=\boldsymbol{\mu}$. If the field is slowly varying, only the first term in this development need be retained, and since the integral over all space of $U(R)$ is $-4\pi\lambda_0^2/15$, one obtains the approximate result

$$\delta\rho(\boldsymbol{\mu})=-(\alpha/15\pi)\lambda_0^2\Delta\rho(\boldsymbol{\mu}). \tag{11}$$

This result agrees with Heisenberg's determination (reference 3, Eq. 40) obtained from the matrix R_S as a result of retaining only one term in the development in powers of g beyond those which represent the singularities.

As a consequence of the existence of an induced charge in the immediate neighborhood of space varying external charges, and the fact that this induced charge is polarized in the manner shown by Eq. (8), the mutual potential energy of external charges must deviate from Coulomb's law when the charges approach one another within a distance of the order of the Compton wavelength. Between like charges, for example, the deviation from the Coulomb potential will be given by the interaction energy of the external charges with that portion of the induced charge due to the neighboring charge which lies within a sphere of which the line connecting the external charges is a radius. Since the induced charge outside of this sphere is of opposite sign to that of the inducing charges this deviation from Coulomb's law must be such as to increase the mutual forces acting between the charges. For charge distributions this deviation could be calculated directly from Eq. (8). For point charges this deviation is most easily determined from the matrix representing the interaction energy. This determination will be made in the next section.

II. Deviation from the Coulomb Potential

Consider two fixed point charges $Z'e$ and $Z''e$ separated by a distance R. In the mutual field of these charges electrons and positrons are created and annihilated, and the equilibrium value of the electron density is obtained from the formulae of the preceding section in which $A_0(\mathbf{r}')$ represents the electrostatic potential of an electron at the point $\mathbf{r}'$ in this electrostatic field. The energy represented by the electron-positron distribution is given by

$$E=\text{Spur}\,(x'k'|Hr|x''k''), \tag{12}$$

where H represents the matrix of the Hamiltonian function, and r is Heisenberg's density matrix after subtraction of the singularities. The evaluation of the Spur in Eq. (12) yields two terms, one of which represents the electromagnetic energy of the electron-positron distribution, namely,

$$E_r=4e\lambda_0^3\int d\boldsymbol{\mu}A^0(\boldsymbol{\mu})(\boldsymbol{\mu}|r|\boldsymbol{\mu}), \tag{12a}$$

where $\boldsymbol{\mu}$ as in the preceding section is in units of λ_0, and the other of which represents the kinetic energy of the distribution. These terms are of opposite sign, and the latter has a magnitude equal to 1/2 the former. Consequently, we may obtain the total energy of the distribution by the introduction of the density matrix as given by Eq. (3) into Eq. (12a) and dividing the result by a factor 2. One would, of course, obtain the same result for the total energy by using the perturbation matrix $V_{r\rho}$ for transitions between negative and positive energy states, and calculation of the total energy from the expression

$$E=-\sum_{r\rho}|V_{r\rho}|^2/(E_r-E_\rho),$$

where r and ρ index respectively the positive and negative energy states. Using the former procedure one obtains

$$E=\frac{\alpha\lambda_0}{128\pi^5}\int d\boldsymbol{\mu}A^0(\boldsymbol{\mu})\int d\mathbf{r}'\int g^2d\mathbf{g}A^0(\mathbf{r}')\{\exp i\mathbf{g}\cdot(\mathbf{r}'-\boldsymbol{\mu})\}\int_{-1}^{1}(1-u^2)\log\{(1+\tfrac{1}{4}g^2)^{1/2}+\tfrac{1}{2}gu\}du. \tag{13}$$

The potentials may now be introduced. With all quantities in natural units one has

$$\int d\boldsymbol{\mu}A^0(\boldsymbol{\mu})\{\exp -i\mathbf{g}\cdot\boldsymbol{\mu}\}=\frac{4\pi e}{g^2\lambda_0}\{Z'\{\exp -\tfrac{1}{2}\mathbf{R}\cdot\mathbf{g}\}+Z''\{\exp\tfrac{1}{2}\mathbf{R}\cdot\mathbf{g}\}\},$$

$$\int d\mathbf{r}'A^0(\mathbf{r}')\{\exp i\mathbf{g}\cdot\mathbf{r}'\}=\frac{4\pi e}{g^2\lambda_0}\{Z'\{\exp\tfrac{1}{2}\mathbf{R}\cdot\mathbf{g}\}+Z''\{\exp -\tfrac{1}{2}\mathbf{R}\cdot\mathbf{g}\}\}.$$

Thus, the energy as represented by Eq. (13) has terms dependent on Z'^2 and on Z''^2 alone and on the

product $Z'Z''$. The former represent the contribution to the proper energy of the charges, and like the proper energy due to its own field the proper energy of the electron-positron distribution due to the point charges is infinite.[6] The interaction energy represented by the terms containing the product $Z'Z''$ is, however, finite for finite distances of separation. One obtains

$$E_{\text{Int.}}=\frac{Z'Z''\alpha e^2}{8\pi^3\lambda_0}\int\frac{dg}{g^2}\{\{\exp i\mathbf{R}\cdot\mathbf{g}\}+\{\exp -i\mathbf{R}\cdot\mathbf{g}\}\}\cdot\int_{-1}^{1}(1-u^2)\log\{(1+\tfrac{1}{4}g^2)^{1/2}+\tfrac{1}{2}gu\}du$$
$$=\frac{Z'Z''\alpha e^2}{\pi^2\lambda_0 R}\int\frac{\sin Rgdg}{g}\int_0^1(1-u^2)\log\{1+\tfrac{1}{4}g^2(1-u^2)\}du. \tag{14}$$

By integrating over g and introducing ordinary units for R

$$E_{\text{Int.}}=-(\alpha/\pi)Z'Z''e^2U(R), \tag{15}$$

where $U(R)$ is defined as in Eq. (7). Since $U(R)$ is always negative the interaction energy is always positive for like charges, as it should be according to the discussion of the previous section. Asymptotic values for $E_{\text{Int.}}$ are easily obtained from Eqs. (9) and (10) for both large and small values of R. The values are:

$$E_{\text{Int.}}\cong-(2\alpha/3\pi)(Z'Z''e^2/R)[\gamma+\log R/\lambda_0+5/6+0(R)] \quad R \text{ small} \tag{16}$$
$$\cong(\alpha\lambda_0^{3/2}/4\sqrt{\pi})(Z'Z''e^2/R^{5/2})e^{-2R/\lambda_0}[1+0(R^{-1})] \quad R \text{ large.} \tag{17}$$

A power series development for $E_{\text{Int.}}$ valid for all values of R, which is useful in particular for small and intermediate values, may be obtained from Eq. (14). By adding and subtracting a term in $\log(1+\frac{1}{4}g^2)$ to the integrand of this equation, it may be written

$$E_{\text{Int.}}=\frac{Z'Z''\alpha e^2}{\pi\lambda_0 R}\int\frac{\sin Rgdg}{g}\left\{(4/3)\log a-\int du[\tfrac{2}{3}\log a-(1-u^2)\log(a+bu)]\right\}, \tag{18}$$

where $a=(1+\frac{1}{4}g^2)^{1/2}$, $b=\frac{1}{2}g$. Since

$$\int_0^\infty\frac{\sin Rgdg}{g}\log(1+\tfrac{1}{4}g^2)=-\pi li(e^{-2R})$$

the first term of Eq. (18) is

$$-\frac{2\alpha}{3\pi}\frac{Z'Z''e^2}{\lambda_0 R}li(e^{-2R})=\frac{2\alpha}{3\pi}\frac{Z'Z''e^2}{\lambda_0 R}\frac{e^{-R}}{(2R)^{1/2}}W_{-1/2,\,0}(2R),$$

where $W_{-1/2,\,0}(2R)$ is the confluent hypergeometric function.[7] The integrand of the second term of Eq. (18) may be developed in powers of b/a valid for all values of g. Integrating first over u and then making the development one obtains

$$\int\frac{\sin Rgdg}{g}\int_{-1}^{1}du\{\tfrac{2}{3}\log a-(1-u^2)\log(a+bu)\}$$
$$=\int\frac{\sin Rgdg}{g}\left\{\frac{16}{9}-\frac{2}{3}\frac{a^2}{b^2}+\frac{4}{3}\log a+\left(\frac{a^3}{3b^3}-\frac{a}{b}-\frac{2}{3}\right)\log(a+b)-\left(\frac{a^3}{3b^3}-\frac{a}{b}+\frac{2}{3}\right)\log(a-b)\right\}$$
$$=\frac{2}{3}\sum_{n=1}^{\infty}\int\frac{\sin Rgdg}{g}\left(\frac{1}{n}-\frac{3}{2n+1}+\frac{1}{2n+3}\right)\left(\frac{b}{a}\right)^{2n}.$$

This integral may be evaluated by complex methods to give a power series in R. Combining the results for the first and second terms of Eq. (18) and returning to ordinary units one obtains finaliy

[6] The contribution to the electrostatic proper energy of a point charge may be obtained by letting $R\to0$ in Eq. (15); it is positive and has a slightly worse singularity than the classical term, since $U\to(\log R)/R$. These polarization terms also lead to divergent positive terms of order α in the proper energy of an electron, giving, in fact, integrals of the form $\alpha\int^\infty(dg/g)\log(1/g)$.

[7] Whittaker and Watson, *Modern Analysis*, 4th ed., p. 339.

for the interaction energy

$$E_{\text{Int.}}=-\frac{2\alpha}{3\pi}\frac{Z'Z''e^2}{R}\Big[li(e^{-2R/\lambda_0})+\frac{3}{2}e^{-2R/\lambda_0}\sum_{n=1}^{\infty}2^n \cdot\sum_{\sigma=0}^{n-1}\sum_{\mu=0}^{n-\sigma-1}\frac{(-2)^{\mu-\sigma}\Gamma(n+\tfrac{1}{2})}{n(2n+1)(2n+3)\Gamma(\tfrac{1}{2})}\frac{(n+\sigma-1)!}{(n+\mu+\sigma)!(n-\mu-\sigma-1)!\sigma!\mu!}\left(\frac{R}{\lambda_0}\right)^{\mu}\Big]. \quad (19)$$

The power series development of the logarithmic function valid for all finite values of the argument is given by Eq. (8a); therefore, one has in Eq. (19) a power series development of $E_{\text{Int.}}$ valid for all finite values of R. One can show that

$$\sum_{\sigma=0}^{n-1}\frac{(-2)^{-\sigma}}{(n+\sigma)(n-\sigma-1)!\sigma!}=\frac{\Gamma(\tfrac{1}{2})}{2^n\Gamma(n+\tfrac{1}{2})}$$

and

$$\sum_{n=1}^{\infty}\frac{1}{n(2n+1)(2n+3)}=\tfrac{2}{3}(5/6-\log 2)$$

as a consequence of which the second term of the bracket in Eq. (19) approaches the value $(5/6-\log 2)$ as R approaches zero. Combining with the first few terms of the series development for li (e^{-2R/λ_0}) one observes that Eq. (19) gives again Eq. (16) for $E_{\text{Int.}}$ valid for small values of R. It is of interest to note that this result agrees in form with that of Furry and Oppenheimer[8] in which the divergences of the previous method are contained in the constant K of their equations.

As has already been mentioned, the results of the theory are valid only insofar as the field intensities can be assumed to be much smaller than the critical field F_c. Thus the results obtained for the deviation from Coulomb potential given above by Eq. (15) can be expected to hold for protons only for distances of separation such that $R\gg\lambda_0(\alpha)^{\frac{1}{2}}$.

III. Scattering of Heavy Particles

The deviations from Coulomb potential considered in the last section become important when the distance of separation of the particles is of the order of the Compton wavelength. These deviations are in principle observable, and may be detected in the scattering of high energy particles. For the case of protons the classical distance of closest approach in units of the Compton wavelength is of the order α for incident particles having energies of the order of one million electron volts. For energies of this order of magnitude one is already beyond the range of validity of the theory, yet, for incident particles of this and somewhat lower energies, deviations from the law of scattering valid for the strict Coulomb potential should be found.

The scattering law for the new potential is easily obtained. Since the deviations from Rutherford scattering will be important only for incident particles of high energy the Born approximation may be used. The perturbation parameter $rV(r)/\hbar v\sim Z'Z''e^2/\hbar v$, the smallness of which determines the validity of the Born method, is for the case of incident protons having kinetic energies of the order of one million electron volts equal approximately to 20α. For this and higher energies the Born approximation will be fairly accurate.

The scattered amplitude according to the Born formula for unit incident flux scattered by a fixed scattering center is

$$f(\theta)=-\frac{2M}{\hbar^2}\int_0^{\infty}\frac{\sin Kr}{Kr}V(r)r^2dr, \quad (20)$$

where $K=(2/\lambda)\sin(\theta/2)$, $\lambda=\hbar/mv$, M is the mass of the incident particle, v its initial velocity, and θ the angle with respect to the direction of the incident beam at which the scattering is observed. Let $Z'e$ and $Z''e$ denote the charge of the incident and scattering particles, respectively. Then from Eq. (15) the mutual potential energy (Coulomb potential plus the deviation from Coulomb potential) is

$$V(r)=(Z'Z''e^2/r)[1-(\alpha/\pi)rU(r)]. \quad (21)$$

All of the integrations can be performed strictly

[8] Furry and Oppenheimer, Phys. Rev. **45**, 245 (1934), Eq. (4.8). A typographical error has put the factor π in the numerator instead of the denominator in two terms of this expression. Also λ_0 here is 2π times the λ_0 used in the expressions given above.

with the result that one obtains for $f(\theta)$

$$f(\theta)=\frac{Z'Z''e^2}{2Mv^2}\csc^2\frac{\theta}{2}\left[1+\frac{\alpha}{3\pi}F(k)\right], \qquad (22)$$

where

$$F(k)=\frac{4}{k^2}-\frac{5}{3}+\left(1-\frac{2}{k^2}\right)\left(1+\frac{4}{k^2}\right)^{1/2}\times\log\frac{(1+\frac{1}{4}k^2)^{1/2}+\frac{1}{2}k}{(1+\frac{1}{4}k^2)^{1/2}-\frac{1}{2}k},$$

$$k=2(Mv/mc)\sin(\theta/2).$$

m is the electron mass, and the negative sign of $f(\theta)$ is dropped since only its absolute value is important. The first term of Eq. (22) gives the ordinary Rutherford scattering; the second term gives the deviation from this scattering law. For small values of k, $F(k)\sim\frac{1}{5}k^2$, and, therefore, the deviation from the Rutherford scattering is finite for all values of θ. For large values of k

$$F(k)\sim 2\log k-(5/3).$$

The form of the function $F(k)$ shows that the deviations from the usual scattering law for particles of a given incident velocity rises rapidly with increasing θ in the neighborhood of $\theta=0$, and then remains practically constant throughout the greater portion of the angular range increasing with θ only as the logarithm of sin $(\theta/2)$. The practical constancy of the deviation together with its small magnitude precludes the possibility of any easy experimental verification of the new potential.[9]

The intensity of scattering into a given solid angle is given by the square of the scattered amplitude $f(\theta)$. For the case of proton scattering by protons (the scattering of protons by hydrogen nuclei) the scattered amplitude in relative coordinates is given by Eq. (22) with M equal to one-half the proton mass. Considering the hydrogen nuclei as initially stationary compared with the high energy incident protons, the intensity of scattering into a solid angle $d\Omega$ measured with respect to the direction of the incident beam is

$$I(\theta)d\Omega=4|f(2\theta)|^2\cos\theta d\Omega. \qquad (23)$$

Exchange may be taken into account in the usual manner by introducing $|f(2\theta)+f(\pi-2\theta)|^2$ for $|f(2\theta)|^2$.

[9] Some recent experimental evidence on the scattering of high energy protons in hydrogen (M. G. White, Phys. Rev. **47**, 573 (1935)) indicates the possible existence of rather large deviations, which in their dependence on energy and angular distribution as well as in the magnitude of the effect bear little resemblance to the predictions given here.

IV. Displacement of Atomic Energy Levels

§1. Secular terms

Because of the failure of the potential energy between electron and nucleus to be strictly Coulombian, the energy levels for the electron are slightly displaced. This displacement may be calculated with the deviation from the Coulombian potential as a small perturbation, or by using the expression for the induced charge to calculate the potential between the nucleus and the induced charge of the electron and the potential between the electron and the induced charge of the nucleus. With the former procedure the displacement in the energy levels is given by

$$\delta E=\int V(r)|\Psi_{nlm}(r\theta\varphi)|^2 d\tau, \qquad (24)$$

where $V(r)$ represents the deviation from Coulomb potential, and Ψ_{nlm} the electron wave function. From Eqs. (15) and (7). $V(r)$ for the interaction of an electron with the nucleus is given by

$$V(r)=\frac{Z\alpha e^2}{\pi r}\int_0^1(1-u^2)du\int_\infty^1\left\{\exp-\frac{2rz}{\lambda_0}(1-u^2)^{-1/2}\right\}\frac{dz}{z}. \qquad (25)$$

For the $1s$ level

$$\Psi_{100}(r\theta\varphi)=-[1/2(2\pi)^{1/2}](2/a)^{3/2}e^{-r/a}, \qquad (26)$$

where $a=\hbar^2/\mu e^2Z$, $\mu=mM/(m+M)$. The integration can be performed strictly to the lowest power in $\lambda_0/a=ZM\alpha/(M+m)$ with the result that

$$\delta E_{1s}\leqq -8Z^2\alpha^3R/15\pi, \qquad (27)$$

where $R=\mu e^4Z^2/2\hbar^2$ is the Rydberg constant. Similarly for the $2s$ level

$$\Psi_{200}(r\theta\varphi)=\frac{1}{8(2\pi)^{1/2}}e^{-r/2a}\left(\frac{1}{a}\right)^{3/2}\left(\frac{2r}{a}-4\right) \qquad (28)$$

and $$\delta E_{2s} \leqq -Z^2\alpha^3 R/15\pi. \quad (29)$$

For p levels the calculation shows that the displacement is of higher order in α, being, in fact, of order α^5. Of the secular terms, therefore, the important ones are the s-terms.[10]

§2. Nonsecular terms

A Fourier resolution of the inducing charge $\rho(rt)$ yields after a Lorentz transformation and substitution into Eq. (8) an expression for a single component of the induced charge given by[11]

$$\delta\rho(K) = X(K)\rho(K), \quad (30)$$

where

$$X(K) = -\frac{\alpha}{2\pi}\int_0^{\pi/2} \cos^3\psi d\psi \cdot \log\left(1+\tfrac{1}{4}K^2\cos^2\psi\right) \quad (31)$$

and the propagation vector K is in units of λ_0^{-1}. For small values of $\mathbf{K}$

$$X(K) \leqq -\alpha K^2/15\pi \quad (32)$$

and accordingly, when only small values of K are important in $\rho(rt)$ Eq. (30) yields the result

$$\delta\rho(rt) = (\alpha/15\pi)\lambda_0^2 \Box\rho(rt) \quad (33)$$

an expression which represents the sum of Eq. (11) for slowly varying space components and Heisenberg's result for pure but slowly varying time components.[12] The order of magnitude of the contribution of transitions within the discrete spectrum to the displacement of the $1s$ electron level may be determined then with the help of Eq. (33), yielding a result which is small of order $Z^4\alpha^6$, and, therefore, negligible in comparison with the secular term. We will, accordingly, consider in more detail only the contribution given by transitions to the continuous spectrum.

Confining our considerations as before to the $1s$ level, the displacement is given by

$$\delta E_{1s} = -\int d\mathbf{k} |V_{1k}|^2/h\nu_{k1}, \quad (34)$$

where $$V_{1k} = Ze\int [\delta\rho(r)/r] d\mathbf{r} \quad (35)$$

and $\delta\rho(r)$ is the induced charge due to the charge representing the transition $1s$ to k. Using plane waves to represent the states of the continuous spectrum, a procedure justified in what follows since little contribution comes from the small values of k, and Eq. (33) for the induced charge, one obtains

$$\delta E_{1s} \leqq -\frac{64\alpha}{225\pi^3 Z}\int \frac{k^2[(1+k^2)^{1/2}-1]dk}{(1+a^2k^2)^2} R. \quad (36)$$

Thus, the integral over k diverges for large k like dk/k, the effect of large components falling off too slowly on account of the k^2 from the d'Alembertian. Aside from the divergence the order of magnitude of the result is $Z^3\alpha^5$. The divergence is, of course, spurious. Convergence may be expected when the true expression for $X(K)$ from Eq. (31) is used. Using again plane waves to represent the states of the continuous spectrum, and Eqs. (30) and (31) for the induced charge, one obtains for the Lth component

$$\delta\rho(Lr) = \frac{e}{8\pi^4}\frac{(2a)^{3/2}\lambda_0^{3/2}}{[1+a^2|\mathbf{K}+\mathbf{k}|^2]^2} X(L)\{\exp i\mathbf{K}\cdot\mathbf{r}/\lambda_0\} \quad (37)$$

with K and k in units of λ_0^{-1}, $a = (\alpha Z)^{-1}(m+M)/M$, k the space vector of the plane wave, and

$$L^2 = K^2 - (k_0 - E_1/\hbar c)^2,$$

where E_1, is the energy for the $1s$ electron, and k_0 is the time component of the propagation vector of the plane wave. The coefficient of $X(L)$ in Eq. (37) in the limit for large a behaves like $\delta(\mathbf{K}+\mathbf{k})$. Since large values of k are important, one can neglect the binding of the electron which is equivalent then in Eq. (37) to replacing $\mathbf{K}$ by $-\mathbf{k}$ in $X(L)$. Therefore, in this approximation using the definition of X from Eq. (31) and substituting $-\mathbf{k}$ for $\mathbf{K}$ in $\mathbf{L}$

[10] These calculations have been made also by E. Brunner to whom we are indebted for having told us of the results.

[11] The derivation of this result is given in the paper of R. Serber appearing in this issue.

[12] Heisenberg, reference 3, Eq. (44).

$$\delta\rho(Lr)=-\frac{\alpha e}{16\pi^5}\frac{(2a)^{3/2}\lambda_0{}^{3/2}}{[1+a^2|\mathbf{K}+\mathbf{k}|^2]^2}\{\exp i\mathbf{K}\cdot\mathbf{r}/\lambda_0\}\int_0^{\pi/2}\cos^3\psi d\psi\log[1+\tfrac{1}{4}\{k^2-(k_0-E_1/\hbar c)^2\}\cos^3\psi]. \tag{38}$$

Integrating over all values of $\mathbf{L}$ and introducing $\delta\rho(r)$ into Eq. (35) one obtains for the dominant term of V_{1k}

$$V_{1k}\sim-\frac{4Z\alpha e^2}{15\pi^2}\frac{(2a)^{1/2}\lambda_0{}^{1/2}}{1+a^2k^2}\log\{1+\tfrac{1}{2}[(1+k^2)^{1/2}-1]\}. \tag{39}$$

For large values of k this expression behaves like $(\log k)/k^2$ instead of like $1/k$ as obtained using the d'Alembertian. The integral for δE_{1s} will, therefore, converge, and the result for the non-secular terms is that δE_{1s} is of the order $Z^3\alpha^5$.

As a consequence of these calculations one finds that the energy levels are depressed, the displacement corresponding to a quantum defect $\Delta=n-n^*$ which is positive. It is not possible, therefore to ascribe any part of the observed discrepancy in the doublet separations of hydrogen to the new potential, since the experimentally observed values of the doublet separations in the Balmer series are always less than those predicted by the relativistic fine-structure theory, whereas, the displacement in the energy levels corresponding to the new potential correspond to an increased separation of the doublet components. Furthermore, the percentage change in the doublet separations would be smaller than the experimentally observed discrepancy of about 3 percent by a factor of at least 10. The nature of the potential necessary to explain the observed results has been considered by Kemble and Present.[13] It needs to be emphasized here, only that the potential to which the electron-positron theory gives rise is not of the requisite character.

The author wishes to express his gratitude for frequent suggestions and help given by Professor J. R. Oppenheimer throughout the course of this investigation and to Dr. R. Serber and Mr. A. Nordsieck for many helpful discussions of the problem.

[13] Kemble and Present, Phys. Rev. **44**, 1031 (1933).

JULY 1, 1935 PHYSICAL REVIEW VOLUME 48

The Raman Spectrum of Heavy Chloroform

R. W. Wood, *Johns Hopkins University* AND D. H. Rank, *Pennsylvania State College*

(Received May 9, 1935)

The Raman spectrum of chloroform made from deuterium has been photographed and the line shifts measured. The three types of isotope effects observed in the spectrum of heavy chloroform have been discussed. By treating different groups of atoms in the molecule as entities satisfactory agreement between calculated and observed values for the isotope displacements can be secured. Some idea of the nature of the role played by the chlorines in the C–H "bending" and "stretching" vibrations is obtained.

THE heavy chloroform, made from deuterium by Dr. F. W. Breuer of the Chemistry Department of Pennsylvania State College, was placed at our disposal for the study of its Raman spectrum. It was contained in a sealed glass tube 6 mm in diameter and 30 cm long, wrapped in black insulation tape with the exception of the lower 5 cm adjacent to the flat Pyrex glass window, the portion occupied by the fluid.

The arrangement of apparatus for irradiating the tube was essentially the same as that described by one of us[1] except that the high potential quartz mercury tube was replaced with the 220-volt Hanovia quartz mercury arc in its metal housing turned to the vertical position. As was shown in the previous paper this disposition prevents a temperature gradient across the diameter of the irradiation tube, with its attendant troublesome refraction, obviating as well the necessity of an air blast. The light from the arc

[1] R. W. Wood, *Raman Spectra of Heavy Water*, Phys. Rev. **45**, 392 (1934).

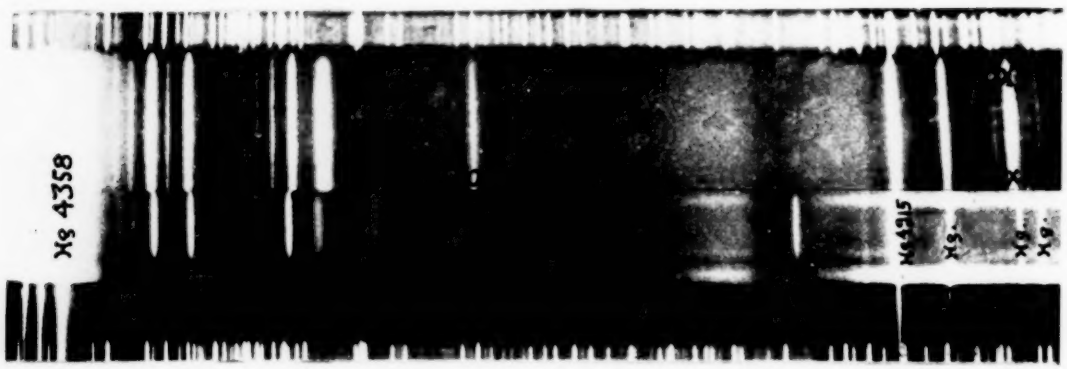

FIG. 1. Raman spectra of light chloroform (above) and heavy chloroform (below).

was focused on the tube by a cylindrical lens consisting of a long tube 4 cm in diameter filled with a solution of sodium nitrite. An absorption cell made from one of the flat glass tubes (in which a certain brand of tooth brush is sold) filled with a strong solution of praseodymium was interposed between the cylindrical lens and the irradiation tube which was backed by a concave cylindrical reflector of this sheet aluminum. A total reflecting prism, immediately below the window of the vertical irradiation tube reflected the emitted light to the achromatic lens which focused the image of the end of the tube on the spectrograph slit. Very full directions for the alignment of tube, prism and lens will be found in the paper referred to above. An exposure of twenty-four hours was given with the large single prism spectrograph of 1-meter focus employed by one of us in work on the Raman effect during the past six years. Excitation by lines of shorter wavelength than 4358 was not employed as chloroform suffers photochemical changes in ultraviolet light.

Spectrograms of ordinary and heavy chloroform are reproduced in Fig. 1. The line marked *x*, due to the vibration of the hydrogen is shifted towards the exciting line (4358) falling at the center of the praseodymium absorption band, the line marked *O*, to a lesser degree, and the other lines by still smaller amounts. A faint trace of the line at 1505 was found on the plate made with ordinary chloroform. It was very broad and hazy and its position is marked with an arrow in Fig. 1 as it may be too faint to reproduce. The $\Delta\nu$ values are given in Table I.

The weighted means of the frequency shifts from the exciting lines which are given in Table I should be accurate within one or two wave numbers.

TABLE I. *Raman spectrum of ordinary and heavy chloroform.* Exciting lines $a = \lambda 4358$, $b = \lambda 4347$, $c = \lambda 4339$.

		$CHCl_3$ $\Delta\tilde{\nu}$	$CDCl_3$ $\Delta\tilde{\nu}$			$CHCl_3$ $\Delta\tilde{\nu}$	$CDCl_3$ $\Delta\tilde{\nu}$
	C	261.4		Γ_2	*b*	668.2	651.2
Γ_1	*b*	261.5	264.1		*a*	668.4	650.5
	a	262.3	261.7	Γ_4	*a*	761.2	737.6
Γ_2	*b*	365.9	368.0	Γ_5	*a*	1215.6	908.3
	a	365.9	366.2	$2\Gamma_4$*	*a*	1505	
	c	670.2		Γ_6	*a*	3018.9	2256.0

Weighted means of frequency shifts

$CHCl_3$	$\Delta\tilde{\nu}$ = 262.0 (15)	365.9 (10)	668.3 (10)	761.2 (10B)	
	1215.6 (5)	1505 (0)	3018.9 (10)		
$CDCl_3$	$\Delta\tilde{\nu}$ = 262.0 (15)	366.5 (10)	650.8 (10)	737.6 (10B)	
	908.3 (5)	2256.0 (10)			

* Could not be measured on comparator. Position could be quite accurately estimated with respect to neighboring iron comparison lines.

DISCUSSION OF RESULTS

The modes of vibration of a symmetrical pentatomic tetrahedral molecule are worked out in Born's *Electromagnetischen Lichttheorie*.[2] This type of molecule gives rise to four distinct vibrational frequencies. Two of these vibrations are triple, one double and the remaining one singly degenerate. It is well known[3] that in the unsymmetrical molecule six distinct frequencies should appear. (The triple vibrations split up into a single and a double vibration.) Chloroform is obviously a molecule of the latter type.

From an inspection of the results given in Table I it is apparent that three distinct types of isotope effects are present in the spectrum of

[2] Max Born, *Electromagnetischen Lichttheorie*, p. 554.
[3] Jenny E. Rosenthal, Phys. Rev. **45**, 538 (1934).

$CDCl_3$. From the magnitude of the isotope shifts we are able immediately to tell the manner in which the hydrogen moves with respect to the other atoms in the molecule in the execution of particular modes of vibration.

We shall show that the isotope effects can be calculated with considerable exactness by treating the chloroform molecule as a simple diatomic oscillator in which composite groups of atoms vibrate as entities.

Case I

The lines in the $CDCl_3$ spectrum unshifted with respect to those of $CHCl_3$ (V_1 and V_2). In this case, effectively, HCl_3 is vibrating against the central carbon atom. It is obvious, however, that the substitution of a deuterium atom for hydrogen in such an oscillator will produce so small a change in the reduced mass as to make the isotope effect too small to be observed. Inspection of the normal modes of vibration of chloroform shows that V_1 and V_2 involve hydrogen bending and stretching. It is apparent, however, that these should be the lowest frequencies of the molecule.

Case II

The lines in the $CDCl_3$ spectrum slightly shifted with respect to those of $CHCl_3$ (V_3 and V_4). To account for this small isotope effect in a simple manner it is only necessary to assume that C–H vibrates as an entity against the chlorine atoms in these particular vibrations. Assuming the frequency of the oscillator can be expressed by the equation

$$\tilde{\nu}_H=(1/2\pi)(f/\mu_1)^{\frac{1}{2}},\quad \mu_1=M_{CH}\cdot M_{Cl_3}/M_{CHCl_3}. \quad (1)$$

A similar expression can be written for $\tilde{\nu}_D$. Since the force constants for the two isotopic molecules are identical, the ratio of the frequencies becomes

$$\tilde{\nu}_H/\tilde{\nu}_D=(M_{CD}\cdot M_{CHCl_3}/M_{CH}\cdot M_{CDCl_3})^{\frac{1}{2}}. \quad (2)$$

A substitution of the numerical data in Eq. (2) yields the calculated values given in Table II. The agreement between the observed and calculated values is all that could be desired from such simple considerations. This agreement seems to show quite definitely that the assumption of CH vibrating as an entity in V_3 and V_4 is not very far from the actual state of affairs.

TABLE II. *Calculated and observed values of doublet separations.*

	$\Delta\tilde{\nu}_H-\Delta\tilde{\nu}_D$ (Obs.)	$\Delta\tilde{\nu}_H-\Delta\tilde{\nu}_D$ (Calc.)
V_3	17.5 cm^{-1}	21.4 cm^{-1}
V_4	23.6	24.9
V_5†	307.3	307.3
V_6	762.9	763.2

† V_5 Calc. and V_5 observed were made to agree purposely by the choice of α.

Case III

The lines in the $CDCl_3$ spectrum greatly shifted with respect to those of $CHCl_3$ (V_5 and V_6). To account for these large isotope displacements in a rough manner it is only necessary to consider the hydrogen atom as vibrating against the rest of the molecule. Such a calculation will give displacements of the correct order of magnitude. V_5 is a double vibration and consists mainly of CH "bending." V_6 is single and is of the type commonly called a CH "stretching" vibration. We can consider V_5 and V_6 to be C–H vibrations to a first approximation. However, we certainly cannot neglect the influence of the other atoms in the molecule on these vibrations. The effect of the chlorines on this simple C–H oscillator leaves two alternatives. The chlorine atoms can vibrate in such a manner as effectively to increase the mass of the carbon atom or effectively increase the mass of the hydrogen atom. A trial calculation showed the latter alternative to be in agreement with experiment. In this case our oscillator is assumed to be $(M_H+\alpha)\longleftrightarrow M_c$. The expression for the ratio of the frequencies becomes.

$$\tilde{\nu}_H/\tilde{\nu}_D=((M_D+\alpha)M_{CH}/(M_H+\alpha)M_{CD})^{\frac{1}{2}}. \quad (3)$$

Using the experimental values of V_{5H} and V_{5D} we are able to determine the value of α from Eq. (3). The value found for α was 0.074 atomic weight units. Once α has been determined it is now possible to calculate V_{6H} or V_{6D} if one or the other is known. The calculated value of the doublet separation is given in Table II.

We are deeply indebted to Dr. F. W. Breuer for the loan of the heavy chloroform we have used. His paper on its preparation will appear elsewhere. One of us (R) has had the benefit of helpful discussions with Dr. W. Altar of the Physics Department, Pennsylvania State College, concerning the modes of vibration of the chloroform molecule.

An Attempt to Observe the Absorption Spectrum of Metastable Nitrogen Molecules

A. A. FROST AND O. OLDENBERG, *Research Laboratory of Physics, Harvard University*

(Received April 30, 1935)

Previous failures to observe the absorption spectrum of metastable N_2 might be explained on the basis of more recent information by the position of the spectrum in an infrared range in which plates are less sensitive and, therefore, the application of high resolving power is difficult. Since at this laboratory a special equipment for the investigation of very faint absorption spectra had been developed for another purpose the problem mentioned was reinvestigated under most favorable conditions with the newly developed plates, types *Q* and *Z*, of the Eastman Kodak Company. Again no absorption spectrum was observed.

THE mechanism of the light emission from active nitrogen has been interpreted in detail by Cario and Kaplan. The main source of energy, which maintains the afterglow through a considerable period of time, consists of the chemical energy of nitrogen *atoms*, most of them in the normal state.[1] Metastable molecules and indirectly metastable atoms are formed in this recombination process. Their concentrations are sufficiently high so that the excitation of the metastable molecules by impacts of the second kind with metastable atoms leads to a characteristic spectrum, observed as afterglow.

It has been reported[2] that active nitrogen, in spite of these metastable atoms and molecules present, does not show an *absorption* spectrum. On the other hand, very powerful absorption of light by metastable *mercury atoms* has been reported by Wood.[3] The absorption spectrum of the metastable N *atoms* is to be expected in the extreme ultraviolet; we are more interested, however, in the absorption spectrum of metastable N_2 *molecules* whose intensity distribution would give an opportunity to find out the details of the processes going on in active nitrogen. It is true that absorption of light is fainter by molecules than by atoms. But this difference might be compensated by higher pressure and a longer column.

At present we know that the absorption spectrum of metastable N_2 is to be expected in the infrared region which within the last years has become much more easily accessible. The high sensitivity of the new plates, types Q and Z, developed in the Research Laboratory of the Eastman Kodak Company[4] makes possible the application of a very high resolving power. This, in turn, is indispensable for the investigation of faint absorption lines.

A particularly sensitive apparatus was built at this laboratory for another investigation of faint absorption spectra of unstable molecules in electric discharges and their decay after interrupting the discharge.[5] It seemed promising to apply this apparatus to the search for the absorption spectrum of metastable N_2 molecules by using a pressure about 5000 times as high and an absorbing column about 10 times as long as the corresponding values in Wood's mercury experiment.

The result was negative. Nevertheless, it seems worth while to give a brief report since the experiment was carried through with a particularly good equipment.

The most favorable conditions for the absorption experiment can be predicted. From the energy level diagram[6] we expect absorption of the first positive group with the lower electronic level $A^3\Sigma$ and the lower vibrational quantum number $v''=0$.[7] Since this group shows a diagonal

[1] G. Cario and J. Kaplan, Zeits. f. Physik **58**, 769 (1929); G. Cario, Zeits. f. Physik **89**, 523 (1934); J. Kaplan, Phys. Rev. **45**, 671 (1934); cf. J. Okubo and H. Hamada, Sci. Reps. Tohoku Imp. Univ. **23**, 281 (1934).

[2] K. F. Bonhoeffer und G. Kaminsky, Zeits. f. physik. Chemie **127**, 385 (1926); A. E. Ruark, P. D. Foote, P. Rudnik and R. L. Chenault, J. Opt. Soc. Am. **14**, 17 (1927). In Cario's papers no absorption spectrum is mentioned, contrary to a remark in a review (Ergebnisse der exakten Naturwissenschaften **8**, 247 (1929)).

[3] R. W. Wood, *Physical Optics*, 3rd ed., p. 606.

[4] C. E. K. Mees, J. Opt. Soc. Am. **25**, 80 (1935)

[5] O. Oldenberg, J. Chem. Phys. **3**, 266 (1935). The main purpose of this apparatus was the investigation of the kinetics of reactions in gases by measuring the concentration of radicals.

[6] G. Herzberg and H. Sponer, Zeits. f. physik. Chemie **B26**, 2 (1934).

[7] We are sure that the vibration of this level is not affected by an unexpected persistence of vibration (J. Franck and A. Eucken, Zeits. f. physik. Chemie **20**, 460 (1933)) since in active nitrogen the excitation process can be recognized by a certain resonance phenomenon building up on this level $v''=0$.

distribution of intensities in the v'/v'' diagram,[8] the vibrational transition $v'=0 \rightarrow v''=0$ at 10,500A is expected with highest intensity. Since high resolving power is required for the most sensitive test for faint and sharp absorption lines a 21-foot grating was used in the first order. The high sensitivity of the Eastman plates, type Z, is available only for rather intense spectra since the failure of the reciprocity law seems to be much more pronounced for these than for ordinary plates. Therefore, the intensity of the spectrum was increased by a cylindrical lens in front of the plate. The wavelength range 10,370–10,470A was investigated with IV–Q plates and the range 10,440–10,540A with I–Z plates. The progress due to the new I–Z plates is demonstrated by the fact that the emission spectrum of the 0→0 band, excited by a current density of only 7.5 ma per cm², could well be photographed with the 21-foot grating in 7 hours (Fig. 1), while previously no measurement or

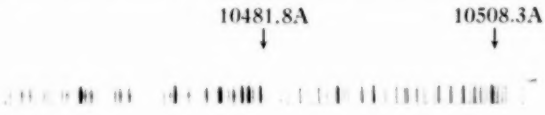

FIG. 1. Nitrogen, first positive group, 0→0 band.

photograph, resolving individual lines, had been published.

The duration of the afterglow is determined by the lifetime of atoms (order of magnitude of many seconds), most of them in their normal state, while in the recombination process the metastable atoms and molecules (lifetime of the metastable states of the order 1/1000 sec. or less) represent only intermediate states which due to their shorter lifetimes have much smaller concentrations than the normal N atoms. For the absorption experiment the most abundant supply of metastable molecules formed per sec. is desirable. The *atoms of the active nitrogen* are a source of metastable molecules of less power than *a uniform electric discharge*. This can be estimated from energy considerations as well as from the comparison of intensities of emission.[9] Therefore it is obviously much better for the absorption experiment to observe the ordinary discharge in which *molecular* nitrogen is being excited directly to the metastable level by the current—instead of the condensed discharge forming *atomic* nitrogen which in turn more indirectly produces metastable molecules. In order to favor the lowest quantum transition of the molecules relatively high pressure was applied. The high intensity of the first positive group, which determines the bright color of the discharge, indicates a large supply of metastable molecules formed per sec. by the radiation process; possibly some more are produced by direct excitation from the normal electronic level. The absorption spectrum during the discharge running can be observed only with a source for the continuous background of predominant intensity. This is represented by a 500-watt bulb.

Active nitrogen is formed only in the presence of *impurities* whose function it probably is to form an adsorbed layer on the glass walls and so prevent the recombination of atoms on the wall. In the uncondensed discharge, however, in which we do not care for a high concentration of atomic nitrogen but instead try to excite directly and concentrate *metastable molecules*, very probably *pure* nitrogen is preferable since the impurities have hardly a chance to favor the production of metastable molecules but might very well partly destroy them by impacts of the second kind. Pure nitrogen was made by decomposition of NaN_3, several times recrystallized and baked out in vacuum.

Since metastable molecules probably have a lifetime smaller than 1/1000 sec., their concentration is expected to fluctuate with the 60 cycle a.c. Therefore a revolving sector in front of the slit was used, transmitting light of the continuous background for the absorption experiment during the periods of maximum current through the N_2 discharge tube, cutting out the intermissions.

In spite of the precautions described no trace

[8] A. H. Poetker, Phys. Rev. **30**, 823 (1930); W. Weizel, *Handbuch der Exp. Phys. Erganzungsband*, Bandenspektren, 1931, p. 356.

[9] In nitrogen of 2 mm with 10 percent dissociation, the partial pressure of metastable molecules is estimated to be only 10^{-4} mm on the following basis: each combination process of two atoms, taking place by a triple collision, leads to one metastable molecule; the rate of combination is derived from Kneser's measurement of the decay of the afterglow (Ann. d. Physik **87**, 725 (1928); the comparison of these rates in nitrogen and hydrogen indicates that in nitrogen only a small fraction of all triple collisions of two atoms with a third particle leads to the formation of a molecule); the lifetime of metastable molecules is assumed to be 1/1000 sec., presumably a too optimistic assumption.

of an absorption spectrum could be detected. The length of the absorbing column of gas was 152 cm. The pressure was varied from 2 to 10 mm, the current increased to 150 ma. The wavelength range around 10,500A, given by Birge's formula for the heads of the first positive group, was investigated as well as the range about 10,420A, given by Poetker's observation, made with small resolving power.[10] The 0→1 absorption band at 8911 did not appear in absorption either.

The failure to observe the absorption spectrum of metastable N_2 might be due to the fact that in the discharge the metastable molecules have no chance for a very long life, since they can be destroyed by the current itself, raising the molecules from the metastable to a higher level from which they go down to the normal level by radiation.[11] *A priori*, we did not expect a very pronounced destruction of metastable molecules by this process. The reason is that the next higher level ($B^3\Pi_g$) which is most probably reached does not readily combine with the normal level so that the radiation process probably leads back to the metastable level.[12]

The experiment, however, proves that the concentration actually is too small although the apparatus is particularly sensitive. In the electric discharge the metastable molecules, although amply produced, presumably have no chance to live long enough for building an appreciable concentration. On the other hand, in the afterglow, the total number of metastable molecules to be produced—one for each pair of atoms combining—is limited by the degree of dissociation caused by the disruptive discharge. Therefore, the slowness of the decay, the very same peculiarity that makes the afterglow conspicuous, indicates that the production of metastable molecules is spread over so long a period that their concentration never reaches the limit required for an absorption experiment.

---

[10] R. T. Birge, Int. Crit. Tab. **5**, 409 (1929); A. H. Poetker, Phys. Rev. **30**, 812 (1927).

[11] An objection against the search for metastable N_2 in the uncondensed discharge might be raised on the following basis: In order to explain the observed quenching of the afterglow by a weak current, it has been suggested that metastable N_2 molecules are reduced to the normal state at a particularly high rate by an electric current (J. Kaplan, Phys. Rev. **33**, 191 (1929)). This assumption, however, turns out not to be adequate for the explanation of the observed facts, considering in particular the more recent results of Wrede (Zeits. f. Physik **54**, 69 (1929)). The destruction of metastable molecules would explain only a *temporary* inability of the active nitrogen to emit light, caused by the destruction of one of the *intermediate* states, but not of the *main source* of energy. It is true that this explanation well applies to the observed *temporary* quenching of the afterglow by heating; in this experiment the active nitrogen, flowing through glass tubes, is dark in the heated zone but starts radiating again beyond this zone, indicating a persistence of the main source of energy, the atoms. On the other hand, the quenching by an electric current is *permanent* (R. J. Strutt, Proc. Roy. Soc. **A92**, 444 (1916)); correspondingly Wrede observed a strong decrease of the concentration of nitrogen atoms by the effect of a current, observed by the effusion method. He concluded that the current creates a modification (for example, ions) which permits molecular formation in a rapid, bimolecular reaction (or possibly wall reaction), without the slow process of triple collisions. It is to be concluded that the observed quenching of the afterglow by a weak current does not indicate a particularly rapid destruction of metastable N_2 by the effect of the current.

[12] The process just considered—destruction of metastables by the current—does not lead to the result that metastables have a maximum concentration for a small current. Assuming that metastable molecules are *formed* by electron impact and *destroyed* either by electron impact or by another independent process (impact of the second kind or radiation), it can be shown by a simple analysis that the concentration of metastables is not decreasing with increasing current but instead increasing with the current according to a power less than the first. Hence strong current was applied in the experiments described.

Hyperfine Structure Formulae for the Configuration p^3s

M. F. CRAWFORD,* *Department of Physics, University of Wisconsin,*
AND
LAWRENCE A. WILLS, *College of the City of New York*

(Received May 10, 1935)

Hfs interval factor formulae for the states of p^3s are derived by the method of Breit and Wills. The formulae for intermediate coupling are expressed in two forms: one involving the coefficients C's, the other the coefficients K's, corresponding to the representation of the functions of the states in intermediate coupling as a linear combination of the (jj) and the (LS) functions, respectively. The (jj)—(LS) transformation matrices as well as the interval factor formulae for (jj) and (LS) coupling are also given.

I. INTRODUCTION

BREIT and Wills[1] extended the relativistic theory of hyperfine structure to intermediate coupling and derived interval factor formulae for the configurations sx, $p\cdot p$, p^2, p^3, p^2s. Recently one of the writers[2] treated the d^2s configuration by the same method. p^3s, a configuration with an unpaired s electron, also merits consideration since it usually gives rise to measurable hyperfine separations. The formulae for this configuration are presented here.

II. WAVE FUNCTIONS AND INTERVAL FACTOR FORMULAE IN INTERMEDIATE COUPLING

The configuration p^3s gives rise to ten states: one with $J=3$, four with $J=2$, four with $J=1$, and one with $J=0$. As the relativistic treatment of hyperfine structure must be made via (jj) coupling, the configuration will be considered first in this coupling. The functions representing the states in (jj) coupling can be conveniently thought of as arising from the coupling of the states of p^3 with an s electron. The states of p^3 are given in Table I. They are designated by

TABLE I. *States of p^3.*

$(j_1, j_2, j_3)=(3/2, 3/2, 3/2)$;			$(3/2, 3/2, 1/2)$;			$(3/2, 1/2, 1/2)$
Resultant $J=$	3/2	;	5/2	3/2	1/2;	3/2
Symbol	$\psi^{3/2}$		$\varphi^{5/2}$	$\varphi^{3/2}$	$\varphi^{1/2}$	$\chi^{3/2}$

Greek letters with their J values indicated by superscripts.

The calculations can be made expediently by using eigenfunctions for a given magnetic quantum number. These functions of p^3 states will be represented by the state symbols with the magnetic quantum number, m, added as a subscript. It is necessary in the calculations to express the three-electron functions in terms of the one-electron functions, which for a given j and m will be represented by symbols of the type $(j)_m$. The three-electron functions for the states with $m=J$, expressed in terms of the one-electron functions, are given here. The functions for other values of m can readily be obtained from these by the method of Gray and Wills.[3] The signs of the p^3 functions and also those of the p^3s functions used in this calculation have been adjusted so as to give magnetic energy matrices identical with those published by Johnson.[4]

(3/2, 3/2, 3/2) Sub-group.

$$\psi_{3/2}{}^{3/2}=(1/\sqrt{6})[(3/2)_{3/2},\ (3/2)_{1/2},\ (3/2)_{-1/2}].$$

(3/2, 3/2, 1/2) Sub-group.

$$\varphi_{5/2}{}^{5/2}=(1/\sqrt{6})[(3/2)_{3/2},\ (3/2)_{1/2},\ (1/2)_{1/2}].$$

$$\varphi_{3/2}{}^{3/2}=(1/\sqrt{5})(1/\sqrt{6})[(3/2)_{3/2},\ (3/2)_{-1/2},\ (1/2)_{1/2}]-(2/\sqrt{5})(1/\sqrt{6})\times[(3/2)_{3/2},\ (3/2)_{1/2},\ (1/2)_{-1/2}].$$

$$\varphi_{1/2}{}^{1/2}=(1/\sqrt{2})(1/\sqrt{6})[(3/2)_{3/2},\ (3/2)_{-3/2},\ (1/2)_{1/2}]-(1/\sqrt{2})(1/\sqrt{6})\times[(3/2)_{1/2},\ (3/2)_{-1/2},\ (1/2)_{1/2}].$$

(3/2, 1/2, 1/2) Sub-group.

$$\chi_{3/2}{}^{3/2}=(1/\sqrt{6})[(3/2)_{3/2},\ (1/2)_{-1/2},\ (1/2)_{1/2}].$$

* This research was carried out during the tenure of a Royal Society of Canada Fellowship.

[1] G. Breit and L. A. Wills, Phys. Rev. **44**, 470 (1933).
[2] M. F. Crawford, Phys. Rev. **47**, 768 (1935).
[3] N. Gray and L. A. Wills, Phys. Rev. **38**, 248 (1931).
[4] M. H. Johnson, Jr., Phys. Rev. **39**, 197 (1932).

Each square bracket in the preceding expressions is an abbreviation for the determinant representation of a three-electron function as a combination of products of three one-electron functions.

The states of p^3s will now be considered. The functions of the s electron will be symbolized by s_m. They can be combined with the functions of the p^3 states without paying attention to symmetry.

$J=3$. The function representing the state with $J=3$, $m=3$, which is independent of coupling, can be written

$$\mathrm{I}=s_{1/2}\varphi_{3/2}{}^{5/2}. \tag{1}$$

The interval factor formula obtained from this function by the procedure of Breit and Wills[1] is

$$A(J=3)=(1/6)a_s+(2/3)a'+(1/6)a''. \tag{2}$$

The a's represent the hyperfine structure interaction or coupling constants as in the paper of Breit and Wills.

$J=2$. The functions representing the four states with $J=2$, $m=2$ in (jj) coupling are

$$\begin{aligned}&\mathrm{I}=s_{1/2}\psi_{3/2}{}^{3/2};\\ &\mathrm{II}=(5/6)^{1/2}s_{-1/2}\varphi_{3/2}{}^{5/2}-(1/\sqrt{6})s_{1/2}\varphi_{3/2}{}^{5/2};\\ &\mathrm{III}=s_{1/2}\varphi_{3/2}{}^{3/2};\quad \mathrm{IV}=s_{1/2}\chi_{3/2}{}^{3/2}.\end{aligned} \tag{3}$$

In intermediate coupling the general function for a state with $J=2$, $m=2$ is

$$(2)_2=C_1\mathrm{I}+C_2\mathrm{II}+C_3\mathrm{III}+C_4\mathrm{IV}. \tag{4}$$

From this we obtain

$$\begin{aligned}A(J=2)=a_s(1/4-(5/12)C_2{}^2)+a'((3/4)C_1{}^2+(14/15)C_2{}^2+(9/10)C_3{}^2+(3/4)C_4{}^2+(2/5\sqrt{6})C_2C_3)\\ +a''((7/30)C_2{}^2-(3/20)C_3{}^2-(2/5\sqrt{6})C_2C_3)+a'''(C_1-C_4)((1/\sqrt{15})C_2-3(2/5)^{1/2}C_3).\end{aligned} \tag{5}$$

$J=1$. The functions representing the four states with $J=1$, $m=1$ in (jj) coupling are

$$\begin{aligned}&\mathrm{I}=(\sqrt{3}/2)s_{-1/2}\psi_{3/2}{}^{3/2}-(1/2)s_{1/2}\psi_{1/2}{}^{3/2};\quad &&\mathrm{II}=-(\sqrt{3}/2)s_{-1/2}\varphi_{3/2}{}^{3/2}+(1/2)s_{1/2}\varphi_{1/2}{}^{3/2};\\ &\mathrm{III}=s_{1/2}\varphi_{1/2}{}^{1/2};\quad &&\mathrm{IV}=(\sqrt{3}/2)s_{-1/2}\chi_{3/2}{}^{3/2}-(1/2)s_{1/2}\chi_{1/2}{}^{3/2}.\end{aligned} \tag{6}$$

In intermediate coupling the general function is

$$(1)_1=C_1\mathrm{I}+C_2\mathrm{II}+C_3\mathrm{III}+C_4\mathrm{IV}. \tag{7}$$

From this we obtain

$$\begin{aligned}A(J=1)=a_s((3/4)C_3{}^2-1/4)+a'((5/4)C_1{}^2+(3/2)C_2{}^2+(5/4)C_4{}^2)+a''((1/2)C_3{}^2-(1/4)C_2{}^2)\\ +a'''[2(5/2)^{1/2}C_2(C_1-C_4)+C_3(C_4+C_1)].\end{aligned} \tag{8}$$

$J=0$. This state has no hyperfine structure and is independent of coupling.

III. Interval Factor Formulae in (jj) and (LS) Coupling, and the $(jj)-(LS)$ Transformation Matrices

The interval factors of the states in (jj) coupling can be obtained directly from the preceding formulae. Consider the states with $J=2$. It is obvious that for one of these in (jj) coupling $C_1=1$, $C_2=C_3=C_4=0$; for another $C_2=1$, $C_1=C_3=C_4=0$; and so on for the others. The (jj) interval factors obtained in this manner are:

$J=3$. Sub-group.

$$s\varphi^{5/2}:\ A(J=3)=(1/6)a_s+(2/3)a'+(1/6)a''. \tag{9}$$

$J=2$. Sub-group.

$$\begin{aligned}&s\psi^{3/2}:\ A(J=2)=(1/4)a_s+(3/4)a'.\\ &s\varphi^{5/2}:\ A(J=2)=-(1/6)a_s+(14/15)a'+(7/30)a''.\\ &s\varphi^{3/2}:\ A(J=2)=(1/4)a_s+(9/10)a'-(3/20)a''.\\ &s\chi^{3/2}:\ A(J=2)=(1/4)a_s+(3/4)a'.\end{aligned} \tag{10}$$

J=1. Sub-group.

$$
\begin{aligned}
&s\psi^{3/2}:\ A(J=1)=-(1/4)a_s+(5/4)a'.\\
&s\varphi^{3/2}:\ A(J=1)=-(1/4)a_s+(3/2)a'-(1/4)a''.\\
&s\varphi^{1/2}:\ A(J=1)=(1/2)a_s+(1/2)a''.\\
&s\chi^{3/2}:\ A(J=1)=-(1/4)a_s+(5/4)a'.
\end{aligned}
\tag{11}
$$

The interval factors of the states in (LS) coupling can be obtained from Eqs. (6, 8) by using the (jj)—(LS) transformation matrices. These matrices are given in Table II.

The interval factors of the states in (LS) coupling, obtained by substituting the appropriate coefficients from the transformation matrices in the general equations, are

$$
\begin{aligned}
&A(^3D_3)=(1/6)a_s+(2/3)a'+(1/6)a''\leqq(1/6)a_s+(4/5)a_p.\\
&A(^3D_2)=(1/12)a_s+(11/12)a'-(2/3)a'''\leqq(1/12)a_s+(3/5)a_p.\\
&A(^5S_2)=(1/4)a_s+(5/6)a'-(1/12)a''+(4/3)a'''\leqq(1/4)a_s.\\
&A(^3P_2)=(1/4)a_s+(3/4)a'\leqq(1/4)a_s+(2/5)a_p.\\
&A(^1D_2)=(5/6)a'+(1/6)a''-(2/3)a'''\leqq a_p.\\
&A(^3S_1)=-(1/4)a_s+(25/18)a'-(5/36)a''+(20/9)a'''\leqq-(1/4)a_s.\\
&A(^3D_1)=-(1/4)a_s+(49/36)a'-(1/9)a''-(20/9)a'''\leqq-(1/4)a_s+(4/5)a_p.\\
&A(^3P_1)=(1/4)a_s+(5/12)a'+(1/3)a''+(2/3)a'''\leqq(1/4)a_s+a_p.\\
&A(^1P_1)=(5/6)a'+(1/6)a''-(2/3)a'''\leqq a_p.
\end{aligned}
\tag{12}
$$

In the nonrelativistic approximation for the p electron a', a'', a''' can be expressed in terms of a_p as follows:

$$
a'=(8/15)a_p,\qquad a''=(8/3)a_p,\qquad a'''=-(1/6)a_p,
\tag{13}
$$

where $a_p=2g\mu_0^2\overline{(r^{-3})}$. The second simplified expression given above for each interval factor is obtained by using these nonrelativistic approximations for the a's.

TABLE II. *Transformation matrices,* $(jj)-(LS)$.

$J=2$	$s\psi^{3/2}$	$s\varphi^{3/2}$	$s\varphi^{1/2}$	$s\chi^{3/2}$	$J=1$	$s\psi^{3/2}$	$s\varphi^{3/2}$	$s\varphi^{1/2}$	$s\chi^{3/2}$
$^3S_2$	$-\sqrt{2}/3$	0	$\sqrt{5}/3$	$\sqrt{2}/3$	$^3S_1$	$-\sqrt{2}/3$	$-\sqrt{5}/3$	0	$\sqrt{2}/3$
$^3D_2$	$1/\sqrt{6}$	$\sqrt{2}/\sqrt{5}$	$2/\sqrt{15}$	$-1/\sqrt{6}$	$^3D_1$	$5/3\sqrt{10}$	$-2/3$	0	$-5/3\sqrt{10}$
$^3P_2$	$-1/\sqrt{2}$	0	0	$-1/\sqrt{2}$	$^3P_1$	$-1/\sqrt{6}$	0	$-\sqrt{2}/\sqrt{3}$	$-1/\sqrt{6}$
$^1D_2$	$-1/3$	$\sqrt{3}/\sqrt{5}$	$-2\sqrt{2}/3\sqrt{5}$	$1/3$	$^1P_1$	$-1/\sqrt{3}$	0	$1/\sqrt{3}$	$-1/\sqrt{3}$

IV. Interval Factors in Intermediate Coupling Expressed in Terms of the Coefficients, K's, of the Transformation Relating the Intermediate to the (LS) States

When the coupling in a configuration tends towards (LS) it is convenient for the application of the theory to have the interval factors expressed in terms of the coefficients, K, that relate the intermediate states to the (LS) states. The interval factors can readily be converted into this form by means of the $(jj)-(LS)$ transformation matrices. In terms of the K's the interval factors are:

$$
\begin{aligned}
A(J=2)=a_s&(1/4-(1/6)K_2^2-(1/4)K_4^2-(\sqrt{2}/2\sqrt{3})K_2K_4)\\
&+a'((5/6)K_1^2+(11/12)K_2^2+(3/4)K_3^2+(5/6)K_4^2+(1/3\sqrt{3})K_1K_2+(1/3\sqrt{6})K_2K_4)\\
&+a''(-(1/12)K_1^2+(1/6)K_4^2-(1/3\sqrt{3})K_1K_2+(\sqrt{6}/9)K_2K_4)\\
&+a'''((4/3)K_1^2-(2/3)K_2^2-(2/3)K_4^2-(2/3\sqrt{3})K_1K_2+(10/3\sqrt{6})K_2K_4).
\end{aligned}
\tag{14}
$$

$$A(J=1)=a_s(-(1/4)K_1^2-(1/4)K_2^2+(1/4)K_3^2-(1/\sqrt{2})K_3K_4)$$
$$+a'((25/18)K_1^2+(49/36)K_2^2+(5/12)K_3^2+(5/6)K_4^2+(\sqrt{5}/9)K_1K_2+(5/3\sqrt{2})K_3K_4)$$
$$+a''((-5/36)K_1^2-(1/9)K_2^2+(1/3)K_3^2+(1/6)K_4^2-(\sqrt{5}/9)K_1K_2-(\sqrt{2}/3)K_3K_4)$$
$$+a'''((20/9)K_1^2-(20/9)K_2^2+(2/3)K_3^2-(2/3)K_4^2-(2\sqrt{5}/9)K_1K_2+(\sqrt{2}/3)K_3K_4). \quad (15)$$

V. Energy Matrices in (*LS*) and (*jj*) Coupling

The coefficients, C, K, that appear in the interval factor formulae are obtainable from the empirical energies of the states of the configuration. To evaluate the coefficients from the energies the energy matrices are required, preferably for both (*LS*) and (*jj*) coupling to correspond to the two forms of the interval factor formulae. Johnson[4] has worked out the energy matrices in (*LS*) coupling. The energy matrices in (*jj*) coupling can readily be obtained from his results by means of the transformations given in Table II; they are presented in Table III. In the table the $J=3$ state is the energy datum level.

The coefficients determined from the empirical energies can be checked by computing the Landé g factors from the coefficients and comparing them with the empirical g's. The g's can be computed most easily via (*LS*) coupling since the matrices for the g's of the (*LS*) states are diagonal. Thus the g of a state with a given J in intermediate coupling is given by $\Sigma_i g_i K_i^2$ summed over all the (*LS*) states with the given J. The g_i's are the g factors of the (*LS*) states and the K_i's are the coefficients in the linear combination that expresses the function of the intermediate state in terms of the functions of the (*LS*) states.

This investigation was carried out under the direction of Professor G. Breit, and the authors wish to thank him for his interest and advice. One of us, M. F. C., takes this opportunity to acknowledge the award of a Fellowship by the Royal Society of Canada, and to thank the Department of Physics of the University of Wisconsin for the privilege of working here.

Table III. *Energy matrices, (jj) coupling.*

	$J=3$ I $=s\varphi^{3/2}$	$J=2$ I $=s\varphi^{3/2}$	$J=2$ II $=s\varphi^{3/2}$	$J=2$ III $=s\varphi^{3/2}$	$J=2$ IV $=s\chi^{3/2}$	$J=1$ I $=s\varphi^{3/2}$	$J=1$ II $=s\varphi^{3/2}$	$J=1$ III $=s\varphi^{1/2}$	$J=1$ IV $=s\chi^{3/2}$	$J=0$ I $=s\varphi^{1/2}$
$J=3$ I	0									
$J=2$ I		$\frac{1}{25}F_2+\frac{3}{2}\bar{a}$	$-\frac{2}{3\sqrt{15}}G_1$	$\sqrt{10}\left(\frac{F_2}{25}+\frac{G_1}{15}\right)$	$\frac{1}{5}F_2$					
II		$-\frac{2}{3\sqrt{15}}G_1$	$\frac{2}{5}G_1$	$-\frac{4\sqrt{2}}{15\sqrt{3}}G_1$	$\frac{2}{3\sqrt{15}}G_1$					
III		$\sqrt{10}\left(\frac{F_2}{25}+\frac{G_1}{15}\right)$	$-\frac{4\sqrt{2}}{15\sqrt{3}}G_1$	$-\frac{1}{5}F_2-\frac{1}{15}G_1$	$-\sqrt{10}\left(\frac{F_2}{25}+\frac{G_1}{15}\right)$					
IV		$\frac{1}{5}F_2$	$\frac{2}{3\sqrt{15}}G_1$	$-\sqrt{10}\left(\frac{F_2}{25}+\frac{G_1}{15}\right)$	$\frac{1}{25}F_2-\frac{3}{2}\bar{a}$					
$J=1$ I						$\frac{1}{25}F_2+\frac{4}{9}G_1+\frac{3}{2}$	$-\sqrt{10}\left(\frac{F_2}{25}-\frac{G_1}{9}\right)$	$-\frac{2}{9}G_1$	$\frac{1}{5}F_2$	
II						$-\sqrt{10}\left(\frac{F_2}{25}-\frac{G_1}{9}\right)$	$-\frac{1}{5}F_2+\frac{5}{9}G_1$	0	$\sqrt{10}\left(\frac{F_2}{25}-\frac{G_1}{9}\right)$	
III						$-\frac{2}{9}G_1$	0	$\frac{6}{25}F_2+\frac{2}{9}G_1$	$-\frac{2}{9}G_1$	
IV						$\frac{1}{5}F_2$	$\sqrt{10}\left(\frac{F_2}{25}-\frac{G_1}{9}\right)$	$-\frac{2}{9}G_1$	$\frac{1}{25}F_2+\frac{4}{9}G_1-\frac{3}{2}\bar{a}$	
$J=0$ I										$\frac{6}{25}F_2$

The Particle Problem in the General Theory of Relativity

A. EINSTEIN AND N. ROSEN, *Institute for Advanced Study, Princeton*

(Received May 8, 1935)

The writers investigate the possibility of an atomistic theory of matter and electricity which, while excluding singularities of the field, makes use of no other variables than the $g_{\mu\nu}$ of the general relativity theory and the φ_μ of the Maxwell theory. By the consideration of a simple example they are led to modify slightly the gravitational equations which then admit regular solutions for the static spherically symmetric case. These solutions involve the mathematical representation of physical space by a space of two identical sheets, a particle being represented by a "bridge" connecting these sheets. One is able to understand why no neutral particles of negative mass are to be found. The combined system of gravitational and electromagnetic equations are treated similarly and lead to a similar interpretation. The most natural elementary charged particle is found to be one of zero mass. The many-particle system is expected to be represented by a regular solution of the field equations corresponding to a space of two identical sheets joined by many bridges. In this case, because of the absence of singularities, the field equations determine both the field and the motion of the particles. The many-particle problem, which would decide the value of the theory, has not yet been treated.

IN spite of its great success in various fields, the present theoretical physics is still far from being able to provide a unified foundation on which the theoretical treatment of all phenomena could be based. We have a general relativistic theory of macroscopic phenomena, which however has hitherto been unable to account for the atomic structure of matter and for quantum effects, and we have a quantum theory, which is able to account satisfactorily for a large number of atomic and quantum phenomena but which by its very nature is unsuited to the principle of relativity. Under these circumstances it does not seem superfluous to raise the question as to what extent the method of general relativity provides the possibility of accounting for atomic phenomena. It is to such a possibility that we wish to call attention in the present paper in spite of the fact that we are not yet able to decide whether this theory can account for quantum phenomena. The publication of this theoretical method is nevertheless justified, in our opinion, because it provides a clear procedure, characterized by a minimum of assumptions, the carrying out of which has no other difficulties to overcome than those of a mathematical nature.

The question with which we are concerned can be put as follows: Is an atomistic theory of matter and electricity conceivable which, while excluding singularities in the field, makes use of no other field variables than those of the gravitational field ($g_{\mu\nu}$) and those of the electromagnetic field in the sense of Maxwell (vector potentials, φ_μ)?

One would be inclined to answer this question in the negative in view of the fact that the Schwarzschild solution for the spherically symmetric static gravitational field and Reissner's extension of this solution to the case when an electrostatic field is also present each have a singularity. Furthermore the last of the Maxwell equations, which expresses the vanishing of the divergence of the (contravariant) electrical field density, appears to exclude in general the existence of charge densities, hence also of electrical particles.

For these reasons writers have occasionally noted the possibility that material particles might be considered as singularities of the field. This point of view, however, we cannot accept at all. For a singularity brings so much arbitrariness into the theory that it actually nullifies its laws. A pretty confirmation of this was imparted in a letter to one of the authors by L. Silberstein. As is well known, Levi-Civita and Weyl have given a general method for finding axially symmetric static solutions of the gravitational equations. By this method one can readily obtain a solution which, except for two point singularities lying on the axis of symmetry, is everywhere regular and is Euclidean at infinity. Hence if one admitted singularities as representing particles one would have here a case of two particles not accelerated by their gravitational interaction, which would certainly be excluded physically. Every field theory, in our opinion, must therefore adhere to the fundamental principle that singularities of the field are to be excluded.

In the following we shall show that it is possible to do this in a natural way, that the question we are raising can be answered in the affirmative.

§1. A Special Kind of Singularity and Its Removal

The first step to the general theory of relativity was to be found in the so-called "Principle of Equivalence": If in a space free from gravitation a reference system is uniformly accelerated, the reference system can be treated as being "at rest," provided one interprets the condition of the space with respect to it as a homogeneous gravitational field. As is well known the latter is exactly described by the metric field[1]

$$ds^2 = -dx_1^2 - dx_2^2 - dx_3^2 + \alpha^2 x_1^2 dx_4^2. \quad (1)$$

The $g_{\mu\nu}$ of this field satisfy in general the equations

$$R^i{}_{klm} = 0, \quad (2)$$

and hence the equations

$$R_{kl} = R^m{}_{klm} = 0. \quad (3)$$

The $g_{\mu\nu}$ corresponding to (1) are regular for all finite points of space-time. Nevertheless one cannot assert that Eqs. (3) are satisfied by (1) for *all* finite values of $x_1, \cdots, x_4$. This is due to the fact that the determinant g of the $g_{\mu\nu}$ vanishes for $x_1 = 0$. The contravariant $g^{\mu\nu}$ therefore become infinite and the tensors $R^i{}_{klm}$ and R_{kl} take on the form $0/0$. From the standpoint of Eqs. (3) the hyperplane $x_1 = 0$ then represents a singularity of the field.

We now ask whether the field law of gravitation (and later on the field law of gravitation and electricity) could not be modified in a natural way without essential change so that the solution (1) would satisfy the field equations for all finite points, i.e., also for $x_1 = 0$. W. Mayer has called our attention to the fact that one can make $R^i{}_{klm}$ and R_{kl} into rational functions of the $g_{\mu\nu}$ and their first two derivatives by multiplying them by suitable powers of g. It is easy to show that in $g^2 R_{kl}$ there is no longer any denominator. If then we replace (3) by

$$R_{kl}^* = g^2 R_{kl} = 0, \quad (3a)$$

this system of equations is satisfied by (1) at all finite points. This amounts to introducing in place of the $g^{\mu\nu}$ the cofactors $[g_{\mu\nu}]$ of the $g_{\mu\nu}$ in g in order to avoid the occurrence of denominators. One is therefore operating with tensor densities of a suitable weight instead of with tensors. In this way one succeeds in avoiding singularities of that special kind which is characterized by the vanishing of g.

The solution (1) naturally has no deeper physical significance insofar as it extends into spatial infinity. It allows one to see however to what extent the regularization of the hypersurfaces $g = 0$ leads to a theoretical representation of matter, regarded from the standpoint of the original theory. Thus, in the framework of the original theory one has the gravitational equations

$$R_{ik} - \tfrac{1}{2} g_{ik} R = -T_{ik}, \quad (4)$$

where T_{ik} is the tensor of mass or energy density. To interpret (1) in the framework of this theory we must approximate the line element by a slightly different one which avoids the singularity $g = 0$. Accordingly we introduce a small constant σ and let

$$ds^2 = -dx_1^2 - dx_2^2 - dx_3^2 + (\alpha^2 x_1^2 + \sigma) dx_4^2; \quad (1a)$$

the smaller $\sigma (> 0)$ is chosen, the nearer does this gravitational field come to that of (1). If one calculates from this the (fictitious) energy tensor T_{ik} one obtains as nonvanishing components

$$T_{22} = T_{23} = \alpha^2 / \sigma / (1 + \alpha^2 x_1^2 / \sigma)^2.$$

We see then that the smaller one takes σ the more is the tensor concentrated in the neighborhood of the hypersurface $x_1 = 0$. From the standpoint of the original theory the solution (1) contains a singularity which corresponds to an energy or mass concentrated in the surface $x_1 = 0$; from the standpoint of the modified theory, however, (1) is a solution of (3a), free from singularities, which describes the "field-producing mass," without requiring for this the introduction of any new field quantities.

[1] It is worth pointing out that this metric field does not represent the whole Minkowski space but only part of it. Thus, the transformation that converts

$$ds^2 = -d\xi_1^2 - d\xi_2^2 - d\xi_3^2 + d\xi_4^2$$

into (1) is

$$\xi_1 = x_1 \cosh \alpha x_4, \qquad \xi_3 = x_3,$$
$$\xi_2 = x_2, \qquad \xi_4 = x_1 \sinh \alpha x_4.$$

It follows that only those points for which $\xi_1^2 \geqq \xi_4^2$ correspond to points for which (1) is the metric.

It is clear that all equations of the absolute differential calculus can be written in a form free from denominators, whereby the tensors are replaced by tensor densities of suitable weight.

It is to be noted that in the case of the solution (1) the whole field consists of two equal halves, separated by the surface of symmetry $x_1=0$, such that for the corresponding points (x_1, x_2, x_3, x_4) and $(-x_1, x_2, x_3, x_4)$ the g_{ik} are equal. As a result we find that, although we are permitting the determinant g to take on the value 0 (for $x_1=0$), no change of sign of g and in general no change in the "inertial index" of the quadratic form (1) occurs. These features are of fundamental importance from the point of view of the physical interpretation, and will be encountered again in the solutions to be considered later.

§2. The Schwarzschild Solution

As is well known, Schwarzschild found the spherically symmetric static solution of the gravitational equations

$$ds^2=-\frac{1}{1-2m/r}dr^2-r^2(d\theta^2+\sin^2\theta d\phi^2)+(1-2m/r)dt^2, \quad (5)$$

($r>2m$, θ from 0 to π, ϕ from 0 to 2π); the variables x_1, x_2, x_3, x_4 are here r, θ, ϕ, t. The vanishing of the determinant of the $g_{\mu\nu}$ for $\theta=0$ is unimportant, since the corresponding (spatial) direction is not preferred. On the other hand g_{11} for $r=2m$ becomes infinite and hence we have there a singularity.

If one introduces in place of r a new variable according to the equation

$$u^2=r-2m,$$

one obtains for ds^2 the expression

$$ds^2=-4(u^2+2m)du^2-(u^2+2m)^2(d\theta^2+\sin^2\theta d\phi^2)+\frac{u^2}{u^2+2m}dt^2. \quad (5a)$$

These new $g_{\mu\nu}$ are regular functions for all values of the variables. For $u=0$, however, g_{44} vanishes, hence also the determinant g. This does not prevent the field equations (3a), which have no denominators, from being satisfied for all values of the independent variables. We are therefore dealing with a solution of the (new) field equations, which is free from singularities for all finite points. The hypersurface $u=0$ (or in the original variables, $r=2m$) plays here the same role as the hypersurface $x_1=0$ in the previous example.

As u varies from $-\infty$ to $+\infty$, r varies from $+\infty$ to $2m$ and then again from $2m$ to $+\infty$. If one tries to interpret the regular solution (5a) in the space of r, θ, ϕ, t, one arrives at the following conclusion. The four-dimensional space is described mathematically by two congruent parts or "sheets," corresponding to $u>0$ and $u<0$, which are joined by a hyperplane $r=2m$ or $u=0$ in which g vanishes.[2] We call such a connection between the two sheets a "bridge."

We see now in the given solution, free from singularities, the mathematical representation of an elementary particle (neutron or neutrino). Characteristic of the theory we are presenting is the description of space by means of two sheets. A bridge, spatially finite, which connects these sheets characterizes the presence of an electrically neutral elementary particle. With this conception one not only obtains the representation of an elementary particle by using only the field equations, that is, without introducing new field quantities to describe the density of matter; one is also able to understand the atomistic character of matter as well as the fact that there can be no particles of negative mass. The latter is made clear by the following considerations. If we had started from a Schwarzschild solution with negative m, we should not have been able to make the solution regular by introducing a new variable u instead of r; that is to say, no "bridge" is possible that corresponds to a particle of negative mass.

If we consider once more the solution (1) from the standpoint of the information we have acquired from the Schwarzschild solution, we see that there also the two congruent halves of the space for $x_1>0$ and $x_1<0$ can be interpreted as two sheets each corresponding to the same physical space. In this sense the example represents a gravitational field, independent of x_2 and x_3, which ends in a plane covered with mass and forming a boundary of the space. In this example, as well as in the Schwarzschild case, a solution free from singularities at all finite points is made possible by the introduction of the modified gravitational Eqs. (3a).

[2] Because of the symmetry about the hypersurface $g=0$, the sign of g does not change at this hypersurface.

The main value of the considerations we are presenting consists in that they point the way to a satisfactory treatment of gravitational mechanics. One of the imperfections of the original relativistic theory of gravitation was that as a field theory it was not complete; it introduced the independent postulate that the law of motion of a particle is given by the equation of the geodesic.[3] A complete field theory knows only fields and not the concepts of particle and motion. For these must not exist independently of the field but are to be treated as part of it. On the basis of the description of a particle without singularity one has the possibility of a logically more satisfactory treatment of the combined problem: The problem of the field and that of motion coincide.

If several particles are present, this case corresponds to finding a solution without singularities of the modified Eqs. (3a), the solution representing a space with two congruent sheets connected by several discrete "bridges." Every such solution is at the same time a solution of the field problem and of the motion problem.

In this case it will not be possible to describe the whole field by means of a single coordinate system without introducing singularities. The simplest procedure appears to be to choose coordinate systems in the following way:

(1) One coordinate system to describe one of the congruent sheets. With respect to this system the field will appear to be singular at every bridge.

(2) One coordinate system for every bridge, to provide a description of the field at the bridge and in the neighborhood of the latter, which is free from singularities.

Between the coordinates of the sheet system and those of each bridge system there must exist outside of the hypersurfaces $g=0$, a regular coordinate transformation with nonvanishing determinant.

§3. Combined Field. Electricity

The simplest method of fitting electricity into the conceptual framework of the general theory of relativity is based on the following train of thoughts. If besides the pure gravitational field other field variables are also present, the field equations of gravitation are

$$R_{ik}-\tfrac{1}{2}g_{ik}R=-T_{ik}, \tag{4}$$

where T_{ik} is the "material" energy tensor, i.e., that part of the mathematical expression of the energy which does not depend exclusively on the $g_{\mu\nu}$. In the case of the phenomenological representation of matter—if it is to be considered as "dust-like," that is, without pressure—one takes

$$T^{ik}=\rho(dx^i/ds)(dx^k/ds),$$

where ρ is the density-scalar, dx^i/ds the velocity-vector of the matter. It is to be noted that T_4^4 is accordingly a positive quantity.

In general the additional field-variables satisfy such differential equations that, in consequence of them, the divergence $T_{ik;\,m}g^{km}$ vanishes. As the divergence of the left side of (4) vanishes identically, this means that among all the field equations those four identities exist which are needed for their compatibility. Through this condition, in certain cases, the structure of T_{ik}, not however its sign, is determined. It appears natural to choose this sign in such a way that the component T_4^4 (in the limit of the special relativity theory) is always positive.

The Maxwell electromagnetic field, as is well known, is represented by the antisymmetric field tensor $\varphi_{\mu\nu}(=\partial\varphi_\mu/\partial x^\nu-\partial\varphi_\nu/\partial x^\mu)$, which satisfies the field equations

$$\varphi_{\mu\nu;\,\sigma}g^{\nu\sigma}=0. \tag{6}$$

These equations have the well-known consequence that the divergence of the tensor

$$T_{ik}=\tfrac{1}{4}g_{ik}\varphi_{\alpha\beta}\varphi^{\alpha\beta}-\varphi_{i\alpha}\varphi_k{}^\alpha \tag{7}$$

vanishes. The sign has been so chosen that T_4^4 is positive for the case of the special relativity theory. If one puts this T_{ik} into the gravitational Eqs. (4), then the latter together with (6) and (7) form a theory of gravitation and electricity.

It so happens that we are forced to put the negative of the above into the gravitational equations if it is to be possible to obtain static spherically symmetric solutions of the equations, free from singularities, which could represent electrical particles. Making this change of sign one finds as the required solution

[3] To be sure, this weakness was formally avoided in the original theory of relativity by the introduction of the energy tensor into the field equations. It was clear, however, from the very beginning that this was only a provisory completion of the theory in the sense of a phenomenological interpretation.

$$\left.\begin{aligned} &\varphi_1=\varphi_2=\varphi_3=0, \quad \varphi_4=\epsilon/r, \\ ds^2=&-\frac{1}{1-2m/r-\epsilon^2/2r^2}dr^2 \\ &-r^2(d\theta^2+\sin^2\theta d\varphi^2)+\left(1-\frac{2m}{r}-\frac{\epsilon^2}{2r^2}\right)dt^2. \end{aligned}\right\} \tag{8}$$

Here m has obviously the significance of a gravitating mass, ϵ that of an electrical charge.

It turns out that also in this case there is no difficulty in forming a solution without singularity corresponding to the solution just given.[4] Curiously enough, one finds that the mass m is not determined by the electrical charge ϵ, but that ϵ and m are independent constants of integration. It also turns out that for the removal of the singularity it is not necessary to take the ponderable mass m positive. In fact, as we shall show immediately, there exists a solution free from singularities for which the mass constant m vanishes. Because we believe that these massless solutions are the physically important ones we will consider here the case $m=0$.

The field equations without denominators can be written

$$\left.\begin{aligned} &\varphi_{\mu\nu}=\varphi_{\mu,\nu}-\varphi_{\nu,\mu}, \quad g^2\varphi_{\mu\nu;\sigma}g^{\nu\sigma}=0, \\ &g^2(R_{ik}+\varphi_{i\alpha}\varphi_k{}^{\alpha}-\tfrac{1}{4}g_{ik}\varphi_{\alpha\beta}\varphi^{\alpha\beta})=0, \end{aligned}\right\} \tag{9}$$

where in the last equation the term in R has been omitted because it vanishes in consequence of (7), by which $T_{\alpha}{}^{\alpha}$ is zero.

If in Eq. (8) (with $m=0$) one replaces r by the variable u according to the equation

$$u^2=r^2-\epsilon^2/2$$

one obtains

$$\left.\begin{aligned} &\varphi_1=\varphi_2=\varphi_3=0, \quad \varphi_4=\epsilon/(u^2+\epsilon^2/2)^{\frac{1}{2}}, \\ ds^2=&-du^2-(u^2+\epsilon^2/2)(d\theta^2+\sin^2\theta d\phi^2) \\ &+[2u^2/(2u^2+\epsilon^2)]dt^2. \end{aligned}\right\} \tag{8a}$$

This solution is free from singularities for all finite points in the space of two sheets and the charge is again represented by a bridge between the sheets. It is the representation of an elementary electrical particle without mass.

[4] If we had taken the usual sign for T_{ik}, the solution would involve $+\epsilon^2$ instead of $-\epsilon^2$. It would then not be possible, by making a coordinate transformation, to obtain a solution free from singularities.

§4. Summary and General Remarks

If one solves the equations of the general theory of relativity for the static spherically symmetric case, with or without an electrostatic field, one finds that singularities occur in the solutions. If one modifies the equations in an unessential manner so as to make them free from denominators, regular solutions can be obtained, provided one treats the physical space as consisting of two congruent sheets. The neutral, as well as the electrical, particle is a portion of space connecting the two sheets (bridge). In the hypersurfaces of contact of the two sheets the determinant of the $g_{\mu\nu}$ vanishes.

One might expect that processes in which several elementary particles take part correspond to regular solutions of the field equations with several bridges between the two equivalent sheets corresponding to the physical space. Only by investigations of these solutions will one be able to determine the extent to which the theory accounts for the facts. For the present one cannot even know whether regular solutions with more than one bridge exist at all.

It appears that the most natural electrical particle in the theory is one without gravitating mass. One is therefore led, according to this theory, to consider the electron or proton as a two-bridge problem.

In favor of the theory one can say that it explains the atomistic character of matter as well as the circumstance that there exist no negative neutral masses, that it introduces no new variables other than the $g_{\mu\nu}$ and φ_{μ}, and that in principle it can claim to be complete (or closed). On the other hand one does not see *a priori* whether the theory contains the quantum phenomena. Nevertheless one should not exclude *a priori* the possibility that the theory may contain them. Thus it might turn out that only such regular many-bridge solutions can exist for which the "charges" of the electrical bridges are numerically equal to one another and only two different "masses" occur for the mass bridges, and for which the stationary "motions" are subject to restrictions like those which we encounter in the quantum theory.

In any case here is a possibility for a general relativistic theory of matter which is logically completely satisfying and which contains no new hypothetical elements.

Magnetic Susceptibilities of Salts of the Iron Group Elements

R. B. JANES, *University of Wisconsin*

(Received May 13, 1935)

Measurements of the paramagnetic susceptibilities of powdered crystals of several salts of the iron group elements have been made over the temperature range 80° to 300°K. The results are in good agreement with the theoretical predictions of Van Vleck and his co-workers in the cases where the theory is applicable. Several of the nickel and cobalt complex salts have susceptibilities which vary in an unusual manner with the temperature.

IN most of the salts of the iron group elements, the metallic ion belonging to this group has an outermost incomplete shell of *3d* electrons. When free the metallic ion shoud have a magnetic moment corresponding to the total angular momentum of the *3d* electrons. However, the crystalline fields due to the groups surrounding the metallic ion in the salt act on this ion and largely destroy the orbital contribution of the ion's electrons to the magnetic moment,[1] leaving a magnetic moment which corresponds fairly closely to the resultant spin momentum of the electrons. If the magnetic moment is due to spin only the ion should be magnetically isotropic with a paramagnetic susceptibility per mole given by the Bose-Stoner expression

$$\chi = N\beta^2 4S(S+1)/3kT, \qquad (1)$$

where S is the resultant spin quantum number, N is Avogadro's number and β is the Bohr magneton. However, the orbital angular momentum is not entirely destroyed, the remnants giving rise to the magnetic anisotropy and deviations from (1) that are observed.

Assuming a crystalline field possessing only rhombic symmetry but with the deviations from cubic symmetry small, Van Vleck[2] has shown that Ni^{++} and Cr^{+++} should be nearly magnetically isotropic and should have mean susceptibilities that deviate only slightly from (1). Co^{++}, however, should show a larger anisotropy and larger deviations from (1). Cu^{++} resembles Ni^{++} and Cr^{+++} but here other factors complicate the situation. Using a complicated perturbation technique and neglecting the effect of the rhombic field, Penney and Schlapp[3] were able to find a simple expression for the mean molar susceptibilities of Ni^{++} and Cr^{+++} which included the coefficient D. No simple formula could be set up for the mean susceptibility of Co^{++}. However Jordahl[4] was able to find a simple expression for Cu^{++}. Penney and Schlapp and Jordahl found that in the case of several Ni^{++}, Cr^{+++} and Cu^{++} hydrated salts, when the experimental value of the mean susceptibility at one temperature is used to find the value of D, the expressions fit very well the experimental data for the other temperatures. The sign of D is found to be positive in all cases. Gorter[5] has shown that the positive sign corresponds to six groups or atoms arranged at the corners of an octahedron around the metallic ion. Thus the results of the calculations give a clue to the arrangement of the groups around the metallic ion in the salt molecule. X-ray investigations, in the cases that they have been carried out, lead to the same arrangement.

The writer has extended the experimental data to other Cr^{+++}, Ni^{++}, Co^{++} and Cu^{++} salts. Powdered crystals of these salts were used throughout. The salts were all carefully purified and analyzed. To determine the susceptibilities of the specimens the Gouy method of weighing a rod of the specimen with and without a magnetic field at right angles to the bottom of the rod was adopted. The magnetic field strength of about 6000 gauss, was held constant by controlling both the temperature of the magnet and the current through its coils. The absolute susceptibilities of the salts were determined by calibrating the rods with an aqueous solution of nickel chloride. The error in the measurement of the relative susceptibilities of the salts at different temperatures was at the most 0.3 percent, but due to the difficulty

[1] For a general discussion see Van Vleck, *Theory of Electric and Magnetic Susceptibilities.*

[2] Van Vleck, Phys. Rev. **41**, 208 (1932).

[3] Penney and Schlapp, Phys. Rev. **42**, 666 (1932).

[4] Jordahl, Phys. Rev. **45**, 87 (1933).

[5] Gorter, Phys. Rev. **42**, 437 (1932).

of determining the correction for apparent densities of the powders when packed into the rods and the inaccuracy in the correction for diamagnetism, the error in the measurement of the absolute susceptibilities was probably about $\frac{1}{2}$ to 1 percent. The susceptibilities were determined at six temperatures, the highest being room temperature and the lowest that of liquid air. For the intermediate temperatures a condenser reflux system, which used liquid air to cool the condenser reflux and ethylene and propane as the gases which were condensed, was built. These condensed gases, boiling under constant pressure, maintained a constant temperature in the bath surrounding the specimen. Propane boiling under atmospheric pressure gave a temperature of about -40°C. By reducing the pressure a temperature of about -70°C could be obtained. Likewise ethylene gave bath temperatures of about -110° and -135°C. The temperature of the test body itself, as measured by thermocouples, could be held constant to about 0.2°C.

Summary and Discussion of Results

Chromium^{+++}

The simple expression for the mean molar susceptibility of the Cr^{+++} ion derived by Penney and Schlapp is

$$\chi=(15N\beta^2/3kT)(1-2\lambda/5D)^2, \qquad (2)$$

where λ is the constant of the orbit-spin interaction. This expression is in good agreement with the Leyden data for the mean susceptibility of chrome alum. Using $\lambda=87$ cm^{-1}, Penney and Schlapp find $D=3730$ cm^{-1} for this salt.

The writer's data for $K_3Cr(SCN)_6\cdot 4H_2O$ are given in Table I. Here κ is the susceptibility per gram of the salt. Since κT is constant within experimental error the data are in good agreement with (2). Using $\kappa T=30.10\cdot 10^{-4}$ a value of $D=1480$ cm^{-1} is obtained. A second run gave an average value of $\kappa T=30.30\cdot 10^{-4}$. With this value $D=1720$ cm^{-1}. This shows that, as Penney and Schlapp have pointed out, too much reliance should not be placed on the numerical value of D. However, the difference between the D for this compound and that found for chrome alum is too large to be accounted for by experimental error, and can be regarded as a rough measure of the differences of the cubic fields in the two compounds.

Table I. *Susceptibility per gram of* $K_3Cr(SCN)_6\cdot 4H_2O$. A diamagnetic correction of 0.44 per gram has been applied.

$\kappa\cdot 10^6$	10.19	13.07	14.59	17.82	20.31	36.64
T°K	295.2	230.7	206.6	169.0	148.5	82.0
$\kappa T\cdot 10^4$	30.08	30.15	30.14	30.12	30.16	30.05

Nickel^{++}

In this case Penney and Schlapp obtain for the mean molar susceptibility an expression

$$\chi=(8N\beta^2/3kT)(1-4\lambda/5D)+4N\beta^2/5D. \qquad (3)$$

The Leyden data for $NiSO_4\cdot 7H_2O$ are in good agreement with (3) except for the points at liquid hydrogen temperatures. Even at these temperatures the disagreement is not serious. Using $\lambda=-335$ cm^{-1}, Penney and Schlapp obtain $D=1485$ cm^{-1}. There is, however, a numerical error in their calculation. D should be 1103 cm^{-1}. The writer's data for several nickel salts are given in Tables II, III, IV and V and Figs. 1 and 2.

If we use $\kappa T=47.30\cdot 10^{-4}$ for $NiSO_4\cdot 6H_2O$ (Table II) at 169°K we get a value of $D=1208$ cm^{-1}. Eq. (3) then fits the experimental data very well as is shown in Fig. 1. The value of D for this

Table II. *Susceptibility per gram of* $NiSO_4\cdot 6H_2O$. The diamagnetic correction used was 0.42 per gram. (See Fig. 1.)

$\kappa\cdot 10^6$	16.13	20.78	23.19	27.96	56.89
T°K	298.5	230.1	205.3	169.0	82.2
$\kappa T\cdot 10^4$	48.14	47.81	47.61	47.25	46.76

Table III. *Susceptibility per gram of* $Ni(NO_3)_2\cdot 6H_2O$. The diamagnetic correction used was 0.37 per gram. (See Fig. 1.)

$\kappa\cdot 10^6$	15.14	19.10	21.28	25.78	29.03	51.73
T°K	293.5	230.0	205.6	169.0	149.3	83.0
$\kappa T\cdot 10^4$	44.43	43.93	43.76	43.58	43.34	42.93

Table IV. *Susceptibility per gram of* $Ni(NO)_2\cdot 4NH_3$. The diamagnetic correction used was 0.39 per gram. (See Fig. 1.)

$\kappa\cdot 10^6$	18.79	23.57	26.57	31.53	63.23
T°K	293.8	231.0	203.1	169.0	82.6
$\kappa T\cdot 10^4$	55.20	54.45	53.97	53.29	52.23

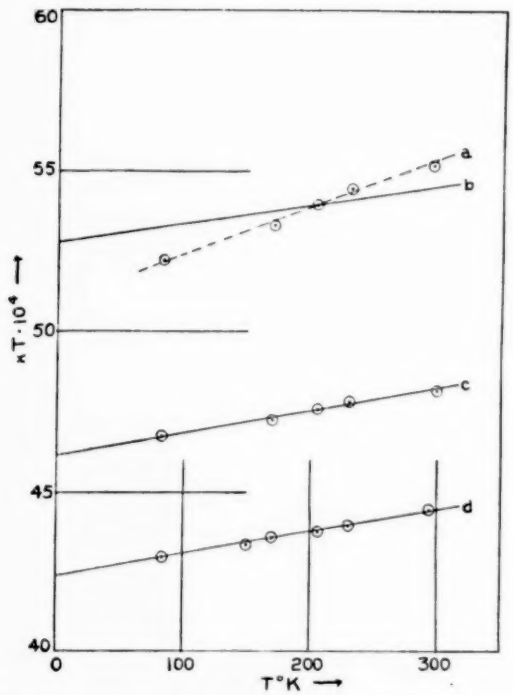

FIG. 1. *a*, the experimental curve for $Ni(NO_2)_2 \cdot 4NH_3$; *b*, the theoretical curve for $Ni(NO_2)_2 \cdot 4NH_3$; *c*, the theoretical curve for $NiSO_4 \cdot 6H_2O$; *d*, the theoretical curve for $Ni(NO_3)_2 \cdot 6H_2O$; the circles in all cases, represent experimental values of $\kappa T \cdot 10^4$.

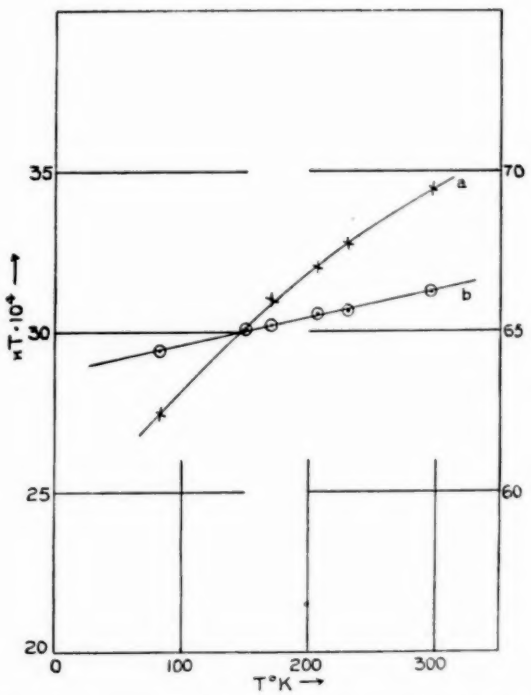

FIG. 2. *a*, experimental curve for $K_2(SCN)_4 \cdot 4H_2O$ (see ordinate scale on right); *b*, experimental curve for $Ni(CN)_2 \cdot C_6H_6 \cdot NH_3$ (see ordinate scale on left).

salt is the same within experimental error as the value for $NiSO_4 \cdot 7H_2O$, showing that the crystalline fields are very similar in the two compounds. This is to be expected because of the similarity of the two salts.

If we use $\kappa T = 43.58 \cdot 10^{-4}$ for $Ni(NO_3)_2 \cdot 6H_2O$ (Table III) at 169°K we get a value of $D = 1106$ cm^{-1}. Eq. (3) is then in good agreement with the experimental results as Fig. 1 shows. The values of the susceptibilities of a second sample fall on a line having the same slope as that of sample one, but the absolute value of the susceptibility is somewhat different. Using the κT value for the second sample at 169°K which is $= 43.95 \cdot 10^{-4}$ we find a value of $D = 1064$ cm^{-1}. The results show that the nitrate has a cubic field closely resembling that of the sulphates. The rhombic fields in the three salts must be of the same order also, for although the presence of a comparatively small rhombic field will not materially change the slope of the theoretical curve given by (3) it will change the value of D necessary to get agreement.

TABLE V. *Susceptibility per gram of* $Ni(CN)_2 \cdot C_6H_6 \cdot NH_3$. The diamagnetic correction used was 0.43 per gram. (See Fig. 2.)

$\kappa \cdot 10^6$	10.56	13.33	14.87	17.87	20.15	35.64
T°K	296.0	230.0	205.5	169.0	149.3	82.5
$\kappa T \cdot 10^4$	31.26	30.66	30.55	30.20	30.09	29.40

Using the experimental value of $\kappa T = 53.97 \cdot 10^{-4}$ for $Ni(NO)_2 \cdot 4NH_3$ (Table IV) at 203.1°K in (3), one obtains $D = 1650$ cm^{-1}. However, as Fig. 1 shows, the theoretical curve does not fit the experimental points at all, and widely different values of D would be secured if values of κT corresponding to other values of the temperature were used. Under these conditions it is hard to predict the type of crystalline field existing in the salt. The salt may have a predominantly rhombic field in which case (3) will not hold, or it may have a predominantly cubic one but with a negative D, in which case (3) will again not hold. The second choice corresponds to a field due to four groups arranged on the corners of a tetrahedron around the metallic ion.[5] Neither choice, however, offers a unique solution. The Bohr magneton number = 3.12 at room temperature is above the spin only value of 2.83.

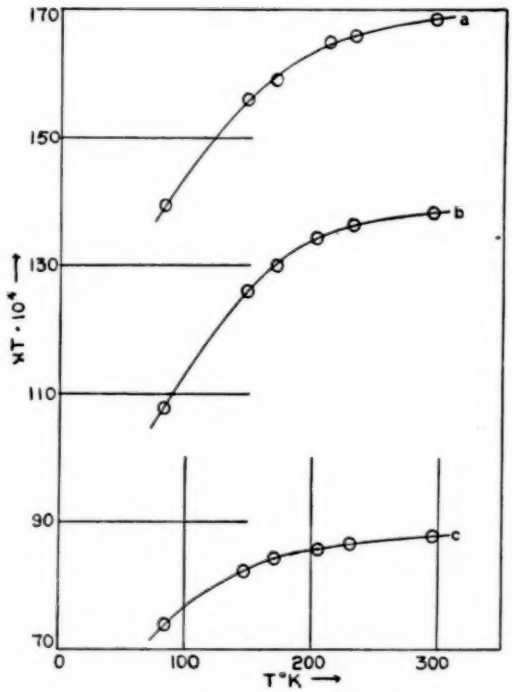

FIG. 3. *a*, experimental curve for $CoSO_4 \cdot 6NH_3$; *b*, experimental curve for $CoCl_2 \cdot 6NH_3$; *c*, experimental curve for $Co(CN)_2 \cdot 2H_2O$.

For $Ni(CN)_2 \cdot C_6H_6 \cdot NH_3$ (Table V) there is no possibility of (3) agreeing with the experimental data. The Bohr magneton number at 300.6°K = 2.27 is below the spin only value. Under these conditions D would be negative and (3) would not be valid. To explain this one could assume that there is a predominantly rhombic or perhaps axial field, which quenches not only the orbital but also part of the spin contribution to the magnetic moment, present in the salt. This case resembles that of $K_2Ni(CN)_4 \cdot H_2O$. This salt has been found to be diamagnetic, and as Pauling has shown,[6] it probably has a predominantly tetrahedral field, which destroys the magnetic moment entirely. The writer has checked the experimental data for this salt, and also finds it to have a diamagnetic susceptibility which is independent of the temperature used.

The Bohr magneton number for NiO (Table VI) at 297.3°K is 1.27. This is far below the spin only value. However, in this salt the "magnetic dilution" is small and exchange forces come in. This case is too difficult to handle theoretically.

[6] L. Pauling, J. Am. Chem. Soc. **53**, 1367 (1931).

TABLE VI. *Susceptibility per gram of NiO.* The diamagnetic correction used was 0.6 per gram.

$\kappa \cdot 10^6$	9.05	8.60	8.46	8.26
T°K	297.3	230.0	199.7	82.3

As Table VI shows, the susceptibility, in contrast to that of other nickel salts, actually decreases with decreasing temperature.

Cobalt^{++}

Here the situation is much more complicated than it is for the other three ions. In Co^{++} a multiplet level lies lowest and as the temperature changes the electron population of each level of the multiplet changes. As the individual levels each contribute a different amount to the susceptibility, we should expect a dependence of the susceptibility on the temperature different from that in the other ions where a singlet level is the lowest. This will be true even if the crystalline field is of the same type considered in these other ions, that is cubic with a positive D.

The Bohr magneton number for $K_2Co(SCN)_4 \cdot 4H_2O$ (Table VII) at 296.8°K is 4.96. The

TABLE VII. *Susceptibility per gram of $K_2Co(SCN)_4 \cdot 4H_2O$.* The diamagnetic correction used was 0.44 per gram. (See Fig. 2.)

$\kappa \cdot 10^6$	23.39	29.38	32.43	39.08	75.69
T°K	296.8	230.3	206.5	169.0	82.5
$\kappa T \cdot 10^4$	69.42	67.66	66.96	66.00	62.43

variation of κT with T resembles that found for the cobalt hydrates which have six water molecules around the metallic ion at the corners of an octahedron. The Bohr magneton number, however, is slightly lower. This compound thus apparently had a predominant cubic crystalline field like those of the hydrates mentioned, although in this case it is impossible to say just what groups surround the metallic ion. Since the Bohr magneton number is closer to the spin only value, the rhombic field is probably larger in this salt. If the metallic ion is surrounded by four groups at the corners of a tetrahedron the sign of D should change,[5] and Co^{++} should then resemble Ni^{++}.[2] The data indicate that such a configuration is probably not present in this salt, as the observed deviations from Curie's law are too large.

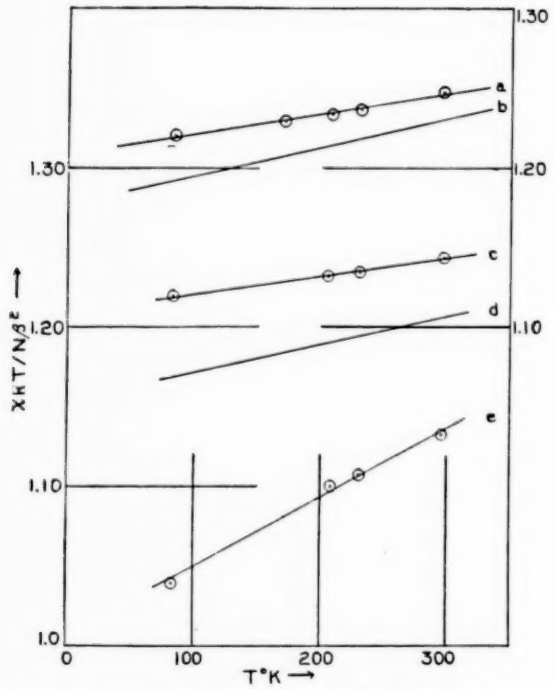

FIG. 4. *a*, experimental curve for $Cu(NH_4)_2(SO_4)_2 \cdot 6H_2O$ (see ordinate scale on right); *b*, Jordahl's theoretical curve for $Cu(NH_4)_2(SO_4)_2 \cdot 6H_2O$ (see ordinate scale on right); *c*, experimental curve for $CuK_2(SO_4)_2 \cdot 6H_2O$ (see ordinate scale on left); *d*, Jordahl's theoretical curve for $CuK_2(SO_4)_2 \cdot 6H_2O$ (see ordinate scale on left); *e*, experimental curve for $CuSO_4 \cdot 4NH_3 \cdot H_2O$ (see ordinate scale on left).

The Bohr magneton for $CoCl_2 \cdot 6NH_3$ (Table VIII) at 292.9°K is 5.09. Although from its composition the crystalline field of this salt should resemble the fields of the hydrates spoken of above, Fig. 4 shows that the variation of κT with T is altogether different. At higher temperatures the curve tends to flatten out so as to give a variation resembling that of the hydrates. Also at room temperatures the Bohr magneton number is of the same order as that of the hydrates. At lower temperatures, however, the value of κT for this salt drops much faster than in the case of the hydrates indicating that the contribution to the susceptibilities of the lower levels of the multiplet is for this salt much smaller, probably going below the spin only values at temperatures below that of liquid air. Possibly at still lower temperatures, when the electrons are largely in the lower levels, the curve will tend to flatten out again at a much lower value of κT. If we had plotted the ordinary curve of the experimentalists, where $1/\kappa$ is plotted against T, we should find that the higher temperature points lie on a straight line and that the lower temperature points lie on another straight line which has quite a different slope. This would seem to indicate a sharp change of some sort inside the crystal at a certain temperature, which is not shown by the κT curve. This second procedure is very artificial and has no real theoretical significance.

TABLE VIII. *Susceptibility per gram of* $CoCl_2 \cdot 6NH_3$. A diamagnetic correction of 0.54 per gram was used. (See Fig. 3.)

$\kappa \cdot 10^6$	47.23	59.11	66.90	77.00	85.11	131.4
T°K	292.9	231.0	200.7	169.0	148.3	82.1
$\kappa T \cdot 10^4$	138.3	136.5	134.3	130.1	126.0	107.8

The Bohr magneton number for $CoSO_4 \cdot 6NH_3$ (Table IX) at 294.2°K is 5.91. The variation of

TABLE IX. *Susceptibility per gram of* $CoSO_4 \cdot 6NH_3$. The diamagnetic correction used was 0.47 per gram. (See Fig. 3.)

$\kappa \cdot 10^6$	57.26	71.72	78.37	93.90	105.1	169.1
T°K	294.2	231.3	210.3	169.2	148.3	82.4
$\kappa T \cdot 10^4$	168.5	165.8	164.8	158.9	155.8	139.4

κT with T resembles that for $CoCl_2 \cdot 6NH_3$. However, at room temperature the Bohr magneton number is higher than in the case of the chloride. This merely means that the susceptibility in the upper levels is not destroyed as much. Such a large value of the Bohr magneton number at room temperature is unusual, however. The lower levels are greatly affected as in the case of the chloride. The crystalline fields are probably a great deal alike in the two cases.

The Bohr magneton number for $Co(CN)_2 \cdot 2H_2O$ (Table X) at 294.5°K is 3.27 while the spin only value is 3.87. In this case the Bohr magneton number at room temperature is much smaller than in the preceding two cases. However, the slope of the κT curve at room temperature is about the same as that of the preceding two cobalt salts. Also, as in the case of the other two

TABLE X. *Susceptibility per gram of* $Co(CN)_2 \cdot 2H_2O$. A diamagnetic correction of 0.32 per gram has been used. (See Fig. 3.)

$\kappa \cdot 10^6$	29.77	37.60	42.02	49.80	55.00	88.93
T°K	294.5	229.7	203.7	169.0	149.3	83.0
$\kappa T \cdot 10^4$	87.68	86.36	85.61	84.16	82.13	73.80

salts, a rapid drop of κT is found at the lower temperatures.

Copper^{++}

Jordahl[4] has found an expression for the principal susceptibilities of Cu^{++} salts which he has applied to Bartlett's[7] data for $Cu(NH_4)_2(SO)_2 \cdot 6H_2O$ and $CuK_2(SO_4)_2 \cdot 6H_2O$. By proper choice of parameters fair agreement can be secured between this expression and the experimental results. However, Bartlett's data are limited to a small range of temperatures around room temperature. The writer has extended the data for the mean susceptibility to lower temperatures in order to check the expression of Jordahl for the mean at these temperatures. This, of course, gives somewhat of a check on the expression for the principal susceptibilities.

In the work on Cu^{++} (Table XI) the author has

TABLE XI. *Susceptibility per gram of* $Cu(NH_4)_2(SO_4)_2 \cdot 6H_2O$. A diamagnetic correction of 0.45 per gram was used. (See Fig. 4.)

$\kappa \cdot 10^6$	3.927	5.009	5.544	6.770	13.640
$T°K$	295.7	229.8	207.0	169.0	83.3
$\chi kT/N\beta^2$	1.247	1.236	1.233	1.229	1.220

plotted $\chi kT/N\beta^2$ instead of κT. If the Cu^{++} ion has the spin only value of 1.73 Bohr magnetons the expression $\chi kT/N\beta^2 = 1$. The diamagnetic correction of 0.45 per gram which was applied to $Cu(NH_4)_2(SO_4)_2 \cdot 6H_2O$ (Table XI) is the same value that Bartlett used. A second sample had susceptibilities lying on a line with the same slope as that of sample one, but the value of $\chi kT/N\beta^2 = 1.240$ at 296.1° was somewhat lower. Jordahl's theoretical curve drawn in accordance with Bartlett's data is also shown in Fig. 4. The agreement between this curve and the writer's data is only fair. This is to be expected as Bartlett's range of temperature was too small to establish the slope accurately and the absolute values cannot be expected to check much better than to about 1 percent. By using the cubic expression for Cu^{++} with a value of $D = 17{,}200$ cm^{-1}, quite good agreement can be secured with the author's data. Of course the more complete expression given by Jordahl could be used but no satisfactory values of the parameters involved in it can be obtained from a knowledge of the mean susceptibilities only. It might be noted, however, that the values of these parameters obtained from Bartlett's data on the principal susceptibilities would have to be changed somewhat in order to be in accordance with the writer's data.

The results for $CuK_2(SO_4)_2 \cdot 6H_2O$ (Table XII)

TABLE XII. *Susceptibility per gram of* $CuK_2(SO_4)_2 \cdot 6H_2O$. The diamagnetic correction used was 0.41 per gram. (See Fig. 4.)

$\kappa \cdot 10^6$	3.541	4.514	5.048	12.51
$T°K$	296.8	230.2	205.6	82.1
$\chi kT/N\beta^2$	1.243	1.234	1.232	1.219

are not in as good agreement with Bartlett's results as they were for the preceding one. The slope agrees fairly well but the writer's absolute values are about 3 percent higher. In fact the values of $\chi kT/N\beta^2$ found by the author agree very well with his values for $Cu(NH_4)_2(SO_4) \cdot 6H_2O$. This means that the cubic expression with $D = 17{,}200$ cm^{-1} will also give good agreement with the data for $CuK_2(SO_4)_2 \cdot 6H_2O$. This is not unexpected as the same thing was found in the case of Ni^{++}. A value of D of the same order will also fit the Leyden data for $Cu(SO_4) \cdot 5H_2O$[4]. It might be noted that if Bartlett's values for $CuK_2(SO_4) \cdot 6H_2O$ were all shifted up by a constant amount good agreement would be secured with the writer's data.

The susceptibilities of $CuSO_4 \cdot 4NH_3 \cdot H_2O$ (Table XIII) are quite different from those in the

TABLE XIII. *Susceptibility per gram of* $CuSO_4 \cdot 4NH_3 \cdot H_2O$. A diamagnetic correction of 0.42 per gram was used. (See Fig. 4.)

$\kappa \cdot 10^6$	5.81	7.28	8.06	19.22
$T°K$	295.0	230.2	206.7	81.9
$\chi kT/N\beta^2$	1.132	1.107	1.100	1.039

other cases suggesting that the field is different. Without data for the principal susceptibilities no satisfactory choice of the field can be made.

The writer wishes to express his thanks to Professor J. H. Van Vleck for continued interest in this work and to Professor C. E. Mendenhall for many helpful suggestions in the experimental arrangements.

[7] B. W. Bartlett, Phys. Rev. **41**, 818 (1932).

Theory of the Work Functions of Monovalent Metals

E. WIGNER AND J. BARDEEN, *Princeton University*

(Received April 30, 1935)

The factors which determine the work function of a metal are described in a qualitative way. The work function is defined as the difference in energy between a lattice with an equal number of ions and electrons, and the lattice with the same number of ions, but with one electron removed. The work function is then found by first calculating the energy of a lattice with n_i ions and n_e electrons. The final formula gives the work functions of monovalent metals in terms of the heats of sublimation. This formula is approximate, and can claim validity only in a qualitative way, as one of the important factors, the electric double layer on the surface, is omitted entirely, and it is assumed that the Fermi energy is as great as if the electrons were entirely free. The values obtained from this formula check very closely with the experimental values for the alkalis, so that it can be concluded that the double layer is probably small for these metals. Finally, the deviations to be expected for other than monovalent metals are considered. A more exact calculation of the work function of one substance (Na) will be given by one of us in an ensuing paper.

(1)

IT is perhaps not quite superfluous to have, in addition to a more exact calculation of a physical quantity, an approximate treatment which merely shows how the quantity in question is determined, and the lines along which a more exact calculation could be carried out. Such a treatment often leads to a simple formula by means of which the magnitude of the quantity may be readily determined. A treatment of this nature has been given by O. K. Rice[1] for the binding energies of the alkalis.

We intend to give here an approximate calculation, on somewhat different lines, of the work functions of monovalent metals, the main result being a formula which relates the work function with the heat of sublimation. We do this for two reasons; first, because a more exact treatment seems to involve a great deal of computational labor, and second, because the connection between the work function and other properties is empirically very pronounced. In fact, Sommerfeld,[2] in his original paper on the electron theory of metals, has already noticed that if one orders the metals according to their work functions (or according to their Volta potentials), the series is the same as if one orders them according to the Fermi energy of the electrons, calculated on the basis of the free electron theory. The greater the Fermi energy, the greater the work function. This fact was rather puzzling on the basis of the naïve free electron theories of that time, but an explanation was given later by Frenkel.[3] Although Sommerfeld and Bethe[4] have shown that the details of his calculations cannot be maintained, we feel that his basic idea is correct, namely that the binding energy of the electrons (i.e., work function) increases with the kinetic energy. The connection between the kinetic and potential energy, as given by the virial theorem in a Coulomb field, has been utilized by Tamm and Blochinzev[5] on the basis of the Fermi-Thomas model. It seems to us, however, that it is dangerous to use the Fermi-Thomas model in this connection, because this model does not yield the metallic bond.[6]

(2)

The work function may be defined as the difference in energy between a lattice with an equal number of ions and electrons, and the lattice with the same number of ions, but with one electron removed. It is assumed in both cases that the lowest electronic states are completely filled, so that the electron is removed from the highest energy state of the neutral metal. It is necessary to specify the position of the electron after its removal from the lattice, because, in general, the work function is different

[1] O. K. Rice, Phys. Rev. **44**, 318 (1933).
[2] A. Sommerfeld, Naturwiss. **15**, 825 (1927); **16**, 374 (1928).
[3] J. Frenkel, Zeits. f. Physik **49**, 31 (1928).
[4] See article by A. Sommerfeld and H. Bethe in the *Handbuch der Physik*, Vol. 24, Berlin, 1933, p. 424.
[5] J. Tamm and D. Blochinzev, Zeits. f. Physik **77**, 774 (1932).
[6] For a discussion of the Fermi-Thomas model as applied to the metallic state, see J. C. Slater and H. M. Krutter, Phys. Rev. **47**, 559 (1935).

for different crystallographic planes. We shall suppose that the electron is at a point in the neighborhood of a surface plane of the crystal, the distance from this plane being small compared with the dimensions of the plane, but large in comparison with atomic dimensions. We shall calculate this energy difference by calculating the energy $E(n_i, n_e)$ of a lattice with n_i ions and n_e electrons where we may suppose that $|n_i - n_e| \ll n_i$ so that effects connected with the finite capacity of the sample may be neglected. For the calculation of $E(n_i, n_e)$ we shall use the method of orbital wave functions. This method requires hardly any modification of the scheme[7] used for $n_i = n_e$, i.e., for uncharged metals.

There is only one important difference, that due to the electric double layer which the electron cloud and the ions may form on the surface of the metal.[8] These double layers are due to the fact that the electron distribution will not be symmetric around the surface ions, as it is around the inner ones. It will extend partly outside of the limits of the spheres surrounding the ions* of the surface, and in the inside of the spheres it will have partly greater, partly smaller densities than in the inner s spheres. This alteration of the charge density may result in double layers on the surface of the metal. The double layers will be such that they generate a constant potential inside the metal. The potential outside the metal, however, will not be constant, but will vary in such a way that the potential differences between the outer neighborhoods of differently oriented crystal surfaces will be equal to the differences in the moments of the double layers of the corresponding surfaces. These differences are revealed experimentally as the differences in the work functions of the different surface planes of the same crystal. This shows, conversely, that the double layer is of the same order of magnitude as these differences, i.e., around $\frac{1}{2}$ to 1 electron volt.[9]

The total energy of the lattice with n_i ions and n_e electrons can be considered as containing three parts: (1) the energy which the lattice would have if the surface ions were surrounded with the same symmetric charge distribution which prevails in the interior; (2) the energy change of the inner ions and electrons due to the double layer on the surface; (3) the energy of this double layer. We shall assume that the electron comes from the interior of the metal, i.e., that the double layer remains unchanged, and that the density of the electrons changes in the interior only. This is, strictly speaking, incorrect, as one can easily see that the density will be practically unchanged in the interior, and that the electron will come from the surface. The result for the work function cannot be incorrect in spite of this, because the energy required to move an electron from the surface to the interior of a metal is of a much smaller order of magnitude than the energy required to remove an electron from the metal (or, the work function). If the energy necessary to move an electron from the surface to the interior were appreciable, the electrons would have already rearranged themselves in the neutral metal. We shall omit in the final result the change in energy of the second and third part of $E(n_i, n_e)$. This is not allowable, of course, but this part of the work function is just equal to the moment of the double layer, and cannot be taken into account without an explicit calculation of the latter, which is reserved for a later paper by one of us.

(3)

We can now use for the calculation of $E(n_i, n_e)$ the scheme of reference 7. The kinetic energy of the ions will be neglected, so that the total energy contains three parts, $\frac{1}{2}\Sigma e_i V_i$ for the ions, $\frac{1}{2}\Sigma e_i V_i$ for the electrons, and the kinetic energy of the latter. The first part can be calculated as follows: First one assumes that the density of electrons everywhere, except in the s sphere of the ion under consideration, is as great as it would be if $n_e = n_i$. Then, the charges outside this s sphere will have no effect on our ion, because the potential of the electrons in every other s sphere will be nullified by the potential of the ion inside.[10] Only the double

[7] E. Wigner and F. Seitz, Phys. Rev. **43**, 804 (1933); **46**, 509 (1934) (I and II); E. Wigner, Phys. Rev. **46**, 1002 (1934) (III); F. Seitz, Phys. Rev. **47**, 400 (1935) (IV).

[8] J. Frenkel, Zeits. f. Physik **51**, 232 (1928).

* "s spheres," reference 7, II.

[9] H. E. Farnsworth and B. A. Rose, Nat. Acad. Sci. **19**, 777 (1935); B. A. Rose, Phys. Rev. **44**, 585 (1933).

[10] We neglect the small correction of Appendix 2, reference 7, II.

layer of the surface will be effective, and we obtain as the first contribution to the energy of the crystal:

$$n_i[(n_e/2n_i)\int|\psi|^2 V dv+\tfrac{1}{2}eD], \qquad (1)$$

where V is the potential of the ion core, D is the moment of the double layer, and the integration must be extended over the s sphere of the ion. The factor n_i comes in, because we have n_i ions, the factor n_e/n_i because there are only that many electrons in the mean in the s sphere; (1) should still be averaged over the wave functions of the different free electrons. The fact that there are $((n_i-1)/n_i)(n_i-n_e)$ electrons missing outside the s sphere introduces a further correction:

$$\tfrac{1}{2}\Sigma e_j\Phi_j, \qquad (1a)$$

where Φ_j is the potential of the missing electrons at the jth ion, and is of the order of magnitude $(n_i-n_e)e/R$ where R is a lateral dimension of the crystal.

The potential energy of the electrons is more complicated. First, again, we can supplement the missing electrons outside the s sphere in which our electron happens to be. The potential energy due to the nearest ion is $\frac{1}{2}V(r)$. To this the electron interaction energy must be added, which, if the charge distribution is assumed to be uniform, amounts to $(n_e/n_i)(3e^2/2r_s-e^2r^2/2r_s^3)$ where r_s is the radius of the s sphere. These two terms give, together with the contribution from the double layer, if averaged over all positions of the electron under consideration in the s sphere:

$$n_e[\tfrac{1}{2}\int|\psi|^2 V dv+0.6e^2n_e/n_ir_s-\tfrac{1}{2}eD] \qquad (2)$$

with definitions similar to those used in (1). The electrons missing outside the s sphere, yield the following correction to the energy:

$$-(n_e/2n_i)\Sigma e\Phi_j. \qquad (2a)$$

Next we must take into account the effects of the different holes. The Fermi hole (exchange energy) gives $-0.458e^2/r_s$ if $n_e=n_i$. One easily sees that r_s must be replaced by $(n_i/n_e)^{\frac{1}{3}}r_s$ if $n_e\neq n_i$. Similarly, if we denote by $r_sf(r_s)$ the correlation function,[11] the correlation energy for one electron is $-e^2f((n_i/n_e)^{\frac{1}{3}}r_s)$. The total contribution from these sources is:

$$-n_e[(0.458e^2/r_s)(n_e/n_i)^{\frac{1}{3}}+e^2f((n_i/n_e)^{\frac{1}{3}}r_s)]. \qquad (3)$$

Finally, the kinetic energy of the electrons gives:

$$-(\hbar^2n_e/2m)\int\psi^*\Delta\psi dv, \qquad (4)$$

which again should be averaged over the different free electron wave functions.

The energy of the double layer due to the electrons and ions inside the crystal is simply:

$$-\tfrac{1}{2}eD(n_e-n_i).$$

This energy will change, even though the double layer itself is unchanged.

If we add all these quantities together, (4) together with the first terms of (1) and (2) gives, because of the Schrödinger equation $-(\hbar^2/2m)\Delta\psi+V\psi=E\psi$ just n_eE, where still the mean value of E over all occupied states of the electrons must be taken. This gives the energy E_0 of the lowest free electron level, augmented by the mean value of the Fermi energy, F, i.e.,

$$n_e(E_0+F(n_e/n_i)^{\frac{2}{3}});$$

$$F=(9\pi/10)(3/2\pi)^{\frac{1}{3}}(R_y/r_s^2). \qquad (5)$$

Thus the total energy is:

$$E(n_i, n_e)=n_e(E_0+F(n_e/n_i)^{\frac{2}{3}})+(n_e^2/n_i)(0.6e^2/r_s)+(1/2n_i)(n_i-n_e)\Sigma\Phi_j-n_e[(0.458e^2/r_s)(n_e/n_i)^{\frac{1}{3}}+e^2f((n_i/n_e)^{\frac{1}{3}}r_s)]-eD(n_e-n_i). \qquad (6)$$

(4)

The derivative of $E(n_i, n_e)$ at $n_i=n_e$ is the work function φ with the negative sign.

$$-\varphi=E_0+5F/3+1.2e^2/r_s-(4/3)(0.458e^2/r_s)-e^2f(r_s)+e^2r_sf'(r_s)/3-eD. \qquad (7)$$

The derivative of the sum in (6) tends to zero with increasing size of the crystal, and has therefore been omitted. If we omit the double layer term, and replace the Fermi energy by its value for free electrons, the only unknown quantity in (7) is E_0. One can express E_0 in terms of the ionization energy I, and the heat of

[11] Represented by the lower curve, Fig. 7, reference 7, III.

TABLE I. *Work functions of the alkalis.*

Metal	r_s	$I+H$	F	$\varphi_{calc.}$	$\varphi_{exp.}$
Li	3.28	7.04	2.07	2.19	2.28[1]
Na	4.00	6.25	1.89	2.15	2.25[2]
					2.46[1]
K	4.97	5.27	1.22	2.20	2.24[1]
					2.24[3]
					2.17[2]
Rb	5.32	5.03	1.07	2.20	2.19[3]
					2.16[1]
Cs	5.73	4.70	.92	2.15	1.96[3]
					1.87[1]
					1.81[4]

[1] A. R. Olpin (see reference 13).
[2] Z. Berkes, Math. Phys. Lapok **41**, 131 (1934).
[3] J. J. Brady, Phys. Rev. **41**, 613 (1932).
[4] K. H. Kingdon, Phys. Rev. **25**, 892 (1925).

sublimation, II,

$$I+II=-(\partial/\partial n_i)E(n_i, n_e)-(\partial/\partial n_e)E(n_i, n_e)$$
$$=-E_0-F-0.6e^2/r_s+0.458e^2/r_s+e^2f(r_s), \quad (8)$$

which, of course, is the result of reference 7. We have, from (7) and (8)

$$\varphi=I+II-\tfrac{2}{3}F-0.6e^2/r_s+0.458e^2/3r_s$$
$$-e^2r_sf'(r_s)/3+eD. \quad (9)$$

Table I gives the work functions of the alkalis as calculated from (9) under the assumption that $D=0$. The Fermi energy for Li was taken from the work of F. Seitz,[12] and the free electron values were used for the remaining metals. The check with the experimental values[13] is extremely good, considering the approximate nature of the theory, and shows that the double layer is probably small for these metals. The double layer may, however, give an important contribution to the work functions of other metals.

The solid curve of Fig. 1 gives the theoretical values of $I+II-\varphi$ in electron volts plotted against r_s in Bohr units. It is assumed that the Fermi energy has its classical free electron value, and that $D=0$. The light broken line connects the experimental values for the monovalent metals. Most of the discrepancy for Li ($r_s=3.28$) is accounted for by the deviation of the Fermi energy from its free electron value.[12] The experimental values of $I+II-\varphi$ for other than monovalent metals are also shown in Fig. 1. A calculation similar to the preceding one could be made for these metals by treating all valence electrons as free. The work function could then be obtained as the difference of quantities which are even greater than those for monovalent metals. One can obtain an orientation, however, by considering only one electron as free, the rest belonging to the "ion" core. There will then be two main modifications of the foregoing considerations. First, the Fermi energy will be even further from its classical value. It will in general be smaller than this if the levels of the last electron all belong to the same Brillouin zone; it may be greater or smaller if they extend over both sides of a gap between two zones. Second, a large part of the cohesion will be due to the interaction of the "ions." Thus in (9), only that part of the heat of sublimation should be inserted which results from the outermost electron. This correction is, indeed, in the right direction to bring the experimental points for these metals closer to the theoretical curve.

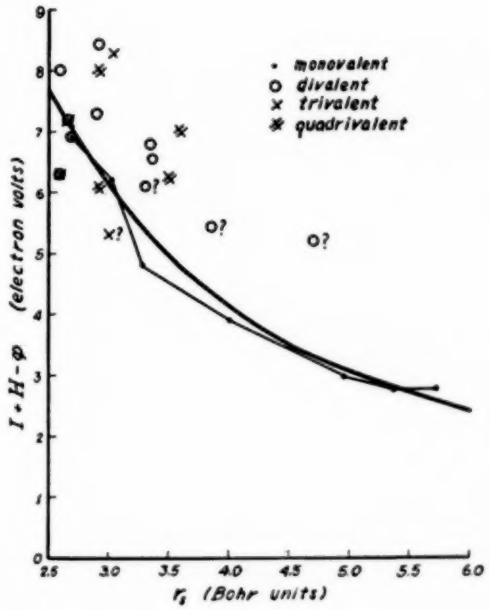

FIG. 1. Theoretical curve of $I+II-\varphi$ for monovalent metals, assuming no surface double layer. Broken line connects experimental values for these metals.

[12] See reference 7, IV.
[13] For the experimental values of the work function, see A. L. Hughes and L. A. DuBridge, *Photoelectric Phenomena*, McGraw-Hill, 1932, p. 75. For the heats of sublimation, see J. Sherman, Chem. Rev. **11**, 93 (1932).

The Energy Distribution of Secondary Electrons from Molybdenum

LELAND J. HAWORTH, *Department of Physics, University of Wisconsin*

(Received April 15, 1935)

Energy distribution curves of secondary electrons from a thoroughly outgassed molybdenum target have been obtained by magnetic analysis with primary electron energies up to 150 volts. In addition to the usual sharp "elastically reflected" peak and the broad, low energy maximum, other maxima and irregularities appear which may be classified as follows: (1) peaks at energies 10.6, 22 and 48 volts less than the primary energy which are due to critical energy losses among the inelastically scattered electrons; (2) "humps" in the curves at secondary energies of 11, 24 and 35 volts, independent of the primary energy. The number of elastically reflected electrons is plotted as a function of primary energy. This curve exhibits several maxima, some of which are correlated with the "critical potentials" giving rise to the peaks of type (1). Others are due to electron diffraction. A discussion of possible applications of modern metallic theories to the present results is given. Two of the peaks of type (1) and all of those of type (2) are tentatively accounted for.

NUMEROUS investigators[1–6] have studied the distribution in energy of secondary electrons emitted by a metal surface when bombarded by a narrow, homogeneous beam of primary electrons. In many of these experiments, however, the specimen did not receive the rigorous heat treatment which photoelectric and thermionic studies indicate is necessary to obtain a comparatively clean surface. For this reason and others the present investigation was undertaken with the intention of studying a metal as free from gas and other impurities as modern vacuum technique will allow.

The energy distribution of secondary electrons from numerous samples of thoroughly outgassed molybdenum was determined by the method of magnetic analysis. The targets used were arranged so that it was possible to make observations with the specimen at high temperatures, the assumption being made that under such conditions the surface would be relatively cleaner than at room temperature. This rendered the use of single crystals not feasible.

The molybdenum used was obtained from two sources, the Elkon Company and the Fansteel Products Company, and in both cases was stated to be extremely pure. No essential differences were detected in the results obtained from samples from the two sources.

[1] H. E. Farnsworth, Phys. Rev. **25**, 41 (1925); **31**, 405 (1928).
[2] C. F. Sharman, Proc. Camb. Phil. Soc. **23**, 523 (1927); **23**, 922 (1927).
[3] E. Rudberg, Proc. Roy. Soc. **A127**, 111 (1930).
[4] T. Soller, Phys. Rev. **36**, 1212 (1930).
[5] J. B. Brinsmade, Phys. Rev. **30**, 494 (1927).
[6] P. Tartakowsky and W. Kudrjawzewa, Zeits. f. Physik **75**, 137 (1932).

Apparatus and Procedure

Primary electrons from the oxide coated filament F_1 (Fig. 1a) traversed the slits of the electron gun and were incident at a 45° angle on the target T. Secondary electrons in the direction of specular reflection passed through the narrow slit S_3 and, under the influence of a uniform magnetic field furnished by a large pair of Helmholz coils, those of the desired velocity traversed the analyzer A (Fig. 1b) and passed into the Faraday collector C. As the path of the primary electrons was along the axis of the field they were undeflected. Primary electrons not striking the target were trapped in the grounded cylinder W.

The electron gun was adapted from a model described by Farnsworth[7] and was in three sections for reasons to be discussed later. A magnetically operated shutter L could be placed in front of F_1 when not actually making observations in order to reduce possible contamination of the target from this source, particularly during the early heating of F_1. It might be mentioned in this connection that on two occasions tungsten filaments were used in place of the oxide coated type with no apparent change in the results obtained.

The analyzer, remodelled from the one previously used by Soller,[4] was of such dimensions as to give a high resolving power ($dV=0.006\ V$).

Most of the targets used were heated by conduction. They consisted of strips of molybdenum 2.5 mm wide and 0.03 mm in thickness bent into hairpin form and held in position at the bent end by a slight tension provided by a weak tungsten

[7] H. E. Farnsworth, J.O.S.A. and R.S.I. **15**, 290 (1927).

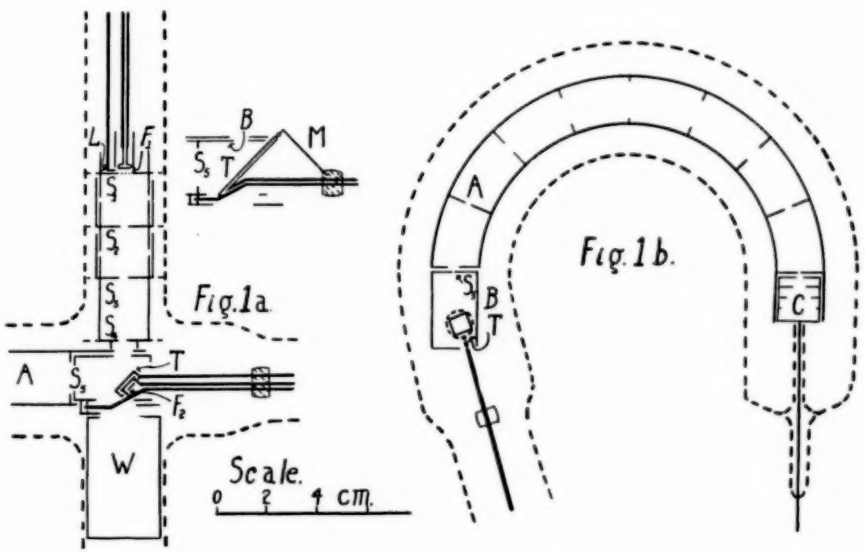

FIG. 1. Experimental apparatus.

spring M (Fig. 1a, inset). Considerable difficulty was experienced from breaking of these filaments at high temperatures because of the tension necessary for exact alignment.

A later and more satisfactory form of target (subsequently referred to as "heater target") consisted of a small cylinder of sheet molybdenum enclosing a non-magnetic pancake filament F_2 of tungsten. The target proper was a thin foil (0.03 mm) of molybdenum mounted on the end of the cylinder and backed by a heavier piece of the same material. The target could be maintained at a temperature of 1400°K by radiation alone during the making of observations and could be heated to any desired temperature by electron bombardment for outgassing purposes. It was found experimentally that the use of alternating current eliminated (by an averaging process) the effect of the very slight magnetic field.

All metal parts of the apparatus were of molybdenum and tungsten with the exception of the small iron armature controlling L. They were enclosed in a Pyrex tube of the shape indicated by the dashed lines of Fig. 1.

The pumping system consisted of a water-cooled mercury diffusion pump backed by a Cenco Hyvac. Two liquid air traps were placed in series between the research tube proper and the diffusion pump, and a third between the latter and the Hyvac. Pressures were measured by a McLeod gauge and an ionization gauge of sensitivity 4×10^{-9} mm Hg per mm deflection of the accompanying galvanometer.

Electrical connections were as follows. The target, the box B surrounding the target, and the analyzer were grounded through a galvanometer, thus affording a measure of the primary current. Switches were so arranged that the current to each could be measured separately. The primary filament was maintained at a negative potential determined by the desired energy of the primary electrons. The grid S_1 was 4.5 volts positive with respect to this filament; S_3S_4 was grounded; and S_2 was held at that potential, usually ground, which gave the maximum current to the target. This arrangement served to give a quite homogeneous beam, which was due in part to the elimination of secondary electrons from the first grid, and in part to a narrower thermal distribution than would have been the case had the entire accelerating potential been applied to this grid. The focusing action of the field between S_1 and S_2 helped compensate for a loss of intensity because of space charge saturation in the region of the cathode. By means of a two-position switch a retarding potential could be applied to S_2, completely stopping the primary beam and affording a method of obtaining the zeros of the various indicating instruments.

Currents to the collector C were amplified by an FP54 vacuum tube circuit of maximum sensitivity 2.5×10^{-16} amperes per mm deflection of the indicating galvanometer.

After assembly the tube was baked at a temperature of 500°C for more than 500 hours, the process being repeated whenever it was necessary to admit air into the system. The furnaces were then removed and special heat treatment of the target begun, the temperature being raised as rapidly as possible without allowing the pressure to rise to too high values. Ultimate outgassing temperatures varied for different specimens. In the case of the heater target the degassing period extended over 3500 hours, the greater part of the last 1000 hours of heating being at temperatures well in excess of 2100°K. On removal the target was found to be firmly welded to its molybdenum backing. Pressures at the end of the degassing period were of the order 2×10^{-8} mm Hg when the specimen was cold and 3 to 4×10^{-8} mm Hg when it was hot. From the behavior on heating and cooling it is believed that the difference was due to gas evolved from the surrounding metal parts (which achieved a bright red temperature) rather than from the target itself.

An analysis of the thermions emitted when the specimen was hot placed the contact potential between a clean target and the analyzer at about 0.8 volt. Application of this correction to the secondary energies just sufficed to make the distribution curves pass through the origin. This contact potential apparently increased by about one volt when the target was exposed to residual gas for a few hours (Fig. 4, curve *e*).

Results

Typical distribution curves for three different primary energies are shown in Fig. 2, curves *a*, *b* and *c*. Abscissae are secondary energies in volts and ordinates are $(K\cdot I_s)/(I_p\cdot E_s)$, where K is a constant, I_s is current to the collector C, I_p is the primary current, and E_s is the secondary energy. Division by E_s is necessary to correct for variable dispersion across the analyzer slits. These results were obtained (as were those of Figs. 3, 4, 5) at the end of the 3500 hour degassing period, the target being at a temperature of 1400°K. Results obtained before outgassing were somewhat similar but the secondary currents were much larger,

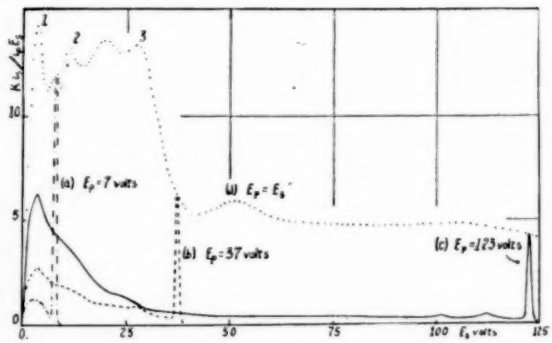

FIG. 2. *a*, *b*, *c*, typical distribution curves. *d*, full velocity curve. Experimental points are indicated in curve *d*.

particularly at very low secondary energies. The general form of the curves of Fig. 2 agrees with the results of other observers.

The high, sharp peak at the high energy end of each distribution curve is due to the so-called "full velocity" or "elastically reflected" electrons, the latter name being given in recognition of the generally accepted belief that they are primary electrons which have been reflected from the target without appreciable loss of energy. Secondary electrons of lower energies are generally assumed to be of two types; "inelastically reflected" electrons; and "true secondary" or "emitted" electrons, i.e. metallic electrons which have received sufficient energy from the primary beam to allow them to escape. The existence of the latter type is proved by the fact that at sufficiently high primary energies the total number of secondaries exceeds that of the primaries.[8] It is generally believed that the large group of secondaries at low energies is composed principally of emitted electrons; that electrons of energies slightly less than the primary energy are mostly inelastically reflected electrons; and that both types are present at intermediate energies.

As previously reported by the author,[9] the distribution curves exhibit a certain fine structure which may be classified under two main headings.

[8] See, for example, P. L. Copeland, Phys. Rev. **46**, 167 (1934).

[9] L. J. Haworth, Phys. Rev. **37**, 93 (1931); **42**, 906 (1932). Later work has somewhat modified the results reported in the first of these two references. The discrete loss peak then found at a loss of 4.7 volts was made to disappear with further outgassing. The positions of the remainder have been more exactly determined. The absence of very low energy secondaries when the target was cold was found to be due to a charging up of the slits of the analyzer. Soller's results[4] were also in error at low energies for this reason.

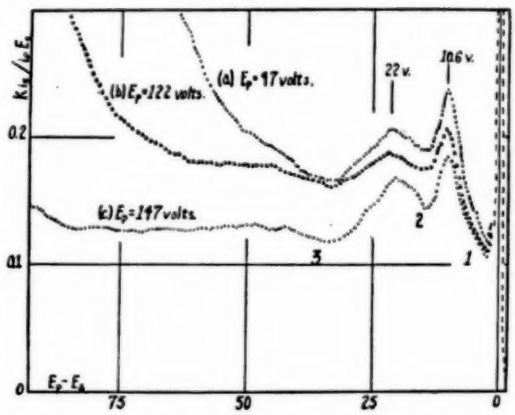

FIG. 3. Discrete loss peaks. Experimental points are indicated.

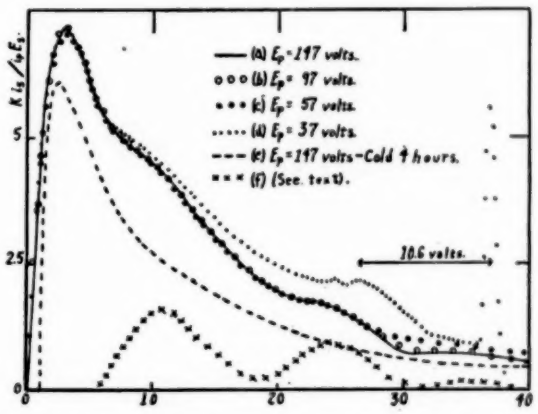

FIG. 4. Low energy secondaries. Ordinates of *b*, *c*, *d*, multiplied by factor to give coincidence with *a* at a secondary energy of 4 volts. *f* represents difference between *a* and extrapolated background. Experimental points are indicated in curves *b*, *c*, *d*, *f*.

(1) In all cases of sufficiently high primary energy, peaks were present in the distribution curves at energies 10.6, 22 and (approximately) 48 volts less than that of the primary electrons (Fig. 3). The first two covered relatively narrow ranges of energy but the third formed part of a wide band extending from an energy about 36 volts less than the primary energy down to a point somewhere near half of the latter. Although these maxima were not at all marked before outgassing the specimen, a hundred or so hours of heat treatment were sufficient to bring them to almost their full prominence. Additional slight "humps" sometimes appeared at energies approximately 17, 31, 43, 66 and 76 volts less than the primary energy but the evidence on this point is not conclusive.

Peaks similar to those just discussed have been observed by Rudberg[3] for various metals. As he has pointed out, they are undoubtedly due to the presence of groups of inelastically reflected electrons which have suffered discrete losses of energy in the process of reflection.

(2) Irregularities in the curves indicate the presence at low secondary energies of a selective emission which is independent of the primary energy. This type of fine structure is illustrated by Fig. 4, in which the scales of ordinates of curves *b*, *c* and *d* have been multiplied by the proper factors to make these curves coincide with curve *a* at a secondary energy of 4 volts. In the energy regions centering about 11, 24 and 35 volts the number of secondaries is abnormally large. This phenomenon was not apparent before several hundred hours of outgassing and in all cases disappeared entirely after a few hours exposure to residual gas (Fig. 4, curve *e*). As is shown by the near coincidence of curves *a*, *b* and *c* the positions and relative magnitudes of these irregularities are practically independent of the primary energy, provided the latter is sufficiently high. In order to study the effect more closely the background of a given distribution curve was extrapolated through the energy ranges of the irregularities and the differences in ordinates between this curve and the experimental curve were plotted on a much larger scale of ordinates. Curve *f*, Fig. 4 was obtained from curve *a* in this manner.

This type of selective emission has not, to the author's knowledge, been previously observed.

It is seen that the distribution curves of Fig. 4 practically coincide over the range of secondary energies from zero to 25 volts for all primary energies of 60 volts or more. The coincidence of the curves for high primary energies in a measure justifies the assumption that the low energy group of secondaries is in such cases made up almost entirely of emitted electrons. As the primary energy is decreased, however, the successive curves are no longer coincident, but diverge rapidly at the higher secondary energies. This is undoubtedly due to the presence of relatively larger numbers of inelastically reflected secondaries of low energies as the primary energy is decreased. For example, the 10.6-volt discrete loss peak is distinctly observable at 26.4 volts in curve *d*.

As molybdenum apparently adsorbs residual gas very quickly even at relatively high tempera-

tures it was felt that perhaps the temperature at which most of the observations were taken (1400°K) was not high enough to assure an absolutely clean surface. For this reason much data was taken under the following conditions. Before each observation the heater target was heated by electron bombardment to a temperature of about 2200°K over a period of 30 seconds. The bombarding potential was then removed, the filament remaining hot, and an observation taken 15 seconds later. That the target was still much above 1400°K was shown by the larger number of thermions being emitted than was the case at that temperature. 15 seconds more were required to obtain instrument zeros, after which bombardment in preparation for the next observation was begun.

Results obtained in this way were not essentially different from those obtained by the usual method. The secondaries were somewhat more numerous and on some occasions the discrete loss peaks were slightly more prominent. The curves were rather irregular because of the rapidly changing conditions under which observations were taken. Curve *a*, Fig. 3, and curve *a* Fig. 4, were obtained in this manner.

Full velocity secondaries

A careful study of a number of the full velocity peaks was made. From their form, together with the calculated slit dispersion, second order dispersion corrections were worked out so that it was possible to compute the area under any peak and hence the number of full velocity secondaries from the observed maximum current to the collector. Observations of this type were taken at close intervals of primary energy from zero to 120 volts, the results for the heater specimen being plotted in curve *d*, Fig. 2.

The principal features of this curve are the relative scarcity of full velocity secondaries at primary energies just greater than zero and the great decrease in their number as the primary energy is increased beyond 30 volts. In addition a number of maxima and minima are present. The positions of the maxima were in approximate agreement for the various specimens, although one or two were sometimes missing. The energies and relative magnitudes of the various maxima are summarized in Table I, the data being from the three most completely outgassed specimens.

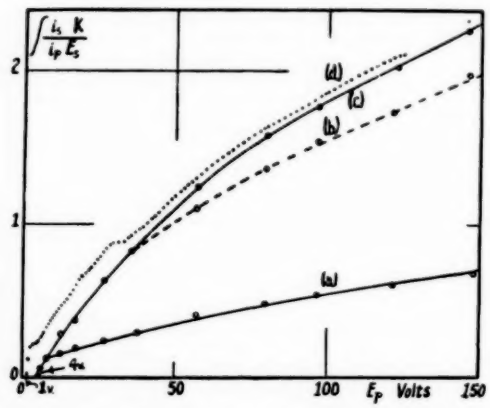

FIG. 5. Integration of distribution curves as functions of primary energy. Curve *a*, integration limits zero to 10 volts (secondary energy); curve *b*, zero to 35 volts; curve *c*, zero to $E_p - 4$ volts; curve *d*, all secondaries included.

TABLE I. *Energies and relative magnitudes of the various maxima.* Intensities *I* range from 5 (very strong) to 1 (very weak). Specimen No. 1, outgassed 1000 hours.; No. 2, 2500 hrs.; No. 3, 3400 hrs. Average values of E_p are weighted.

	E_p	I	E_p	I	E_p	I	E_p	I	E_p	I	E_p	I	E_p	I	E_p	I
No. 1	3.3	5			14.5	3	21.5	3	29.5	3	51.5	2	No data taken			
No. 2	3.8	3	7.8	2	13.0	4	21.5	2	28.5	1	50.0	2	78.5	2	101	2
No. 3	3.5	3	7.5	2	11.5	3	20.0	3	28.5	2	51.0	4			101	1
Aver.	3.6		7.6		12.0		20.8		28.8		50.7		78.5		101	

Integration of distribution curves

The total number of secondary electrons (per primary electron) in any given range of energy could be determined by measurements of the areas under the distribution curves. The results of such integrations are plotted as functions of primary energy in Fig. 5, the various curves representing integrations over different ranges of secondary energy.

No secondary electrons of any energy were observed when the primary energy was less than one volt. For primary energies less than 4 volts* only full velocity secondaries appeared. At higher primary energies the secondaries covered the whole energy range from zero up to the energy of the primaries. The number of secondaries in each energy range increased steadily with increasing primary energy, the greatest increase being at low secondary energies. That curves *c* and *d* rise

* Throughout this paper the primary energies given have been corrected for the contact potential between the cathode and the target. This correction amounted to three volts so that, for example, the value of four volts at which slow secondaries first appeared corresponded to a reading of seven volts on the voltmeter indicating the primary energy.

more rapidly than b is because of their wider integration limits. The general form of curve d is similar to that given by Petry[10] and others who have plotted the (total secondary)/(total primary) ratio, including all directions of emergence. The irregularities are not, however, of the same nature. This may be because of their integration over all directions. A more likely explanation is, however, the fact that only a few primary energies were used in obtaining curve c and that curve d was built from curve c by adding the areas of many full velocity peaks to the ordinates of a smooth curve drawn through the few experimental points of curve c. Thus the fine structure of curve d is not necessarily correct.

Discussion

Various theoretical studies[11] have shown that in a metal lattice the tightly bound "atomic" electrons behave almost identically as in an isolated atom but that the energy spectrum at the higher energies characteristic of the "valence" or "free" electrons is markedly different. For a given direction of motion in the crystal the allowed states lie in bands with forbidden intervals between. When all directions of motion are considered the bands overlap so that no energies are absolutely forbidden but, as Kronig[12] has shown, certain energies are much more probable than others.

The situation in an ideal one-dimensional crystal is shown in Fig. 6. The dashed lines represent the potential field which approaches the value indicated by the line AA at an infinite distance from the crystal. The "conduction" or "free" electrons distribute themselves among the lower states of band 1 in accordance with a normal Fermi distribution so that, since there are two allowed states per atom in each band, half of the states in the first band will be occupied in a monovalent metal. The energy spread W_i among the filled levels at 0°K is given by a well-known formula of Sommerfeld. The situation in molybdenum is somewhat complicated by the fact that in the free atom there is not a closed shell inside the valence shell so that the number of "free" electrons is not definitely known. If, however, we assume one such per atom we get $W_i = 5.9$ volts. The additional energy necessary to allow the highest energy conduction electron to escape from the metal is the thermionic work function ϕ. According to DuBridge[13] $\phi = 4.15$ volts for molybdenum.

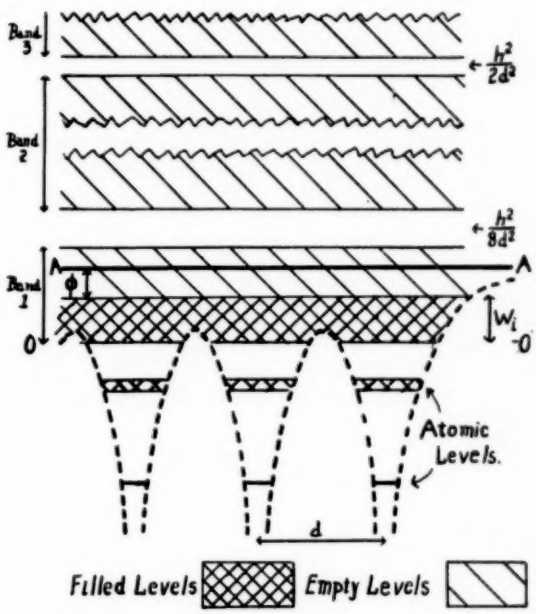

Fig. 6. Energy levels in an idealized crystal. d is the spacing between atoms.

Three types of secondary electrons are possible in addition to the elastically reflected primaries. They are: (1) inelastically reflected primaries; (2) emitted "free" or "conduction" electrons; and (3) emitted atomic electrons. We are thus interested on the one hand in the processes by which the primary electrons may lose energy and on the other hand in the processes by which electrons within the metal may absorb sufficient energy to escape.

Elastically and inelastically reflected electrons

Primary electrons may lose energy to either the atomic or the free electrons. Energy absorbed by an atomic electron will result in its ejection from the atom, giving rise to the excitation of soft x-rays. The energy transferred in such a process must be not less than that necessary to enable the ejected electron to occupy the lowest vacant conduction level. Froehlich[14] has studied the excitation of free electrons by primary electrons

[10] R. L. Petry, Phys. Rev. **26**, 346 (1925).
[11] See J. C. Slater, Rev. Mod. Phys. **6**, 209 (1934) for a complete bibliography.
[12] R. de L. Kronig, Zeits. f. Physik **75**, 191 (1932).
[13] L. A. DuBridge, Phys. Rev. **42**, 52 (1932).
[14] H. Froehlich, Ann. d. Physik **13**, 229 (1932).

for a rather simple model. He has found that certain selection rules require that the excited electron be lifted to at least the second allowed energy band and that the most probable transitions are those to the second band. Kronig and Penney[15] have obtained the same result in the case of excitation by radiation. Thus there seems to be a minimum to the energy which one of these electrons may absorb, but on the other hand few of them have very high energies after excitation.

Whatever the process, then, there is apparently a more or less definite lower limit (call it $W_{\min}$) to the energy which a primary electron can lose, so that no inelastically reflected secondaries should appear at energies greater than $E_p - W_{\min}$. This probably accounts for the sharp minimum just before the full velocity peak in the curves of Fig. 3.

The sharpness of the discrete loss peaks indicates that the banded structure of the upper energy levels is playing an important role. Excitation of the conduction electrons could give rise to such peaks only if some sort of selection rules or discontinuous transition probabilities such as those of Froehlich govern the process. Furthermore the ejection of atomic electrons would account for sharp edges only on the low loss sides of the discrete loss peaks unless transitions to the upper conduction levels are somewhat discontinuous. Kronig[12] has explained the fine structure of x-ray absorption spectra by assuming that this is the case.

A definite relationship exists between the irregularities of Fig. 3 and certain of those of the full velocity curve (*d* of Fig. 2). This is to be expected. As the primary energy is increased from zero the number of elastically reflected electrons should suffer sharp decreases at energies just sufficient to give rise to the processes responsible for the discrete loss peaks. That is, there should be a sort of critical potential effect. A primary electron may surrender up to $E_p+\phi$ volts of energy and still be able to occupy one of the unfilled conduction levels. In Table II values for this expression corresponding to various points E_c at which curve *d*, Fig. 1, "breaks" downward are listed together with the lowest energy losses E_1 found in the different discrete loss peaks. In computing the latter account was taken of the nonhomogeneity of the primary beam and the imperfect resolving power of the analyzer. The term values of the lowest x-ray states are listed in line 4 for comparison. These are taken from Siegbahn[16] and were determined from measurements of the *L* and *M* emission spectra. The Y_{I} and Y_{II} term values probably represent multiple excitations. The $N_{\text{IV, V}}$ and Y_{II} values seem too low to be consistent with our calculated value of W_i but this may arise from inaccuracies in their determination because of the rather indirect way in which they were measured. It is seen that the agreement between $E_c+\phi$ and E_1 is good and that in cases one and three the x-ray term values are sufficiently close to the experimental values to make it seem likely that it is the excitation of these levels which is responsible for the irregularities in question. Thus the large decrease in the number of elastically reflected electrons as the primary energy is increased beyond 30 volts seems to represent a sort of absorption edge for the $N_{\text{II, III}}$ x-ray states.

TABLE II.

	1	2	3
E_c	3.6	12.0	28.8
$E_c+\phi$	7.8	16.1	33.0
E_1	7.5	17.0	35.0
$E_{\text{x-ray}}$	$\left\{\begin{matrix}4.5(N_{\text{IV, V}})\\5.5(Y_{\text{II}})\end{matrix}\right\}$	$23.3(Y_{\text{I}})$	$38.2(N_{\text{II, III}})$

The phenomenon of electron diffraction may also enter into the results represented by the full velocity curve. This is merely another way of saying that when a primary electron has a momentum component perpendicular to some set of net planes of a crystal of such a value that the corresponding energy falls in one of the forbidden bands, the electron will be specularly reflected from that set of net planes. Simple assumptions indicate that in the present case maxima arising from this cause should appear in the full velocity curve at energies given by

$$E_{p(\max)} = (75\, n^2/d^2) - 2W_a$$

where n is an integer, d is the spacing between Bragg planes and W_a+E_p is the energy which the electron possesses within the crystal. Calculated values for this expression are listed in the first

[15] R. de L. Kronig and W. G. Penney, Proc. Roy. Soc. **A133**, 255 (1931).

[16] M. Siegbahn, Zeits. f. Physik **88**, 559 (1934).

TABLE III.

$E_{\text{theor.}}$	10.1	25.4	40.6	55.8	86.0	101.3
$E_{\text{exp.}}$	7.6	20.2	—	50.7	78.5	101
Difference	2.5	5.2		5.1	7.5	0.3

line of Table III, where we have assumed a value for W_a given by $W_a=\phi+W_i=10.05$ volts. In the second line are listed values from Table I which seem to correspond. If this interpretation is correct our value for W_a seems somewhat too small.

It is probable that both "critical potential" and electron diffraction effects influence the number of full velocity secondaries but whether or not the assignments we have made are correct is problematical.

Emitted electrons

The emitted electrons may receive their energy directly from the primary electrons or there may be some intermediate process such as the photoelectric action of soft x-rays. In either case it is to be expected on general grounds that the energies of most of the emitted electrons will be low. This is true in the case of electrons ejected from isolated atoms by either electrons or radiation and the results of Froehlich[14] and Kronig and Penney[15] indicate that fairly low energies are most probable among excited conduction electrons.

The large, low energy group of emitted electrons covers a range of energies which is approximately the same as the range of energy which includes most of those electrons which can with certainty be classed as inelastically reflected. This would seem to indicate that most of the emitted electrons originated in the conduction levels as somewhat greater energy transfers would be necessary to give rise to emitted atomic electrons.

The relative scarcity of secondaries at energies just above zero may be the result of a high internal reflection coefficient for very slow electrons; or it may be possible that such energies are improbable because of the banded structure of the allowed states.

Fig. 5 shows that when the primary energy is less than about 4 volts, only elastically reflected secondaries are observed. This may be explained as follows. We have seen that most inelastically reflected electrons have lost at least 7.5 volts of energy. Thus they cannot escape unless the primary energy is greater than this value. Furthermore, in order to have appreciable excitation it is necessary that the primary energy available for that purpose be greater than $W_{\min}=7.5$ volts. Thus, in order to have any emitted electrons it is necessary that $E_p+\phi\geq 7.5$ volts, or $E_p\geq 3.35$ volts, not far from the experimental value mentioned above.

The fixed energy groups may be a result of the irregular density of the allowed energy states above the filled conduction levels. That is, if the number of states is particularly large in a certain energy range, one should expect a large number of secondaries at the corresponding energies. Measurements by Zinn[17] on the fine structure of x-ray absorption spectra for molybdenum indicate, according to Kronig's[12] interpretation, that transitions to states in the regions near 14, 41 and 79 volts above the highest unoccupied conduction level are unusually numerous. Measured from the same origin our first and third fixed energy groups would be centered around 15 and 39 volts, in good agreement with two of Zinn's values. The presence of the discrete loss groups precluded the possibility of determining whether an additional fixed energy group existed in the neighborhood of 79 volts.

It is possible to account for the 24-volt fixed energy group by an entirely different process. We have seen that it seems likely that the $N_{\text{II, III}}$ x-ray levels are strongly excited. Transitions of the type $N_{\text{IV, V}}\rightarrow N_{\text{II, III}}$ would give rise to x-rays of energy 33.7 volts (or somewhat less if, as previously suggested, the $N_{\text{IV, V}}$ term value listed is too low). Photoelectrons ejected by this radiation would have energies between $33.7-(\phi+W_i)$ and $33.7-\phi$ or, roughly, between 23.5 and 29.5 volts, thus accounting, perhaps, for the 24-volt fixed energy group.

It is thus possible to find reasonable explanations for most of the experimental results. However, both theory and experiment are as yet too incomplete to render these explanations anything but tentative. The experimental work is being continued on other metals.

It is a pleasure to express my sincere thanks to Professor C. E. Mendenhall who suggested the problem and who has given generously of his time during the progress of the work.

[17] W. H. Zinn, Phys. Rev. **46**, 659 (1934).

Secondary Emission of Electrons from Complex Targets*

PAUL L. COPELAND, *Department of Physics, Montana State College*

(Received April 18, 1935)

Secondary emission of electrons from complex targets formed by the condensation of some substances on others has been investigated. The change in the secondary emission with the primary energy appears to be dominated by the overlying element in the low energy range and by the base metal in the range of high primary energies. The total secondary emission in certain ranges may be less or greater than that obtained from either constituent of the complex target when used alone.

THE writer[1] has made studies concerning the general form of the curves obtained when the magnitude of the secondary emission is plotted against the energy of the primary electrons. The correlation of secondary emission with atomic number suggested that complex targets (formed by the condensation of thin films of some substances on others) might show the properties of the superficial layer for primaries of low energy and the properties of the base material for primaries of higher energy.

The apparatus and procedure used for measuring the ratio of the secondary emission to the primary current was of the usual type. The geometry of the arrangement is shown schematically in Fig. 1. A metal plate, T, was inserted to act as a target, and provision was made to control the evaporation of some material from the filaments F and F' a part of which recondensed on this target. In practice the collector of the secondaries, C, was made about 100 volts positive with respect to the target. The net currents to the target and collector were measured. The ratio, R, of the secondary current to the primary current was obtained through division of the collector current by the sum of the collector and target currents.

The first results were obtained from targets formed by a deposit of platinum on aluminum. The tube was evacuated and baked for several hours at about 450°C. Before evaporating any of the platinum, the secondary emission of the aluminum was obtained as a function of the primary energy. Curve 1 of Fig. 2 shows these results. In this figure the abscissas represent the energy of the primary electrons in volts and the ordinates are the common logarithms of the corresponding ratios, R. After curve 1 was obtained, the platinum filaments were heated by an electric current to such a temperature that appreciable evaporation of the platinum took place. After several minutes of this evaporation, the platinum was allowed to cool, and the secondary emission from the target was again measured as a function of the primary energy. The first result of the condensation of platinum on the aluminum appeared to be a lowering of the secondary emission a few percent throughout the entire range of primary energies used. After several such stages of platinum evaporation, curve 2 was obtained. Depositing still more platinum on the aluminum resulted in the curves labelled 3, 4, 5 and 6 (taken in this order although separated in general by data omitted here).

The first result of depositing platinum on aluminum is to decrease the secondary emission a few percent throughout the entire range of primary energies used. As the film thickness is increased, however, the emission for the lower primary energies shows a variation more and

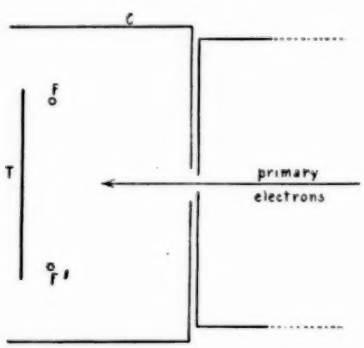

FIG. 1. Apparatus.

* The material in this paper was obtained in the George Eastman laboratories at M. I. T. and was presented before the Washington Meeting of the Am. Phys. Soc., April 28, 1934. Phys. Rev. **45**, 763 (1934).

[1] Copeland, Phys. Rev. **46**, 167 (1934).

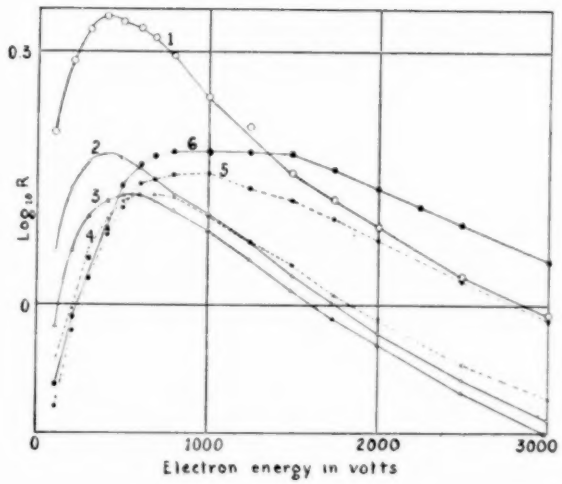

FIG. 2. Platinum on aluminum.

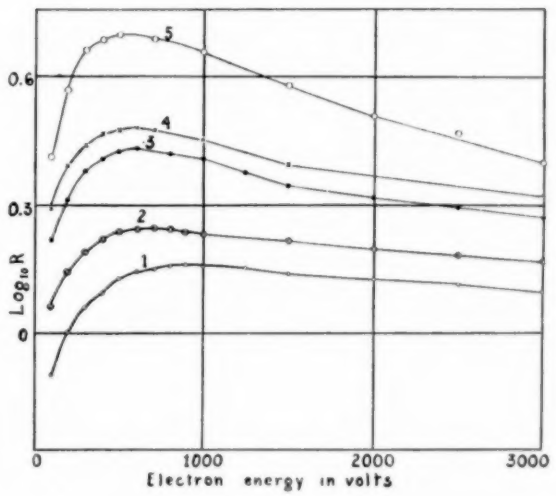

FIG. 3. Calcium on gold.

more characteristic of the platinum, while at higher energies the rate of variation of the secondary emission is certainly characteristic of the aluminum. For the thickest of the platinum films (estimated to be about 7.5×10^{-6} cm thick) for which results are shown by curve 6, the results are very similar to those obtained from thick plates of platinum for primary energies less than 1500 electron volts, while for higher primary energies the secondary emission decreases at a rate characteristic of aluminum rather than platinum.

The most striking fact is that the total secondary emission obtained from a complex target may differ from that obtained using either of the constituent elements, and that it is not a weighted average of the two. For intermediate film thicknesses (curves 3, 4 and 5) the secondary emission is lower than that obtained either from a simple aluminum target or from a simple platinum target over the whole range of high primary energies.

The converse of this case is obtained by depositing a film of calcium on a gold target. (The experimental arrangement was similar to Fig. 1. The target, T, was a gold plate and the platinum filaments were replaced by a small spiral of tungsten wire containing the calcium metal.) The result obtained from the gold target after very limited heat treatment is shown by the first curve of Fig. 3. The evaporation of a small amount of calcium a part of which is deposited on the gold, raises the emission a few percent throughout the entire range of energies used. Results obtained with the thicker films (curves 3, 4 and 5) show that the emission increases more rapidly at low energies than it does for the simple gold target. Curves 3 and 4 show that the emission begins to decrease more rapidly than it does for the simple gold target. For both of these curves the slope changes at about 1500 volts and the rate of decrease in the secondary emission beyond this point is quite similar to that obtained from clean gold. Depositing still more calcium on the gold results in the maximum being shifted to lower primary energies as shown by curve 5. The rapid decline of the secondary emission characteristic of calcium then continues to a primary energy in the order of 2000 volts.[2]

Results similar in general nature were obtained for lithium on tantalum and for germanium on gold.

A very interesting result was obtained by condensing the vapor of an ordinary motor oil onto a gold base. Fig. 4 represents the results obtained. The first effect (as before) is an increase in the secondary emission. For intermediate film thicknesses (shown by curves 4 and 5) the secondary emission rises to a maximum in the region at which the earlier work has shown a maximum for surfaces dominated by grease contamination. For curve 5 the rate of decline of

[2] The results are probably influenced by some degree of alloying. After the removal of the target, inspection revealed that the part of the target on which the primary electrons were incident showed coloring which differed from other parts of the surface.

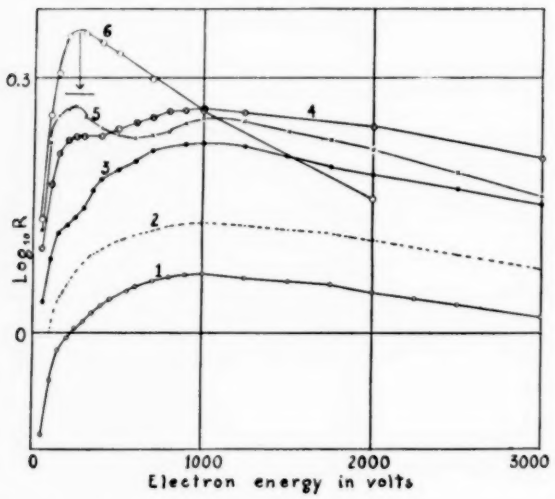

FIG. 4. Oil on gold. Note: All ordinates of curve 6 should be lowered as indicated.

secondary emission just above the maximum is characteristic of the superficial layer. At primary energies slightly higher, the secondary emission again increases and comes to a second maximum at a primary energy quite close to that at which a maximum emission is obtained from the gold alone. The appearance of the double maximum is quite striking, and it suggests the dominance of the overlying film at low energies and the dominance of the base metal at high energies in determining the rate at which the secondary emission changes with the energy of the incident electrons. Fig. 4 is a complete converse of Fig. 2. The emission is raised instead of lowered, and for intermediate film thicknesses, the total secondary emission is greater throughout the entire high energy range than it is for either the simple gold target or for a thick film of the overlying substance.[3]

The films used in these experiments are relatively thick. The work function would hardly be expected to change after the addition of the first few atomic layers. The major portion of the changes in secondary emission must be ascribed to some other cause. The results suggest that the depth to which the primaries penetrate is the controlling factor. This naturally alters the distance through which secondaries diffuse in reaching the surface. These experiments can best be understood on the hypothesis that for a certain primary energy electrons scattered from the primary beam at a certain depth below the surface are more effective than any others in the production of secondaries. This optimum depth varies with the material and with the primary energy. Placing a relatively good scattering agent at the optimum depth naturally increases the secondary emission. Conversely, if at the optimum depth a relatively poor scattering agent is placed, the emission from the surface is reduced. On this basis a complex target may have a total secondary emission in some energy ranges which is either above or below that of either of the constituents alone.

[3] Although the films studied here were not entirely stable, the main features of the variation of secondary emission with primary energy and with film thickness were verified by repeated trials on the same film and for films formed in several evaporation sequences.

JULY 1, 1935 PHYSICAL REVIEW VOLUME 48

Corrections to H. Kayser's "Tabelle der Schwingungszahlen" [1]

(Received March 30, 1935)

PROFESSOR H. KAYSER of Bonn, Germany has submitted the following table of corrections to his well-known and useful *Tabelle der Schwingungszahlen*. He states that these errors occurred on account of the bad state of his eyes. They have been found by himself and others, mostly by Dr. W. F. Meggers to whom he expresses his best thanks.

Because of the great usefulness of these tables to spectroscopists, and at the specific request of many readers of the *Physical Review*, these corrections to the tables are here presented.

EDITOR

[1] Verlag von S. Hirzel, Leipzig, 1925.

Corrections to Kayser's Tabelle der Schwingungszahlen

Page	Line	Now reads	Should read
1	2006.9	1290.0	1190.0
1	2009.8	4063.6	4003.6
1	2015.9	9854.7	8954.7
3	2101.5	6889.8	6989.8
3	2108.8	052.47	0524.7
3	2110.4	6933.2	6931.2
3	2110.5	6701.1	6706.7
3	2117.1	194.20	1942.0
3	2138.2	5851.1	5351.1
3	3 from end	100.5	110.5
4	2157.4	3749.2	3747.2
4	2184.5	6279.8	6269.8
4	2290	2290	2190
5	2240.5	1906.7	1900.7
7	2300.1	9296.0	6296.0
7	2309.5	8607.0	8607.5
7	2321.0	7163.2	7162.2
8	2385.0	1582.6	1592.6
9	2422.1	7394.9	7394.2
9	3 from end	211.1	121.1
10	2463.4	8262.2	8202.2
10	2471.9	4249.6	4248.6
10	2472.7	2941.2	2940.2
10	2481.3	8921.8	8928.8
11	2500.4	8955.0	8155.0
11	2430	2430	2530
11	2530.3	091.32	0913.2
12	2583.5	9660.8	9560.8
12	8 from end	20.4	30.4
13	2611.4	8229.5	8221.5
13	2616.5	0766.1	0760.1
13	2622.6	1923.9	1873.9
13	2622.7	1828.6	1728.6
13	2622.8	1683.3	1583.3
13	2622.9	1537.9	1437.9
13	2631.0	2799704.5	3799704.5
13	2645.9	4308.5	8308.5
13	2647.8	7597.3	5597.3
14	2665.0	3741231.1	3751231.1
14	2666.0	9824.1	3749824.1
14	2666.1	8683.5	9683.5
15	2703.2	8214.2	8224.2
15	2703.2	8214.2	8224.2
15	2703.3	8077.4	8087.4
15	2731.9	9372.7	9374.7
15	2738.0	1225.5	1222.5
16	2750.3	4844.3	4894.3
16	2794.4	6533.2	7533.2
17	2849.8	8089.7	7989.7
17	2849.9	7966.6	7866.6
17	2850.0	7843.6	7743.6
17	3 from end	80.2	88.2
18	2850.0	7843.6	7743.6
18	2845	2845	2855
18	2856.4	9894.5	9884.5
21	3011.8	9301.2	9309.2
22	3047	3047	3057
22	3069.0	7466.6	7446.6
22	3074.4	1720.4	1725.4
27	8 from end	17.0	18.0
27	8 from end	18.8	17.8
28	3400.	2930335.7	2940335.7
30	3481	3481	3471
31	2530	2530	3530
31	3528	3528	3538
32	3566.3	3239.0	3229.0
32	3568.7	1353.9	1343.9
35	3730.0	2670205.7	2680205.7
36	3752.0	4990.7	4490.7
37	3841.9	2133.4	2143.4
37	3842.0	2065.6	2075.6
37	3842.1	1997.9	2007.9
39	3925.6	6652.8	6662.8
39	3933.3	1647.4	1677.4
42	4051	4051	4061
42	4080.8	8810.7	9810.7
45	4227.6	4784.6	4744.6
48	4351.7	6309.0	7309.0
48	4376.9	4072.4	4082.4
48	4389.2	7671.8	7681.8
49	4420.1	1764.2	1759.2
49	4422.7	0434.6	0429.6
49	4424.5	9515.1	9510.1
49	4446.7	8129.7	8229.7
50	4452.1	5003.8	5502.8
53	4613.8	8805.8	6805.8
53	4621.1	3372.9	3382.9
53	4641.9	3679.1	3689.1
55	4713.5	1074.2	0974.2
55	4713.7	0984.1	0884.1
55	4740.2	9627.6	9027.6
56	4759.1	0657.1	0652.1
56	4766.9	7114.8	7214.8
56	4767.1	7026.8	7126.8
56	4767.3	6938.8	7038.8
56	4777.1	2738.9	2736.9
56	4796.9	4198.9	4098.9
57	4802.1	1831.2	1842.2
57	4804.3	0988.8	0888.8
57	4808.7	8934.8	8984.8
57	4320	4320	4820
57	4822.8	2996.7	2906.7
57	4832.7	8650.4	8660.4
57	4835.1	7623.6	7633.6
58	4852.3	0294.5	0304.5
58	4865.1	4984.0	4884.0
58	4865.3	4899.5	4799.5
58	4867.5	3875.8	3870.8
58	4879.5	8869.8	8819.8
58	4889.9	4412.4	4462.4
59	4930.1	7797.1	7792.1
59	4932.9	6691.1	6641.1
59	4935.1	5717.6	5737.6
59	4938.1	4456.9	4506.9
59	4943.3	2367.4	2377.4
60	4964.7	3620.1	3660.1
60	4972.7	0470.6	0420.6
60	4979.1	7886.6	7836.6
60	4989.7	3561.2	3571.1
60	4993.3	2176.7	2126.7
61	5016.1	3016.4	3026.4
61	5037.7	4461.1	4481.1
61	5038.7	4097.2	4087.2
61	5044.3	1879.6	1884.6
61	5044.4	1835.3	1845.3
61	5044.5	1796.0	1806.0
61	5044.6	1756.7	1766.7
61	5044.7	1717.4	1727.4
61	5044.8	1678.1	1688.1
61	5044.9	1643.9	1648.9
62	5058.9	6163.0	6165.0
62	5099.3	0558.7	0508.7
63	5122.5	1679.5	1629.5
63	5140.7	4770.1	4720.1
63	5144.7	3258.1	3208.1
63	5149.7	1371.4	1321.4
64	5162.5	6558.1	6508.1
64	5164.9	5603.3	5608.3
64	5179.3	0276.8	0226.8
64	5198.7	3013.8	3023.8
65	5209.5	9032.2	9037.2
65	5213.9	7467.7	7417.7
65	5225.1	3357.8	3307.8
65	5245.3	5989.6	5939.6
65	5247.9	4985.3	4995.3
65	5250.3	4114.5	4124.5
66	5250.3	4114.5	4124.5
66	5251.7	3669.9	3616.9
66	5258.3	1277.6	1227.6
66	5264.3	9010.7	9060.7
66	5272.5	6157.2	6107.2
66	5275.7	4947.1	4957.1
66	5276.9	4576.2	4526.2
66	5282.1	2611.2	2661.2
66	5298.9	6610.6	6660.6
66	5299.5	6457.0	6447.0
67	5301.7	5614.2	5664.2
67	5311.7	2164.2	2114.2
67	5311.8	2178.8	2078.8
67	5311.9	2093.4	2043.4
67	5317.5	0011.4	0061.4
67	5324.3	7610.3	7660.3
67	5327.7	6412.0	6462.0
67	5338.1	2856.2	2806.2
67	5338.9	2575.6	2525.6
67	5339.9	2124.9	2174.9
68	5357.1	6114.0	6164.0
68	5358.1	5865.7	5815.7
68	5367.3	2637.5	2617.5
68	5367.9	2459.4	2409.4
68	5384.9	6579.8	6529.8
68	5385.3	6382.0	6392.0
69	5419.9	4531.1	4541.1
69	5421.9	3810.7	3860.7
70	5452.2	3617.7	3613.7
70	5493.6	8795.7	9795.7
70	5493.7	8762.6	9762.6
71	5511.1	4015.1	4017.1
71	5549.3	1580.0	1530.0
72	5576.1	2861.6	2871.6
72	5588.1	9011.5	9021.5
72	5599.1	5501.8	5506.8
74	5666.9	4184.9	4144.9
75	5723.3	6710.4	6760.4
76	5758.0	6232.7	6233.7
76	5759.0	5933.2	5932.2
76	5782.7	8867.7	8817.7
78	5867.2	3819.3	3919.3
79	5923.9	7660.6	7610.6
79	5925.1	7258.8	7268.8
79	5934.6	4267.8	4567.8
79	5935.6	4584.0	4284.0
81	6006.7	4397.1	4347.1
81	6009.8	3498.2	3489.2
81	6028.1	8434.2	8439.2
81	6041.1	4860.4	4870.4
82	6058.5	0167.7	0117.7
82	6059.3	9889.8	9899.8
82	6078.1	4791.6	4796.6
83	6122.9	2752.1	2762.1
83	6124.7	2232.2	2282.2
83	6136.7	9070.4	9090.4
83	6150	6150	6140
84	6177.7	8268.6	8278.6
84	6186.5	5926.6	5976.6
84	6189.3	5250.6	5245.6
84	6189.4	5229.5	5219.5
84	6189.5	5203.4	5193.4
84	6189.6	5177.3	5167.3
84	6189.7	5151.2	5141.2
84	6189.8	5125.1	5115.1
84	6189.9	5099.0	5089.0
84	6190.0	5072.9	5062.9
84	6190.1	5041.8	5036.8
85	6222.2	6705.5	6705.0
85	6229.3	4863.8	4873.8
85	6238.7	2405.7	2455.7
85	6244.1	1019.9	1069.9
85	6246.1	0507.2	0557.2
86	6252.3	8980.0	8970.0
86	6296.3	7791.1	7796.1
88	6358.3	2323.6	2313.6
89	6420.3	7120.1	7130.1
90	6478.1	3231.9	3236.9
91	6533.9	0056.6	0057.6
93	6624.7	9036.3	9086.3
94	6665.9	9754.1	9759.1
97	6826.9	4370.3	4390.3
98	6874.3	4393.0	4293.0
98	6883.5	2399.3	2349.3
99	6904.9	7878.2	7848.2
99	6914.7	5795.2	5796.2
100	6955.9	7262.8	7232.8
100	6966.7	5094.7	5004.7
100	6981.2	2034.2	2024.2
100	6994.1	9393.0	9383.0
103	827.0	8857.9	1208857.9
105	903.3	6749.5	6748.5

Corrections to "Vorwort"

III	17	ν_0	t_0
III	last	ν_0	λ^2
III	last	ν^6	λ^6
V	20	2596129.9	2596129.4
V	23	2596115.8	2596115.3

Corrections to $(n-1)\times 10^7$

100	6950	2553.39	2753.39
100	6960	2553.31	2753.31
100	6970	2553.23	2753.23
100	6980	2553.15	2753.15
100	6990	2553.07	2753.07

Professor H. Kayser

Bonn, Germany,
March 9, 1935.

LETTERS TO THE EDITOR

Prompt publication of brief reports of important discoveries in physics may be secured by addressing them to this department. Closing dates for this department are, for the first issue of the month, the twentieth of the preceding month; for the second issue, the fifth of the month. The Board of Editors does not hold itself responsible for the opinions expressed by the correspondents.

Gamma-Rays from Nitrogen Bombarded with Deuterons

It is known[1] that nitrogen bombarded with deuterons yields several homogeneous groups of alpha-particles, and at least two groups of protons. The reactions are probably

$$N^{14}+H^2 \rightarrow C^{12}+He^4, \quad (1)$$
$$N^{14}+H^2 \rightarrow N^{15}+H^1. \quad (2)$$

Lawrence, McMillan and Henderson[2] have investigated the alpha-particle spectrum down to about 6-cm range, and the proton spectrum down to about 10-cm range. From the differences in energy of the particle groups found, they inferred that there are excited levels of 3.8 and 4.7 MEV associated with the alpha-particle emission, and a level of 4.7 MEV associated with the proton emission. It should be kept in mind that in reaction (1), as far as the experimental data are concerned, the excited levels could be either in the C^{12} or in the alpha-particle.

We have studied the gamma-radiation emitted from nitrogen bombarded with deuterons, by means of a cloud chamber. Fig. 1 shows the energy spectrum of recoil electrons obtained from 2400 photographs taken at 900 kv bombarding voltage, 80 microamperes deuteron current and 1500 gauss magnetic field. The target used was ammonium chloride, and to minimize chemical decomposition it was bombarded only for about $\frac{1}{2}$ second, at the time of each expansion of the cloud chamber. In order to increase the resolution in the spectrum, only those tracks making angles less than $7\frac{1}{2}$ degrees with the direction of the radiation were recorded. The intercepts in the electron energy spectrum (shown as dotted lines), after having 0.2 to 0.25 MEV added to them in accordance with the theory of Compton collisions, indicate that the principal gamma-ray lines are 1.9, 3.1, 4.0, 5.3 and 7.0 MEV.

It is seen that these gamma-ray lines (except the 4 MEV line) do not represent directly the differences between the total energy released in the reaction and the energies of the various particle groups. They would represent these differences only if the excited nucleus could make no other transition than to the ground state; if transitions to intermediate levels are permitted, which is reasonable to expect, the gamma-rays observed will be related, but not in a direct way, to the energies of the particle groups. To correlate the gamma-rays and particles in the present case it is easy to construct simple level diagrams which are consistent with the data, but it is of course not possible to make one that is unique, on the basis of the present incomplete data. The alpha-particle energies indicate levels at 4.7 and 3.8 MEV, and the gamma-ray energies indicate, in addition, a level at 7, and possibly one at 5.3 MEV. The group of alpha-particles corresponding to the excitation of the 7-MEV level would be expected to have a range, in Lawrence, McMillan and Henderson's experiment, of 4.5 cm, which is considerably below the region for which they give data. The group corresponding to the 5.3 MEV level would have a range of 6.2 cm, and would lie just at the lower limit of their curve.

The height of the potential barrier which keeps the excited C^{12} from splitting up into three alpha-particles, or into one alpha-particle and Be^8 does not necessarily constitute a limitation upon the energy to which C^{12} may be excited. The excitation may be thought of as being within one of the constituent alpha-particles, and indeed the high observed value of the excitation (7 MEV) inclines one toward this view. One does not know how much different the levels in such a bound alpha-particle would be from those in a free alpha-particle; if they are nearly the same, the question of whether the observed excitation is in the C^{12} or in the ejected alpha-particle will be difficult to answer, on the basis of the present measurement of the gamma-ray energies. If both kinds of excitation occur, however, one might expect to find doublet structure in the alpha-particle energy groups, one member of each doublet corresponding to the excitation of a level in a bound alpha-particle, and the other to the excitation of the corresponding level in the ejected alpha-particle.

The number of protons emitted in reaction (2) is roughly a thirtieth of the number of alpha-particles from reaction (1), and therefore the contribution to the gamma-ray spectrum from this source can be neglected.

H. R. CRANE
L. A. DELSASSO
W. A. FOWLER
C. C. LAURITSEN

Kellogg Radiation Laboratory,
California Institute of Technology,
June 14, 1935.

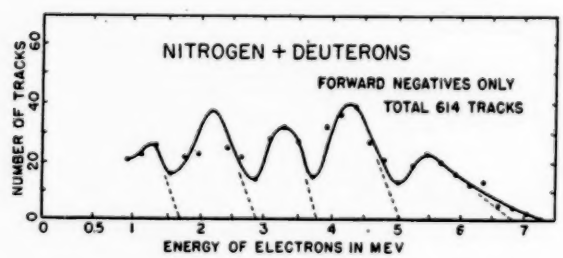

FIG. 1. Energy spectrum of recoil electrons produced by the gamma radiation from nitrogen bombarded with deuterons.

[1] Lewis, Livinston and Lawrence, Phys. Rev. **44**, 55 (1933).
[2] Lawrence, McMillan and Henderson, Phys. Rev., **47**, 273(1935).

The Origin of the "Extra Rings" in Electron Diffraction Patterns[1]

The diffraction patterns produced by electrons differ from the diffraction pattern produced by x-rays not only in the intensity distribution but also in the appearance of new lines.

These can be produced (a) by surface layers, since cross gratings may also produce sharp rings and (b) by the refraction of electrons on "electron smooth" surfaces. If the electron beam enters and leaves at the same crystal surface the Bragg equation $\sin\vartheta = n\lambda/2d$ has to be replaced by $\sin\vartheta' = n\lambda/2d(1-4d^2V_0/150n^2)^{\frac{1}{2}}$[2] and this may lead also to the appearance of lines not existing in the x-ray diffraction pattern. For low velocity electrons it has been found[3] that between the ordinary interference maxima there appear new maxima at a distance halfway between the regular maxima (so-called "fractional orders"). It has been assumed that these are due to an adsorbed gas layer (e.g., hydrogen).[4]

In the case of fast electrons, rings have been observed which are entirely inside the ordinary diffraction pattern and which also have been interpreted as fractional orders.[5] There is no theoretical reasoning to lead to the existence of such fractional orders.

During the last two years we have been using a new method[6] for making thin films for electron diffraction. The substance to be investigated is deposited in a high vacuum upon a volatile material which is later pumped off, leaving the free film. For most experiments purest naphthalene has been used. The following substances have been investigated: aluminum, cadmium, copper, cuprous oxide, gold, lead, lead oxide, nickel, silicon and silver. For all these substances we have found electron diffraction patterns containing sharp "inner rings" in positions similar to those reported by Rupp for gold. It is possible to interpret these rings as fractional orders of the ordinary interference maxima. Such an interpretation would necessarily lead to the expectation that the values of $\sin\vartheta/\lambda$ are different for different substances. Table I gives a summary of the values of $\sin\vartheta/\lambda$ as observed in our experiments. For comparison we have added the values from Rupp's work on gold. (Au(R) in table).

TABLE I. *$\sin\vartheta/\lambda$ for various substances and "inner rings."*

Ag					0.107	0.121	0.134	(0.141)			0.178
Al				0.077		.121		.137			
Au					.106	.121	.134				.178
$Cu+Cu_2O$					.106	.120	.134				
Cd					.108	.118		.138			
Ni					.105	.120	.133				.174
Pb		0.058		0.080	.105	.121		.138			
Si					.107	.120	.133		0.146		
Au(R)	0.054	.061	0.072	.082	.108	.124					.176
$C_{10}H_8$			.068	.077	.108	.120	.134	.140	.147	0.165	.175

The values of $\sin\vartheta/\lambda$ are identical for the different substances indicating that the diffraction pattern is not due to the substance itself but to an adsorbed surface layer. Since our films were produced by depositing on naphthalene we suspected that a thin layer of naphthalene might be responsible for the diffraction pattern observed.[7] An x-ray powder pattern of the naphthalene used in our experiments gave values for $\sin\vartheta/\lambda$, most of which are identical with the ones of the extra inner electron diffraction rings. The similar values which Rupp has found for $\sin\vartheta/\lambda$ in the absence of naphthalene are apparently due to adsorbed layers of organic substances which have similar spacing due to the similar C–C distances. Rupp states expressly that his rings cannot be due to traces of grease vapor since at the high voltages used (200 kv) the vacuum would break down in the presence of vapor. We have found that the adsorbed layers cannot be driven off by heating the film up to 500°C and also withstand electron bombardment.

The fact that the rings appear extremely sharp leads to the conclusion that we are dealing not only with thin crystal layers but with random orientated cross gratings. Also in this case, as has been shown by Laue,[8] sharp diffraction patterns are observed. This conclusion is further supported by the intensity distribution which shows characteristic differences from the distribution in space lattices.[9] The intensity sets in sharply at a certain angle and falls off from there. In some of our diffraction patterns we observe a blackening starting from one ring and filling continuously the interval on the plate to the next ring.

Recently we have been able to obtain thin films for electron diffraction by depositing on ammonium chloride which is later driven off by heating to 200°C in a vacuum. In this case no "inner rings" have been observed.

That these rings can be produced by contact with organic vapors (grease, oil) we have shown in the following manner: Two gold films have been made under exactly the same conditions. One film was exposed to organic vapors (from a grease joint), the other one was held in a perfect vacuum. The first film gave "inner rings," the second not. After exposing the second film to grease vapor the "inner rings" have been observed too. Our experiments seem to indicate that even the presence of small naphthalene nuclei, so sparsely distributed that they themselves will not give a diffraction pattern, will induce the deposition of other organic matter which will then produce cross gratings responsible for the "inner rings" observed.

Summarizing we conclude that the so-called fractional orders, as observed in the diffraction of fast electrons, are due to adsorbed layers of organic substances forming thin crystalline layers and random orientated cross gratings.

K. LARK-HOROVITZ
H. J. YEARIAN
J. D. HOWE

Physical Laboratory,
Purdue University,
June 1, 1935.

[1] Grateful acknowledgment is made to the American Philosophical Society for a grant-in-aid of this research. K.L-H.

[2] K. Lark-Horovitz and H. J. Yearian, Phys. Rev. **43**, 376 (1933).

[3] L. H. Germer, Zeits. f. Physik **54**, 408 (1929); E. Rupp, Ann. d. Physik **5**, 453 (1930).

[4] This interpretation, however, is difficult to understand because of the strong intensity of the fractional orders.

[5] E. Rupp, Ann. d. Physik **10**, 933 (1931).

[6] K. Lark-Horovitz, H. J. Yearian and E. M. Purcell, Phys. Rev. **45**, 123 (1934); J. D. Howe and E. M. Purcell, Phys. Rev. **47**, 329 (1935).

[7] The experiments with Au, Ag, Cu, Cu_2O, Cd, Ni deposited on naphthalene and interpreted as above have been reported at the Pittsburgh meeting of the Am. Phys. Soc.

[8] M. Laue, Zeits. f. Krist. **82**, 127 (1932).

[9] A. Steinheil, Zeits. f. Physik **89**, 50 (1934).

Gamma-Rays from Boron Bombarded with Protons

We have found a rather weak gamma-radiation emitted when boron is bombarded with protons, and have investigated the spectrum, by measuring the energy of recoil electrons in a cloud chamber. The intensity is certainly not more than 1/10 that obtained from boron bombarded with deuterons under the same conditions, and probably is not far from the upper limit of 1/50 placed upon it by our earlier investigations with an ionization chamber.[1] McMillan[2] has reported radiation from proton bombardment, but no comparison with the deuteron effect can be made from the data he has given.

Fig. 1 shows the energy spectrum of negative secondary electrons obtained from 3000 cloud chamber photographs taken at 900 kv bombarding voltage, 100 microamperes ~~deuteron~~ current and 1500 gauss magnetic field. The glass wall of the chamber was the source of the secondary electrons. The upper curve includes all measurable negative electron tracks, and the lower contains only those which were ejected with an initial angle of less than $7\frac{1}{2}$ degrees with the direction of the incident gamma-radiation. The curves, when corrected according to the theory of Compton collisions, indicate gamma-ray lines at 2.5, 4.2, 5.7, 7.5, 9.8, and 13 (?) MEV. A few high energy pairs were obtained, which are plotted at the bottom of the figure, according to their total energy, which includes the energy equivalent of the rest masses of the two electrons. Each dot represents a pair. The extreme upper limit of the gamma-ray spectrum is probably best given by the pairs, since the probability of pair production increases rapidly with energy, while the number of recoil electrons decreases. The upper limit indicated by the pairs is clearly about 14.5 MEV.

The only reaction involving boron and protons which can release sufficient energy to make possible the emission of the observed 14.5 MEV gamma-ray appears to be

$$B^{11}+H^{1}\rightarrow C^{12}. \qquad (1)$$

From Bethe's[3] values for the masses of the atoms involved, or, by using the value 13 MEV for the energy released in the reaction

$$B^{11}+H^{2}\rightarrow C^{12}+n^{1} \qquad (2)$$

observed by Bonner and Brubaker,[4] and by assuming that the energy contributed by the bombarding proton is approximately 0.9 MEV, we obtain about 15 MEV for the excess energy in reaction (1). This fits well within the accuracy of the experiment, and constitutes perhaps the most unambiguous evidence we have for the simple capture of a proton with the emission of the excess energy entirely as gamma-radiation. This naturally implies that the C^{12} nucleus is capable of existing in an excited state corresponding to 14.5 MEV and of making one or more radiative transitions from this to the normal state, in spite of the fact that the energy it contains is more than sufficient to cause it to split up into three rather energetic alpha-particles; that is, alpha-particles having enough energy to clear easily their mutual potential barrier. This seems to invalidate the argument advanced by Bethe[5] for the maximum value of the mass of C^{12}, namely, that the excitation energy cannot exceed the binding energy of one of the alpha-particles with respect to the other two by more than about 0.7 MEV. The observation of several such high energy gamma-rays from light nuclei has led us to postulate, as suggested in the accompanying letter,[5] that the excitation need not be due entirely to the mutual arrangement or motion of the three alpha-particles, but may consist, at least in part, of excitation within one or more of the alpha-particles themselves, and that this internal alpha-particle energy is not strongly coupled—that is to say, not easily transferred—to the three-alpha-particle system.

The possibility that some of the lower energy lines may arise from the reaction

$$B^{11}+H^{1}\rightarrow 3He^{4}, \qquad (3)$$

in which the energy release is about 11 MEV,[6] cannot with certainty be ruled out. The alternative way of accounting for the lower lines is by postulating that the majority of the excited C^{12} nuclei make the transition from the 14.5 MEV level to the ground level by way of intermediate levels. We have not measured quantitatively the excitation curve for the radiation, but the intensity seems to rise considerably more steeply with voltage than is to be expected from the Gamow penetration of the proton alone: it was not possible to obtain appreciable intensity, even of the lower energy lines, at 700 kv. This seems to indicate that all of the radiation is the result of the capture process, although if a very large portion of the energy in reaction (3) were used up in excitation, the three alpha-particles might have a low probability of coming apart through their mutual barrier, and the gamma-rays from this process would in that case also exhibit a high sensitivity to bombarding voltage. The capture of a proton by B^{10} to form the radioactive isotope C^{11} could release as much as 9 MEV, but from the known rate of formation[7] of C^{11} we can be sure that the gamma-rays would be too feeble to account for any of the observed lines. It is reasonable to assume that in reaction (1) the proton is captured only when its kinetic energy is such as to make the total energy of the resulting system correspond just to that of the excited C^{12}; the voltage excitation curve should there-

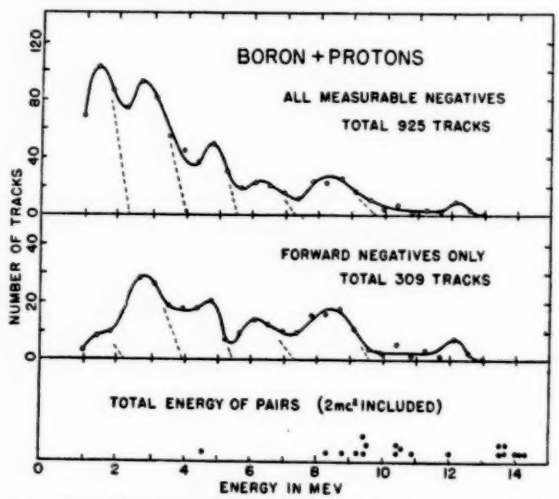

FIG. 1. Recoil electrons and pairs produced by the gamma-radiation from boron bombarded with protons.

fore exhibit a rather sharp maximum, and from the results of our experiments one can estimate that if such a sharp maximum exists it must lie in the neighborhood of the voltage used, namely 0.9 MEV.

H. R. Crane
L. A. Delasso
W. A. Fowler
C. C. Lauritsen

California Institute of Technology,
Kellogg Radiation Laboratory,
June 14, 1935.

[1] Lauritsen and Crane, Phys. Rev. **45**, 493 (1934).
[2] McMillan, Phys. Rev. **46**, 868 (1934).
[3] Bethe, Phys. Rev. **47**, 633 (1935).
[4] Bonner and Brubaker, Unpublished.
[5] Crane, Delsasso, Fowler and Lauritsen, Phys. Rev. **48**, 100 (1935).
[6] Cockroft, Int. Conf. Phys., London, 1934.
[7] Lauritsen and Crane, Phys. Rev. **45**, 493 (1934); Cockroft, Int. Conf. Phys., London, 1934. Estimates of the efficiency of this process vary among experimenters, possibly because it is a capture process, and is therefore sensitive to bombarding voltage. Our most recent estimate is that, under our experimental conditions at 900 kv, from 100 to 500 C^{11} atoms are formed per second per microampere proton current.

A Note on the Spectra of Jupiter and Saturn

In addition to the many rotation-vibration bands of methane, the spectra of Jupiter and Saturn contain also the harmonic rotation-vibration bands of ammonia at 7920A and 6474A. First photographed in the planetary spectrum by V. M. Slipher,[1] they have since been traced to the ammonia molecule by R. Wildt,[2] and by T. Dunham, Jr.[3]

It is the purpose of this note to show that the bands are of the parallel type; namely, the fourth and fifth harmonics of the fundamental ν_1 at 3337 cm^{-1}.

Employing equivalent path lengths of ammonia up to 315 meter-atmospheres, the bands at 7920A and 6474A were photographed, as was also a band at 5520A.[4] These three bands possess identical structures, indicating that they are harmonics of the same fundamental vibration. In fact, the parallel fundamental at 3337 cm^{-1} and the above bands are connected by the formula:

$$\nu_N = 3389.N - 50.N^2 - 2.N^3,$$

where N is the order of the harmonic.[5]

The structure of the fourth, fifth and sixth harmonics is clearly represented by the photograph and intensity trace shown in Fig. 1.[6] The harmonic bands of ν_1 should each consist of two nearly superimposed bands; that is, the band lines should be double in virtue of the ability of the nitrogen atom to pass through the plane of the hydrogens on its way from one position of equilibrium to the other. Dennison and Uhlenbeck[7] have shown the manner in which the doubling depends upon the amplitude of the nitrogen atom in the case of the harmonic vibrations of ν_2, the second parallel fundamental of ammonia. By applying this analysis to the harmonics of ν_1, a zeroth approximation to the doubling of the state $N\nu_1$ can be obtained. In the vibration ν_1 as opposed to the vibration ν_2 there is considerable motion of the hydrogens in their own plane. This motion renders it more difficult for the nitrogen atom to penetrate the hydrogen plane and thus decreases the doubling of the levels $N\nu_1$ below what it would be for a similar amplitude of oscillation of the nitrogen atom in the motion $N'\nu_2$. A somewhat better approximation can therefore be achieved by reducing the zeroth approximation to one-half or one-third its value. For example, the band $5\nu_1$ should exhibit a doubling in the neighborhood of 15 cm^{-1}. Several such line pairs have been located, but complete ordering of the lines has not yet been accomplished.

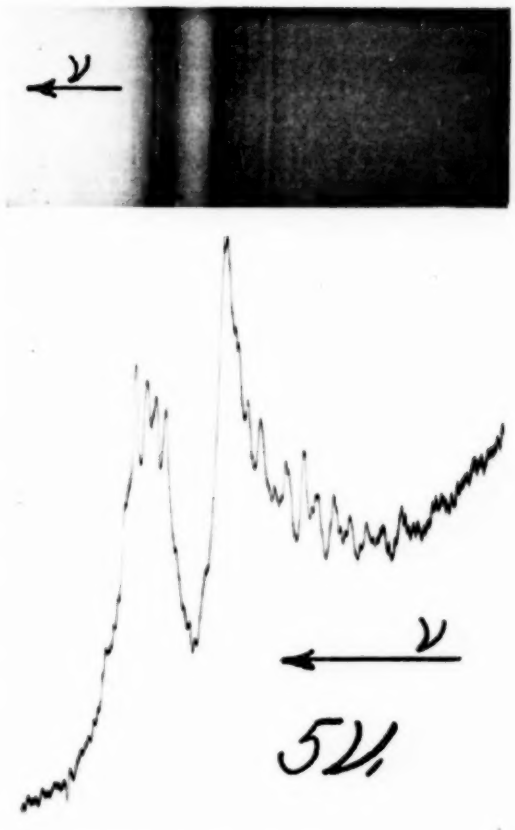

Fig. 1.

Arthur Adel

Lowell Observatory and
University of Michigan,
June 18, 1935.

[1] Slipher, Lowell Observatory Bulletin 42; Popular Astronomy, **37**, 140 (1929).
[2] Wildt, Ver. der Univ. Sternw. zu Gött. Heft 22 (1932).
[3] Dunham, P. A. S. P. **45**, 42 (1933).
[4] For a description of the apparatus see A. Adel and V. M. Slipher, Phys. Rev. **46**, 902 (1934). Eastman P, B and G plates were used.
[5] In the mode of vibration ν_1 the hydrogen nuclei move along median lines of the basal triangle while the nitrogen atom moves along a perpendicular to the plane of the hydrogens. See D. M. Dennison and J. D. Hardy, Phys. Rev. **39**, 938 (1932).
[6] In the present experiment, this band was photographed with a glass Hilger E-I. With higher resolving power, each line seen in the figure splits into several fine ones. See R. M. Badger, Phys. Rev. **35**, 1038 (1930). It appears very likely that this hyperfine structure is caused by the failure to superimpose of the lines:

$$\begin{matrix} J \to J' \\ K \to K' \end{matrix} \Big) K = 0,\ 1,\ \cdots J \qquad J < J',$$

in virtue of the differing values of $(1/A - 1/C)$ in the ground and excited vibrational states. A and C are, of course, the moments of inertia of the ammonia molecule.
[7] D. M. Dennison and G. E. Uhlenbeck, Phys. Rev. **41**, 313 (1932).

Mass Ratio of the Lithium Isotopes

The mass ratio of the isotopes of Li as determined from measurements of the $^1\Pi \rightarrow {}^1\Sigma$ blue-green band system by Jenkins and McKellar[1, 2] stands in definite disagreement with the mass ratio determined by Costa[3] and by Bainbridge,[4] who used the mass spectrograph, and also with the ratio recently obtained by Oliphant, Kempton and Rutherford,[5] who used the data from certain nuclear transformations. The last three determinations are in excellent agreement as shown in Table I.

The red system of Li_2 is a $^1\Sigma \rightarrow {}^1\Sigma$ transition,[6] has no Q branches, and fewer superpositions of lines than the blue-green system. In the $(v',0)$ progression especially these red bands offer an excellent opportunity for the determination of the mass ratio. We have photographed this system in absorption, in the first order of a 21-foot, 30,000-lines-per-inch grating for the purpose of examining the discrepancy in the band-spectrum value of the mass ratio. This seemed worth doing in view of the fact that no such discrepancy has been discovered in the case of other diatomic molecules except the hydrides ($H^2 : H^1$). For the hydrides there is, however, at least qualitative theoretical justification[7] for the difference in the mass ratio obtained from band spectra and mass spectrograph.

In the analysis of the Li_2 bands the procedure was as follows. The first ten or twelve lines in the P and R branches of each Li^7Li^7 and Li^6Li^7 band in the progression 0,0 to 5,0 were measured against second order iron lines. From the wave numbers of these lines Δ_2F's were obtained for the upper and lower states, and the rotational constants, (B_v), calculated from the equation

$$\Delta_2F/4(K+\tfrac{1}{2}) = B_v + 2D(K+\tfrac{1}{2})^2, \qquad (1)$$

where the term in $(K+\frac{1}{2})^2$ was treated as a small correction term to be subtracted from the left side. D'' and D'''^i were taken from McKellar, and D' and D'^i were evaluated from measurements to high quantum numbers in the (3,0) Li^7Li^7 and Li^6Li^7 bands. D' and D'^i were taken to be the same in all bands of each type of molecule, a perfectly safe assumption since even a ten percent change in D is just barely appreciable in its effect on a B calculated by Eq. (1) when lines of $K<13$ are used. Finally, the B_v'''s and α_v'''s were obtained by least-squares solution of $B_v' = B_v - \alpha_v'(v+\frac{1}{2})$, and the B_v''''s by adding $\alpha_v''/2$ and $\alpha_v'''^i/2$ from McKellar to our B_0'' and $B_0'''^i$. The results are listed in Table I, together with the values of the mass coefficient $\rho(=(\mu'/\mu'^i)^{\frac{1}{2}})$ calculated therefrom.

Next, the band origins, ν_0, were computed from the equation,

$$\nu = \nu_0 + (B'+B'')M + (B'-B'')M^2 + 2(D'+D'')M^3, \qquad (2)$$

where $M=-K''$ for P lines and $M=(K''+1)$ for R lines. Observed frequencies of good lines (10 to 15 for each band except the Li^6Li^7 (0,0) which had only four unobscured) were substituted for ν, the average B_0'', and B_v'''s, smoothed by the equation $B_v' = B_e' - \alpha_e'(v+\frac{1}{2})$, were substituted for B' and B'', and the corresponding ν_0's computed. The average ν_0 for each band is given in Table I, together with an estimate of the probable error. As before the term involving the D's is small, amounting to about 0.04 cm^{-1} at $K=10$.

From the series of band origins, first, second and third differences were formed and, from the small, erratic third differences $(=6y_e'\omega_e')$, $y_e'\omega_e'$ was calculated for the Li^7Li^7 and Li^6Li^7 series. In the equation

$$\nu_0(v,0) = \nu_e + [\omega_e'(v'+\tfrac{1}{2}) - \omega_e''/2] - [x_e'\omega_e'(v'+\tfrac{1}{2})^2 - x_e''\omega_e''/4] + y_e'\omega_e'(v'+\tfrac{1}{2})^3 \qquad (3)$$

$y_e'\omega_e'(v'+\frac{1}{2})^3$ was calculated using the values of $y_e'\omega_e'$ obtained as described above, $\omega_e''/2$ and $x_e''\omega_e''$ were obtained from McKellar's work[3] and ν_e, ω_e', and $x_e'\omega_e'$ then calculated by least squares for the Li^7Li^7 and Li^6Li^7

TABLE I.

Band	B_0''	$B_0'''^i$	B_v'	$B_v'^i$	$\nu_0(v,0)$	$\nu_0^i(v,0)$	$\nu_0^i - \nu_0$	$\rho - 1$
0,0	0.6690	——	0.4949	0.5360	14,020.616 ±0.02	14,018.602 ±0.06	2.014 ±0.07	0.0425 ±0.0014
1,0	.6696	0.7252	.4898	.5305	14,272.950 ±.02	14,281.113 ±.02	8.161 ±.03	.04049 ±.00015
2,0	.6691	.7248	.4837	.5232	14,522.107 ±.02	14,540.160 ±.02	18.053 ±.03	.04064 ±.00007
3,0	(.6681)[8]	.7248	(.4767)[8]	.5179	14,768.148 ±.02	14,795.822 ±.02	27.674 ±.03	.04067 ±.00004
4,0	.6692	.7240	.4744	.5113	15,011.073 ±.02	15,048.180 ±.02	37.107 ±.03	.04075 ±.00003
5,0	.6693	.7248	.4687	.5050	15,250.906 ±.02	15,297.170 ±.02	46.264 ±.03	.04078 ±.00003
	Av. .6693 ±.0001	Av. .7248 ±.0002	$B_e' = .4974$ ±.0003	$B_e'^i = .5393$ ±.0003	$\nu_e = 14,068.295$ ±.03	$\nu_e^i = 14,068.337$ ±.03	Using shift in 4,0 and 5,0:	
	$B_e'' = .67285$ ±.0001	$B_e'''^i = .72895$ ±.0002	$\alpha_e' = .00519$ ±.0002	$\alpha_e'^i = .00623$ ±.0002	$\omega_e' = 255.523$ ±.004	$\omega_e'^i = 265.931$ ±.008	$\rho = 1.04077$ ±.00003	
					$x_e'\omega_e' = 1.603$ ±.005	$x_e'^i\omega_e'^i = 1.733$ ±.01		
					$y_e'\omega_e' = .0047$	$y_e'^i\omega_e'^i = .0053$	Best value (average of above and $\omega_e'^i/\omega_e'$):	
	$\rho = (B_e'''^i/B_e'')^{\frac{1}{2}} = 1.04080$ ±.0003		$\rho = (B_e'^i/B_e')^{\frac{1}{2}} = 1.0413$ ±.0005		$\rho = \omega_e'^i/\omega_e' = 1.04073$ ±.00004		$\rho = 1.04075$ ±.00004	
			$\rho = (\alpha_e'^i/\alpha_e')^{\frac{1}{2}} = 1.060$ ±.03		$\rho = (x_e'^i\omega_e'^i/x_e'\omega_e')^{\frac{1}{2}} = 1.040$ ±.01		Bainbridge: 1.04074 ±.00003	
							Oliphant, Kempton, and Rutherford: 1.040758 ±.000012	
							Costa: 1.04075 ±.0001	

molecules. The constants and the corresponding values of ρ are given in Table I.

The calculated electronic isotope shift ($\nu_e^i - \nu_e = 0.042$ cm^{-1}) is about equal to the probable error in its determination. If we assume it to be exactly zero, we can calculate $(\rho-1)$ from the equation for the vibrational isotope effect,

$$\nu_0^i - \nu_0 = (\rho-1)\{[\omega_e'(v'+\tfrac{1}{2}) - \omega_e''(v''+\tfrac{1}{2})] - (\rho+1)[x_e'\omega_e'(v'+\tfrac{1}{2})^2 - x_e''\omega_e''(v''+\tfrac{1}{2})^2] + (\rho^2+\rho+1)[y_e'\omega_e'(v'+\tfrac{1}{2})^3 - y_e''\omega_e''(v''+\tfrac{1}{2})^3]\}. \quad (4)$$

$(\rho-1)$ calculated from this equation is relatively insensitive to small errors in ω_e and $x_e\omega_e$ or large errors in $y_e\omega_e$; its uncertainty arises largely from errors in determining the *difference* between origins and $(\rho-1)$ should be very accurate for the bands with the largest shift. The errors stated assume zero electronic shift; the uncertainty in this quantity would approximately double the probable error. The small terms involving $x_e\omega_e$ and $y_e\omega_e$ in Eq. (4) are adequately taken care of in the calculation by assuming an approximately correct ρ in their coefficients. The values of $(\rho-1)$ obtained are given in Table I. The trend in these values indicates that there is a small electronic isotope shift of sign opposite to that of the shift calculated by the use of Eq. (3); but in either case the magnitude of the shift is about the same as, or less than its probable error.

In Table I we have given as our best value of ρ the mean of the two most accurate values obtained from the isotope vibrational shift averaged with the value obtained from ω_e^i/ω_e. It is in good agreement with the value of ρ obtained by other methods. The other, less accurate, determinations differ from the best value, with minor exceptions, by less than the probable errors. The molecular constants have been determined with much greater precision than by Wurm.

Since these results have to do largely with the constants of the upper $^1\Sigma$ state of Li_2 they do not conflict directly with the results of McKellar and Jenkins (who used the $^1\Pi \rightarrow {}^1\Sigma$ bands) except in the ratio $(B_e''^i/B_e'')^{\frac{1}{2}}$ for which they secured 1.0422 ± 0.0006. It would be desirable to measure a v'' progression to secure a direct check on the vibrational constants of the lower state, common to the two band systems.

G. M. Almy
G. R. Irwin

Physics Department,
University of Illinois,
Urbana, Illinois,
June 18, 1935.

[1] F. A. Jenkins and A. McKellar, Phys. Rev. **44**, 325 (1933).
[2] A. McKellar, Phys. Rev. **43**, 215 (1933).
[3] J. L. Costa, Ann. de physique **4**, 425 (1925).
[4] K. T. Bainbridge, Phys. Rev. **44**, 56 (1933).
[5] M. L. E. Oliphant, A. E. Kempton and Lord Rutherford, Proc. Roy. Soc. **149**, 406 (1935).
[6] K. Wurm, Zeits. f. Physik **59**, 35 (1929).
[7] R. de L. Kronig, Physica **1**, 617 (1934).
[8] In the (3,0) bands there is nearly exact coincidence of P and R branch lines for low K. The Δ_2F's were thereby distorted in the Li^7Li^7 band, and yielded low values of B' and B'', which were excluded in the calculation of B_0'' (average) and B_e'.

The Ultraviolet Absorption Spectrum of Hydrogen Fluoride

It was suggested by Professor Mulliken that an investigation of the ultraviolet absorption spectrum of hydrogen fluoride might be of interest since there were reasons[1] to suspect that there should be discrete band absorption by diatomic HF somewhere in this region. By using the hydrogen continuous spectrum as a source, absorption spectra were obtained with the hydrogen fluoride at pressures of from 2 to 76 cm of mercury. Absorbing path lengths of 15 and 30 cm were used. Two band systems were found. One system extends from 3200A to 2400A with a maximum of absorption at approximately 2800A. The second system extends from about 2300A to shorter wavelengths beyond the range of the grating spectrograph in air. The absorption in this system shows no diminution in intensity to wavelengths as short as 1950A.

The structure of both band systems indicates that, contrary to the original expectation, the absorbing molecule is a polymer of hydrogen fluoride. With the dispersion used, 14A per mm, no rotational structure was resolved. The bands are typically polyatomic, having regions of some regularity followed by regions of considerable complexity, due probably to overlapping of bands with various vibrational quantum number assignments. A prominent frequency appearing in the longer wavelength system is 244 cm^{-1} and in the shorter wavelength system 376 cm^{-1}. It is planned to attempt a vibrational analysis of the bands in the near future.

The work of Simons[2] on the molecular weight of gaseous hydrogen fluoride as a function of the temperature and pressure tends to indicate that the polymer present is $(HF)_6$, that the polymerization is nearly complete at room temperatures, but that at 100°C the polymer is almost entirely dissociated. In harmony with the theory that the two band systems belong to the polymer, the absorption by the gas is found to be very decidedly weaker at 100°C than at room temperature, although perhaps not so much so as one would have expected from Simons' report.

To obtain windows for the absorption tubes capable of transmitting ultraviolet light but of a material not attacked by gaseous hydrogen fluoride is a problem of great difficulty. The problem was partially solved by using windows of fluorite, which may or may not remain transparent after contact with the gas for several minutes. The necessary rapid exposures were made possible by use of the high intensity hydrogen tube source developed by Stevens.[3] It was found in the course of the work that this source could be greatly improved by constructing the enclosing jacket of metal instead of glass.

Kohei Siga*
Harold J. Plumley

Ryerson Laboratory,
University of Chicago,
June 10, 1935.

[1] Cf. the roughly estimated U(r) curves for HF given by L. Pauling, J. Am. Chem. Soc. **54**, 998 (1932).
[2] J. H. Simons, Chem. Rev. **8**, 213 (1931).
[3] D. S. Stevens, Rev. Sci. Inst. **6**, 40 (1935).
* Following the untimely death of Mr. Siga, the work has been taken over by the second author.

The Carbon Reactions and the Corrected Mass-Scale

A crucial feature of Professor Bethe's correction of the helium-oxygen ratio from disintegration data,[1] by which he derives a new set of mass values for the lighter elements which eliminates many of the disturbing inconsistencies hitherto encountered in disintegration reactions, is his assumption that the mass difference between C^{13} and C^{12} is directly measured by the 14- to 18-cm protons emitted in the reaction $C^{12}+H^2 \rightarrow C^{13}+H^1$, without including the energy of the observed 3 MEV gamma-rays. This assumption was quite in keeping with all available data, including a special series of observations made here in which the expected 40-cm proton group, if present at all, was shown to be less than 1/1500 of the intensity of the main group. The carbon isotopes are connected by the alternative mode of disintegration under deuteron bombardment:

$$C^{12}+H^2 \rightarrow N^{13}+n^1;\ N^{13} \rightarrow C^{13}+e^+$$

for which the maximum positron energy is known to be in the vicinity of 1.4 MEV, and it was immediately evident that even a crude determination of the maximum energy of the emitted neutrons would distinguish between the alternative 3 MEV and 6 MEV reaction-energies. To eliminate the possibility that the proton and neutron reactions are both accompanied by gamma-rays and to provide a further check on Professor Bethe's assumption, in that no quanta corresponding to a reaction-energy exceeding that of the proton reaction should be present, observations on the gamma-ray energies using a cloud chamber in a magnetic field were also necessary or desirable.

Since the sum of the mass of one positron and one negatron plus the observed maximum energy of the positrons emitted by N^{13} plus the new mass-difference between proton and neutron equals or exceeds the energy observed in the proton reaction, the neutrons emitted in the alternative reaction should have a maximum energy equal to or less than that contributed by the bombarding deuterons, provided the gamma-rays accompany a shorter range proton group as Professor Bethe has suggested. We already knew that the carbon neutrons gave recoil deflections which were large compared to those of high speed protons as observed with a linear amplifier, and we expected our calibrations to show the maximum neutron energy to be well above that of the bombarding beam, but calibrations and further observations made just after the recent Physical Society meeting gave the data of Fig. 1, showing that the maximum energy of the carbon neutrons is about 0.25 MEV greater than the energy of the bombarding deuterons, in rough agreement with Professor Bethe's assumption. In the absence of a convenient camera, the observations here given were made visually with a cathode-ray oscillograph. The linear amplifier calibrations, with polonium alpha-particles and recoil protons (Po), made immediately before and after the neutron observations, show that a deflection of 5 mm corresponds to approximately 0.202 MEV[2] (5770 ion pairs). Taking 7.6 mm from Fig. 1 as the deflection corresponding to the head-on collision of a carbon neutron of maximum energy with a nitrogen nucleus (air was used in the 4-mm ionization chamber), the energy of the latter is 0.31 MEV, and by comparison with Chadwick the maximum neutron energy is 1.20 MEV at a deuteron energy of 950 kv. It is difficult to estimate the accuracy of this determination of the carbon neutron energy, but it would appear to be within 0.2 MEV. Immediate visual comparison with the neutrons from beryllium (also bombarded by deuterons) showed that the recoils due to the latter were obviously of higher energy, were distributed over a much wider energy range and presented a much less definite upper limit.

Additional evidence for a low energy for the C+D neutrons is given by experiments which showed them to be

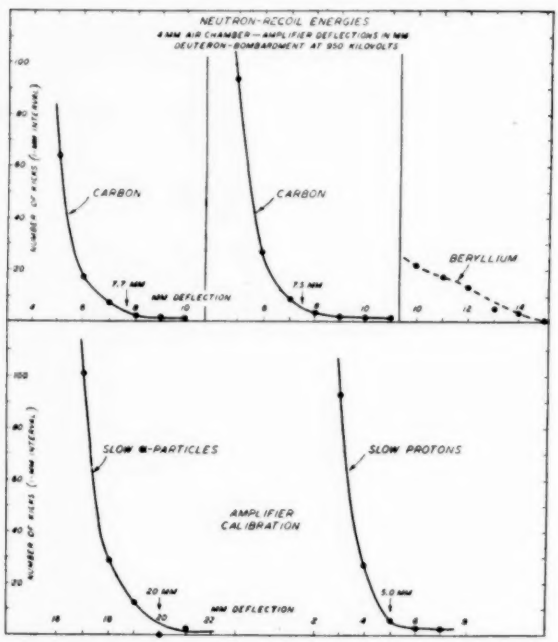

FIG. 1. Determination of maximum energy of neutrons from carbon bombarded by deuterons.

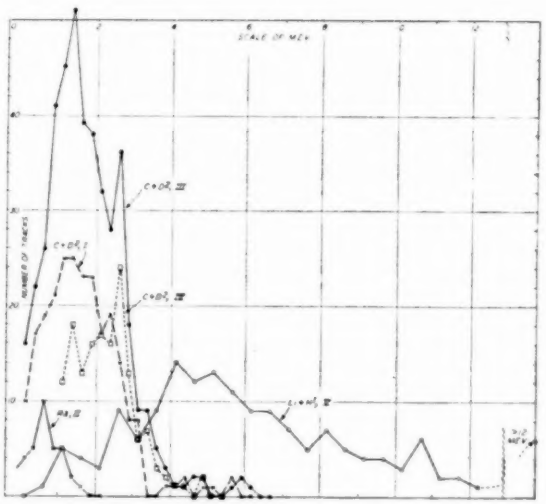

FIG. 2. Energies of gamma-ray electrons, cloud chamber 850 gauss.

five times as effective as Be+D neutrons in the production of Fermi radioactivity.

A further check on the energy of the carbon neutrons was obtained by a cloud chamber comparison of the neutron recoils due to the carbon reaction and those due to the bombardment of deuterons by deuterons. A total of thirty-seven recoil protons due to the latter averaged 47.9 mm in reduced range, whereas forty-eight recoil protons due to the carbon neutrons averaged only 12.6 mm in reduced range. The energy of the neutrons from the deuteron reaction has been given as about 2 MEV by the Cambridge investigators. These cloud chamber measurements do not give a good determination of the energy of the carbon neutrons because of the probable inclusion of several unrecognized forks due to neutron-disintegrations. Although the observed energy of the carbon neutrons is somewhat higher than would be expected on the basis of the new mass values, it clearly contradicts the neutron energy of 4 to 5 MEV predicted by the old mass values, which required the 3 (4) MEV gamma-rays to accompany the 14- to 18-cm protons.

Measurements on the gamma-rays emitted by carbon under deuteron bombardment at 950 kv, using a cloud chamber in a magnetic field of 850 gauss, are shown in Fig. 2. Preliminary observations having indicated a preponderance of low-energy electrons, the first measurements were made with a 7/8-inch lead filter between the target and the chamber, giving the data of curve I. To insure against error, a few observations were made with 1 mg of radium approximately in the position of the target, yielding curve II. These observations indicated the maximum gamma-ray energy from carbon to be about 3.5 MEV (3.7 MEV if arbitrarily corrected for Compton recoil), and since this quantum-energy is near the minimum of the absorption coefficient curve, higher as well as lower energies are discriminated against and it consequently seemed desirable to make observations with less absorption. The data of curve III, taken with a 1/8-inch lead filter, indicate a maximum quantum energy of about 4 MEV (or even slightly more if corrected for Compton recoil), and this indication is sustained when the measurements are restricted to "forward" negative tracks, plotted as curve IV. No tracks were measured which had uniformly curved length of less than 10 cm, most of them being well above this length, and no attempt was made to measure the few doubtfully straight tracks above 7 MEV. Very few positrons were identifiable in the carbon observations, in contrast to the brief series of photographs made with protons bombarding lithium, data of curve V, which showed forward electrons of both signs up to very high energies. Using the new mass values, there is no possibility that such a high energy gamma-ray could arise in any reaction involving the formation of N^{13}, and consequently it must accompany a short range proton group as postulated by Professor Bethe. However, the indicated maximum energy of the gamma-ray equals or even exceeds the total energy observed in the known proton reaction (3.6 MEV, including recoil, at 0.95 MEV deuteron energy), and consequently the protons which accompany the gamma-rays must have an energy near zero. If this is the case, they should have great difficulty in penetrating the carbon barrier outward, and the gamma-ray process should be very infrequent compared to the 14- to 18-cm protons. This is not the case according to our measurements, the proton yield being about 3 per 10^6 at 950 kv, and by numerous experiments, including a direct cloud chamber comparison of the high energy electrons from 1 mg of radium with those from carbon, we find that the gamma-ray yield can hardly be under 1 per 10^6 incident deuterons. Thus until some way is found to account for the large intensity of these hard gamma-rays the carbon reactions cannot be considered to be in a satisfactory state, even with the new mass values. The old mass values seem to be completely excluded, however, even by these carbon observations alone, unless the proton and neutron reactions both lead to excited states.

We are grateful to Professor Bethe for taking an active interest in these measurements.

M. A. Tuve
L. R. Hafstad

Department of Terrestrial Magnetism,
Carnegie Institution of Washington,
Washington, D. C.,
June 3, 1935.

[1] H. Bethe, Phys. Rev. **47**, 633 (1935).
[2] H. Schulze, Zeits. f. Physik **94**, 104 (1935).

Higher Order Derivatives in the Interaction "Ansatz" of the Fermi Theory[1]

Since there are theoretical arguments[2] for introducing higher order derivatives in the interaction of the heavy particle with the electron-neutrino field, we have investigated the effect of such a change on the form of the continuous electron or positron spectra. We shall consider only the light nuclei so that the influence of the nuclear charge Z may be neglected; furthermore we shall take the neutrino mass μ equal to zero.

The polar four-vector which is needed to make up the interaction energy may be formed with the help of the gradient vector $\partial/\partial x_i$ and the quantities γ_i, M_{ij} and k_{ijk}.[3] The possibilities with the gradient alone, for example, are:

$$(m+1,\ m)_i=\frac{\partial}{\partial x_i}\cdot\frac{\partial^m\psi\dagger}{\partial x_\alpha\cdots\partial x_\beta}\cdot\frac{\partial^m\varphi}{\partial x_\alpha\cdots\partial x_\beta}, \tag{1}$$

$$(m,\ m+1)_i=\frac{\partial^m\psi\dagger}{\partial x_\alpha\cdots\partial x_\beta}\cdot\frac{\partial}{\partial x_i}\cdot\frac{\partial^m\varphi}{\partial x_\alpha\cdots\partial x_\beta}. \tag{2}$$

The order of the derivatives of $\psi\dagger$ and φ must differ by unity only, because otherwise factors like $\partial^2\psi\dagger/\partial x_\alpha\partial x_\alpha$ or $\partial^2\varphi/\partial x_\alpha\partial x_\alpha$ would occur. From the second order Dirac wave equations for the electron and neutrino, which, with $Z=0$ and $\mu=0$ are

$$\partial^2\psi\dagger/\partial x_\alpha\partial x_\alpha+\psi\dagger=0,\quad \partial^2\varphi/\partial x_\alpha\partial x_\alpha=0,$$

such factors would cause the vector to vanish or to reduce to one of the forms (1) or (2). Making use also of the first order Dirac equations

$$(\partial\psi\dagger/\partial x_\alpha)\cdot\gamma_\alpha+\psi\dagger=0,\quad \gamma_\alpha(\partial\varphi/\partial x_\alpha)=0,$$

one can reduce all the other four-vectors, involving γ_i, M_{ij} and k_{ijk}, to three types and their linear combinations.[4] These three types are (1), (2) and

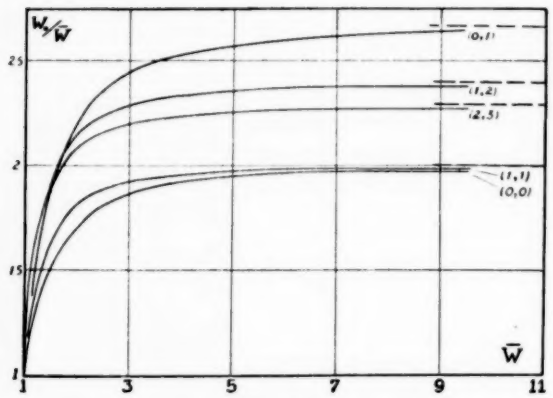

FIG. 1.

$$(m,\ m)_i=\frac{\partial^m\psi\dagger}{\partial x_\alpha\cdots\partial x_\beta}\cdot\gamma_i\cdot\frac{\partial^m\varphi}{\partial x_\alpha\cdots\partial x_\beta}. \qquad (3)$$

Four-vectors of the type (1) can be immediately excluded. Since the order of the derivative of the electron wave function is higher than that of the neutrino wave function, these vectors would lead to energy distributions which give greater weight to high electron energies than the original Fermi theory. This, as we have seen in I, §2, is in conflict with the experimental facts. The energy distribution resulting from the four-vectors (2) and (3) for different values of m are:

(0,0): $P\sim W(W^2-1)^{1/2}(W_0-W)^2$,
(0,1): $P\sim W(W^2-1)^{1/2}(W_0-W)^4$,
(1,1): $P\sim W(W^2-1)^{1/2}(4W^2-1)(W_0-W)^4$,
(1,2): $P\sim W(W^2-1)^{1/2}(4W^2-1)(W_0-W)^6$,
(2,2): $P\sim W(W^2-1)^{1/2}[(4W^2-1)^2-4W^2](W_0-W)^6$,
(2,3): $P\sim W(W^2-1)^{1/2}[(4W^2-1)^2-4W^2](W_0-W)^8$.

(0,0) is the original Fermi distribution for $Z=0$, which is just the statistical factor; (0,1) is the distribution proposed in I, §4. In these equations W is the *total* energy of the electron measured in units.

Although, in order to make a definite decision, a direct comparison of the above formulae with the experimental distributions should be made, an indication can be obtained by considering the relation between the average energy $\overline{W}$ and the maximum energy W_0. In Fig. 1 we have plotted $W_0/\overline{W}$ as a function of $\overline{W}$ for the different formulae. $\overline{W}$ is chosen as abscissa since it can be determined experimentally much more accurately than W_0. The curves corresponding to interactions of the type (3) all approach an asymptote at $W_0/\overline{W}=2$. The type (2) curves also have horizontal asymptotes but these vary with m and are given by $W_0/\overline{W}=(4m+8)/(2m+3)$.

From the empirical material now available it seems that one can already exclude interactions of the type (3). They lead to distributions which have about the same degree of asymmetry as the simple statistical factor (0,0) and are therefore just as unsatisfactory (see I, §2). The recent results of Crane, Delsasso, Fowler and Lauritsen[5] on the high energy β-ray spectra of B^{12}, Li^8 and F^{20} may allow a decision on the value of m in the interactions of type (2). The average energies of these spectra are respectively $\overline{W}=9.0$, 8.6, 4.8 in our units; the upper energies are about $W_0=23$, 22, 11.5. If the average energies can be regarded as correct within a few percent then, by finding a lower limit to W_0, one can set a lower limit to $W_0/\overline{W}$. All the interactions whose asymptotes are below this value can then be eliminated. For example, in the case of Li, if $W_0\geqq 20$, $\overline{W}=8.6\pm 0.1$, then $W_0/\overline{W}\geqq 2.3$ so that already the (2,3) interaction is excluded. The distribution curve given by (2,3) is also quite unlike the empirical energy distribution.

Of course, theoretically, also linear combinations of interactions of the different types or of different orders are possible. Since, however, interactions of type (3) and of type (2) for larger m give comparatively symmetrical distributions, already the study of the asymmetry of the high energy β-ray spectra will make it possible to restrict the amount with which the higher order derivatives can be present in the interaction function.

E. J. KONOPINSKI
GEORGE E. UHLENBECK

University of Michigan,
June 16, 1935.

[1] This is an extension of our paper (hereafter cited as I) in the Phys. Rev. **48**, 7 (1935) to which reference is made for further details. We continue to use the same notation, units, etc.
[2] W. Heisenberg, Zeeman Jubilee Papers, Nijhoff, The Hague, 1935, p. 108.
[3] See Pauli, *Handbuch der Physik*, Vol. 24, 1, p. 220.
[4] For an example of such a reduction see I, §4.
[5] Crane, Delsasso, Fowler and Lauritsen, Phys. Rev. **47**, 887, 971 (1935).

Concerning the Possibility of a Unified Interpretation of Electrons and Protons

The purpose of this note is to show: (a), that it is formally possible to construct irreducible equations of the Dirac type which are invariant under the extended Lorentz group and contain more than four components and, (b), that these equations suggest the examination of the feasibility of interpreting the fundamental physical particles in terms of particles of a single kind. Such an interpretation would possess certain attractive features, but in view of several difficulties (the one concerning the magnetic moment of the proton being perhaps the most important) it is at present doubtful that the procedure indicated below can be made successful. The equations in question contain one or more four-vectors, denoted below by B's, whose physical meaning, if they have any, is at present obscure. For the sake of brevity we shall not consider the general case,* but shall let an example illustrate the trend of the argument.

The Dirac equation for the electron can be written in the form

$$\{\alpha_K P_K+\beta c\}\psi=0, \qquad (1)$$

where $\alpha_0=1$, where α_1, α_2 and α_3 are square roots of unity which anticommute with each other and with β, and where

$$\beta^2=m^2, \qquad (2)$$

and

$$P_K=p_K+e/c\cdot A_K. \qquad (3)$$

Now, the relations (2) and (3), introduced essentially by classical analogy, are not strictly necessary for the Lorentz invariance of (1), and the question arises whether it is possible to convert (1) into an irreducible equation of more than four components by relinquishing (2) and (3).

The following example shows that the formal answer is in the affirmative. Let $\alpha_0=1$, let α_1, α_2 and α_3 be

$$\begin{vmatrix} \alpha_1 & 0 \\ 0 & \alpha_1 \end{vmatrix}, \quad \begin{vmatrix} \alpha_2 & 0 \\ 0 & \alpha_2 \end{vmatrix}, \quad \begin{vmatrix} \alpha_3 & 0 \\ 0 & \alpha_3 \end{vmatrix}, \tag{4}$$

respectively, let

$$\beta = \begin{vmatrix} M\alpha_m & 0 \\ 0 & m\alpha_m \end{vmatrix} \tag{5}$$

and let

$$P_K = p_K + e/c \cdot A_K + ib \begin{vmatrix} 0 & -\rho_1 \\ \rho_1 & 0 \end{vmatrix} B_K + b' \begin{vmatrix} 0 & \rho_1 \\ \rho_1 & 0 \end{vmatrix} B'_K; \tag{6}$$

the α's and ρ_1 in (4), (5) and (6) are those of Dirac; M, m, b and b' are real constants, M being unequal to m and not both b and b' being zero; B_K and B'_K are components of four-vectors. The invariance of the resulting equation under rotations in four-space can be proved in the usual manner. The invariance under a reflection of the three space-axes follows from the fact that the matrix

$$\begin{vmatrix} \alpha_m & 0 \\ 0 & -\alpha_m \end{vmatrix}$$

anticommutes with each matrix in (4) and commutes with every other operator in the equation. Further, no matrix other than a multiple of unity commutes with each matrix in (4), with (5), and with the matrix part of (6); the equation thus possesses no nontrivial constants of motion in an arbitrary field and is consequently in general irreducible. The quantities $\varphi\cdot\psi$, $-\varphi\cdot\alpha_1\psi$, $-\varphi\cdot\alpha_2\psi$ and $-\varphi\cdot\alpha_3\psi$ transform like the contravariant components of a four-vector, and the divergence of the four-vector vanishes at least when the B_K and the B'_K do not involve the p's.

Let us use the term *koniton* to denote a hypothetical particle whose behavior is described by an equation which allows for more than one value of the magnitude of the rest-mass, and regard the last two terms in (6) as small. The states of the koniton described by (1), (4), (5) and (6) can then be approximately classified into four groups: 'heavy' states (rest-mass of the koniton equal to M) of positive and of negative kinetic energy, denoted below by $+H$ and $-H$, respectively, and 'light' states (rest-mass m) of positive and of negative kinetic energy, denoted below by $+L$ and $-L$, respectively.

The following modification of Dirac's original electron-proton theory now suggests itself: We assume that the fundamental constituents of matter are konitons, that their states of negative kinetic energy are nearly all filled, and that konitons in $+L$ and $+H$ states are electrons (negatrons) and antiprotons, respectively, while holes in $-L$ and $-H$ states are positrons and protons, respectively.[1] Two long-lived types of matter are then possible:

A. *Terrene matter:* konitons of positive kinetic energy in $+L$ states, holes in $-H$ states; atoms consist of positive nuclei surrounded by electrons; free positrons and antiprotons are short-lived.

B. *Contraterrene matter:* konitons of positive kinetic energy in $+H$ states, holes in $-L$ states; atoms consist of negative nuclei surrounded by positrons; free electrons and protons are short-lived. Contraterrene matter (the formal feasibility of which is, strictly speaking, independent of the validity of the conjecture regarding the existence of konitons) may be expected actually to exist in some parts of space.**

Some of the koniton-transitions might perhaps be of interest in connection with cosmic rays: $-L\rightarrow -H$ transitions (conversions of protons into positrons with the possibility of production of very fast positrons), $+H\rightarrow +L$ transitions (conversions of antiprotons into electrons with the possibility of production of very fast electrons), the explosive transformation of matter into radiation in a collision of a terrene and a contraterrene body, etc. We must emphasize, however, that although the procedure indicated here can take care of the difference of the masses and the oppositeness of the charges of the proton and the electron, it is at present doubtful that it can be made to account for the experimental data regarding the field of a proton.

The writer is much indebted to Professor G. Breit for correspondence regarding this work and in particular for showing that certain eight-component equations considered by the writer are reducible; and to Professor E. U. Condon, Dr. A. H. Fox, Professor H. P. Robertson and Dr. F. Seitz for helpful discussion.

V. ROJANSKY

Union College,
Schenectady, New York,
May 20, 1935.

[1] The alternative identification obtained by interchanging the words *electrons* and *positrons* and also the words *protons* and *antiprotons* in this sentence, accompanied by appropriate changes in the statements below it, would lead to nearly (if not precisely) the same physical nferences.

Added June 14: *The general case of modifications of the kind illustrated below and intended primarily to raise the dimensionality of the representation is meant; the possibility of combining these with the modifications used by Pauli in his equation for the magnetic neutron has not yet been studied. **Since writing this note the writer has learned that in informal discussions various theoretical physicists have speculated upon the possibility that in some parts of space matter is composed of atoms whose nuclei are charged negatively and whose extra-nuclear constituents are positrons. However, nothing appears to have been published on the subject and, in any case, the explicit mathematical structure proposed in the present note is new.

On the Polarization of Electrons by Double Scattering

The polarization effect predicted by Mott as a consequence of Dirac's theory of the electron does not seem to be in agreement with observations. A previous attempt by Sauter to attribute this divergence to the screening of the nuclear field has not met with success.

In analyzing the theoretical and experimental situation two possibilities seem to be open, which might account for the discrepancy: (a) The production of *virtual* pairs, though not of very large influence on the scattering itself, might be of great importance as far as the polarization

(scattering asymmetry) is concerned; (b) deviation of the nuclear field from the purely Coulombian type. We want to report briefly in this letter on our calculations in reference to (b).

The main source of error in these calculations comes from the fact that the polarization effect, as calculated by Mott, is not a second order effect but is only to a fraction given by a second order perturbation calculation. On the other hand, rigorous calculation can only be made (with great effort) for the purely Coulombian case. We therefore shall be satisfied with the semi-quantitative information as given by the second order approximation.

Results

Gamow potentials or potentials slowly decreasing inside of the nucleus do not affect the polarization appreciably. Repulsive potentials decrease the polarization the more, the less "penetrable" for electrons the nucleus becomes. The Klein paradox prevents the assumption of a strictly "impenetrable" nucleus which has been used with success for neutron scattering. Taking a repulsive potential of the type $V=b/r^5$ where the constant b is so determined as to make V of appreciable importance on the surface of the nucleus and cutting off the potential to prevent divergencies near $r=10^{-13}$ cm annihilates the polarization effect completely. Because of the fact that the eigenfunctions for the static problem are made very small by potentials like V near the nucleus, previous calculations on isotope hyperfine structure by Breit and collaborators and others do not become affected (except perhaps in the case of the fine structure of hydrogen).

O. Halpern

New York University,
University Heights.

J. Schwinger

College of the City of New York,
June 6, 1935.

The Cleavage and X-Ray Planes of Calcite Crystals

In the process of aligning a pair of calcite crystals on a double crystal spectrometer it was noted that the usual telescope method of adjustment did not give the minimum width of a line in the (1+1) position. This was true even though the cleaved surface was parallel to the axis of rotation (within 10″), and in the (1−1) position, the rocking curve width was the theoretical width for a perfect crystal. An investigation of this has brought out the surprising fact that in many cleaved calcite crystals, which possessed good optical surfaces, the cleaved surface does not coincide with the true atomic or x-ray plane.

When the adjustment of a pair of crystals has been completed, a fluoroscopic examination of the x-ray line, reflected in the (1−1) position from the second crystal, shows that as the crystal is slowly rotated through the angle in which reflection takes place the line appears and disappears uniformly over its entire height. If the crystal planes are not parallel, the line will appear first at either the top or the bottom and correspondingly disappear at the bottom or top. In fact, if one has sufficient intensity and a good fluorescent screen the adjustment of a double crystal spectrometer can be more quickly and accurately made by this method than by the usual ionization chamber method.

After having made the above adjustments in the (1−1) position as accurately as possible, a fluorescent screen examination of the (1+1) reflection showed that it appeared at the top or bottom indicating that the crystal planes which diffracted the x-rays were not parallel in this position. It was necessary to tilt the second crystal approximately 30′ of arc about a horizontal line in order to make the planes parallel. By setting the second crystal 15′ from its initial position and then tilting the first in the opposite direction by 15′, it was found that the x-ray lines for both the (1+1) and the (1−1) appeared and disappeared uniformly.

After adjusting the crystals as above, which might be called an x-ray method, it was found (Table I) that the

Table I. *Copper K series.*

$K\alpha_1$		$K\alpha_2$		$K\beta$	
Present	Bearden[1] Shaw	Present	Bearden Shaw	Present	Bearden Shaw
37.8″	39.9″	47.5	51.5	68.5	72.5

[1] J. A. Bearden and C. H. Shaw, Phys. Rev. in press.

(1+1) line widths for the copper $K\alpha_1$, α_2, β lines were about 5 percent less than had been obtained previously by Bearden and Shaw. Since these widths are so much less than any found by previous investigators, it is probable that the same effect has been present in their experiments. In the case of the long wavelengths (titanium K series) the difference is small (about one percent).

Six different pairs of crystals have been tested and in every case the cleavage and x-ray planes were not parallel. The angle between the cleavage and x-ray planes was not the same for all crystals. It varied from 2′ to about 16′ of arc in the various crystals. It also varied as the crystal was rotated about a line normal to the crystal surface. Five pairs of these crystals had been cut from a very perfect block of Iceland calcite by the knife and hammer method. One pair was cut by the milling machine method and this gave the minimum observed angle of 2′. This probably indicates that the method of splitting is responsible for the effect, but it is not clear why the surface should have good optical properties and still not be parallel to the atomic plane. It is necessary that there be present a regular succession of breaks which are small compared to the wavelength of light which continues over the entire surface of the crystal. This, together with the fact that there are always a large number of large visible "steps" on the crystal surface, makes it difficult to find a satisfactory explanation.

J. A. Bearden
H. H. Roseberry

Johns Hopkins, University.
June 15, 1935.

Correction on Previous Reports Concerning the Hyperfine Structure of Y II Lines

In a recent letter to the editor and at the Washington meeting of the American Physical Society the writers[1] reported some structure appearing in the spectrum of yttrium II. At that time, the structure was considered to be hyperfine structure. A more detailed examination has shown that this is not true, and it is the purpose of this letter to correct the error. Since the original report was submitted, the same lines have been photographed when using a different sample of yttrium. This new sample was obtained from A. D. Mackay in New York. With the new sample the same results were obtained for the line λ4900, but the intensity ratio of the components to the line λ4786 was found to vary with the samples. The consistent behavior of the line λ4900 may be explained by assuming that the component is a heretofore unidentified fine structure line in the spectrum of yttrium I. The wave number of this component is found to check the wave number of the yttrium I transition $^4F_{2\frac{1}{2}}{}^0-{}^4F_{3\frac{1}{2}}$ calculated from the data given by Meggers and Russell.[2]

Because of the small dispersion of the spectrograph used, and the numerous Y lines in the neighborhood of λ4854, it was impossible to get photographs on which the interference fringes of the lines did not overlap. This situation prevented an accurate check of the intensity ratio for the components of λ4854.

Both samples were examined for impurities and faint traces of erbium and gadolinium were found. These impurities are estimated to be less than one percent and the observed structure cannot be explained by their presence. Furthermore, the structure of the lines λ4786 and λ4854, which certainly exists, is not explainable as radiation from known terms in yttrium I or yttrium II. At present, the writers are unable to explain this structure, a brief resumé of which is given in Table I. Apparently it is not hyperfine

TABLE I. *Structure of yttrium lines.*

λ obs.	ν obs.	ν calc.	Int. ratio (Chem. Dept.)	Int. ratio (Mackay)	Identification
4900.130	20401.94		3.9	3.9	Y II $^3F_3 - {}^3D^0_2$
.098	20402.07	20402.0	1	1	Y I $4F^0_{2\frac{1}{2}} - {}^4F_{3\frac{1}{2}}$
4786.580	20885.92		3.7	1.6	Y II $^3F_3 - {}^3D^0_3$
.529	20886.14	?	1	1	?
4854.962	20591.75			1	?
.870	20592.14	?		1.8	Y II $^3F_2 - {}^3D^0_1$

structure; a conclusion which agrees with the results of Schüler and Schmidt.[3]

P. GERALD KRUGER
C. N. CHALLACOMBE

University of Illinois,
June 5, 1935.

[1] Kruger and Challacombe, Phys. Rev. **47**, 509 (1935); **47**, 798 (1935).
[2] Meggers and Russell, Bur. Standards J. Research **2**, 733 (1929).
[3] Schüler and Schmidt, Naturwiss. **22**, 838 (1934).

On Bitter's Patterns

F. Bitter,[1] by the sedimentation method, has obtained regular striations on ferromagnetic single crystals. His results suggest that the line-up of the magnetic moments in these crystals is not homogeneous. There is hardly any doubt that Bitter's patterns are characteristic for the thermodynamically stable state of solid iron, nickel, etc. His experiments therefore constitute a direct proof for the contention, that a *perfect* (thermally stable) crystal cannot completely be described by an ideal atomic lattice, but that there exist *secondary structures*, whose characteristic lengths D are large compared with the ordinary lattice constants $d \sim 10^{-8}$ cm.

I here advance in a preliminary way a suggestion concerning the characteristic lengths D of magnetic secondary structures.

The energy of a magnetic moment μ in an effective field H is proportional to $H\mu$. Associated with it is a Larmor frequency, roughly given by

$$\nu = H\mu/h, \tag{1}$$

where h is Planck's constant. *All of* the magnetic moments μ throughout the crystal are in a state of *cooperative* interaction,[2] the theory of which necessitates the consideration of *retardation* effects, caused by the finiteness of the velocity of light c. Because of these retardation effects the magnetization will form a system of *standing waves*, with the wavelength prototype

$$D = c/n\nu = ch/nH\mu = (ch/nH_s\mu)H_s/H, \tag{2}$$

where H_s is the field at saturation and n a pure number of the nature of a refractive index. It is approximately $\mu H_s = k\Theta$, where Θ is the temperature of the Curie point. Finally

$$D = (ch/nk\Theta)H_s/H. \tag{3}$$

As H increases, D decreases, in accordance with Bitter's experiments. D is minimum for $H = H_s$. Let $\Theta = 1000°$Abs. and $k = 1.37 \times 10^{-16}$ ergs, then

$$D_{\min} = 1.4 \times 10^{-3}/n \text{ cm}, \tag{4}$$

which is of the same order as the smallest observational values.

The stabilization of the standing waves in a fixed position is probably due to the presence of imperfections and to surface actions. In a perfect real crystal imperfections would be absent, and the surface should hardly be capable of fixing the standing waves in a definite position, so that in this case the striations will probably be washed out.

A more complete theory must take into account the crystalline structure. Also it is clear, that crystals possess a multitude of normal modes, which may account for the complexity of the observed patterns.

Similar considerations can be advanced concerning the ordinary secondary structure in all crystals. In this case the standing waves are associated with the *optical* normal modes.[3] In passing we remark that the present quantum theory of the metallic state must, in some important instances, be at fault, because of the neglect of electromagnetic retardation effects.

F. ZWICKY

California Institute of Technology,
June 6, 1935.

[1] F. Bitter, Phys. Rev. **38**, 1903 (1931).
[2] F. Zwicky, Phys. Rev. **43**, 270 (1933).
[3] For the characteristic lengths involved see F. Zwicky, Proc. Nat. Acad. Sci. **19**, 822 (1933).

THE AMERICAN INSTITUTE OF PHYSICS

INCORPORATED

GOVERNING BOARD

For The American Physical Society:

KARL T. COMPTON, *Chairman*
Massachusetts Institute of Technology

GEORGE B. PEGRAM, *Secretary*
Columbia University

JOHN T. TATE
University of Minnesota

For The Optical Society of America:

E. C. CRITTENDEN
Bureau of Standards

PAUL D. FOOTE
The Gulf Companies

F. K. RICHTMYER
Cornell University

For The Acoustical Society of America:

HARVEY FLETCHER
Bell Telephone Laboratories

VERN O. KNUDSEN
University of California at Los Angeles

WALLACE WATERFALL
The Celotex Company

For The Society of Rheology:

E. C. BINGHAM
Lafayette College

A. STUART HUNTER
du Pont Rayon Company

S. E. SHEPPARD
Eastman Kodak Company

For The American Association of Physics Teachers:

HOMER L. DODGE
University of Oklahoma

PAUL E. KLOPSTEG
Central Scientific Company

FREDERIC PALMER
Haverford College

ADMINISTRATIVE STAFF

HENRY A. BARTON, *Director* JOHN T. TATE, *Adviser on Publications*

MADELINE M. MITCHELL, *Editorial Secretary*

Office: 11 East 38th Street, New York, New York

JOURNALS

THE PHYSICAL REVIEW

REVIEWS OF MODERN PHYSICS

PHYSICS

JOHN T. TATE, *Editor*
J. W. BUCHTA, *Assistant Editor*
E. C. BINGHAM, *Rheology Editor*

THE JOURNAL OF THE OPTICAL SOCIETY OF AMERICA

THE REVIEW OF SCIENTIFIC INSTRUMENTS WITH PHYSICS NEWS AND VIEWS

F. K. RICHTMYER, *Editor*

JOURNAL OF THE ACOUSTICAL SOCIETY OF AMERICA

F. R. WATSON, *Editor*

THE JOURNAL OF CHEMICAL PHYSICS

HAROLD C. UREY, *Editor*

THE AMERICAN PHYSICS TEACHER

DUANE ROLLER, *Editor*

The American Institute of Physics is a membership corporation of which five societies are the founding members. These five societies are the principal national societies devoted to pure and applied physics in America. Their names, and those of their representatives who form the Governing Board of the Institute, are given above. The principal work of the Institute is the publication of journals sponsored by the societies or by itself. The names and the editors of the journals are also listed above.

The broad purpose of the Institute is to represent, in all matters of wide or common interest, the five thousand or more members and subscribers associated with the Founder Societies and the journals. It aims to advance the science and profession of physics, and to promote cooperation between pure research, the applied sciences and the industries. To achieve these aims, it is greatly in need of an endowment and is empowered by law to administer grants and funds of any kind.

CONTENTS

PHYS. REV. 48 (1935) JULY 1

Schematic Representation of the Anomalous Scattering by Suitable Nuclear Fields . . . . . LEE H. HORSLEY 1

On the Fermi Theory of β-Radioactivity . . . . . E. J. KONOPINSKI AND G. E. UHLENBECK 7

Discussion of the β-Decay Theory . . . . . R. L. DOLECEK 13

Shapes and Wavelengths of K Series Lines of Elements Ti 22 to Ge 32 . . . . . J. A. BEARDEN AND C. H. SHAW 18

Measurement of the Absolute Probability of K-Electron Ionization of Silver by Cathode Rays . . . . . J. C. CLARK 30

Direct and Fluorescence Excitation of the K Level in Thick Targets of Gold . . . . . K. B. STODDARD 43

Remarks on the Systematics of Isotopes . . . . . GUIDO BECK 47

Linear Modifications in the Maxwell Field Equations . . . ROBERT SERBER 49

Polarization Effects in the Positron Theory . . . . . E. A. UEHLING 55

Raman Spectrum of Heavy Chloroform . . R. W. WOOD AND D. H. RANK 63

Attempt to Observe the Absorption Spectrum of Metastable Nitrogen Molecules . . . . . A. A. FROST AND O. OLDENBERG 66

Hyperfine Structure Formulae for the Configuration p^2s . . . . . M. F. CRAWFORD AND LAWRENCE A. WILLS 69

Particle Problem in the General Theory of Relativity . . . . . A. EINSTEIN AND N. ROSEN 73

Magnetic Susceptibilities of Salts of the Iron Group Elements . R. B. JANES 78

Theory of the Work Functions of Monovalent Metals . . . . . E. WIGNER AND J. BARDEEN 84

Energy Distribution of Secondary Electrons from Molybdenum . . . . . LELAND J. HAWORTH 88

Secondary Emission of Electrons from Complex Targets. PAUL L. COPELAND 96

Corrections to H. Kayser's "Tabelle der Schwingungszahlen" 98

Letters to the Editor:

Gamma-Rays from Nitrogen Bombarded with Deuterons . . . . . H. R. CRANE, L. A. DELSASSO, W. A. FOWLER AND C. C. LAURITSEN 100

Origin of the "Extra Rings" in Electron Diffraction Patterns . . . . . K. LARK-HOROVITZ, H. J. YEARIAN AND J. D. HOWE 101

Gamma-Rays from Boron Bombarded with Protons . . . . . H. R. CRANE, L. A. DELSASSO, W. A. FOWLER AND C. C. LAURITSEN 102

Note on the Spectra of Jupiter and Saturn. . . . . ARTHUR ADEL 103

Mass Ratio of the Lithium Isotopes. . . . . G. M. ALMY AND G. R. IRWIN 104

Ultraviolet Absorption Spectrum of Hydrogen Fluoride . KOHEI SIGA AND HAROLD J. PLUMLEY 105

Carbon Reactions and the Corrected Mass-Scale . . . . . M. A. TUVE AND L. R. HAFSTAD 106

Higher Order Derivatives in the Interaction "Ansatz" of the Fermi Theory . . . . . E. J. KONOPINSKI AND GEORGE E. UHLENBECK 107

Concerning the Possibility of a Unified Interpretation of Electrons and Protons . . V. ROJANSKY 108

On the Polarization of Electrons by Double Scattering . . . O. HALPERN AND J. SCHWINGER 109

Cleavage and X-Ray Planes of Calcite Crystals . . . J. A. BEARDEN AND H. H. ROSENBERRY 110

Correction on Previous Reports Concerning the Hyperfine Structure of Y II Lines . . . . . P. GERALD KRUGER AND C. N. CHALLACOMBE 111

On Bitter's Patterns . . . . . F. ZWICKY 111

LANCASTER PRESS INC., LANCASTER, PA.